Trends in groundwater quality in relation to groundwater age

Nederlandse Geografische Studies / Netherlands Geographical Studies

ISSN 0169-4839

Netherlands Geographical Studies 384

Trends in groundwater quality in relation to groundwater age

Ate Visser

Utrecht 2009

Koninklijk Nederlands Aardrijkskundig Genootschap
Faculteit Geowetenschappen Universiteit Utrecht

This publication is identical to a dissertation submitted for the title of Doctor at Utrecht University, The Netherlands. The public defence of this thesis took place on 15 May 2009.

Dit proefschrift werd (mede) mogelijk gemaakt met financiële steun van de Europese Unie, als onderdeel van het Geïntegreerde Onderzoeksproject AquaTerra van het 6e Kader Programma, alsmede van TNO - Bouw en Ondergrond, en Deltares.

ISBN 978-90-6809-427-5

Graphic design, cartography and figures:
GeoMedia (Faculty of Geosciences, Utrecht University)

Printed in the Netherlands by A-D Druk b.v. – Zeist

Contents

Figures

Tables

1 Introduction

1.1 Rationale: Protecting groundwater quality

Groundwater is a valuable natural resource and as such should be protected from chemical pollution (EU 2006). This is particularly important for groundwater dependent ecosystems where groundwater contributes significantly to surface water (Van Ommen 1986; Rozemeijer and Broers 2007) and where groundwater is used as drinking water such as in the European Union and the United States (Solley *et al.* 1993).

The quality of groundwater and surface water is usually characterized by its chemical composition: groundwater and surface water of good quality have low concentrations of pollutants like nitrate and pesticides. Ideally, the concentrations of pollutants in groundwater meet drinking water standards, for example 50 mg/l NO_3 in the EU (EU 1991). Increasing concentrations of pollutants or indicators of pollutants are perceived as a deterioration of groundwater quality.

Groundwater quality is threatened by point sources of pollution, such as leaky oil tanks, septic tanks, landfills, etc., and by diffuse sources of pollution. Diffuse agricultural pollution is the largest threat to groundwater quality at a regional scale in many areas of the US (Spalding and Exner 1993; Nolan *et al.* 1997), the UK (Foster *et al.* 1982), the EU (Strebel *et al.* 1989), China (Zhang *et al.* 1996), Iran (Jalali and Kolahchi 2008), Japan (Kumazawa 2002) and increasingly in developing countries like India (Bijay-Singh *et al.* 1995). The most common form of agricultural pollution of groundwater is the leaching of high concentrations of nitrate, but artificial pesticides and heavy metals present in manure and fertilizers also threaten groundwater quality. Upward trends in nitrate concentrations were found throughout Europe, and linked to changes in agricultural practices (Strebel *et al.* 1989).

Awareness of the pollution of surface water (Ackermann *et al.* 1970; Wolman 1971) and groundwater (Oakes *et al.* 1981; Foster *et al.* 1982) led to the implementation of measures aimed at reducing the input of pollutants into the natural system (EU 1975; MacDonnell and Guy 1991). For example, the Dutch Manure Act (1986; Mol *et al.* 2001) was aimed at reducing the amount of nitrate leaching from agricultural land. The EU Nitrates directive (EU 1991; Goodchild 1998) forces EU member states to take measures against pollution caused by nitrates from agricultural sources. The EU Water Framework Directive (EU 2000) aims at the integral management of surface water and groundwater. It is the most advanced regulatory framework for the protection of all natural waters in the European Union in order to achieve "good status" by the end of 2015. The recently adopted EU Groundwater Directive (GWD, EU 2006) on the protection of groundwater against pollution in the EU member states specifies the environmental objectives of the WFD with regards to groundwater within so-called "groundwater bodies".

Because of the long travel times of pollutants through groundwater bodies, early detection of deterioration is necessary to efficiently protect groundwater quality. Therefore, the GWD not only requires member states to demonstrate good groundwater chemical status, but also to

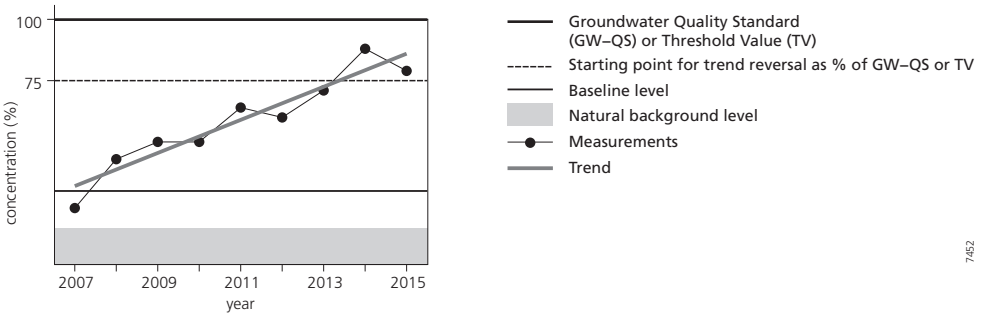

Figure 1.1 Elements of trend and trend reversal assessment (after (Grath *et al.* 2008))

identify and reverse significant and sustained upward trends in the concentrations of pollutants that may threaten future groundwater quality. According to the GWD, a groundwater body is at risk of failing to achieve good chemical status if it shows a significant and sustained upward trend in the concentration of a pollutant and the upper 95%-confidence limit of the concentration of the pollutant exceeds 75% of the Quality Standard (QS) or Threshold Value (TV). This point is defined as the starting point for trend reversal, at which the EU member state is required to implement measures to reverse the trend. This concept is illustrated in Figure 1.1.

Trend detection as required by the GWD is dedicated to detect trends in the concentrations of pollutants resulting from anthropogenic sources and distinguish these from natural variation with an adequate level of confidence and precision (GWD, Annex V, art 2(a)(i)). Obviously, variations due to climatic or meteorological factors might complicate trend detection, but also spatial and temporal variation of leaching of pollutants towards the groundwater table, variation in travel times of sampled groundwater and variable hydrogeochemical processes along the groundwater flow path. These uncertain factors result in unexplained variations in the measured concentrations of pollutants in groundwater, which may obstruct the detection of the underlying trend of anthropogenic origin. This motivates policy-makers to ask the scientific community to develop trend detection techniques that reduce the variability not related to anthropogenic influences and improve the confidence of trend detection.

To address the challenges of the WFD, a number of working groups was asked to design a common implementation strategy (CIS) and produce "guidance documents" for the implementation of the WFD. The mandate of the Groundwater Working Group (WGC) required the development of practical guidance and technical specifications for the derivation of threshold values, the assessment of status compliance (both quantitative and chemical) and the assessment of groundwater trends and trend reversal. The research for this thesis was conducted in the years that the specific content of the GWD was negotiated and the Guidance documents were further developed. The focus of the guidance document on "statistical aspects of the identification of groundwater pollution trends, and aggregation of monitoring results" (Grath *et al.* 2001) left little room to include conceptual understanding of the factors determining groundwater quality. In recent years, it was generally realized that a conceptual understanding of the groundwater systems is essential for the characterization of chemical status and the detection of trends (Grath *et al.* 2007). However, no concrete methods were available yet to relate chemical status and trends to the character of the groundwater body or historical contamination.

1.2 Aim and general research question

The aim of this work was to develop and improve tools to detect trends in groundwater quality considering the reactive transport of pollutants from the ground surface to the monitoring screen. The emphasis was on including the travel time of pollutants in the methods for trend detection, because several analytical techniques to determine the travel time or age of samples groundwater have become widely available over the past decades. The working *hypothesis* was that including more information on pollutant transport, in particular travel time, in the analysis of groundwater quality monitoring data will lead to an improved efficiency to detect these trends and a better understanding of the detected trends. Also, groundwater age will provide a direct link between observed concentrations of pollutants in groundwater and the historical application of these pollutants on agricultural land. In relation to this aim, the general research question of this thesis was formulated as:

"*What is the value of groundwater age in the detection of trends in groundwater quality?*"

The overall research question is elaborated through a series of sub-questions, which are presented in section 1.6.

1.3 Study area and scope

The research presented in this thesis was conducted within the scope of work package TREND 2, named "Trends in groundwater and surface water quality", of the EU 6th Framework Program Integrated Project "AquaTerra" (Gerzabek *et al.* 2007). AquaTerra aims to provide the scientific

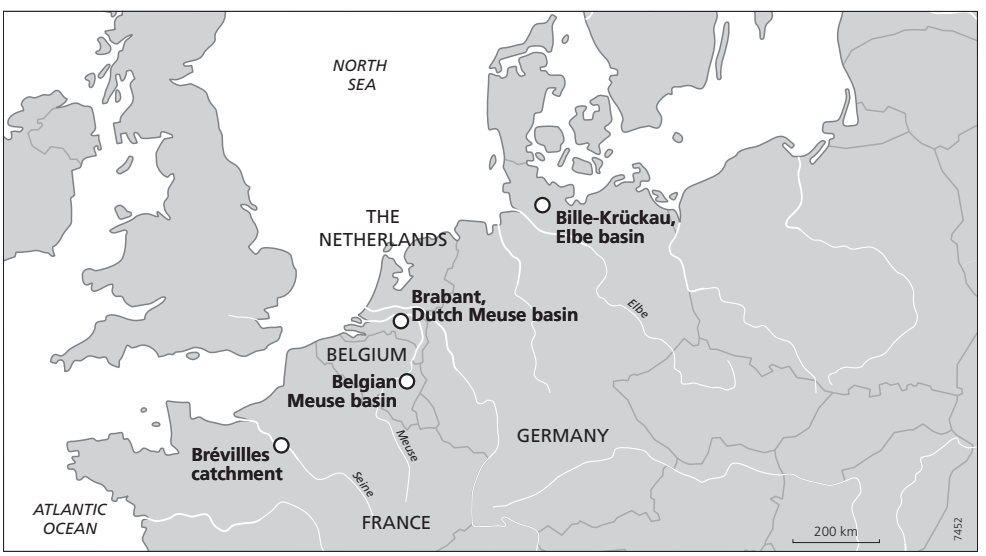

Figure 1.2 Locations of the TREND 2 test sites in Europe.

basis for improved river basin management, through a better understanding of the river-sediment-soil-groundwater system.

Work package TREND 2 was dedicated to the development of operational methods to assess, quantify and extrapolate trends in groundwater systems. Several statistical techniques, modeling techniques and combinations of both are available for trend analysis and some promising techniques were tested, including groundwater age dating and transfer-function approaches. These techniques were tested at four sites, covering a wide range of settings present in Europe, including unconsolidated lowland deposits in the Netherlands (Brabant, Dutch Meuse Basin) and Germany (Bille-Krückau watershed, Elbe Basin), chalk aquifers in Belgium (Belgian Meuse Basin) and a fractured aquifer with a thick unsaturated zone in France (Brévilles catchment) (Figure 1.2).

1.3.1 Study area

The study area of the research presented in this thesis was the province of Noord-Brabant, the Netherlands. Noord-Brabant (5100 km^2) covers most of the Sand Meuse groundwater body in the south of the Netherlands. The subsurface consists of fluvial unconsolidated sand and gravel deposits from the Meuse River, covered by 2-30 meters of Middle- and Upper-Pleistocene fluvio-periglacial and aeolian deposits consisting of fine sands and loam. It is a flat area with altitudes ranging from mean sea level (MSL) in the north and west to 30 m above MSL in the southeast. The area is drained by a natural system of brooks, extended in the 20th century with drains and ditches to allow agricultural practices in the poorly drained areas. Groundwater tables are generally shallow as result, usually within 1-5 meters below the surface. Net groundwater recharge is around 300 mm/y resulting in a downward groundwater flow velocity of about 1 m/y in recharge areas (Broers 2004a).

Today, Noord-Brabant is one of the areas in Europe which is most affected by agricultural pollution. Intensive livestock farming, now covering 62% of the area, produces a large surplus of nitrogen-rich manure. Because of the vulnerability of Noord-Brabant to agricultural pollution, a groundwater quality monitoring network was installed in 1980, and extended in 1990, consisting of nested piezometers with a diameter of 5 cm and a screen length of 2 meters at a depth of about

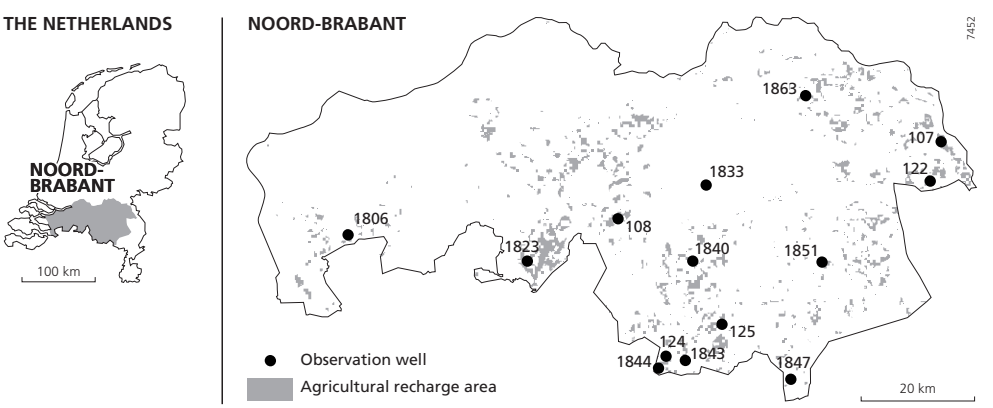

Figure 1.3 Locations of the observation wells from which groundwater quality data and $^3H/^3He$ ages were collected.

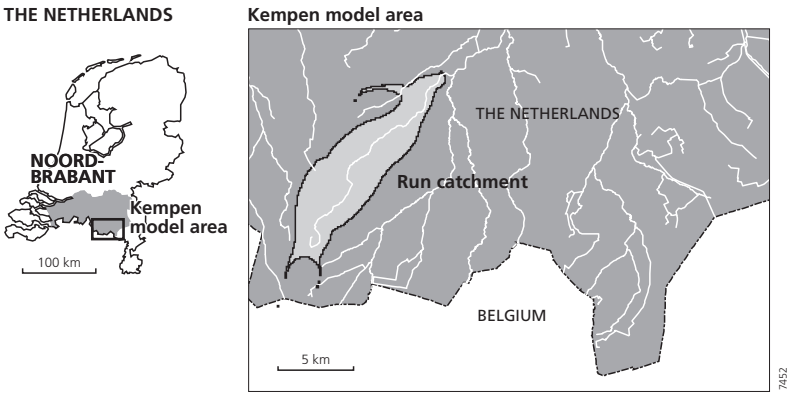

Figure 1.4 Location of the Run catchment within the numerical groundwater flow and transport model of the Kempen Area.

10 and 25 meters below surface (Van Duijvenbooden 1993; Broers 2002). Measurements of field parameters (pH, electrical conductivity and dissolved oxygen), concentrations of major cations (Na, K, Ca, Mg, Fe, Al and NH_4), anions (Cl, NO_3, SO_4, HCO_3 and PO_4) and trace metals (As, Cd, Cu, Ni, and Zn) are collected annually as part of the national or provincial monitoring effort.

The focus of this study was a selection of 14 monitoring wells located in agricultural recharge areas (Figure 1.3). These areas are homogeneous in land use history and hydrogeochemistry (Broers and Van der Grift 2004). Recharge areas lack a superficial drainage network; have relatively deep groundwater levels, relatively permeable soils and a relatively high topographical position. These areas are especially vulnerable to diffuse groundwater pollution because groundwater and thus contaminants can easily reach deeper parts of the aquifer. The long time-series from the selected wells of the groundwater quality monitoring network were used in this thesis, in conjunction with groundwater ages determined with $^3H/^3He$ in the 34 screens of the 14 wells in agricultural recharge areas.

The impact of groundwater on surface water quality is strongly related to the range of travel times in discharging ground water (Raats 1977; Van Ommen 1986; Duffy and Lee 1992; Broers *et al.* 2007; Rozemeijer and Broers 2007). Predictions of the breakthrough of spatially diffuse contamination can be based on distributed contaminant transport models (Van der Grift and Griffioen 2008); or on a combination of the travel time distribution of a catchment derived from a numerical model with land use and contamination history (Broers *et al.* 2007). To assess the accuracy of travel time distributions in numerical models, the distribution of groundwater travel times in the small catchment of the Run stream was studied using a numerical groundwater flow and transport model that covered the Kempen region in the south-east of Noord-Brabant (Figure 1.4).

1.3.2 Factors determining the concentrations of pollutants in the study area

In the agricultural recharge areas of the Sand Meuse groundwater body, four factors that determine the concentrations of pollutants measured in groundwater monitoring wells are

considered relevant: (1) the deposition of pollutants at the ground surface, (2) leaching of these pollutants to the water table and the travel time of pollutants through the groundwater flow system towards the monitoring location, (3) hydrogeochemical processes along the groundwater flow path altering the concentrations of pollutants, and (4) mixing of groundwater during sampling. These factors are discussed briefly below, to outline the scope of this thesis.

Historical concentrations of pollutants at the water table can be reconstructed using a regional scale mineral balance based on records of atmospheric deposition, manure applications, and fertilizer sales (Van der Grift and Griffioen 2008). A detailed description of the mineral balance in Noord-Brabant is presented in the Appendix of Chapter 2. Even though the large difference between natural land cover and agricultural land is removed by selecting monitoring wells with presumably agricultural land use in their catchment areas, it is very likely that the actual historical concentrations at the water table vary spatially as well as temporally. Also, leaching processes can lead to unpredictable temporal variations in the concentrations of pollutants (Bjerg and Christensen 1992; Broers *et al.* 2004a). These are some of the sources of variation that obscure the anthropogenic trends.

Once pollutants have crossed the water table, they are transported by groundwater flow to the location of sampling. Along the groundwater flow path, hydrogeochemical processes alter the concentrations of pollutants (Glynn and Plummer 2005). Uncertainty about these geochemical processes is a complicating factor for trend detection.

The agricultural load of cations, in particular potassium (K) and heavy metals, is affected by the exchange with the cation exchange complex of the subsoil (Ceazan *et al.* 1989). Previous studies in the area show that cation exchange leads to the retardation of the K front and the delayed arrival of K at the monitoring screen (Griffioen 2001; Broers and Van der Grift 2004). The total sum of cations (SUMCAT) remains constant if cation exchange is the only process that is taking place, although individual cations may exchange individually with the cation exchange complex. Therefore, SUMCAT can be used as a conservative chemical indicator to detect anthropogenic trends in groundwater quality.

Earlier work indicated that nitrate reduction by pyrite oxidation (Kölle *et al.* 1985; Postma *et al.* 1991) is the dominant process of nitrate removal in the study area of this thesis (Broers 2004b; Broers and Van der Grift 2004) providing natural attenuation of nitrate pollution (Hiscock *et al.* 1991; Korom 1992). On the other hand, arsenic, nickel and zinc enclosed in pyrite may be released by nitrate-induced pyrite oxidation (Kölle *et al.* 1985; Van Beek *et al.* 1989; Broers 2004b). If pyrite oxidation by nitrate reduction takes place, the oxidation capacity (OXC), defined as the weighted sum of NO_3 and SO_4, remains constant before and after pyrite oxidation (Postma *et al.* 1991). OXC behaves as a conservative indicator that can also be used to detect anthropogenic trends in groundwater quality (Broers and Van der Grift 2004).

Given the character of the aquifer, it is assumed that piston flow transports pollutants between recharge and sampling. The sharp gradients that are found in vertical profiles of tritium concentrations in similar aquifers (Robertson and Cherry 1989; Postma *et al.* 1991) suggest that the effect of dispersion is limited. Moreover, dispersion is not expected to affect the long-term anthropogenic trends resulting from diffuse pollution from agriculture. Because groundwater quality samples used in this study were collected from short well screens (2 m), little mixing occurs during sampling and groundwater samples have a distinct travel time. Uncertainty about the travel time of sampled groundwater complicates the aggregation of trends or monitoring data across a groundwater body. Assuming increasing travel times with depth, grouping of data

according to sampling depth can be used to facilitate trend aggregating. Additionally, dating groundwater using environmental tracers may help to remove this source of uncertainty from the detection of trends.

Several other factors may also influence the concentrations of pollutants in groundwater. A thick unsaturated zone delays the arrival of pollutants at the water table that were applied at the land surface. There are few methods to determine the travel time through a thick unsaturated zone. An unsaturated zone with variable thickness may result in apparent groundwater age inversions, whereby older groundwater overlies younger groundwater. Dual porosity aquifers cause non-linear mixing of old and young groundwater complicating the analysis of the concentrations of pollutants in groundwater. Long sampling screens or convergent flow lines of discharging groundwater also cause mixing of older and younger groundwater. In such samples the groundwater quality or concentrations of pollutants are mostly determined by the distribution of groundwater ages in the sample. None of these factors is relevant, because of the shallow groundwater levels, single-porosity granular aquifers, and short sampling screens in the study area of this thesis.

1.3.3 Scope

The value of groundwater age in the detection of trends was studied under a set of conditions which define the scope of the thesis: the specific aim of trend detection within the context of the WFD and GWD; the historical contamination, character of the groundwater body and monitoring network in the study area; the available time-series from this network; and the financial resources to apply groundwater age tracers. Because only anthropogenic trends are the objective of trend detection, we defined trends in groundwater quality, according to Loftis (1996), as "changes in groundwater quality over time, at a given location or over a given region, which are related to water quality or land-use management." Variations or trends due meteorological of climatic factors, as well as variations in application, leaching, travel times or geochemical reactions are considered undesired noise to be distinguished from the long-term anthropogenic trends.

Previous studies have already provided a decent understanding of the groundwater flow system in the selected areas and many of the occurring geochemical reactions are known beforehand. The aim of this study was to detect trends, considering these factors, but not to acquire additional knowledge on the characteristics of the groundwater body. The monitoring network has been installed with the particular aim of signaling deterioration of groundwater quality and considering the characteristics of the groundwater body. Therefore, the design and operation of the monitoring network (Broers 2002) are beyond the scope of this study. The time-series used contained annual measurements of pollutant concentrations. No attention was given in this thesis to dealing with seasonal fluctuations which may be present in the time-series of higher monitoring frequency in systems with quick response time such as fractured or karst aquifers. Both the character of the groundwater system and monitoring network, as well as the funding of the project allowed the accurate determination of groundwater ages at the well screens with environmental tracers. This may be more difficult or even impossible in different groundwater systems (fractured or karst aquifers, thick unsaturated zones) or available monitoring networks (supply wells with long screens, springs, discharge points). The unique combination of the conditions of this research resulted in findings that in some respects may be site-specific and obviously not all conclusions and recommendations hold when the aim, contamination history, groundwater system, or available resources, in terms of data and funding,

are different. Therefore, a comparison of the different experiences at the four test sites of the TREND 2 partners of the AquaTerra project is presented as part of this thesis (Chapter 4).

1.4 Overview of research on groundwater quality and trend detection

1.4.1 Groundwater quality monitoring networks

Groundwater quality monitoring networks and programs are already in place in many countries. Unfortunately, only few monitoring networks have been properly described in scientific literature (Leahy *et al.* 1993; Van Duijvenbooden 1993; Kim *et al.* 1995; Juhler and Felding 2003; Ward *et al.* 2004; Daughney and Reeves 2005; Lee *et al.* 2007; Rosen and Lapham 2008 and references therein). The objectives of these monitoring networks are diverse: to signal threats to drinking water supplies, monitor the spread of point-source pollution, detect the intrusion of salt water in coastal areas or detect the threat of agricultural pollution to regional groundwater quality. Each of these objectives requires a different monitoring network (location and type of wells) and monitoring program (sampling scheme). Regional monitoring networks have three purposes: 1) assessing groundwater quality, 2) detecting changes in groundwater quality, and 3) relating these changes to land use practices. The design and operation of monitoring networks should depend on the monitoring objectives, as well as the characteristics of the monitored groundwater body (Broers 2002). Ideally, such monitoring networks consist of dedicated monitoring wells, often sampling groundwater from a specific depth. In practice, studies in trends in groundwater quality often rely on existing time-series of measurements, sampled from existing wells. These existing wells can be a collection of municipal or agricultural water supply wells, springs or discharge points, or a combination thereof.

The distinction between monitoring wells with short screens and water supply wells is important because the former sample from a specific point in the aquifer while the latter have long screens drawing water from the entire groundwater body. This difference can influence the sampled concentration of nitrate, because the mixture sampled from a supply well contains a portion of old, pre-agricultural groundwater with no nitrate (Nolan *et al.* 1997). Data from supply wells should therefore be regarded as a sampling a different sub-population (Alley 1993).

Results from the Dutch National Groundwater Quality Monitoring Network

The Dutch national groundwater quality monitoring network was installed in 1980 to assess national groundwater quality and impact of agriculture (Van Duijvenbooden *et al.* 1985). Because of the vulnerability of groundwater in the province of Noord-Brabant to agricultural pollution, the national network was extended in 1990 by a Provincial monitoring network (Van Duijvenbooden 1993). The data from the national and provincial monitoring networks in the Netherlands have been used to investigate the hydrogeochemistry of groundwater (Frapporti *et al.* 1993; Frapporti 1994). Spatial trends in groundwater quality have been analyzed by statistical interpolation of measured concentrations of 25 groundwater quality variables to produce median concentrations for 4×4 km blocks (Pebesma and de Kwaadsteniet 1997). For 12 variables, maps of changes in groundwater quality were made by spatial interpolation of short-term predictions calculated for each well screen from time series of yearly measurements over 5-7 years, using a simple regression model for variation over time and taking location-specific time-prediction uncertainties into account. Groundwater quality in the Netherlands was systematically mapped

in 1992 (Van Drecht *et al.* 1996; Reijnders *et al.* 1998) and again in 2000 (Reijnders *et al.* 2004). These reports provide the weighed mean concentration of various pollutants in physical geographical units in the Netherlands, as well as the percentage of the area of each unit where concentrations are expected to be above the threshold. The report distinguishes between shallow and deep groundwater, implicitly incorporating groundwater age in the analysis. They also reported changes in Dutch groundwater quality between 1984 (the first year of operation) and 1993 or 2000 (Van Drecht *et al.* 1996; Reijnders *et al.* 1998; Reijnders *et al.* 2004). The changes in groundwater quality are based on the differences in weighted mean concentrations between the two years and reported for each physical geographical unit. They found that the nitrate concentrations increased between 1984 and 1993 in shallow groundwater under sandy areas in the centre of the Netherlands by 1.9 mg/l on average. Also the number of nitrate concentrations above the threshold value increased in this period. Surprisingly, few changes were detected for the period between 1984 and 2000.

1.4.2 Detecting trends in groundwater quality

Loftis (1996) provides a comprehensive overview of relevant studies on trends in groundwater quality. Most trend assessment studies have used available data from existing monitoring networks. The advantage of using existing data is the possibility to study changes in water quality, without the need to wait for the time-series to be collected. The disadvantages of existing data are the often non-ideal method of sample collection, and sometimes irregular time-series. Even when groundwater quality data are used from a dedicated monitoring network, changes in the methods of sample storage and laboratory analyses may result in artificial trends (Frapporti *et al.* 1994).

If existing time-series are used for trend detection, the method of data analysis and trend detection should be chosen based on the objectives of the study, the historical contamination and the type of sampling. In any case, the method for trend detection should be robust and capable of dealing with irregular time series, containing missing values, and possibly having a non-normal distribution. A number of authors have discussed and compared the power of statistical methods available for the detection of trends (Loftis *et al.* 1991b; Esterby 1996; Yue *et al.* 2002).

Grouping monitoring locations and time-series to improve trend detection

In general, the efficiency of trend detection may be improved by including information of pressures, hydrology and geochemistry by grouping wells accordingly (Broers and Van der Grift 2004; Broers et al. 2008). Obviously, wells receiving water from natural areas should be analyzed separately from wells receiving agriculturally polluted water. Grouping of monitoring data should also consider the depth of sample collection, because groundwater travel times generally increase with depth in unconsolidated aquifers (Broers 2004a). The depth of the well screen is especially important for the detection of trends in groundwater quality in relation to agricultural pollution because the shallower screens in unconsolidated granular aquifers may show that the quality of younger (post-1990) groundwater is improving thanks to manure legislation, while the deeper wells still show the decline of quality in older (pre-1980) groundwater as the result of the intensification of agriculture. These concepts were included in the design of the Dutch national and provincial monitoring networks (Van Duijvenbooden 1993; Broers 2002). Although agricultural areas in a given groundwater body may have a similar input history, field-to-field variation in manure and fertilizer application and crop uptake, and even within-field year-to-year variation in leaching concentrations, result in unexplained variations in the measured

concentrations of pollutants. Grouping monitoring data before applying trend detection techniques may therefore be beneficial.

Trends in time-series

Trends can be determined in individual time-series using simple linear regression or a non-parametric test for trends like the Mann-Kendall test (Broers 2002; Broers and Van der Grift 2004; Batlle-Aguilar et al. 2007). The choice between using linear regression or the Mann-Kendall test should be based on the normality of the distribution of observations (Batlle-Aguilar *et al.* 2007). After the detection of trends in individual monitoring wells, it is necessary to aggregate the observed trends to supply a representative trend for the groundwater body or parts of the groundwater body (Broers and Van der Grift 2004). Stuart *et al.* (2007) also determined the trends for single boreholes and then spatially averaged these. They found this approach less sensitive to 'missing data', while preserving information about the spatial distribution of trends within the water body. Daughney and Reeves (2006) used non-parametric methods (Mann-Kendall) to detect trends in individual time-series. They clustered monitoring locations using hierarchical cluster analysis based on observed water quality parameters, rather than using additional information to separate beforehand.

Analyzing trends in vertical profiles

Trend detection is usually limited to the analysis of time series of individual wells or groups of wells. Hallberg and Keeney (1993) showed that trends in groundwater quality can also be detected using concentration-depth information, because depth and groundwater age are interrelated under natural flow conditions. This phenomenon is most pronounced in groundwater recharge areas. The combined use of time series information and time-averaged concentration-depth profiles helps detect temporal changes in groundwater quality. The vertical concentration profiles are especially useful for understanding trends of reactive pollutant concentrations. A vertical 1D numerical reactive transport model may provide insight into the transport and hydrogeochemistry of reactive pollutants (Broers and Van der Grift 2004).

Using age tracers to analyze groundwater quality

The capability to detect trends in groundwater quality can be improved by the application of environmental tracers (Cook and Solomon 1997) to determine the exact or approximate age of groundwater. Foster *et al.* (1982) aggregated data from UK aquifers and related the observed concentrations to tritium levels and land use change. Bronswijk en Prins (2001) directly related groundwater concentrations in the Netherlands to the time of recharge determined from ^{3}H profiles (Robertson and Cherry 1989; Meinardi 1994).

The application of modern groundwater dating methods that can determine an exact age of groundwater has been a great improvement in groundwater quality studies (Böhlke and Denver 1995; Johnston *et al.* 1998; Böhlke 2002; MacDonald *et al.* 2003; Klump *et al.* 2006; Osenbrück *et al.* 2006). Laier (2004) used CFC groundwater dating to identify trends in individual monitoring wells related to time of recharge. Wassenaar *et al.* (2006) detected trends in nitrate concentrations dated with $^{3}H/^{3}He$. Tesoriero *et al.* (2007) linked concentrations of nitrate and pesticides like atrazine and its degradation product DEA to groundwater age along flow paths at several locations throughout the US. The concentrations in relation to time of recharge compared well to the land use and pesticide history.

Recently, a number of trend studies from the U.S. Geological Survey National Water-Quality Assessment program (NAWQA) were published that used groundwater dating to link measured concentrations to the time of recharge (Burow *et al.* 2008; Debrewer *et al.* 2008; Rosen and Lapham 2008; Rupert 2008; Saad 2008). These studies commonly recognized the value of age dating because it increases the utility of existing short-term time-series.

1.5 Overview of research on groundwater age

1.5.1 Concept of groundwater age

Groundwater age is the time that has elapsed since water passed the water table and became groundwater (Goode 1996; Bethke and Johnson 2008). The terms groundwater travel time or groundwater residence times are technically more correct, indicating they refer to the time that water has traveled or resided as groundwater, rather than the time the water itself has existed as such. The terms groundwater age and groundwater travel time are used interchangeably in this thesis.

The concept of groundwater age has greatly improved our understanding of groundwater systems (Glynn and Plummer 2005). It is very useful because it relates to the moment when groundwater recharged which is also often the moment when pollutants enter the water cycle. The view of the concept of groundwater age has changed over recent years. Today, a groundwater sample is seen not as water that recharged the groundwater system at a point in the past, but as a mixture of waters that have resided in the subsurface for varying lengths of time (Bethke and Johnson 2008). In this perspective, a groundwater sample may have a mean age, which is merely a useful statistical characteristic of the distribution of groundwater ages present in the sample. The spread of the age distribution depends on aquifer characteristics, but also on the type of groundwater sample.

1.5.2 Sample type

Within a single groundwater sample, a range of groundwater ages may be present. Mixing of older and younger may occur during groundwater flow or during sampling. Hydrodynamic dispersion in granular aquifers causes limited mixing. Converging flow lines or dual porosity systems or sampling groundwater from a well with a long screen causes substantial mixing. If a groundwater sample contains a wide distribution of groundwater age, the mean age of groundwater becomes meaningless. For example, if a groundwater sample has an age of 40±1 years, it is free from pollutants introduced 30 years ago. If a sample has a mean age of 40±20 years, the pollutant will be present in the groundwater sample. This concept of age spread is essentially important for all analyses performed on concentrations in groundwater samples.

Samples from long-screened wells, springs, galleries, production wells, fractured aquifers etcetera are mixed-samples. Samples from dedicated monitoring wells in systems with little mixing due to hydrodynamic dispersion can be considered point-samples. It is assumed that all groundwater in a sample collected from the national and provincial monitoring networks in the Netherlands has recharged within a period of 5 years. If the spread of groundwater age is so limited, the traditional view of a single groundwater age of the sample can also be adopted. For samples with such a distinct age, several analytical techniques are available to determine the age of the groundwater sample.

1.5.3 Groundwater age tracers

Several authors have provided complete overviews of groundwater dating (Ekwurzel *et al.* 1994; Cook and Solomon 1997; Bethke and Johnson 2008), but the following overview is limited to the aspects of groundwater dating relevant for this thesis.

Tritium

Tritium (^{3}H) is a radioactive isotope of hydrogen and was the first environmental groundwater age tracer (Kaufman and Libby 1954; Nir 1964). It has a half-live of 12.32 years and decays to ^{3}He emitting an electron (ß-decay). Large amounts of tritium were introduced into the atmosphere by nuclear tests in the 1950s and 1960s. Tritium atoms bonded with oxygen and hydrogen to form water molecules that became part of the hydrological cycle. The historical concentrations of tritium in precipitation show a distinct peak in 1963 at the height of the nuclear bomb tests. As a result, high tritium concentrations can be found in groundwater that recharged just after 1963. By sampling a vertical profile of tritium concentrations in areas with downward groundwater flow, it is possible to accurately determine the location of the tritium peak and interpolate the rest of the age profile. This approach requires a high resolution tritium profile. A logarithmic age-depth profile can already be fitted (Meinardi 1994; Broers 2004a) using tritium measurements from two short monitoring screens above each other. The approximate age of water in a single screen can be estimated by de-convoluting a time-series of tritium measurements (Maloszewski and Zuber 1993).

^{3}H/^{3}He

In 1969, Tolstikhin and Kamenski (1969) suggested measuring both tritium and its decay-product ^{3}He. The age of groundwater (τ) can then be estimated based on the ratio between the two and the decay constant of tritium (λ = 0.05626 y^{-1}):

$$\tau = \lambda^{-1} \ln\left(\frac{^3He^*}{^3H} + 1\right) \qquad (1.1)$$

Twenty years later, the first applications of ^{3}H/^{3}He dating of groundwater were published (Takaoka and Mizutani 1987; Poreda *et al.* 1988; Schlosser *et al.* 1988). These showed that dating groundwater with ^{3}H/^{3}He requires separating the tritiogenic fraction of dissolved ^{3}He from the naturally occurring atmospheric equilibrium concentration. It appeared that besides the atmospheric equilibrium (Ozima and Podosek 2002) and tritium decay, two more sources of ^{3}He have to be distinguished: excess air (Heaton and Vogel 1981) and radiogenic ^{3}He from U/Th-decay (Schlosser *et al.* 1989). Separating the tritiogenic fraction requires the simultaneous measurement of ^{3}He, ^{4}He and Ne, and preferably also the heavier noble gases Ar, Kr and Xe for a more accurate separation. Several approaches (Stute *et al.* 1995; Aeschbach-Hertig *et al.* 1999; Aeschbach-Hertig *et al.* 2000) have been developed for analyzing noble gas data and separating tritiogenic ^{3}He.

Transient tracers CFCs and SF_6

Several man-made chemicals can also be used to date groundwater. The increased use of chlorofluorocarbons (CFCs) in refrigerators and as propeller gas since the 1950s raised their concentrations in the atmosphere (Walker *et al.* 2000). Similarly, the increased use of sulfur-

hexafluoride (SF_6) as electric insulator and blanket gas since 1970 resulted in an increasing atmospheric SF_6 concentration (Maiss and Brenninkmeijer 1998). Because CFCs and SF_6 are soluble in water, their concentrations in groundwater increased as well. Measuring their concentrations in groundwater and relating the measured concentrations (or ratios of concentrations) to reconstructions of atmospheric mixing ratios has successfully been used to date groundwater (Thompson and Hayes 1979; Busenberg and Plummer 1992; Dunkle *et al.* 1993; Oster *et al.* 1996; Busenberg and Plummer 2000). Because these tracers rely on their changing concentrations in the atmosphere, CFCs and SF_6 are referred to as transient tracers. Recently, trifluoromethyl sulfurpentafluoride (SF_5CF_3) was added to the list of transient tracers (Busenberg and Plummer 2008).

Limitations of groundwater age tracers

$^3H/^3He$ seems to be an ideal tracer to determine the age of groundwater, because it relies on the radioactive decay of ^3H that is actually part of the water molecule. The decay product is a noble gas that is transported conservatively in groundwater under normal circumstances. However, several studies have revealed weaknesses of the $^3H/^3He$ dating method. Tritiogenic ^3He must be confined below the water table. The accuracy of the $^3H/^3He$ dating method depends on the ability of the saturated zone to retain ^3He against diffusive loss at the water table (Solomon *et al.* 1992). Also, the concentrations of ^3H in recharging groundwater have been highly variable. Mixing of older and younger water by dispersion and diffusion may result in apparent ages that are different from the actual mean groundwater age (Solomon and Sudicky 1991; Solomon *et al.* 1993; Engesgaard *et al.* 1996; LaBolle *et al.* 2006). Also, in dual-domain groundwater systems (LaBolle *et al.* 2006; Neumann *et al.* 2008), like stagnant water in aquitards or the matrix-component of dual porosity systems, diffusive transport of ^3H and ^3He between the two domains can result in differences between the apparent and true mean age.

By deriving the age directly from the concentrations of tracers, these tracers are very sensitive to contamination, local sources or degradation. There are early reports on elevated CFC concentrations near urban areas (Oster *et al.* 1996) or elevated SF_6 concentrations near industrial or urban areas (Santella *et al.* 2003; Santella *et al.* 2008). SF_6 has recently been reported to have a terrigenic source as well (Koh *et al.* 2007). CFCs and SF_6 are assumed to be chemically inert so their concentrations in groundwater are not expected to change do to geochemical reactions with the subsurface. However, several studies have reported the degradation of CFCs in anoxic environments (Lovley and Woodward 1992; Happell *et al.* 2003; Hinsby *et al.* 2007; Sebol *et al.* 2007; Horneman *et al.* 2008).

Degassing

All these groundwater age tracers rely on conservative transport of dissolved gases in groundwater. However, these gases are only transported conservatively if they do not come in contact with a gas phase below the water table (Fry *et al.* 1995). If a gas phase forms below the groundwater table, the dissolved tracer gases re-partition between the gas and water phases. The result is a decrease of the concentrations of the tracer gases in the water phase. This process is referred to as degassing.

There is an expanding body of literature describing depleted tracer gas concentrations in groundwater as the result of degassing (Solomon *et al.* 1992; Baedecker *et al.* 1993; Revesz *et al.* 1995; Blicher-Mathiesen *et al.* 1998; Van Breukelen *et al.* 2003; Purtschert *et al.* 2004; Amos *et al.*

2005; Fortuin and Willemsen 2005; McNab *et al.* 2007). For example, denitrification of nitrate to N_2 may form a gas phase below the groundwater table (Blicher-Mathiesen *et al.* 1998). Degassing by denitrification has also been supported by laboratory experiments (Istok *et al.* 2007).
The question is whether degassed groundwater can still be dated using these tracers. This requires understanding the transport of these tracers through both the gas and water phase. Both laboratory experiments (Gupta *et al.* 1994; Holocher *et al.* 2002; Amos and Mayer 2006b; Balcke *et al.* 2007) and numerical model simulations (Holocher *et al.* 2003; Amos and Mayer 2006a; Balcke *et al.* 2007) have provided insight in the partitioning behavior of trace gases in the presence of a gas phase.

1.5.4 Modeling groundwater age

The concept of groundwater age has also been studied using a variety of models, ranging from simple analytical formulations to complex numerical distributed 3D transport models. For example, groundwater flow in recharge areas with little superficial drainage can be approximated by two-dimensional vertical flow towards a fully penetrating drain. For this situation an analytical formula for the distribution of groundwater age can be used (Vogel 1967). A more elaborate approach is the manual or numerical construction of a groundwater flow net (Van Elburg *et al.* 1992), from which groundwater ages can be derived. Since the development of numerical models of groundwater flow, these have also been used to simulate the distribution of groundwater age in aquifers. There are three methods to simulate groundwater ages in numerical models (Castro and Goblet 2005): particle tracking, the breakthrough of a block-front or direct age simulations.

Particle tracking
Fictional particles are released at the surface of the numerical model and their pathways are followed through the groundwater flow pattern in the model. Particle tracking relies on an analytical approximation of the groundwater flow pattern within rectangular model cells (Pollock 1988). This approximation makes it quick, but only advective transport is considered. Dispersion may be included by introducing a random-walk component (Weissmann *et al.* 2002; Salamon *et al.* 2006).The weak point of particle tracking approach is the presence of weak sink cells in the numerical model. Sink cells, containing abstraction wells or drainage features, are "weak" if they capture only a part of the water flowing into the model cell. Weak sinks pose a problem because an analytical approximation of the flow pattern does not exist for weak sinks and it is undetermined whether a particle reaching a weak sink cell should be discharged by the sink or allowed to pass the cell. This adds an element of uncertainty to the age results of a particle tracking analysis.

Breakthrough of a block-front in a transport model
Simulations of the transport of a fictional tracer by advective groundwater flow, diffusion and dispersion can be used to calculate the groundwater age in the model. The tracer is applied to the surface of the model (as if it were dissolved in precipitation) from a certain time onward. The arrival time of the tracer at a location in the model represents the age of groundwater at that location. Because of mixing, hydrodynamic and numerical dispersion, the arrival of the tracer may be smoothened. The spread of groundwater age as the result of mixing can be derived from the shape of the breakthrough curve.

Direct simulation of groundwater age
Groundwater age can be simulated directly as the concentration of a solute "age" which concentration is measured in units of time (Goode 1996; Engesgaard and Molson 1998). This fictional solute has a zeroth-order source: each year the concentration of age increases with one year. The benefit of this method is that it provides a modeled age in each cell, rather than the break-through of a tracer which has to be analyzed to derive the age. The second benefit is that it could be used in transient simulations. Thirdly, the spread of groundwater age can be simulated simultaneously (Varni and Carrera 1998).

Groundwater age simulations have been applied in various ways. The direct comparison of tracer ages with modeled ages has been used as a target to calibrate the numerical model (Castro *et al.* 1998; Janssen *et al.* 2008). In relation to trends in groundwater quality, the results of groundwater age simulations indicate areas with young groundwater that are vulnerable to pollution (Broers and Van Geer 2005) or predict pollutant concentrations by combining groundwater age with the pollution history of the area (Kauffman *et al.* 2001; Zoellmann *et al.* 2001).

1.6 Specific research questions and thesis outline

The general research question formulated in relation to the aim, scope and focus of this thesis ("*What is the value of groundwater age in the detection of trends in groundwater quality?*") was elaborated through a series of sub-questions, which are answered in the individual chapters of this thesis. Most chapters have been published as articles in international peer-reviewed journals and have been included without modifications. Two lines of research are combined in this thesis: (1) investigating trends in groundwater quality in relation to groundwater ages and (2) determining groundwater age of sampled groundwater and in numerical models. The thesis consists of two parts. Each part deals with one line of research and consists of three chapters.

PART I: TRENDS IN GROUNDWATER QUALITY

Can we detect trends and demonstrate trend reversal in groundwater quality using groundwater age?
The measured concentrations of pollutants can be directly related to the time of recharge determined by $^{3}H/^{3}He$ groundwater dating. The time of recharge can then function as an objective basis for the aggregation of groundwater quality data of an entire groundwater body. The aggregated data can be analyzed for trends and trend reversal in groundwater quality. This method of trend detection is presented in Chapter 2.

Can we understand the trends of concentrations of reactive solutes using groundwater age?
The concentrations of reactive solutes can also be analyzed in relation to groundwater age, using the aggregation method presented in Chapter 2. This approach is used in Chapter 3, to investigate the hydrogeochemical processes controlling the transport of pollutants. The trends in measured concentrations were compared to the results of a 1D reactive numerical hydrogeochemical model, in order to understand the effects of chemical reactions on trends in groundwater quality.

Which method is best suitable for the detection of trends in groundwater quality given the characteristics of the available data, hydrogeological settings, and objectives?
The collaboration of the four research groups in work package TREND 2 formed the basis for a comparison of hands-on experience with different trend detection methods for groundwater quality. Chapter 4 presents a comparison of different methods for the detection of trends in groundwater quality in terms of prerequisites, costs, the system under study, the understanding of the system and the potential for extrapolation.

PART II: GROUNDWATER AGE

Can we date groundwater that is affected by geochemical reactions and subsequent degassing?
Denitrification of nitrate from agricultural pollution leads to the formation of gas bubbles below the water table. These bubbles cause "degassing" and affect the transport of the tracer gases that are used to determine the groundwater age. Chapter 5 presents a method to determine the groundwater age based on degassed groundwater.

What is the fate of N_2 bubbles in the subsurface and how accurate are tracer ages of degassed groundwater?
A two-phase numerical groundwater flow and transport model was used to investigate the behavior of a gas phase below the water table. To aim was to reproduce the measured concentrations of tracer gases. The model was also used to assess the accuracy of the method presented in Chapter 5. These results are presented in Chapter 6.

How can we derive accurate travel time distributions in regional scale models in order to predict trends in surface water quality?
The contribution of groundwater to surface water quality is related to the travel time distribution of discharging groundwater. Such a travel time distribution can be quickly calculated based on a particle tracking analysis in numerical groundwater flow models. However, so-called weak sinks in the flow model pose a problem to the particle tracking theory. Chapter 7 presents an objective method to calculate the travel time distribution, avoiding the problem of weak sinks.

The last chapter of this thesis (Chapter 8) summarizes the answers to the general research question and the six sub-questions and combines the conclusions of the individual chapters. These conclusions inspire new research questions, which are discussed in the final sections of the thesis.

PART I

TRENDS IN GROUNDWATER QUALITY

2 Demonstrating Trend Reversal of Groundwater Quality in Relation to Time of Recharge determined by $^{3}H/^{3}He$

Groundwater age dating reveals trends and trend reversal in groundwater quality

This chapter has been published as:
Ate Visser, Hans Peter Broers, Bas van der Grift and Marc F.P. Bierkens (2008) *Demonstrating Trend Reversal of Groundwater Quality in Relation to Time of Recharge determined by $^{3}H/^{3}He$*, Environmental Pollution 148(3): 797-807, doi:10.1016/j.envpol.2007.01.027

Abstract
Recent EU legislation is directed to reverse the upward trends in the concentrations of agricultural pollutants in groundwater. However, uncertainty of the groundwater travel time towards the screens of the groundwater quality monitoring networks complicates the demonstration of trend reversal. We investigated whether trend reversal can be demonstrated by relating concentrations of pollutants in groundwater to the time of recharge, instead of the time of sampling. To do so, we used the travel time to monitoring screens in sandy agricultural areas in the Netherlands, determined by $^{3}H/^{3}He$ groundwater dating. We observed that concentrations of conservative pollutants increased in groundwater recharged before 1985 and decreased after 1990. Thereby, we demonstrated trend reversal of groundwater quality. From this research we concluded that $^{3}H/^{3}He$ dating can be used to facilitate (re)interpretation of existing groundwater quality data. The presented approach is widely applicable in areas with unconsolidated granular aquifers and large agricultural pressures on groundwater resources.

2.1 Introduction

Over the last 40 years, the development of intensive livestock farming in sandy areas in Noord-Brabant (in the south of the Netherlands) has greatly increased the use of agricultural contaminants (e.g. nitrate). These areas are vulnerable to agricultural contamination, because groundwater and contaminants can easily reach deeper parts of the aquifer.

Following the awareness of diffuse groundwater contamination, legislation was put into effect in the Netherlands to reverse upward trends of contaminant concentrations in shallow groundwater and bring concentrations down below quality standards. Both the EU Nitrates Directive (EU 1991) and the Dutch Manure Law (1986) aim at reducing agricultural inputs to the

groundwater system. It has also lead to the establishment of national and regional groundwater quality monitoring networks in the Netherlands, with the purpose of quantifying the magnitude of the contamination, to identify significant upward trends in concentrations and to guide the implementation of manure reduction legislation (Van Duijvenbooden 1993; Broers 2002; Fraters *et al.* 2004). The time series of these Dutch monitoring networks are now long enough to detect trends and trend reversals in concentrations of contaminants in recent groundwater, caused by increasing or decreasing agricultural pollution. In fact, the detection of trends in groundwater quality and the demonstration of trend reversal are key aspects of the new EU Groundwater Directive, which is supposed to become enacted in 2006 (EU 2005). In line with the concepts used in the Groundwater Directive, we embraced the trend definition given by Loftis (Loftis *et al.* 1991a; 1996) who consider a temporal trend as a change in groundwater quality over a specific period in time, over a given region, which is related to land use or water quality management.

It is difficult to detect trends in the regional groundwater quality for a number of reasons (Broers and Van der Grift 2004): (1) the uncertainty of the travel time of groundwater and contaminants to the monitoring screens, (2) attenuating processes retarding the arrival of contaminants at the monitoring screen, such as sorption or chemical reactions with the subsurface, (3) noise caused by short term temporal variation of concentrations, for example as a result of crop rotation, and (4) variation of concentrations in separate monitoring screens as a result of large scale spatial variation in inputs. The Dutch monitoring network consists of standardized multi-level monitoring wells with fixed screens at specific depths. Other monitoring networks may have less uniform well completion with unknown depth of borehole penetration, which is an additional complicating factor for trend analysis. To detect trends in regional groundwater quality, we need to find a way to aggregate the data from individual monitoring screens to a regional scale and, at the same time, reduce the effects of the aforementioned sources of error.

Earlier work on trend analysis for agricultural pollution problems used different ways of aggregating monitoring data. Foster *et al.* (1982) aggregated data from UK aquifers and related the observed concentrations to tritium levels and land use change. Frapporti (1994) aggregated data using a water type approach and was able to detect upward trends in nitrate concentrations using data of the Dutch National Monitoring Network. Broers and van der Grift (2004) and Broers *et al.* (2004a) aggregated time series data using data from fixed depth, assuming a relatively homogeneous travel time distribution with groundwater age increasing with depth in the aquifer. Bronswijk en Prins (2001) directly related groundwater concentrations in the Netherlands to the time of recharge. However, all of these studies were based on groundwater age determinations based on tritium measurements (Robertson and Cherry 1989; Meinardi 1994). Laier (2004) successfully used CFC groundwater dating (Busenberg and Plummer 1992) to identify trends in individual monitoring wells.

In this study, we applied an alternative approach to trend analysis that is promising for the aggregation of time series in individual monitoring points to trends that represent larger areas or groundwater bodies. The approach is based on relating observed concentrations of contaminants in groundwater to the time of recharge of the sampled groundwater. As a check for consistency, we also reconstructed the historical concentrations of contaminants in recharging groundwater in agricultural recharge areas of the province of Noord-Brabant based on statistical data of atmospheric deposition, manure and fertilizer use and crop harvesting. This reconstruction of historical concentrations was compared with the recharge concentrations obtained from groundwater dating, leading to two independent assessments of possible trend reversal.

We analyzed the obtained relation between concentration and recharge year to (1) demonstrate a trend reversal in groundwater quality, and (2) to correlate the concentration – recharge year relation to the historical concentrations of agricultural contamination in recharging groundwater.

2.2 Methods

2.2.1 Study area and data

Noord-Brabant is one of the areas in Europe which is most affected by agricultural pollution, because intensive livestock farming in the area produces a large surplus of manure. Agricultural land covers 62% of the province of Noord-Brabant, which lies in the south of the Netherlands and has a total area of 5100 km². The agricultural area of the province of Noord-Brabant is vulnerable to diffuse groundwater pollution with nitrate because groundwater and contaminants can easily reach deeper parts of the aquifer. The subsurface consists of fluvial unconsolidated sand and gravel deposits from the Meuse River, overlain by a 2-30 m thick cover of Middle- and Upper-Pleistocene fluvio-periglacial and aeolian deposits consisting of fine sands and loam. In some areas pyrite occurs in the subsurface (Broers 2004b). Nitrate reduction by pyrite oxidation is described by the following reaction (Postma *et al.* 1991):

$$5\,FeS_2 + 14\,NO_3^- + 4\,H^+ \rightarrow 5\,Fe^{2+} + 10\,SO_4^{2-} + 2\,H_2O + 7\,N_2 \qquad (2.1)$$

Noord-Brabant is a relatively flat area with altitudes ranging from 0 m above Mean Sea Level (MSL) in the north and west to 30 m above MSL in the southeast. Groundwater tables are generally shallow, usually within 1-5 meters below the surface. A natural network of brooks, which developed in equilibrium with a shallow groundwater table, drained the area before 1900. To allow for agricultural use of the poorly drained areas, the natural drainage was artificially extended during the 20th century, resulting in a dense network of ditches, drains and small watercourses.

The geohydrological situation was mapped to identify homogeneous recharge areas for the design of the groundwater quality network of Noord-Brabant (Broers 2002). Homogeneous

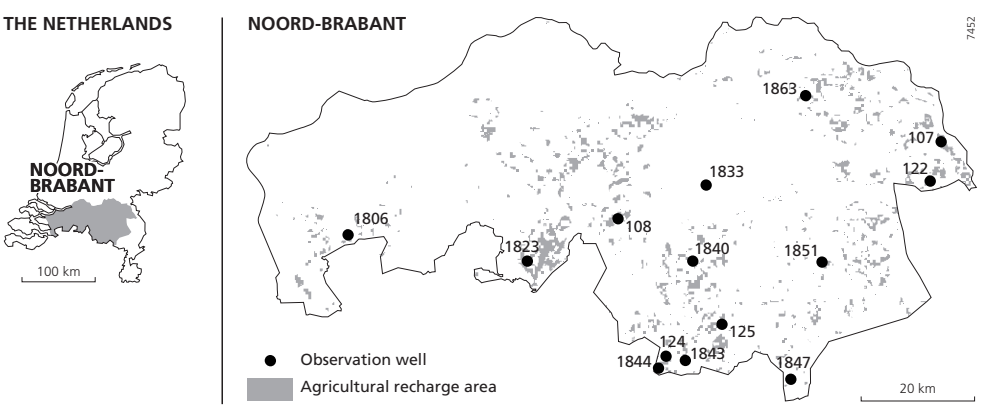

Figure 2.1 Locations of 14 selected wells in agricultural recharge areas.

recharge areas lack a superficial drainage network; have relatively deep groundwater levels, relatively

permeable soils and a relatively high topographical position. Monitoring wells were placed within the largest of the homogeneous areas, using stratified sampling (Broers and Van der Grift 2004).

We selected the 14 monitoring wells in recharge areas (Figure 2.1), such that the land use in the catchment area of each selected monitoring well was intensive livestock farming: mixed land use of mainly grassland and maize land. The wells consist of purpose built nested piezometers with a diameter of 2 inch and a screen length of 2 meters at a depth of about 8 and 25 meters below surface (Van Duijvenbooden 1993; Broers 2002). Three wells had an additional screen at about 4 meters below surface. The locations of the 31 screens we used are listed in Table 2.1. Measurements of field parameters (pH, EC and dissolved oxygen), concentrations of major cations (Na, K, Ca, Mg, Fe, Al and NH4), anions (Cl, NO_3, SO_4, HCO_3 and PO_4) and trace

Table 2.1 Well locations, screen depths and $^3H/^3He$ travel times

Location					^3H [TU]	$^3He^*$ [TU]	Travel time [years]
Well Number	Depth [m]	Screen Number	North deg°mm'ss"	East deg°mm'ss"			
107	7	1	51°37'52"	5°57'38"	7.9	5.7	10
107	24	3	"	"	11.2	36.5	26
108	8	1	51°30'38"	5°08'02"	10.1	4.8	7
108	24	3	"	"	14.3	66.2	31
122	9	1	51°34'10"	5°55'54"	9.2	3.7	6
122	24	3	"	"	8.5	22.4	23
124	8	1	51°17'33"	5°15'32"	8.6	4.8	8
124	26	3	"	"	8.4	7.6	11
125	12	1	51°20'33"	5°24'01"	9.7	10.5	13
125	23	3	"	"	10.6	32.0	25
1806	5	1	51°28'54"	4°26'59"	9.1	0.9	2
1806	23	3	"	"	12.4	28.9	21
1823	8	1	51°26'32"	4°54'22"	8.8	3.9	6
1823	18	3	"	"	10.4	10.3	12
1833	8	1	51°33'52"	5°21'31"	9.6	13.7	16
1833	19	3	"	"	14.2	118.9	40
1840	10	2	51°26'39"	5°19'44"	9.6	4.9	7
1840	24	4	"	"	8.9	37.2	29
1843	3.5	1	51°17'06"	5°18'21"	8.6	0.7	1
1843	8	2	"	"	9.8	2.3	4
1843	23	4	"	"	10.9	68.5	35
1844	4.5	1	51°16'17"	5°14'35"	9.3	1.3	2
1844	8	2	"	"	9.2	2.1	4
1844	23	4	"	"	12.6	36.4	24
1847	8	1	51°15'22"	5°34'27"	8.3	1.8	4
1847	24	3	"	"	15.4	64.1	29
1851	9	1	51°26'31"	5°39'14"	10.0	32.7	26
1851	23	3	"	"	21.6	129.3	35
1863	3.5	1	51°42'20"	5°36'49"	10.2	2.2	3
1863	10	2	"	"	15.7	67.1	30
1863	22	4	"	"	11.3	72.4	36

metals (i.e. Cd, Cu, Ni, and Zn) are collected annually as part of the national or provincial monitoring effort. For this paper, we have applied our method for trend demonstration to *nitrate* and *potassium*, and two additional chemical indicators: *sum of cations* and *oxidation capacity*. As mentioned before, nitrate can be reduced by pyrite in the subsurface, and downward transport of agricultural potassium is retarded compared to conservative chloride due to cation-exchange (Griffioen 2001). The latter two composite chemical indicators are transported conservatively under most circumstances (Broers and Van der Grift 2004).

The *sum of cations* is useful as a conditionally conservative indicator when cation-exchange processes dominate the transport of the cations and mineral dissolution does not occur. Moreover, the sum of cations is an indicator of the total load of solutes in the groundwater.
The *oxidation capacity* is defined as the weighted sum of molar concentrations of NO_3 and SO_4 after Postma *et al.*(1991):

$$OXC = 5 * [NO_3] + 7 * [SO_4^{2-}] \quad (2.2)$$

OXC behaves conservatively during the process of nitrate reduction by pyrite oxidation assuming that no denitrification by organic matter occurs below the groundwater table. We assumed that sulfate reduction does not occur at relevant depths in these aquifers, based on Broers and Buijs (1997) who only found significant amounts of H_2S which indicate an ongoing process of sulfate reduction in the deepest parts of the aquifer, deep below the Fe/NO_3 redox cline.

2.2.2 Groundwater age dating

In this study, we used $^3H/^3He$ groundwater dating (Tolstikhin and Kamenski 1969; Schlosser *et al.* 1988) to determine the travel time of groundwater to the monitoring screen. $^3H/^3He$ groundwater dating is based on the radioactive decay of tritium and the containment of the decay product ^3He in groundwater. $^3H/^3He$ directly yields a travel time and can be applied to a single sample, whereas ^3H alone requires a depth profile to locate the ^3H-bomb peak (Schlosser *et al.* 1988). Groundwater travel times were determined from $^3H/^3He$ samples that we collected in 2001 and 2005 and measured by the Bremen Mass Spectrometric Facility for the Measurement of Helium Isotopes, Neon, and Tritium in Water (Sültenfuß *et al.* 2004). The groundwater travel times were calculated from the ratio between tritiogenic helium and tritium (Table 2.1) as (Tolstikhin and Kamenski 1969):

$$\tau = \lambda^{-1} \ln\left(\frac{^3He^*}{^3H} + 1\right) \quad (2.3)$$

with groundwater travel time (τ), tritium decay constant (λ) and measured tritium (^3H) and tritiogenic helium ($^3He^*$) concentrations in Tritium Units (TU). 1 TU represents a ratio of 1 atom of tritium per 10^{18} atoms of hydrogen and corresponds to 2.488×10^{-12} cm^3 STP ^3He or 1.11×10^{-16} moles of ^3He per kg water: 1 TU of ^3H will decay to 1 TU of ^3He. The calculation of travel times is discussed in detail in Chapter 5.

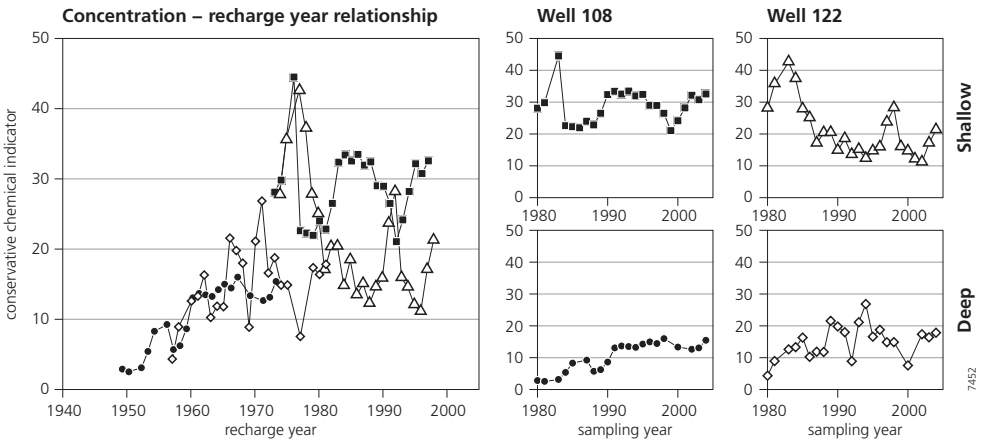

Figure 2.2 The concentrations of a conservative chemical indicator (OXC) sampled from the shallow (8m) and deep (24m) screens of observation wells 108 and 122 (right) plotted at the recharge year of the sampled groundwater (left). The result is the *concentration – recharge year relationship*, from which a clear trend can be observed that was not visible in the individual time series.

2.2.3 Transposition of time series to time of recharge: constructing the concentration -recharge year relationship

We used the $^{3}H/^{3}He$ travel times to relate the observed concentration time series in the monitoring screens directly to the time of recharge. Thus we obtained a direct relation between all observed concentrations and a single independent variable: the time of recharge. With this relation, we aggregated the time series of concentrations from the national and regional monitoring network in the province of Noord-Brabant, the Netherlands.

As an example of how this works, we consider the time series of a conservative chemical indicator (OXC), collected from wells 108 and 122 of the national monitoring network. (Figure 2.2, right) Large variation exists in the individual time series and no clear trends can be observed. However, knowing the travel time to each screen, we can relate the observed concentration to the recharge year of the groundwater sample. (Figure 2.2, left) In this figure, an overall upward trend can be observed in groundwater that recharged before 1980. As such, groundwater travel time is a key variable to aggregate observed concentrations in individual monitoring screens.

We analyzed the resulting *concentration – recharge year* relationship in three ways. Firstly, we used a LOWESS smooth (Cleveland 1979) to aggregate the median trend in all observations. The span parameter of the LOWESS smooth was 0.5 in all figures in this paper. Two extra LOWESS smooths were calculated through the residuals above and below the first LOWESS smooth. These are the upper and lower quartile of the conditional distribution of the concentrations as a function of the recharge year (Helsel and Hirsch 1995). They indicate the spread and symmetry of the distribution of concentrations around the middle LOWESS smooth; fifty percent of the measured data falls between the upper and lower smooth.

Secondly, we correlated the three LOWESS smooths through all observations to the reconstructed historical concentrations in recharging groundwater, which were based on atmospheric deposition and manure statistics. A good correlation between reconstructed

historical concentrations and the observed concentrations would indicate that future concentrations are well predictable.
Thirdly, to significantly determine trend reversal, two simple linear regression lines were fitted, one through all concentration data with a recharge time of before 1980 ("old water"), and one through all concentration data with a recharge time of after 1990 ("young water"). Trend reversal was considered significant if the regression line changed from significantly upward in "old water" to significantly downward in "young water".

2.2.4 Reconstruction of historical concentrations in recharging groundwater

To quantify the historical inputs, we constructed an annual mineral balance for the root zone of agricultural recharge areas in the province of Noord-Brabant. We considered four sources (*atmospheric deposition, animal manure, artificial fertilizer* and *lime*); and two sinks (*crop uptake* and *denitrification in the unsaturated zone*). We assumed that the surplus of this balance leaches to the groundwater. For a detailed description of the mineral balance we refer to the Appendix.

A catchment to basin scale approach demands an averaged input curve for all agricultural land in a specific area, instead of the detailed information for individual land use types. In this case, we have constructed the aggregated input curve for the recharge areas with intensive livestock farming – where more maize is present than on average in the province – to compare it to the measurements of groundwater quality in these vulnerable areas. To do so, we weighted the net deposited loads for each land use type by the relative area covered by that land use type in agricultural recharge areas.

We calculated the concentrations in recharging groundwater by dividing the annual mineral surplus by the annual precipitation surplus since 1970. We did not consider using annual precipitation surpluses to calculate annual concentrations, because the reaction of shallow groundwater concentration on varying precipitation surplus is very non-linear. The counteracting effects of dilution and increased leaching at increased surplus depend heavily on processes in the unsaturated zone in previous years.

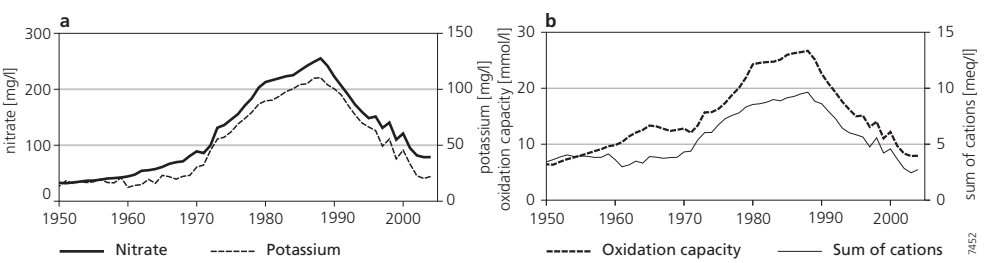

Figure 2.3 Reconstructed historical concentrations in recharging groundwater based on the annual mineral balance (Appendix) of nitrogen and potassium (a), and conservative chemical indicators (b). All indicators show a peak in the late 1980's when the use of manure was at its maximum.

2.3 Results

2.3.1 Reconstructed historical concentrations in recharging groundwater

The most important change in land use was the introduction of maize in 1970 in the Netherlands. Maize is the only crop on which an unlimited amount of manure and fertilizer can be applied. The introduction of maize also incited the development of intensive livestock farming in Noord-Brabant. We plotted the reconstructed historical concentrations in recharging groundwater in Figure 2.3. We found that the historical concentrations in recharging groundwater of nitrate

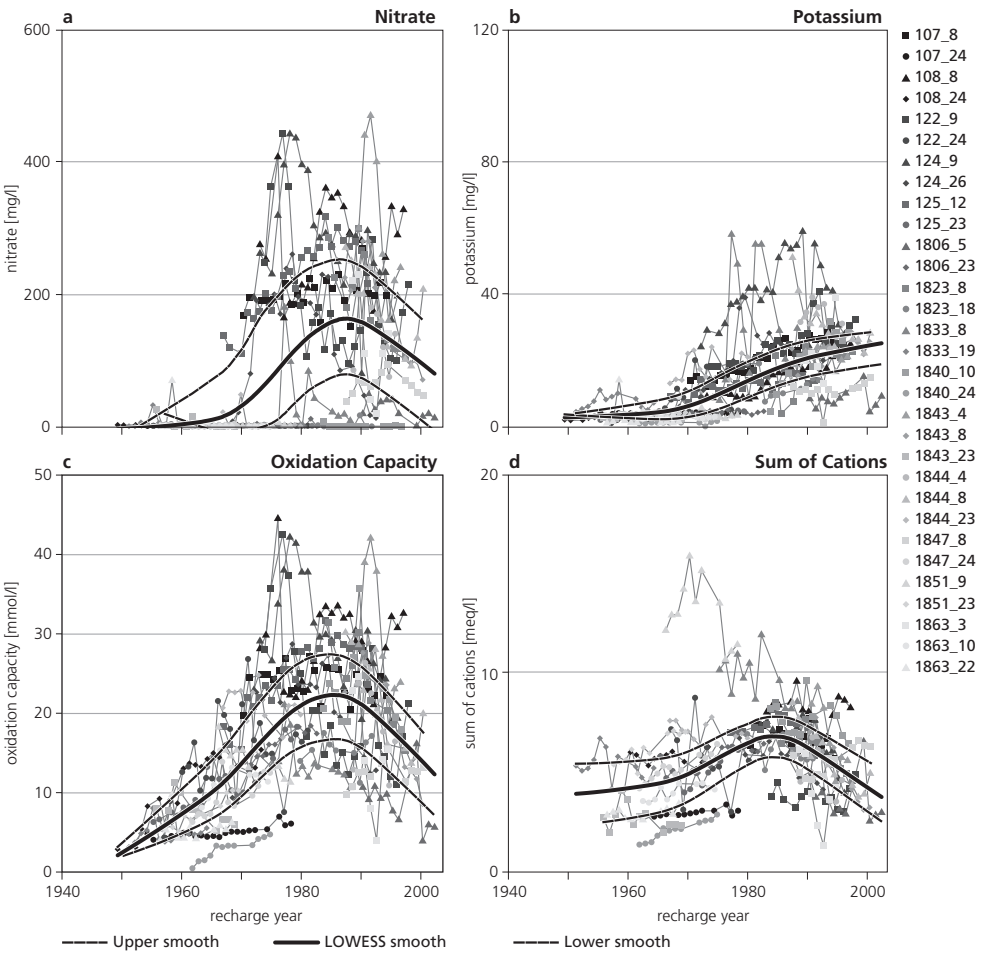

Figure 2.4 The observed *concentration – recharge year relationship* of nitrate (a), potassium (b), oxidation capacity (c) and sum of cations (d). Measured concentrations are plotted in the year in which the sampled groundwater recharged, considering the groundwater travel time determined with $^{3}H/^{3}He$. A LOWESS smooth (black line) is used to show the overall trend in these data. Dashed black lines indicate the upper and lower LOWESS smooths, which indicate the spread of concentration data around the middle LOWESS smooth.

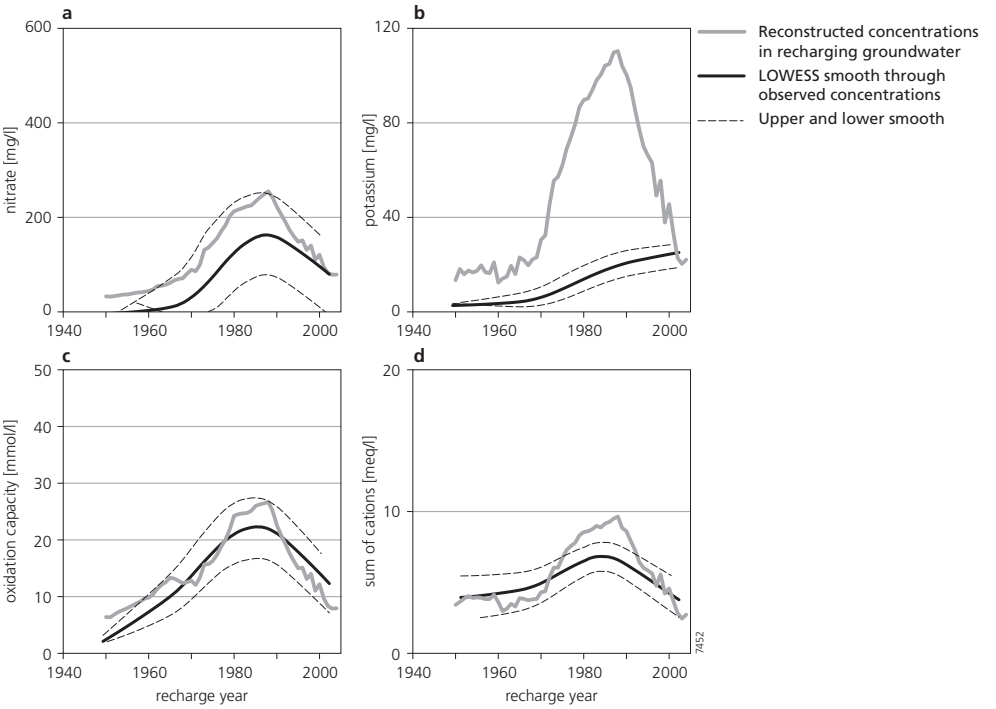

Figure 2.5 Comparison of the LOWESS smooth through the observed *concentration – recharge year relationship* (solid black line with dashed upper and l ower smooths) with reconstructed historical concentrations in recharging groundwater (grey line). Reactive substances (top) show large discrepancies with reconstructed concentrations, whereas conservative indicators (bottom) are consistent with the predicted trends.

and potassium (Figure 2.3a) and oxidation capacity and sum of cations (Figure 2.3b) increased between 1950 and the mid '80s as a result of increased application of manure and fertilizer. The highest reconstructed average nitrate concentration in recharging groundwater was over 250 mg/l in 1988. Concentrations decreased after 1990 as the result of the measures proscribed by the Dutch Manure Law (1986) and the EU Nitrates Directive (EU 1991) aimed at reducing the application of manure, causing a reversal of the upward trend in historical concentrations in recharging groundwater. This reconstruction was aimed at capturing the trends in concentrations, rather than yielding accurate predictions of concentrations at specific years. The consistent regional approach, rather than on the plot-scale, makes this reconstruction useful for comparison with regionally aggregated data of concentrations in groundwater.

2.3.2 Trends in observed aggregated concentrations

Figure 2.4 shows the concentration – recharge year plots for nitrate (a), potassium (b), oxidation capacity (c) and sum of cations (d). These figures include the data of 31 time series sampled from 2 or 3 depths in the 14 observation wells, plotted at the time of recharge determined by $^{3}H/^{3}He$. Individual time series show a large amount of temporal variation and a range of concentrations is present at every recharge year. We did not remove outliers, to show that this approach is

robust and rather insensitive to outliers. For example, two time series of sum of cations are clearly affected by calcite dissolution and could be considered outliers, because one of the underlying assumptions for sum of cations – no mineral dissolution – is not valid. Nevertheless, the LOWESS smooth is hardly affected by the two time series. So despite the large amount of variation, aggregating the trends using upper, middle and lower LOWESS smooths revealed distinct trends of the concentrations with time.

We observed that the aggregated concentrations of *oxidation capacity* and *sum of cations* increased towards a peak in the mid 1980s, and decreased in younger groundwater (Figure 2.4c and d). The individual measurements however showed a large variation around the LOWESS smooth. The upper and lower smooths indicate that 50% of the monitoring data is within a maximum bandwidth around the middle smooth of 10 mmol/l for oxidation capacity and 2 meq/l for sum of cations. Nevertheless, the upper and lower LOWESS smooths showed the same upward and downward trends as the middle LOWESS smooth.

Nitrate showed a similar pattern with a pronounced peak in 1985 and decreasing concentrations afterwards (Figure 2.4a). However, the nitrate trends were probably affected by the reactivity of nitrate with the subsurface. Many time series of nitrate concentration in older water showed consistently low values, probably caused by complete denitrification by pyrite oxidation or organic matter in the saturated zone. Again the middle LOWESS smooth showed an upward trend before 1980, but the spread was much wider, caused by the complete denitrification in some of the time series. A downward trend was also present in young groundwater.

Table 2.2 Statistics of the correlation between reconstructed historical concentrations and LOWESS smooth through observed concentrations of nitrate, potassium, oxidation capacity and sum of cations.

	nitrate			**potassium**		
	lower LOWESS smooth	**middle LOWESS smooth**	**upper LOWESS smooth**	**lower LOWESS smooth**	**middle LOWESS smooth**	**upper LOWESS smooth**
correlation coefficient *r*	0.89	0.88	0.98	-0.01	-0.02	0.38
significance	***	***	***	-	-	-
intercept	-42.95	16.72	86.37	12.30	17.85	15.25
slope	0.49	0.59	0.70	0.00	0.00	0.09
R^2	0.80	0.78	0.96	0.00	0.00	0.15
	oxidation capacity			**sum of cations**		
	lower LOWESS smooth	**middle LOWESS smooth**	**upper LOWESS smooth**	**lower LOWESS smooth**	**middle LOWESS smooth**	**upper LOWESS smooth**
correlation coefficient *r*	0.97	0.97	0.95	0.97	0.96	0.95
significance	***	***	***	***	***	***
intercept	4.05	8.01	11.96	1.07	2.25	4.07
slope	0.50	0.56	0.61	0.51	0.49	0.40
R^2	0.93	0.95	0.90	0.95	0.92	0.91

(Significance of t-test that Pearson's product-moment correlation coefficient = 0 (P>|t|); <0.001: ***; <0.005: **; <0.01: *; -)

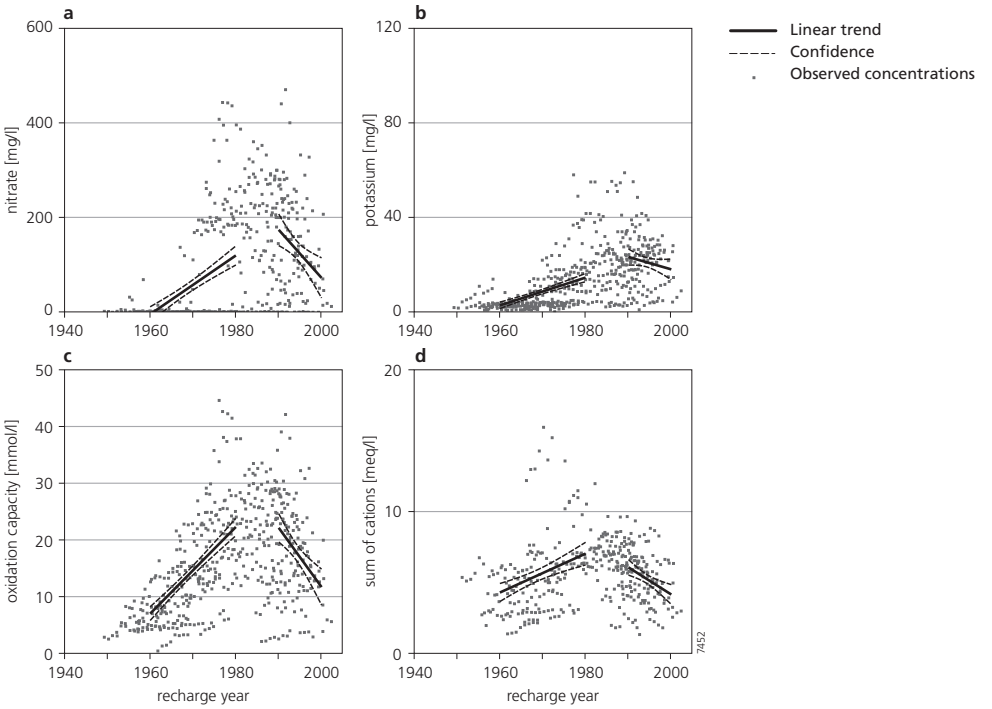

Figure 2.6 Linear trends through *concentration – recharge year* data show significant trend reversal between 1980 and 1990 for nitrate (a), oxidation capacity (c) and sum of cations (d). Potassium (b) showed no significant trend reversal.

Potassium concentrations showed completely different trends (Figure 2.4b). The upper, middle and lower LOWESS smooth of potassium were constantly increasing, even in young groundwater, but this trend was not yet reversed. Downward transport of agricultural potassium is retarded (compared to conservative chemicals) due to cation-exchange (Griffioen 2001). Concentrations slowly increased with recharge year, and the maximum has not been reached. This is in agreement with reactive transport modeling of potassium by Broers and Van der Grift (2004) who showed that the potassium front slowly moves downward and that the maximum concentrations have not yet reached the uppermost monitoring screens.

To compare the reconstructed historical concentrations with the LOWESS smooths through the observed concentration – recharge year relationship, we plotted both in Figure 2.5. The trends in the LOWESS smooth through the observed concentration recharge year relationship agreed well with the trends in the reconstructed historical concentrations in recharging groundwater of oxidation capacity and sum of cations (Figure 2.5): upward before 1980, downward after 1990. In both cases, the reconstruction did overestimate the peak in observed concentrations, but this did not alter the agreement between the trends.

The reconstructed historical concentrations of nitrate in recharging groundwater structurally overestimated the LOWESS smooth through observed concentrations. This was caused by the removal of nitrate by denitrification in the saturated zone, which affected some of the time series. However, the median aggregated nitrate trend showed trend reversal around 1985, similar to

conservative chemical indicators. The close resemblance between the reconstructed and observed trends in OXC concentration indicates that OXC acts as a conservative chemical indicator in our situation. From that we derive that our assumption (that the main mechanism of nitrate removal is the oxidation of pyrite) is valid here. Earlier studies showed the presence of abundant pyrite in the Noord-Brabant subsoil (Broers 2002, 2004b; Broers and Van der Grift 2004) and the removal of nitrate by pyrite (Postma *et al.* 1991).

The reconstructed potassium concentrations largely overestimated the observed concentrations. Although the reconstructed concentrations showed a trend reversal in the '80s, the aggregated median trend was increasing slowly into the 1990s. These results are in agreement with the results of Broers and Van der Grift (2004) who modeled the retarding effect of cation exchange between potassium, and calcium and magnesium described by Griffioen (2001).

We found an excellent correlation between the reconstructed historical concentrations in recharging groundwater and the middle LOWESS smooth through the *observed concentration – recharge year relationship*. Pearson's product-moment correlation coefficients (*r*) were as high as 0.97, and 0.96 for *oxidation capacity* and *sum of cations* respectively. These correlations were all significant at the 0.001-level. However, the relationships were not proportional. The regression lines had a considerable positive intercept and a slope angle of less than 1 (Table 2.2). This indicated that the reconstructed concentrations overestimated high concentrations and underestimated lower concentrations, as seen in Figure 2.5. The high and significant correlation coefficients for oxidation capacity and sum of cations show that aggregation of multiple time series indeed reduces spatial and temporal variations.

2.3.3 Trend reversal

By fitting linear regression lines through the concentration – recharge year data (Figure 2.6), we found significant upward trends in the concentrations of *nitrate*, *oxidation capacity* and *sum of cations* in "old water". These trends were reversed to significant downward trends in "young water" (Table 2.3) and therefore trend reversal is significant for conditionally conservative chemical indicators (*oxidation capacity* and *sum of cations*). Trend reversal is also significantly demonstrated for nitrate, despite the fact that nitrate removal by pyrite oxidation affected the absolute concentrations of nitrate. We found no significant trend in the concentrations of potassium in "young water", so trend reversal was not demonstrated for potassium. This is caused by its sorption to the subsurface, illustrating the behavior of reactive substances.

Table 2.3 Statistics of linear regression lines through concentration – recharge year data show significant trend reversal for nitrate, oxidation capacity and sum of cations.

	nitrate		**potassium**		**oxidation capacity**		**sum of cations**	
period	<1980	>1990	<1980	>1990	<1980	>1990	<1980	>1990
slope	6.32	-9.17	0.59	-0.53	0.77	-1.01	0.14	-0.21
significance	***	**	***	-	***	***	***	***

(Significance of t-test that slope = 0 (P>|t|); <0.001: ***; <0.005: **; <0.01: *; -)

2.4 Discussion and conclusions

We demonstrated trend reversal by relating the observed concentrations in groundwater to the time of recharge determined by $^{3}H/^{3}He$ dating. In this study, we aggregated all time series in agricultural recharge areas in the province of Noord-Brabant. With this approach we removed three of the four aforementioned difficulties with trend detection: (1) groundwater dating removes the variation in travel time towards the monitoring screen, and aggregation averages out both (3) short-term variations and (4) spatial variations. Attenuating and retarding processes that affect the arrival of contaminants at the monitoring screen (2) were partly removed by choosing two chemically conservative indicators, such as oxidation capacity and sum of cations to demonstrate trend reversal.

The advantages of relating time-series of groundwater quality to their time of recharge are twofold: (a) every time series provides information over a range of recharge years, and (b) data of multiple time series is available for each recharge year. Existing time series can thus be aggregated efficiently and trends are more easily observed from a limited number of time series, because spatial and temporal noise is reduced by aggregation. It can be applied to other (existing) datasets of groundwater quality, if the following conditions are plausible. 1) The travel times to the screens are constant. This is valid when no large-scale changes in the hydrological system take place. 2) The monitoring screen should be sufficiently short to be able to sample groundwater with distinct travel times. The screen should not sample a large range of travel times, which is usually the case with pumping wells or spring waters. 3) There exists a long-term trend in input concentrations that spans many years, which is caused by diffuse agricultural pollution. 4) Dispersion or mixing along the groundwater flow lines is limited. The character of the aquifer should not cause mixing of older and younger groundwater, which might be the case in aquifers with dual porosity. All these conditions are fulfilled in the sandy agricultural areas of Noord-Brabant, and probably in many unconsolidated granular aquifers, which are typically threatened by agricultural pollution.

We showed that groundwater dating is useful to demonstrate trends in groundwater quality. Our method – relating observed concentrations to the time of recharge – can be used to demonstrate trend reversal, to correlate observed concentrations to the historical inputs and to improve future predictions of groundwater quality. By aggregating a large number of time-series, the method is robust and insensitive to outliers, subsurface heterogeneity, and spatial and temporal variation in inputs.

2.A Appendix: Mineral Balance

We obtained estimates of *atmospheric deposition* from research done to quantify acidifying deposition by the Dutch National Institute for Public Health and the Environment (RIVM) and the Netherlands National Precipitation Chemistry Network (Buijsman 1989). RIVM publishes annual model estimates of average national wet and dry deposition of nitrogen (NOx and NHy) and sulphur (SOx) since 1980 (Bleeker and Erisman 1996) and estimates of deposition in the province of Noord-Brabant for selected years. For the period before 1980, we used estimates by Stuyfzand (1991), who used a linear model to estimate atmospheric nitrogen and sulphur deposition from emission data for the period 1920-1980, calibrated on the period 1983-1987.

We based estimates of cation deposition on measurements of station 231 of the Dutch National Precipitation Chemistry Network (KNMI/RIVM, 1982-2001) located at the centre of Noord-Brabant. Data are available since 1978 (RIVM 1979-1981, 1986-1988, 1989-1995), and on the website of RIVM since 1992 (RIVM 2005). For the period before 1978, we used the average of the first five available years.

Because the application of manure and fertilizer depends on land use, we distinguished three land use categories: grass, arable land and maize. We obtained annual estimates of land use surface area for each category from the online database of Statistics Netherlands (CBS 2006).
Animal manure is the main contributor of most minerals leaching to groundwater in Noord-Brabant. Because the concentrations of minerals in manure are not the same for all kinds of livestock, we constructed a detailed manure mineral balance for the province of Noord-Brabant, differentiating between types of livestock. CBS published figures on animal manure production since 1950 (CBS 1976-1992). We obtained data from Statline (CBS 2006) for the period 1994 to present. The figures on manure production were specified for dairy cows, calves, pigs (for meat production), sows (with piglets) and poultry.

We used data from Van der Grift and Van Beek (1996) who assembled data of the concentrations of minerals in manure, published by Evers (2000). The composition of animal manure was assumed to be constant in time, except for concentrations of N, and K which are published annually by CBS since 1980 (N) or 1995 (K) (Van Eerdt 1999; CBS 2006)

We considered the manure requirements and limitations of grass, maize and crops on arable land, given by the Commission Fertilizing Grassland and Crops. (Hoeks 2002) We assumed all animal manure is applied to agricultural land in Noord-Brabant in four steps. The first step is the application of 4/10 of the total dairy cow manure production on grassland, representing the deposition during the grazing season. Secondly, additional manure is applied during the rest of the year up to an equivalent of 180 kg K_2O/ha/yr. The amount of K_2O in applied manure may not exceed 180 kg K_2O/ha/yr because higher loads can cause diseases in cattle. Thirdly, the remainder

Table 2.A1 Distribution of artificial fertilizers over national area of grassland, arable land and maize

Fertilizer type:	grassland	arable land	maize
Nitrogen	75%	25%	
Phosphor	30%	70%	
Potassium	20%	80%	

Table 2.A2 Concentrations of minerals in crops.

crop	N (%)	K (%)	Ca (%)	S (%)
grass	3.2	2.1	0.5	0.3
potatoes	0.3	0.02	0.02	0.03
sugar beets	0.5	0.03	0.1	0.05
wheat	2.3	0.2	0.2	0.3
maize	1.2	1.0	0.1	0.1

of the manure is applied to arable land to a maximum of 250 kg N/ha/yr, from the different sources in the following order: remaining dairy cow manure, calves manure, pigs manure, sows manure and poultry manure. The application of manure to arable land is limited to a maximum load of 250 kg N/ha/yr from animal manure because most crops – except for maize, which is treated separately – do not tolerate higher loads. Finally, the manure surplus left after applying manure to the grassland and arable land is applied to maize land. No limit applies to the amount of manure used on maize.

The nationally applied amounts of artificial fertilizers (since 1950 reported by the Agricultural Economical Institute LEI (2006)) were distributed over the total national area of grassland, arable land and maize following the distribution key table (Table 2.A1) published by CBS (1987). This national average of fertilizer application per unit area was converted to the amount of fertilizer applied in Noord-Brabant, by comparison with a study by Menke (1992), reporting fertilizer application for agricultural lands in Noord-Brabant for the years 1985 and 1990.

Van der Grift and Van Beek (1996) estimated the use of lime fertilizers since 1950. The Agricultural Economical Institute (LEI 2006) published the national use of lime fertilizers since 1975 online. We used the regional estimates of lime fertilizer application by Menke (1992) to calculate the lime fertilizer application in agricultural recharge areas in Noord-Brabant.

Summing the aforementioned contributions of atmospheric deposition, manure, fertilizer and lime yielded the gross deposited loads. We then subtracted crop uptake from deposited loads, to calculate the composition of the water leaching from the root zone. We obtained historical crop yield data from CBS and from Van der Grift and Van Beek (1996) and converted these to crop mineral uptake using average mineral concentrations in crops published by Evers (2000) (Table 2.A2). We assumed that on arable land the following three crops are used in equal and fixed proportions: potatoes, sugar beets and wheat.

We calculated nitrogen uptake by crops and denitrification losses in the unsaturated zone according to the Solute Prediction from Regional distributed Agricultural Deposition (SPREAD) model, developed by Kiwa (Beekman 1998).

The annual surplus of nutrients, cations and heavy metals deposited on the land surface since 1950, is calculated for each land use category (grassland, arable land and maize) as the sum of atmospheric deposition, manure, fertilizer and lime application minus the crop uptake and denitrification.

3 Trends in pollutant concentrations in relation to time of recharge and reactive transport at the groundwater body scale

This chapter has been published as:
Ate Visser, Hans Peter Broers, Ruth Heerdink and Marc.F.P. Bierkens (2009) *Trends in pollutant concentrations in relation to time of recharge and reactive transport at the groundwater body scale*, Journal of Hydrology, in press, doi: 10.1016/j.jhydrol.2009.02.008

Abstract

To quantify the threat of pollutants to present and future groundwater quality requires detecting trends in groundwater quality. We related the measured concentrations of pollutants from selected monitoring locations in the Sand Meuse groundwater body to the time of recharge determined by $^{3}H/^{3}He$ as a means to aggregate the measurements and detect trends that are significant for the entire groundwater body. The aim of this study was to (1) define under what conditions the concentrations of reactive solutes may be related to travel times; (2) identify solute specific trends; (3) assess which geochemical processes are responsible for these trends using a geochemical model (PHREEQC); and (4) distinguish between different types of trends.

The observed trends in the concentrations of Cl are solely the result of historical changes in chloride concentrations in recharging groundwater. Cation exchange influences the trends in the concentrations of K and Ca, and heavy metals, and to a lesser extent also Na and Mg. Trends in the concentrations of NO_3 and SO_4 are the combined result of changing recharge concentrations and the process of pyrite oxidation. Fe, As, Ni and Zn are released during pyrite oxidation and these trends are indirectly the result of changing land use practices.

We distinguish three types of trends in the concentrations of solutes related to time of recharge. These are the result of: (1) the anthropogenic trends in historical concentrations in recharging groundwater unaltered during conservative transport through the groundwater body, (2) anthropogenic trends in recharge concentrations altered by reactions during transport, and (3) geochemical reactions in the subsurface that are triggered by anthropogenic changes in the recharge concentrations of other solutes.

3.1 Introduction

Water resources are threatened by the introduction of pollutants (e.g. nitrate) in groundwater bodies. Pollutants leach from agricultural lands and are transported by groundwater flow, possibly

to points in the groundwater body that are vulnerable to such pollutants, such as drinking water supplies or groundwater dependent ecosystems. To quantify the threat of these pollutants to present and future groundwater quality and to protect groundwater from deterioration requires monitoring, detecting trends in groundwater quality and relating these trends to changes in land use or agricultural practices. Detecting trends in groundwater quality at the groundwater body scale is a challenging task because of (Broers and Van der Grift 2004):

- the long travel times of groundwater to the well screens;
- the obscuring, attenuating or retarding effect of physical and chemical processes on solute breakthrough;
- the spatial variability of contaminant concentrations in recharging groundwater, in hydrologic residence time, and in reactive properties of the aquifer sediments;
- the short-term natural temporal variability of groundwater composition at the monitored depths.

Detecting trends that are significant for the entire groundwater body requires the aggregation of either the concentration measurements from a number of monitoring locations or the aggregation of trends that are detected in individual monitoring locations. The EU Groundwater Directive (EU 2006) specifically asks for "the way in which the trend assessment from individual monitoring points within a body or a group of bodies of groundwater has contributed to identifying that those bodies are subject to a significant and sustained upward trend in concentration of any pollutant or a reversal of that trend". Trend detection as required by the GWD is dedicated to detect trends in the concentrations of pollutants resulting from anthropogenic sources and distinguish these from natural variation with an adequate level of confidence and precision (GWD, Annex V, art 2(a)(i)).

Groundwater dating has been applied as a tool for aggregating groundwater quality data and analyzing trends therein by relating the measured concentrations of pollutants to the time of recharge of the sampled groundwater (Böhlke and Denver 1995; MacDonald *et al.* 2003; Wassenaar *et al.* 2006; Burow *et al.* 2007; Tesoriero *et al.* 2007). The resulting concentration – travel time relationship can be linked directly to historical records of land use or agricultural practices. Recent publications presenting studies from the U.S. Geological Survey National Water-Quality Assessment program (NAWQA) in which concentrations are directly related to recharge time of groundwater conclude that groundwater travel times are invaluable to the detection of trends in existing groundwater quality data (Burow *et al.* 2008; Debrewer *et al.* 2008; Rosen and Lapham 2008; Rupert 2008; Saad 2008).

Relating solute concentrations to time of recharge was often limited to conservative solutes. The term conservative solutes is used here to indicate solutes that do not interact with the subsurface and are transported by groundwater flow without changes in concentration along the flow path due to degradation, sorption et cetera. Relating solute concentrations to recharge time should only carefully be applied to reactive solutes that may be subject to concentration changing processes (Tesoriero *et al.* 2007). If the measured concentrations have been changed by geochemical reactions, they no longer represent the historical recharge concentrations and may show trends that are different from the trends in agricultural practices. On the other hand, the differences between reconstructed and observed trends, in combination with concentration measurements of reaction products can provide information on the degradation rates of contaminants in aquifers (Burow *et al.* 2007; Tesoriero *et al.* 2007).

The aim of this study was to (1) define under what conditions the concentrations of reactive solutes may be related to travel times; (2) identify solute specific trends in concentrations in relation to recharge time; (3) assess how geochemical processes are responsible for the observed trends using a geochemical model; and (4) distinguish between different types of trends resulting from changing land use practices, reactive transport, or a combination of these factors.

This work combines two approaches of analyzing groundwater quality data: geochemical modeling of concentration profiles (e.g. Postma *et al.* 1991) and trend detection in relation to travel times (e.g. Chapter 2). Postma *et al*. (1991) aggregated concentration measurements of solutes related to nitrate induced pyrite oxidation from eight multilevel samplers along a flow line in an unconfined sandy aquifer in Denmark. The data were aggregated based on the depth of the sampler relative to the redoxcline. This depth aggregation was only possible because the vertical component of groundwater flow was practically constant. Geochemical modeling of nitrate and sulfate concentrations along the vertical component of groundwater flow confirmed that pyrite oxidation was the dominant process of nitrate removal in this aquifer.

This work further extends on the analysis of trends in the concentrations of solutes collected from the monitoring network in the unconfined sandy groundwater body Sand Meuse in the south of the Netherlands presented in Chapter 2 of this thesis, in which time-series of measured concentrations were related to the time of recharge determined by $^{3}H/^{3}He$ to remove variation in travel times of groundwater collected at the same depth. This variation of travel times was the result of the monitoring wells being placed far apart using a stratified random sampling strategy (Broers 2002) to represent the entire groundwater body with a limited number of wells. The concentrations of nitrate and potassium related to the time of recharge presented in Chapter 2 showed trends that appeared to have been altered by geochemical processes such as pyrite oxidation or cation exchange. To confirm whether these reactions are plausible causes for these trends, we used the 1D reactive transport model PHREEQC (Parkhurst and Appelo 1999).

3.2 Methods

3.2.1 Study area and data

We analyzed a selection of the dataset of solute concentrations collected since 1980 by the national groundwater monitoring program in the province of Noord-Brabant, the Netherlands. Noord-Brabant (5100 km^2) covers most of the Sand Meuse groundwater body in the south of the Netherlands. It is a flat area with altitudes ranging from mean sea level (MSL) in the north and west to 30 m above MSL in the southeast. The subsurface consists of fluvial unconsolidated sand and gravel deposits from the Meuse River, covered by 2-30 meters of Middle- and Upper-Pleistocene fluvio-periglacial and aeolian deposits consisting of fine sands and loam. The occurrence of pyrite in these sediments is thought to be the cause of nitrate reduction in this groundwater body (Broers 2004b). Groundwater tables are generally shallow, usually within 1-5 meters below the surface.

Today, Noord-Brabant is one of the areas which is most affected by agricultural pollution in Europe. Intensive livestock farming, now covering 62 % of the area, produces a large surplus of manure and the surplus of nitrogen applied to agricultural land exceeded 250 kg/ha/y. The surplus of nitrogen applied to agricultural land shows an upward trend until the late 1980s as the result of the intensification of agriculture, and a decreasing trend afterwards thanks to the Dutch

manure legislation (1986) and EU Nitrates Directive (EU 1991). Because of the vulnerability of Noord-Brabant to agricultural pollution, a groundwater quality monitoring network was installed consisting of nested piezometers with a diameter of 5 cm and a screen length of 2 meters at a depth of about 8 and 25 meters below surface (Van Duijvenbooden 1993; Broers 2002). Because the screens were limited in length, little mixing occurs during sampling and we may assume that piston flow transports pollutants between recharge and sampling. Therefore these wells sample groundwater with a distinct travel time. Measurements of field parameters (pH, electrical conductivity and dissolved oxygen), concentrations of major cations (Na, K, Ca, Mg, Fe, Al and NH_4), anions (Cl, NO_3, SO_4, HCO_3 and PO_4) and trace metals (As, Cd, Cu, Ni, and Zn) are collected annually as part of the national or provincial monitoring effort. Groundwater travel times at the monitoring screens have been determined by $^3H/^3He$ dating, as described in Chapter 5.

The focus of this study was a selection of 14 multilevel monitoring wells (34 screens in total) located in agricultural recharge areas (Figure 3.1a). These areas are homogeneous in land use history and geohydrological situation (Broers and Van der Grift 2004). Recharge areas lack a superficial drainage network; have relatively deep groundwater levels, relatively permeable soils and a relatively

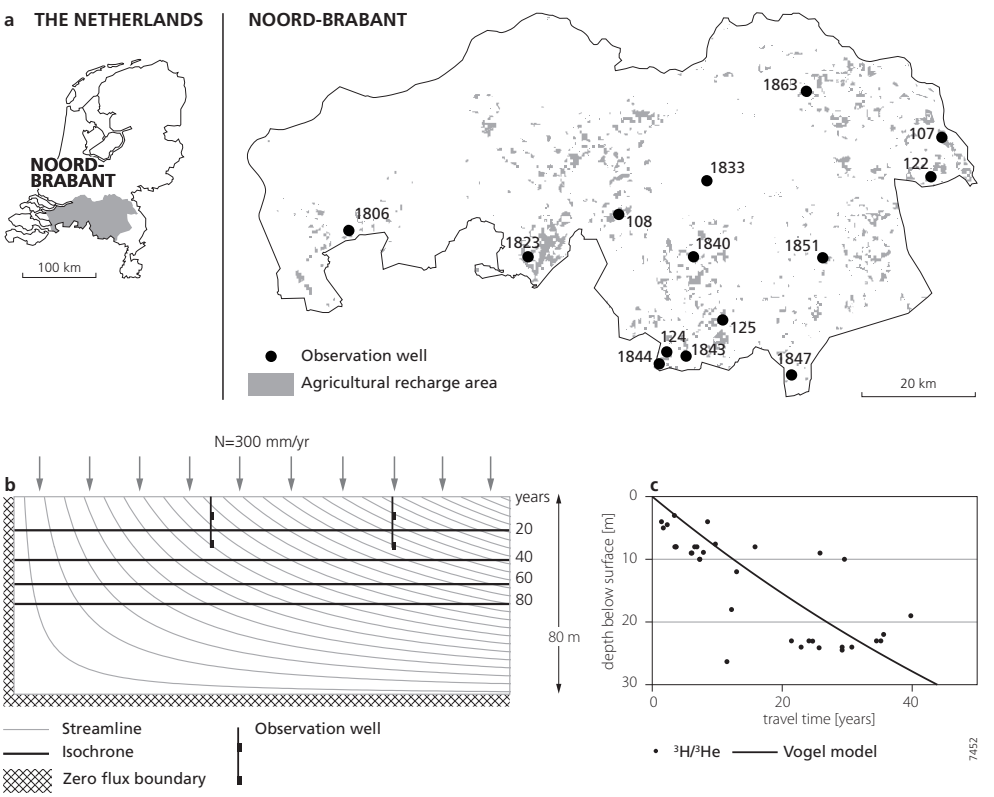

Figure 3.1 Location of monitoring wells and agricultural recharge areas in Noord-Brabant, The Netherlands (a), travel time distribution in 2D groundwater flow model (b) and apparent $^3H/^3He$ travel times in monitoring wells (c).

high topographical position. These areas are especially vulnerable to diffuse groundwater pollution because groundwater and thus contaminants can easily reach deeper parts of the aquifer.

Groundwater flow in homogeneous recharge areas can be simplified to a two-dimensional model (Vogel 1967) with impermeable west and bottom boundaries and a fully penetrating drain at the east boundary (Broers 2004a; Broers and Van der Grift 2004). Although groundwater flow is in both the horizontal and vertical directions, groundwater with the same travel time is found at the same depth (i.e. the isochrones are horizontal). Travel times of sampled groundwater increase logarithmically with depth, independent of the horizontal position (Figure 3.1b). If agricultural pollution is diffuse and homogeneous within the selected areas, the concentrations of non-reactive pollutants depend on travel time alone (Broers and Van Geer 2005). In a homogeneous system with horizontal isochrones, the concentrations of pollutants depend on the depth of sampling and vertical profiles of concentrations could be used to aggregated data from the agricultural recharge areas, similar to Postma *et al* (1991). However, $^{3}H/^{3}He$ dating of groundwater sampled from the selected wells showed that travel times in groundwater sampled from the same depth varied by as much as 20 years (Figure 3.1c). This variation of travel times is the reason to abandon depth profiles to aggregate concentrations, but instead relate the concentrations of solutes to the time of recharge. Because these areas are assumed to be homogeneous in land use history, concentrations of pollutants are determined by travel time, rather than by the horizontal location of the monitoring wells within the selected area of the groundwater body.

3.2.2 Analyzing trends in the concentrations of reactive solutes in relation to time of recharge

The recharge time of sampled groundwater determined by $^{3}H/^{3}He$ was used to aggregate the monitoring data from the 14 wells scattered across the Sand Meuse groundwater body. Measurements of pollutant concentrations were related directly to the estimated time of recharge of the groundwater sample and data from all 34 screens were plotted together in a single figure. This approach requires advective groundwater flow with little dispersion (piston-flow) to ensure that a groundwater sample has a distinct age, rather than being a mixture of groundwater with a range of ages. Additionally, the contamination history upstream of the monitoring wells should be similar. The character of the aquifer and the careful selection of "agricultural" monitoring wells ensured these conditions were fulfilled.

Because of the temporal variations in time-series of pollutant concentrations, it is beneficial to use as many measurements as possible in a single trend detection analysis. However, relating entire time-series of solutes to the time of recharge implicitly assumes conservative transport of that particular solute, as we will illustrate below. Therefore it is necessary to clearly define under which conditions, the measurements of reactive solute concentrations may be related to the time of recharge.

To illustrate the effect of reactive transport on measured solute concentrations in relation to time of recharge, we will show one example a conservative solute (chloride) and two examples of reactive solutes (nitrate and potassium). All three examples (Figure 3.2) plot the entire time-series of concentration measurements of chloride, nitrate and potassium, sampled between 1980 and 2004, from the shallow screen (12 m below surface) and deep screen (25 m below surface) of well 125. The groundwater age in the shallow screen was determined to be 13 years, and this time-series plotted between 1967 and 1991. The groundwater age in the deep screen was determined

to be 25 years, and this time-series plotted between 1955 and 1979. These two time-series, both covering the period between 1967 and 1979, are ideal to study the effect of reactive transport. The two screens do not sample from the exact same groundwater flow path. However, because the trends in recharge concentrations are assumed to be homogeneous within the catchment area of the monitoring well, both screens should show approximately the same trends, if a solute is transported conservatively.

Example 1: Conservative transport of chloride
The time-series of chloride concentrations from the shallow and deep screen largely overlap (Figure 3.2a). The measured concentrations are close to 1 mmol/l, and elevated concentrations are found in groundwater that has recharged before 1970. Unfortunately, neither time-series shows a clear typical anthropogenic trend. The overlapping time-series indicate that, assuming the same trends in recharge concentrations, no changes in chloride concentration occur along the groundwater flow path and chloride is transported conservatively between the water table and the monitoring screen. For such a conservative solute, it is valid to relate the entire time-series of concentrations to the time of recharge. Trends in this figure relate directly to the historical recharge concentrations. Additionally, because no changes in concentrations are expected along the flow path, the oldest measurements represent present-day concentrations of chloride in groundwater with an age of 49 years that recharged around 1955. Although it is beyond the scope of this study, this shows that the concentrations of solutes in samples collected in the past are suitable to be used to assess trends in groundwater that is older than the age of groundwater at the monitoring screen, but only if the solute is transported conservatively.

Example 2: Nitrate and denitrification
This example shows the effect of nitrate reduction at a redoxcline, located between the shallow and deep screen (Figure 3.2b). High and increasing concentrations of nitrate were found in the entire time-series collected from the shallow screen. The concentration measured in 2004 represents the recharge concentration in 1991, if no nitrate reduction takes place above the shallow screen. The high oxygen concentration (7.22 mg/l) measured in the shallow screen indicates oxic conditions where nitrate reduction is indeed unlikely. The groundwater sampled in 1980 recharged in 1967, and because nitrate reduction is unlikely upstream of the shallow screen, the concentration measured in this sample represents the recharge concentration in 1967.

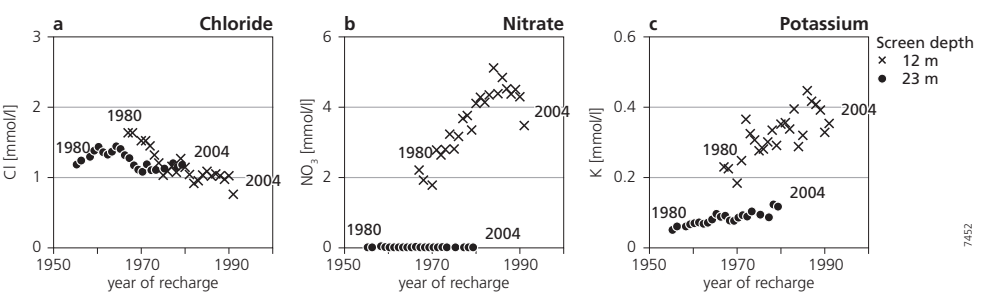

Figure 3.2 Time-series of the concentrations of chloride, nitrate and potassium measured at 12 and 23 m below the surface, plotted at the time of recharge of the sample.
Labels (1980 and 2004) indicate the year the sample was taken.

If nitrate were transported conservatively after passing the shallow screen, the concentration measured in the shallow screen in 1980, representing groundwater recharged in 1967, would be present in groundwater with an age of 37 years.

The time-series of nitrate concentrations sampled between 1980 and 2004 from the deep screen cover the recharge period 1955-1979 and all measured concentrations are below the detection limit. The absence of nitrate in the deep screen shows that nitrate is removed from groundwater between the upper and lower screen. This indicates the redoxcline is located between the shallow and deep screen. Given the horizontal redoxcline extending laterally, it is highly unlikely that groundwater with an age of 37 years still contains nitrate. Therefore the concentrations measured in the shallow screen in 1980 do not reflect the nitrate concentration in 37-year-old water in 2004 and it is not justified to extrapolate the trends found in this time-series to represent present-day trends in groundwater with an age between 13 and 37 years. Also, nitrate concentrations measured below the redoxcline do not reflect the concentrations at the time of recharge, because these have obviously been affected by nitrate reduction.

This shows that care should be taken when relating entire time-series to the time of recharge. The entire time-series related to time of recharge is only suitable for a direct comparison with reconstructed recharge concentrations if one can be sure that the concentrations have not been altered along the flow path between the time of recharge and the time of sampling. In this case, high dissolved oxygen concentrations indicating oxic groundwater could serve as an indicator for (locally) conservative transport of nitrate.

Example 3: Potassium and cation exchange

This example shows the effect of cation exchange (Ceazan *et al.* 1989) along the flow path (Figure 3.2c). The concentrations of potassium in groundwater sampled from the shallow screen show an upward trend. Potassium concentrations in the deep screen show a weaker trend at a much lower level. If potassium were transported conservatively, concentrations measured in the deep screen would overlap those measured in the shallow screen from the same recharge period. However, the differences between concentrations from the deep screen and the shallow screen show that the concentration of potassium is altered along the flow path. Potassium is not transported conservatively but in this case subject to cation exchange. As a result, the concentrations measured in the shallow screen can not be related to recharge concentrations (the concentration measured in 2004 in 13 year old groundwater does not equal the recharge concentration in 1992); and the concentrations measured in previous years do not represent concentrations in groundwater older than the groundwater sample (concentrations measured in 1980 in 13 year old groundwater do not represent concentrations in 37 year old groundwater in 2004).

3.2.3 Character of solutes related to recharge time

Before measured time-series of concentrations can be related to the expected time of recharge, it has to be decided whether the solute should be considered conservative or reactive. All possible processes such as the degradation of pesticides, production of pesticide-metabolites, release of solutes from the sediment or pH buffering should be considered when deciding on the character of the solute. We distinguished three different solute characters:

- *Conservative solutes* (for example Cl) are transported by groundwater flow without changes in concentration occurring during groundwater flow. If the same groundwater was sampled again further along the flow path, conservative solutes are detected at the same

concentration. Because concentrations of conservative solutes do not change along the flow path, concentrations of conservative solutes measured in previous years are representative of groundwater that is older than sampled groundwater. Therefore, entire time-series of solute concentrations can be related to the time of recharge (e.g. Chapter 2; Laier 2004): the entire time-series are valid to assess trends in older groundwater as well as to compare directly to reconstructions of the historical concentrations of solutes at the time of recharge.

- *Locally conservative solutes* are typically influenced by processes occurring at a specific location in the aquifer, such as nitrate reduction and pyrite oxidation at the redoxcline. The concentrations of *locally conservative solutes* (for example nitrate) remain constant in time, as long as the redox conditions of the sediment along the groundwater flow path do not change. The data set of time-series should then be divided in an oxic and an anoxic part. Only the time-series of concentrations measured in oxic groundwater may be used to estimate recharge concentrations. Concentrations measured in the past in the oxic part of the aquifer remain valid only for the oxic part, but may not be used to assess trends in older groundwater because that may have crossed the redoxcline. If no further reactions are expected to take place, the concentrations measured in the anoxic part of the aquifer in previous years may be used to assess trends in concentrations in older groundwater.
- The concentrations of *reactive solutes* are expected to change continuously along the groundwater flow path and are typically influenced by processes such as cation exchange. All concentrations included in a single analysis should be sampled within a few years and the concentration – recharge year relationship only represents the trends in groundwater quality at a certain moment in time. Measurements made in the past may not be used to assess trends in older groundwater today, nor can they be related to reconstructed recharge concentrations directly. Concentrations measured in previous year may be related to recharge year as well, but only to provide a separate trend analysis representative for that particular moment.

Three conceptual figures of groundwater flow illustrate the differences types of transport of solutes: conservative, locally conservative and reactive transport (Figure 3.3). *Conservative* solutes are transported through the aquifer without changes in concentration; *locally conservative* solutes are only transported in the non-reactive (oxic) part of the aquifer; *reactive* solutes are subject to reactions along the entire flow path and their concentrations change continuously.

In this study, we only related the entire time-series of solutes to the time of recharge if the transport of that solute could be considered conservative. We transposed entire time-series of

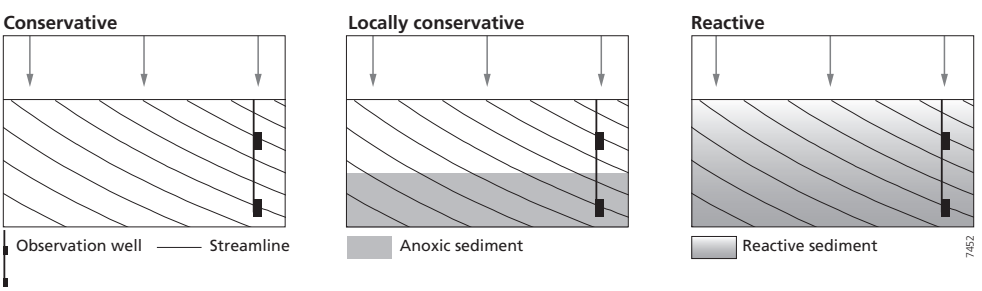

Figure 3.3 Conceptual figures of groundwater flow to illustrate the differences types of transport of *conservative*, *locally conservative* and *reactive solutes*

nitrate and sulfate, providing the distinction between oxic and anoxic groundwater. For reactive solutes, we only used the concentrations measured between 2002 and 2004 to assess the trends in pollutant concentrations that were present in the groundwater body in 2003. We revealed solute specific aggregated regional trends in concentrations by using a LOWESS smooth (Cleveland 1979) to remove scatter due to short term variations in leaching and horizontal variations of the recharge concentrations. These trends are relevant within the scope of the EU GWD to assess the vulnerability of groundwater bodies to future deterioration of groundwater quality.

3.2.4 Model description and relevant geochemical processes

To test whether the suggested processes could actually have resulted in the observed patterns we used a geochemical reactive transport model (PHREEQC-2 version 2.15, Parkhurst and Appelo 1999). The aim of the model was to reproduce the observed trends in reactive solutes to test whether the suggested processes could have caused these trends. The model was intentionally not calibrated towards a better fit with the data. Instead, differences between the model and the measurements were used to gain more information either about the reactive processes or on the validity of the inputs of the model. In this case, geochemical modeling to reproduce observed trends is preferred over a geochemical analysis of aquifer sediments, because this study requires effective geochemical parameters at the groundwater body scale, which are difficult to derive from laboratory measurements.

3.2.5 1D transport in relation to travel time

The 1D model represented a groundwater flow path along which solutes are transported and may react with the sediment. The 1D model simulates concentrations in relation to the travel time along the groundwater flow path, rather than the traveled distance. This allowed for direct comparison between model and measurements related to time of recharge. Each cell of the model represented the volume of groundwater that recharged within one year. Each year, the groundwater solutions in each cell were shifted one cell forward and a new recharging groundwater solution was introduced into the first cell. This approach is very similar to simulating the transport of reactive solutes in a vertical 1D column in which horizontal flow is neglected. To be able to convert literature estimates of reactivity parameters that are related to sediment mass into values related to travel time we had to assume a single recharge rate, porosity and sediment bulk density.

3.2.6 Concentrations of solutes in recharging groundwater

The initial concentrations in the model were based on a study on natural background levels in groundwater (Griffioen *et al.* 2008). The concentrations of solutes in recharging groundwater were reconstructed using an annual mineral balance for agricultural land in Noord-Brabant. We considered three sources (atmospheric deposition, animal manure, and artificial fertilizer); and two sinks (crop uptake and denitrification in the unsaturated zone). For a detailed description of the mineral balance we refer to the Appendix of Chapter 2. Estimates of atmospheric deposition of N and S were based on a large scale study of fertilizing and acidifying deposition the Netherlands (Eerens *et al.* 2001). Because most research has focused on the deposition, uptake and leaching of nitrogen and potassium from agricultural land, it was more difficult to provide reliable estimates of the reconstructed concentrations for other elements.

3.2.7 Simulated processes

Based on previous work in the agricultural recharge areas of the Sand Meuse groundwater body (Griffioen 2001; Broers 2004b; Broers and Van der Grift 2004; Fest et al. 2007; Van der Grift and Griffioen 2008), the following processes were considered to be relevant to trends in solute concentrations in relation to time of recharge. These were the processes that we simulated using PHREEQC:

- pH buffering by gibbsite in oxic groundwater
- cation exchange
- oxygen consumption by degradation of dissolved organic matter
- pyrite oxidation induced by nitrate, indicated by NO_3, SO_4 and Fe
- pH buffering by goethite precipitation in anoxic groundwater
- release of heavy metals during pyrite oxidation.

Concentrations of Al in most groundwater in the Netherlands are saturated with respect to gibbsite, considering complexation with dissolved organic carbon (Fest *et al.* 2007). This indicates that groundwater in the Netherlands is buffered by the dissolution of gibbsite, releasing Al^{3+} and OH^-. Therefore we simulated the mineral phase gibbsite in equilibrium with the groundwater solution in the oxic part of the model.

Cation exchange was simulated by three individual exchangers: X, Y and Z. The first cation exchanger (X) represents clay minerals. In this model every cation may be sorbed to clay, except H^+. The second (Y) and third (Z) cation exchangers represented organic matter. In this model every cation may be sorbed to organic matter, also H^+. Since they are able to sorb H^+ they may act directly as pH-buffer. The first exchanger may buffer pH indirectly by exchanging Al produced by gibbsite dissolution.

Equations 3.1-3.3 describe the exchange of Na (for example) with the three exchangers, in which $[Na^+]$ represents the aqueous activity of Na and $\beta_{X\text{-}Na}$ is the equivalent fraction of Na absorbed to exchanger X. Each of these half reactions has a logK associated with it, defining the affinity of the exchanger for the cation, relative to other cations. Table 3.1 lists the logK values used. To illustrate the effect of the cation exchange complex and test its sensitivity, we used two sets of values for the cation exchange capacity (CEC) representing the high and low end of the range of concentrations of clay and organic matter found in the sediments in Noord-Brabant.

Table 3.1 logK of cation exchange half reactions

logK	X	Y	Z
H^+	-	5.08	3.08
Na^+	0	-0.85	-0.85
K^+	0.7	-0.7	-0.7
Ca^{+2}	0.8	0	0
Mg^{+2}	0.6	-0.3	-0.3
Fe^{+2}	0.44	0	0
Ni^{+2}	0.6	-	1
Zn^{+2}	0.8	1	1
Al^{+3}	0.67	0.9	0.9

Table 3.2 Characteristics of PHREEQC model runs.

Name	CEC (mmol/l)			Mineral phases	
	X	Y	Z	cells 1-15	cells 16-80
no CEC	-	-	-	gibbsite	pyrite and goethite
low CEC	0.03	0.001	0.001	gibbsite	pyrite and goethite
high CEC	0.1	0.08	0.08	gibbsite	pyrite and goethite
conservative	-	-	-	-	-

$$Na^+ + X^- = Na\text{-}X;\ logK = \log(\beta_{X\text{-}Na}/[Na^+]) \quad (3.1)$$

$$Na^+ + Y^- = Na\text{-}Y;\ logK = \log(\beta_{Y\text{-}Na}/[Na^+]) \quad (3.2)$$

$$Na^+ + Z^- = Na\text{-}Z;\ logK = \log(\beta_{Z\text{-}Na}/[Na^+]) \quad (3.3)$$

Oxygen consumption was simulated using a first order kinetic reaction with CH_2O, representing dissolved organic matter. The degradation rate for O_2 was 0.22 y^{-1}. The chemical reaction of pyrite oxidation depends on whether the produced Fe(II) is also oxidized by NO_3. If all Fe(II) remains in solution, pyrite oxidation consumes acid (Equation 3.4), while if all Fe(II) is also oxidized by NO_3 and subsequently precipitated as Fe(OH)3, pyrite oxidation produces acid (Equation 3.5). The reaction can also be made neutral with respect to acid production (Equation 3.6).

$$5FeS_2 + 4\ H^+ + 14\ NO_3^- = 10\ SO_4^{-2} + 5Fe^{+2} + 7N_2 + 2H_2O \quad (3.4)$$

$$2FeS_2 + 6\ NO_3^- + 4\ H_2O = 4\ SO_4^{-2} + 2Fe(OH)_3 + 3N_2 + 2H^+ \quad (3.5)$$

$$9FeS_2 + 26\ NO_3^- + 6H_2O = 18\ SO_4^{-2} + 4Fe(OH)_3 + 5Fe^{+2} + 13N_2 \quad (3.6)$$

3.2.8 Conservative chemical indicators

If geochemical processes are expected to have influenced solute concentrations, conservative chemical indicators can be constructed that are insensitive to these processes to demonstrate the effect of trends in recharge concentrations (Broers and Van der Grift 2004). In this study we used the oxidation capacity (OXC) and the sum of cations (SUMCAT) as conservative chemical indicators. OXC behaves as a conservative solute if pyrite oxidation by nitrate reduction takes place (Postma *et al.* 1991) because the weighted sum of NO_3 and SO_4 remains constant before and after pyrite oxidation. The ratio between NO_3 consumed and SO_4 produced ranges between 1.4 to 1.5 depending of the formulation (Equation 3.4 or 3.5). Following Postma (Postma *et al.* 1991), we used a ratio of 1.4 and defined the oxidation capacity as:

$$OXC = 5*[NO_3] + 7*[SO_4] \quad (3.7)$$

A requirement for the use of OXC is that all oxygen is consumed before groundwater reaches the pyrite. Oxygen concentrations show that in this aquifer, oxygen is removed from groundwater within 5 years. This makes the use of OXC as a conservative indicator possible.

The total sum of cations remains constant if cation exchange is the only process taking place, although individual cations may exchange individually with the cation exchange complex. Dissolution of minerals, such as calcite, will increase the sum of cations. Pyrite oxidation will also increase the sum of cations by releasing Fe^{2+} or H^{+} (depending on the formulation of the reaction, Equation 3.4 or 3.5). The contribution of pyrite oxidation to the sum of cations ranges between 1/3 to 3/7 meq/l per mmol NO_3 reduced, depending on the formulation. With reconstructed recharge concentrations of NO_3 up to 4 mmol/l, the contribution of pyrite oxidation to SUMCAT is 1.5 meq/l at most. Hence, we considered the sum of cations a conservative solute, despite this possibly non-conservative behavior.

3.3 Results of trend analysis in relation to recharge time

The measured concentrations related to time of recharge were analyzed, together with the modeled concentrations, in the following ways. First, we discuss the *aggregated regional trend* based on a LOWESS smooth through the measurements. For *conservative* solutes, the LOWESS smooth was fitted through all aggregated time-series related to time of recharge. For *locally conservative* solutes, the LOWESS smooth was fitted through measurements of concentrations in oxic (NO_3 > 0.5 mmol/l) and anoxic (NO_3 < 0.5 mmol/l) groundwater samples separately. For *reactive* solutes, the LOWESS smooth was fitted through concentration measurements sampled between 2002 and 2004. Second, the aggregated regional trends were compared to the model results. The conservative model run represents the reconstructed historical concentrations in recharging groundwater, while differences between the aggregated regional trend and the conservative model run may indicate that the observed trends have been altered by geochemical processes. The comparison between the aggregated regional trend with the reactive model runs reveal how geochemical processes may have altered the changes in historical recharge concentrations. Third, the type of trend is distinguished, based on the combination of the observed regional trends and the model results.

3.3.1 Chloride

The aggregated regional trend (Figure 3.4, black line) in the concentrations of chloride (Cl), based on the entire time-series of concentrations, shows constant concentrations in groundwater that has recharged before 1985, but a downward trend in groundwater that has recharged after 1985. The downward trend agrees with the modeled concentrations (grey line) in young groundwater, although the observed concentrations are slightly lower. Because Cl does not partake in any reaction, all model runs yielded the same result. The trends in Cl concentrations are the direct result of the anthropogenic trends in historical in concentrations in recharging groundwater unaltered by conservative transport through the groundwater body.

3.3.2 Solutes related to pyrite oxidation

The aggregated regional trends for oxidation capacity (OXC, Figure 3.5a, black line), based on the entire time-series of measurements, are typical of anthropogenic influences and changes in agricultural practices. An upward trend is present in groundwater that has recharged before 1980, while a downward trend is present in groundwater that has recharged after 1990. These trends are also present in the results for OXC of both the conservative model run (orange line) and the

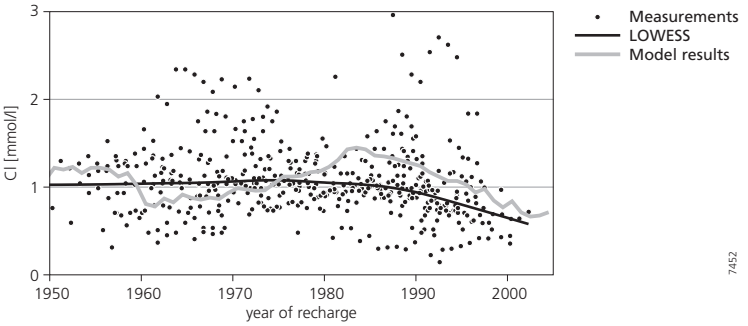

Figure 3.4 Concentrations of Cl related to recharge time, together with model results.

reactive model run (pink). The very small difference between the conservative and reactive model results in the anoxic part of the model is due to the reaction of Fe(II) with NO_3. The trends in OXC are the direct result of the anthropogenic trends in recharging groundwater transported through the groundwater body without changes in concentrations.

The aggregated regional trends of nitrate (NO_3) in oxic groundwater (Figure 3.5b, dashed black line), based on the entire time-series, are again typical of agricultural practices: upward before 1980 and downward after 1990. The trend in anoxic groundwater (dotted black line) plotted along the horizontal axis, because all measurements on which this trend was based were below 0.5 mmol/l by definition. In the underlying measurements, the distinction was made between the oxic (dots) and anoxic (crosses) samples, as well as between the samples collected in 2004 (black) and samples collected in previous years (grey). This distinction showed that the oldest groundwater sample collected in 2004 that still contained NO_3 had a groundwater age of 15 years and had recharged in 1990. The aggregated regional trends compared favorably with the results of the conservative model run (orange line) and the results in the oxic part of the reactive model run (red line). This indicates that the reconstructed recharge concentrations are accurate. Although the trends in the oxic part of the aquifer appear to be the direct result of the anthropogenic trends in recharging groundwater transported through the groundwater body without changes in concentrations, the absence of NO_3 in older groundwater shows that the anthropogenic trends in recharge concentrations are altered by reactions during transport.

The aggregated regional trends of sulfate (SO_4) in oxic groundwater (Figure 3.5c, dashed black line), based on the entire time-series, are again typical of anthropogenic influences. The aggregated regional trends of SO_4 in anoxic groundwater (dotted black line) are typical of anthropogenic influences, but the concentrations in anoxic groundwater are higher, showing the release of sulfate by nitrate-induced pyrite oxidation. The conservative model run (orange line) and the results in the oxic part of the reactive model run (red line) show the same trends, but slightly underestimate the absolute concentrations. The anoxic part of the reactive run showed the release of sulfate, but overestimated the measured concentrations, which could indicate that another source of electrons other than pyrite is present, for example sediments containing reactive organic matter. Like for nitrate, the trends in the oxic part of the aquifer appear to be the direct result of the anthropogenic trends in recharging groundwater transported through the groundwater body without changes in concentrations. However, the elevated concentrations of sulfate in anoxic groundwater show that the anthropogenic trends in recharge concentrations are

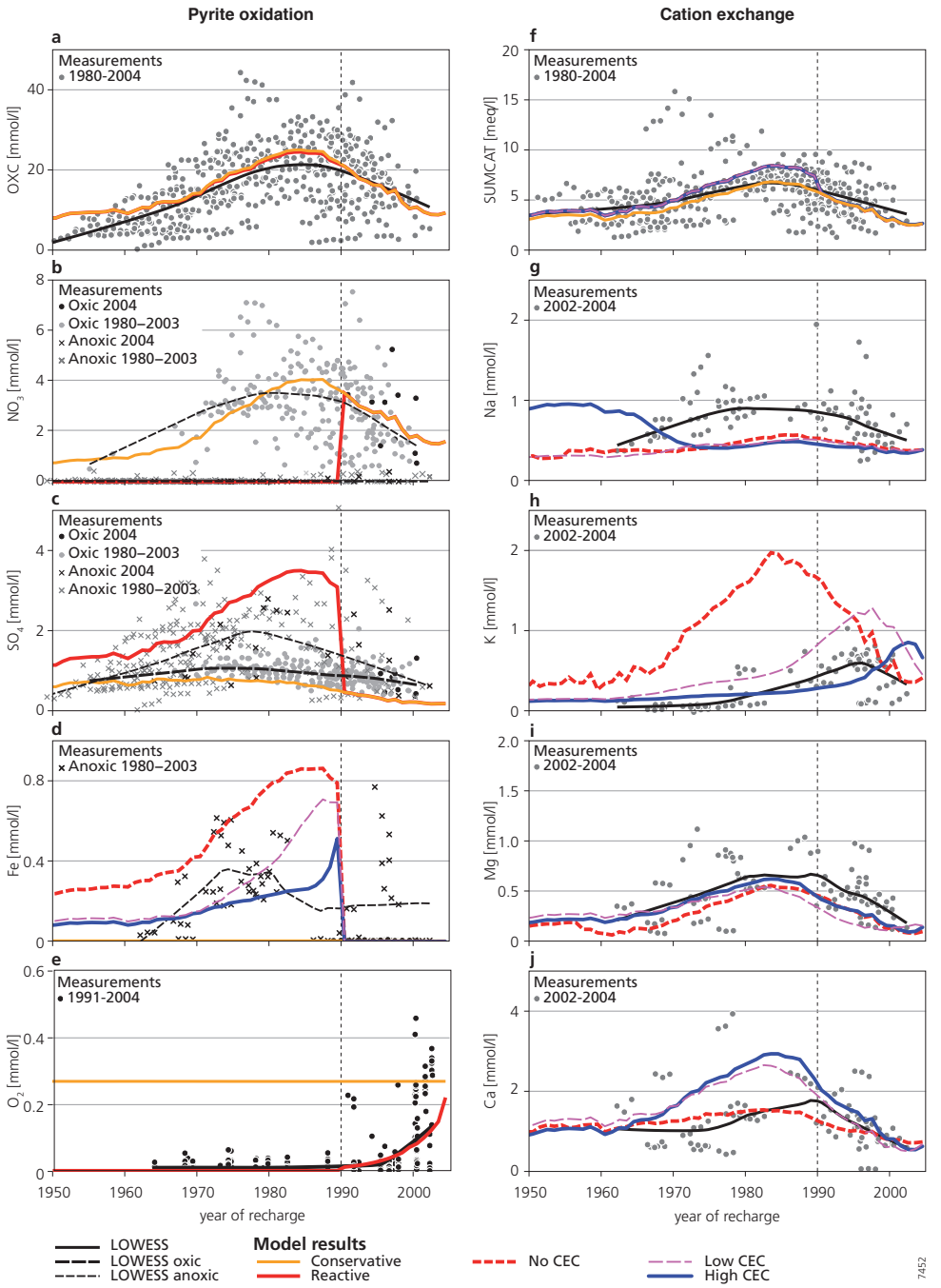

Figure 3.5 Concentrations of solutes related to pyrite oxidation and cation exchange related to the time of recharge, together with model results. Vertical dashed line indicates location of redoxcline in model.

altered by reactions during transport that are triggered by changes in the recharge concentrations of another solute, in this case NO_3.

The aggregated regional trends of iron (Fe) in oxic groundwater (Figure 3.5d, dashed black line), based on the concentrations measured between 2002 and 2004, plotted along the horizontal axis, because Fe is oxidized to Fe(III) in oxic water, which is highly insoluble and precipitates as $Fe(OH)_3$. The aggregated regional trends of iron (Fe) in anoxic groundwater (dotted black line) show Fe concentrations up to 0.8 mmol/l; indicating a source of Fe is present in anoxic groundwater. The presence of Fe in anoxic groundwater is another qualitative indication of pyrite oxidation. A quantitative mass balance comparison with NO_3 removed and SO_4 produced by pyrite oxidation is impossible because part of the Fe released by pyrite oxidation may have been oxidized to Fe(III) by NO_3 and precipitated, and Fe was also subject to cation exchange. The conservative model predicted no Fe, because no source of Fe was present in the reconstructed recharge concentrations. The reactive models predicted various trends, all showing the release of Fe in 16-year-old groundwater, at the modeled redoxcline. After release by pyrite oxidation, Fe is transported conservatively further by the no-CEC model run (red line), while Fe was subject to cation exchange in the low-CEC (purple line) and high-CEC (blue line) model run. The range of modeled concentrations is similar to the range of measured concentrations in anoxic groundwater, indicating that the release of Fe by pyrite oxidation and subsequent cation exchange are both responsible for the trends in Fe concentrations in anoxic groundwater. The aggregated regional trends of Fe are clearly the result of geochemical reactions occurring during transport that are triggered by the presence of NO_3 in recharging groundwater.

The aggregated regional trend of oxygen (O_2, Figure 3.5e, black line) was based on the entire time-series of O_2 measurements. However, the entire time-series was plotted at the recharge time of the most recent (2004) groundwater sample, rather then being transposed entirely, which is an exception to the other solutes. This approach is valid for O_2 alone, because there is no trend in the concentrations of O_2 in recharging groundwater, and provides as much data as possible for the trend analysis. The aggregated regional trend showed an exponential decrease in young groundwater. O_2 is completely consumed before groundwater reaches the redoxcline and this indicates that pyrite oxidation occurs by nitrate reduction only. The results of the reactive model (red line), with which the O_2 consumption was simulated with a 1st order kinetic process, fitted the observed trends well. The aggregated regional trend of O_2 were not related to anthropogenic influences, but solely the result of the geochemical properties of the groundwater body.

3.3.3 Cations

The aggregated regional trends for sum of cations (SUMCAT, Figure 3.5f, black line), based on the entire time-series of measurements, are again typical of anthropogenic influences and changes in agricultural practices. An upward trend is present in groundwater that has recharged before 1980, while a downward trend is present in groundwater that has recharged after 1990. These trends are also present in the results of the conservative model run (orange line) for OXC. All reactive model results, no-CEC (red line), low-CEC (purple line), and high-CEC (blue line) overlap, indicating that SUMCAT is unaffected by cation exchange. The difference between the conservative and reactive model results in the anoxic part of the model is due to the contribution of pyrite oxidation to SUMCAT. The contribution of pyrite oxidation is minor compared to the larger trends in SUMCAT, which are largely the direct result of the anthropogenic trends

in recharging groundwater transported through the groundwater body without changes in concentrations.

The aggregated regional trends of the four major cations, sodium (Na), potassium (K), magnesium (Mg), and calcium (Ca), were based on the concentrations measured between 2002 and 2004 (Figure 3.5g-3.5j, black lines). The aggregated regional trends of Na, Mg and Ca all showed the typical agricultural influences. In contrast, the aggregated regional trend of K is entirely different. The modeled concentrations of Na were systematically below the aggregated trend. There was very little difference in the simulated concentrations of Na between the no-CEC (red line), low-CEC (purple line), or high-CEC (blue line) run. These small differences illustrated the low affinity of the cation exchange complex for Na. The high concentrations of Na in old groundwater show the retarded flushing of high concentrations initially present in the model. Because the effect of cation exchange on Na concentrations is limited, the difference between the measured and modeled Na concentrations must be the result of errors in the recharge concentrations. These errors may be due to inaccurate estimates of Na contents of manure, fertilizer or crops. Because Na is very limited subject to cation exchange, the aggregated regional trends of Na appear to be the direct result of the anthropogenic trends in recharging groundwater transported through the groundwater body without changes in concentrations.

The unique aggregated regional trend of K indicates the effect of a reaction affecting the concentrations of K along the flow path. Instead of typical upward trends before 1980 and downward trends after 1990, aggregated regional trend of K shows a slow but steady upward trend from 1970 to 1995 and only a slight downward trend in younger groundwater. While the no-CEC (red line) model run predicts the typical agricultural trends, the low-CEC (purple line) and high-CEC (blue line) model runs show trends that are similar to the observed trend. This reproduction of the observed trends indicates that cation exchange simulated by the reactive model is responsible for the trend in K concentrations. The aggregated regional trend of K was clearly the result of the anthropogenic trends in recharge concentrations being altered by reactions during groundwater flow.

The similarities between the results of the different model runs for Mg indicate the low affinity of Mg for the cation exchange complex and limited participation of Mg in cation exchange. The modeled trends accurately reproduce the aggregated regional trend of Mg, which was largely the direct result of the anthropogenic trends in recharging groundwater transported through the groundwater body without changes in concentrations.

The aggregated regional trend of Ca, similar to the characteristic anthropogenic trend, was hardly affected by a few very high Ca concentrations that are likely the result of calcite dissolution. The no-CEC (red line) model results closely resembled the observed trends, while the low-CEC (purple line) and high-CEC (blue line) overestimate the concentrations of Ca in groundwater that has recharged before 1990. The differences between the model runs show the effect of Ca release by cation exchange. The large amount of Ca released from the cation exchange complex in the model was the combined result of a high initial concentration of Ca and the high affinity of the exchange complex for Ca resulting in a high occupancy of Ca at the exchange complex; the replacement of Ca from the complex by K; and the production of Fe by pyrite oxidation and subsequent exchange with Ca. Although the model results indicate that Ca concentrations are affected by reactive transport, the aggregated regional trend of Ca appears to be the direct result of the anthropogenic trends in recharging groundwater transported through the groundwater body without changes in concentrations.

3.3.4 pH

The aggregated regional trends for pH and Al were based on samples collected between 2002 and 2004 (Figure 3.6a and 3.6b, black line). The aggregated trend for pH shows a steady decline from higher values in anoxic groundwater that recharged around 1960 to lower values in younger and oxic groundwater; while the aggregated regional trend for Al shows a small increase in groundwater that recharged after 1990. The lower pH (down to ~ 4.5) combined with higher Al concentrations in recent oxic groundwater indicate that pH is buffered by Al-hydroxides during recharge. Anoxic water appears to be buffered by goethite precipitation during pyrite oxidation. The aggregated trend of pH was insensitive to a small number of groundwater samples (triangles) with a pH above 6, which also showed high calcite saturation indices indicating these samples had been affected by calcite dissolution.

The mutual effects of pH-buffering and Al-solubility were very clear from the modeled concentrations. The results from the no-CEC run (red line) without cation exchange in young water, the pH was about 4.4 and Al concentrations were approximately 25 µmol/l. The measured concentrations of Al well above the modeled results are the result of Al-complexation with dissolved organic matter (Fest *et al.* 2007). In the model runs with a low (purple line) or high (blue line) cation exchange capacity, Al was quickly exchanged for other cations and the modeled pH was buffered more.

Pyrite oxidation by nitrate reduction appeared to buffer pH at or above 5, by partial precipitation of produced Fe as Fe(III)-hydroxides. Although pyrite oxidation is often associated with acidification, this is only the case if oxygen is electron acceptor. In this case, oxygen is removed before groundwater reaches the redoxcline and pyrite oxidation by nitrate does not cause acidification. Therefore it is more likely that pyrite oxidation by nitrate reduction follows the stoichiometry of the reactions described by Equation 3.4 or 3.6; rather then that of Equation 3.5, which would lead to acidification.

The aggregated regional trends for pH were the result of the anthropogenic trends in acidifying precipitation being buffered by reactions during groundwater flow, while the aggregated regional trends of Al are the result of geochemical reactions that are triggered by higher concentrations of another solute, in this case H^+.

3.3.5 Nickel, zinc and arsenic

The aggregated regional trends for nickel (Ni, Figure 3.7a), zinc (Zn, Figure 3.7b), and arsenic (As, Figure 3.7c) were based on samples collected between 2002 and 2004, and for oxic (dashed black line) and anoxic (dotted black line) samples separately. Neither of these LOWESS smooth lines shows a very clear trend, because of the limited amount of data points and the large variation in the measured concentrations. The aggregated regional trends of Ni, Zn and As show elevated concentrations in anoxic groundwater, but these trends are not very clear because of the limited amount of data points and the large variation in the measured concentrations. Ni and Zn were also detected in oxic samples, and the aggregated trend of Zn shows a pattern similar to the trend in K. The modeled concentrations of Ni show its release during pyrite oxidation, and the effect of subsequent cation exchange.

The model results for Zn show two effects: the anthropogenic trends that are present in the conservative run (orange) and oxic part of the no-CEC run (red), are altered by cation exchange in the low-CEC (purple) and high-CEC (blue) run. Additionally, Zn is also released during pyrite oxidation, resulting in elevated concentrations in anoxic groundwater (except

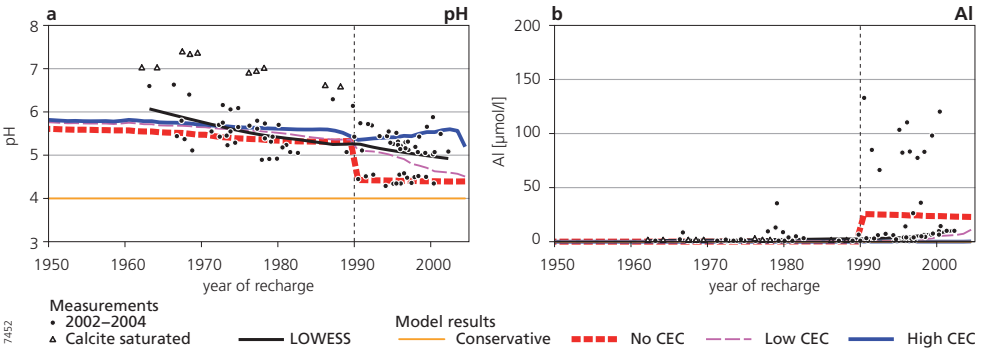

Figure 3.6 Measurements of pH and Al concentrations related to the time of recharge, together with model results.

for the conservative run). Subsequent cation exchange results in various trends in modeled Zn concentrations in anoxic groundwater. High concentrations of As measured in anoxic groundwater indicate that As is released by pyrite oxidation (Broers and Buijs 1997) The presence of As in anoxic groundwater is reproduced by the reactive model runs, but the absolute concentration is overestimated by a factor 20. Either the concentration of As in pyrite was estimated too high or there is a sink for As present, possibly complexation with Fe-hydroxides. The simulated concentrations could not accurately predict the measured level of concentrations, but the trends that were observed in the measurements could be reproduced and show that the

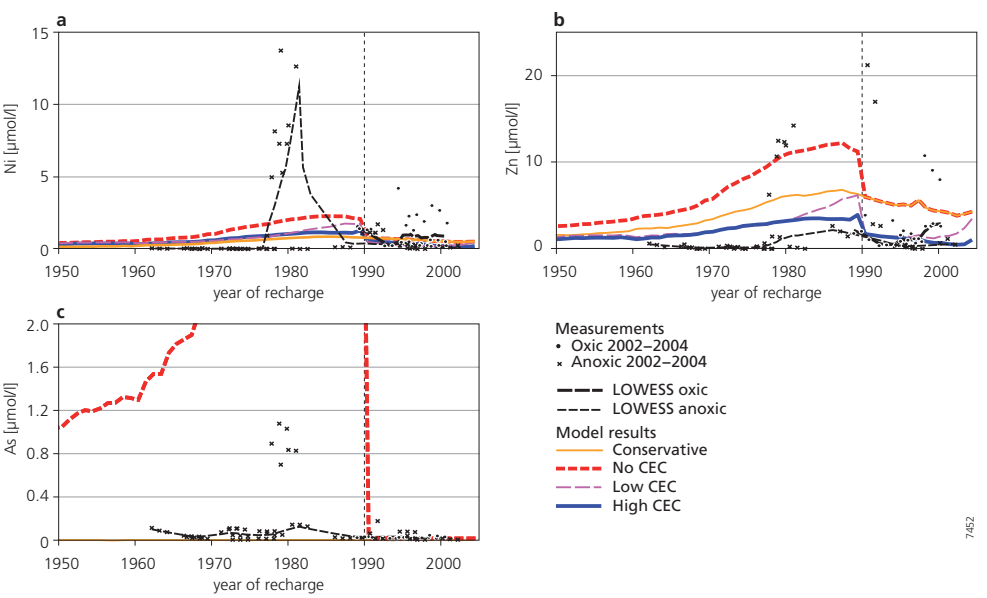

Figure 3.7 Measurements of Ni, Zn and As concentrations related to the time of recharge, together with model results.

processes influencing the concentrations of heavy metals are plausible. The aggregated regional trends for Zn are partially the result of anthropogenic trends in recharge concentrations altered by reactions during transport, while the aggregated regional trends for Ni, As, and partially for Zn, are the result of geochemical reactions in the subsurface that are triggered by anthropogenic changes in the recharge concentrations of other solutes, in this case pyrite oxidation triggered by anthropogenically elevated nitrate concentrations.

3.4 Discussion

3.4.1 Possibilities, limitations and requirements for relating pollutant concentrations to travel time

Relating concentrations of solutes in groundwater to the estimated recharge time of groundwater provides new approaches for the analysis of trends in groundwater quality, also for reactive solutes, as required by the EU Groundwater Directive (EU 2006). Using this approach, we were able to detect aggregated regional trends in the concentrations of both conservative and reactive pollutants. Because of the variability in pollutant concentration measurements, using a larger number of measurements in a single analysis is preferable, to discern the regional anthropogenic trend from short-term temporal variation. This approach benefits from the aggregation of existing time series from selected homogeneous areas of a groundwater body. The land use and pollution history of the selected areas, which are aggregated in a single analysis, must be similar and should not contain a systematic spatial trend. The flow system of the groundwater body must be characterized by piston flow with little dispersion. Also the monitoring network should allow for the collection of groundwater samples with a distinct travel time. Therefore, data from water supply wells with long screens that sample mixed water with a range of travel times are unsuitable for direct comparison with reconstructed recharge concentrations. If solute concentrations are to be related to recharge time, the character should be identified first. Three types of solutes can be distinguished:

- conservative solutes, which are not affected by geochemical reactions
- locally conservative solutes, which only react with the sediment at one place and are transported conservatively before the reaction takes place
- reactive solutes, which may react continuously with the sediment or other solutes along the entire flow path.

Each type of solute requires a different approach to relate their concentrations to recharge time (Table 3.3). The entire time-series of conservative solutes are suitable for an aggregated regional trend assessment, as presented in this study; to link directly to historical recharge concentrations; or to assess trends in older groundwater. The same approaches of trend detection are applicable to locally conservative solutes, upon the condition that only parts of the data-set (before or after the reaction has taken place) are used in the same analysis. Only a short period of the time-series of reactive solutes are suitable for an aggregated regional trend assessment, but the observed aggregated trends can neither be linked directly to historical recharge concentrations, nor can they be used to assess trends in older groundwater. To understand the effect of geochemical reactions on the shapes of the aggregated regional trends of reactive solutes, relate measured

Table 3.3 Character of solute and suitable data for different approaches of trend detection in relation to time of recharge.

	Aggregated regional trend assessment	Direct link to historical recharge concentrations	Assess trends in older groundwater
conservative solute	entire time-series	entire time-series	entire time-series
locally conservative solute	separate analysis, before and after reaction, based on entire time-series	entire time-series before reaction	entire time-series after reaction
reactive solute	short period only (~3 years)	not possible	not possible

concentrations to historical recharge concentrations, or assess trends in older groundwater, requires the use of a reactive transport model.

3.4.2 Identified solute specific trends and responsible geochemical processes

Relating concentrations to recharge time revealed solute-specific aggregated regional trends (Table 3.4) that are the result of solute specific geochemical processes. Changing historical recharge concentrations are solely responsible for trends in the concentrations of conservative solutes like Cl, OXC, and SUMCAT. A combination of changing recharge concentrations and cation exchange caused the trends of K and Zn concentrations. A combination of recharge concentrations and nitrate induced pyrite oxidation cause the trends in NO_3 and SO_4 concentrations. The trend in O_2 concentrations is caused by sediment geochemistry alone because recharge concentrations are invariable. The trend in pH in oxic groundwater is the result of sediment geochemistry through dissolution of Al-hydroxides, which is also the cause for trends in Al concentrations; while the pH-trend in anoxic groundwater is the result of buffering by goethite precipitation. The historical concentrations of nitrate in recharging groundwater are indirectly responsible for the trends in SO_4, Fe, As, Ni, and Zn, due to nitrate-induced pyrite oxidation. Trends in Fe, Ni and Zn in anoxic groundwater are in turn influenced by cation exchange.

Table 3.4 Relevant geochemical processes and types of trends observed in the concentrations of solutes in relation to time of recharge.

	Cl	OXC	NO_3	SO_4	Fe	O_2	SUMCAT	Na	K	Mg	Ca	pH	Al	As	Ni	Zn
Processes																
Cation exchange					X			X	X	X	X		X		X	X
Pyrite oxidation			X	X	X		x					X		X	X	X
Sediment geochemistry						X						X	X			
Types of trends																
Conservative	X	X	o	o			X		X		X	X				
Direct reactive			X							X			X			X
Indirect reactive				X	X									X	X	X

X indicates influence. x indicates negligible influence. o indicates only valid under oxic conditions.

3.4.3 Types of trends

In summary, we distinguish three types of trends in the concentrations of solutes related to time of recharge (Table 3.4). Trends of the first type are the result of the anthropogenic trends in historical in concentrations in recharging groundwater unaltered by conservative transport through the groundwater body, referred to as *conservative* trends in Table 3.4. These trends are only caused by changing recharge concentrations and are found in the concentrations of conservative solutes, and also in the concentrations of locally conservative solutes that have not yet reached reactive parts of the aquifer. For example, the trends in nitrate concentrations in the oxic part of the aquifer show trends typical for a conservative solute.

Trends of the second type are the result of anthropogenic trends in recharge concentrations that are altered by reactions during transport, referred to as *direct reactive* trends. The leaching of solutes from agricultural land causes these trends, but they are transformed by reactions with the subsurface. For example, the elevated concentrations of K in young groundwater are the result K leaching from agricultural land, but the trends in K concentrations are the result of the retarded transport of K through the groundwater body due to the exchange of K with the cation exchange complex, for example.

Trends of the third type are the result of geochemical reactions in the subsurface that are triggered by anthropogenic changes in the recharge concentrations of other solutes. This type of trends is referred to as *indirect reactive* trends, because these trends indirectly caused by anthropogenic trends in recharge concentrations, rather than being directly the result of pollutants present in the recharge concentrations. For example, the elevated concentrations of Fe, As and heavy metals in anoxic groundwater are the result of nitrate-induced pyrite oxidation. This last type of trend is most difficult to assess because the pollutant is not present in recharging groundwater, while its release due to anthropogenic changes in the natural system poses a threat to groundwater quality nonetheless. This type of trends also includes the formation of de-ethylatrazine (DEA) upon the degradation of atrazine (Pinault and Dubus 2008), or the release of nickel from pyretic sediments subject to water table decline (Larsen and Postma 1997).

3.4.4 Requirements and possibilities of a reactive stream tube model in relation to travel time

Relating concentrations to recharge year provides the basis for constructing a 1D transport model with travel time as the independent variable, rather than distance. Such a stream tube model is similar to a 1D model in the vertical dimension, but it has the advantage that variations in travel times at a specific depth are removed, and that modeled concentrations can be compared directly to the aggregated regional trends related to time of recharge. Reproducing the observed aggregated regional trends in reactive solute concentrations with a geochemical model reveals how geochemical processes are responsible for these trends and helps to distinguish between trends that are directly or indirectly the result of reactive transport. It also showed weak points in the historical reconstruction of recharge concentrations.

These stream tube models require basic knowledge about the geochemical reactions taking place in the groundwater body. This knowledge may be obtained from the measured concentrations related to time of recharge. The parameterization of the model can be based on literature, laboratory investigations of sediment reactivity or obtained by inverse modeling and calibration. The most difficult challenge is probably to obtain accurate reconstructions of recharge concentrations. These must be based on historical data of atmospheric deposition and agricultural

practices and are very important if the geochemical parameterization is based on calibration. Especially the concentrations in manure, fertilizer or crops of less "interesting" cations, such as Na, are often poorly documented.

Once calibrated, these stream tube models may provide predictions of future groundwater quality by simulating reactive transport of pollutants through the groundwater body. Different stream tube models are probably required to simulate the reactive transport of areas with different hydrology and land use. The ensemble of stream tube models provides the status of groundwater quality for the entire groundwater body in relation to travel times. Combining these with the distribution of groundwater travel times within the groundwater body provides an accurate description of groundwater quality status at the groundwater body scale. Combining these reactive stream tube models with the travel time distributions of discharging groundwater (see Chapter 7) then provides the contribution of pollutants in groundwater to surface water quality.

3.5 Conclusions

Groundwater dating has successfully been applied as an approach for detecting trends in groundwater quality by a number of studies (Böhlke and Denver 1995; MacDonald *et al.* 2003; Wassenaar *et al.* 2006; Burow *et al.* 2007; Tesoriero *et al.* 2007; Burow *et al.* 2008; Debrewer *et al.* 2008; Rosen and Lapham 2008; Rupert 2008; Saad 2008). The aggregation of monitoring data from monitoring wells scattered across a groundwater body by relating all measurements of pollutant concentrations to the time of recharge provides the basis for detecting aggregated regional trends. These aggregated regional trends are particularly suited to comply with the requirements for trend detection of the EU Groundwater Directive. A large number of measurements can be incorporated in a single trend analysis, which is beneficial because of the temporal variations in time-series of pollutant concentrations. The application of a LOWESS smooth proved to be particularly helpful to reveal the aggregated regional trend.

In this chapter we provided a framework for selecting the appropriate data for aggregation and trend detection analysis, depending on the character of the solute and the purpose of the trend detection exercise. To identify the specific conditions for relating the concentrations of a pollutant to the time of recharge, it must first be characterized as being a conservative, a locally conservative, or a reactive solute.

The analysis of aggregated regional trends of locally conservative and reactive solutes benefits greatly from a comparison with the results of a reactive stream-tube model. Our results show how geochemical reactions in the subsurface alter the anthropogenic trends in recharge concentrations, or produce new trends by releasing pollutants during geochemical reactions. This comparison also serves to define the type of the aggregated regional trend: conservative, direct reactive or indirect reactive.

The distinction between conservative, direct reactive and indirect reactive trends is important to correctly interpret trends in groundwater quality data in relation to historical changes in recharge concentrations of anthropogenic origin. Trend detection should be particularly perceptive of indirect reactive trends, which are the result of the reactions of other solutes with the subsurface. These trends pose a hidden threat to groundwater quality because these pollutants have not been introduced into the system through recharge, but are released within the groundwater body. Extrapolation of these indirect reactive trends certainly requires the use of a reactive stream-tube

model to assess the threat to future groundwater quality. The parameterization of such models and the reconstructions of recharge concentrations are challenging tasks, but the simulation of reactive transport of pollutants through the groundwater body is essential for predictions of future groundwater quality and the contribution of pollutants in groundwater to surface water quality.

4 Comparison of methods for the detection and extrapolation of trends in groundwater quality

This chapter is to be submitted for publication as:
Ate Visser, Igor Dubus, Hans Peter Broers, Serge Brouyère, Marek Korcz, Ruth Heerdink, Bas van der Grift, Philippe Orban, Pascal Goderniaux, Jordi Batlle-Aguilar, Nicolas Surdyk, Nadia Amraoui, Hélène Job, Jean Louis Pinault, and Marc Bierkens. *Comparison of methods for the detection and extrapolation of trends in groundwater quality*.

Abstract

Land use changes and the intensification of agriculture since the 1950s have resulted in a deterioration of groundwater quality in many European countries. For the protection of groundwater quality, it is necessary to (1) assess the current groundwater quality status, (2) detect changes or trends in groundwater quality, (3) assess the threat of deterioration and (4) predict future changes in groundwater quality. A variety of approaches and tools can be used to detect and extrapolate trends in groundwater quality, ranging from simple linear statistics to distributed 3D groundwater contaminant transport models. In this paper we report on a comparison of four methods for the detection and extrapolation of trends in groundwater quality: (1) statistical methods, (2) groundwater dating, (3) transfer functions, and (4) deterministic modeling.

Our work shows that the selection of the method should firstly be made on the basis of the specific goals of the study (only trend detection or also extrapolation), the system under study, and the available resources. For trend detection in groundwater quality in relation to diffuse agricultural contamination, the most important aspect is whether the nature of the monitoring network and groundwater body allow the collection of samples with a distinct age or produce samples with a mixture of young and old groundwater. We conclude that there is no single optimal method to detect trends in groundwater quality across widely differing catchments.

4.1 Introduction

Land use changes and the intensification of agriculture since the 1950s have resulted in increased pressures on natural systems. For example, the diffuse pollution of groundwater with agricultural contaminants such as nitrate and pesticides has resulted in a deterioration of groundwater quality (Foster *et al.* 1982; Strebel *et al.* 1989; Spalding and Exner 1993). The amount of nitrogen deposited on agricultural land, and possibly leaching to groundwater, shows similar trends for most European countries and the United States (Figure 4.1): upward until the late 1980s and

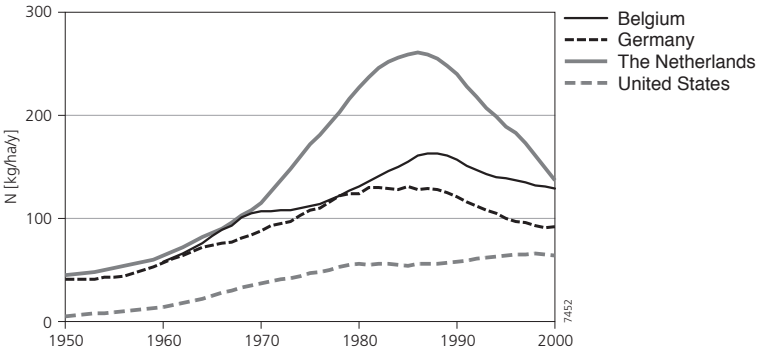

Figure 4.1 Estimates of nitrogen deposition on agricultural land in Belgium (data courtesy of Gembloux Agricultural University), Schleswig-Holstein, Germany (data from (Behrendt *et al.* 2003)), Noord-Brabant, the Netherlands (see chapter 2, Appendix); and the United States (including pasture land, data courtesy of USGS).

stabilization or decreasing trends afterwards. The transfer of these contaminants to deeper groundwater and surface water represents a major threat to the long-term sustainability of water resources across the Europe and elsewhere (Nolan *et al.* 1997).

For the protection of groundwater quality in the European Union (EU), the Water Framework Directive (WFD, EU 2000) and the Groundwater Directive (GWD, EU 2006) require member states to achieve good chemical status of their groundwater bodies by the year 2015. To achieve this, these directives ask member states to delineate groundwater bodies and assess the present chemical status of these groundwater bodies. To detect possible threats to future groundwater quality, the GWD asks for the detection of sustained upward trends in the concentrations of pollutants. If upward trends are found, these should be reversed when the concentration of the pollutant reaches 75% of the threshold value. The GWD also lays down requirements on the implementation of measures necessary to reverse any significant and sustained upward trend. In the context of the WFD and GWD, the scientific community will be asked the following with respect to groundwater quality: (1) assess the current status, (2) detect changes or trends, (3) assess the threat of deterioration by relating them trends to historical changes in land use, (4) predict future changes by extrapolating present day trends and possibly predict trend reversal in response to legislation.

The WFD requires groundwater quality monitoring networks to be operational by the year 2007, but the awareness of the threat to groundwater quality has already led to the installation of monitoring networks in many countries such as Korea (Kim *et al.* 1995; Lee *et al.* 2007), Denmark (Juhler and Felding 2003), the Netherlands (Van Duijvenbooden 1993), New Zealand (Daughney and Reeves 2005), Palestine (Almasri and Ghabayen 2008), the US (Leahy *et al.* 1993; Rosen and Lapham 2008), and the UK (Ward *et al.* 2004). These networks have since produced time-series of monitoring data which have been used to detect and quantify changes in groundwater quality (Broers et al. 2004a; Broers and Van der Grift 2004; Daughney and Reeves 2006; Reynolds-Vargas et al. 2006; Batlle-Aguilar et al. 2007; Burow et al. 2007; Stuart et al. 2007; Xu et al. 2007).

These studies showed that trends in groundwater quality are difficult to detect. Most often the period of interest is longer than the period of record (Loftis 1996) and available time series are typically rather short and sparse because of the high costs of sampling and analysis. The

lack of substantial data usually limits the application of statistical methods to rather simple approaches, rather than more complex time series analysis tools. Other factors complicating trend detection are: variations in the duration and pathways of the transport of contaminants towards monitoring location by groundwater flow, variations in application of contaminants at the ground surface, in space and time, and (partial) degradation of contaminants in the subsurface (Broers and Van der Grift 2004). Additionally, the travel time of sampled groundwater may be uncertain, in particular because the groundwater sample may represent a range of travel times. Whether the character of the groundwater flow system causes mixing of groundwater, for example in dual porosity systems, and whether the groundwater sample contains a mixture of groundwater, for example from springs or production wells is an important factor for the success of trend detection in groundwater quality. This difference can influence the sampled concentration of nitrate, because the mixture sampled from a supply well contains a portion of old, pre-agricultural groundwater with no nitrate (Nolan *et al.* 1997). Data from supply wells should therefore be regarded as a sampling a different sub-population (Alley 1993). In situations where samples contain groundwater with a distinct age, several studies have used groundwater age tracers to enhance the interpretation of measured concentrations of pollutants (Böhlke and Denver 1995; Böhlke *et al.* 2002; MacDonald *et al.* 2003; Laier 2004; Tesoriero *et al.* 2005; Wassenaar *et al.* 2006).

To assess whether an upward trend in the concentration of a contaminant will threaten groundwater quality, a variety of tools can be used to detect and extrapolate trends in groundwater quality. These range from linear statistics (Broers and Van der Grift 2004; Batlle-Aguilar et al. 2007; Stuart et al. 2007); relating trends to changing land use patterns (Gardner and Vogel 2005; Jiang *et al.* 2006; Lapworth *et al.* 2006; Ritter *et al.* 2007) and predict future trends based on land use scenarios (Almasri and Kaluarachchi 2005; Di *et al.* 2005); Trends in

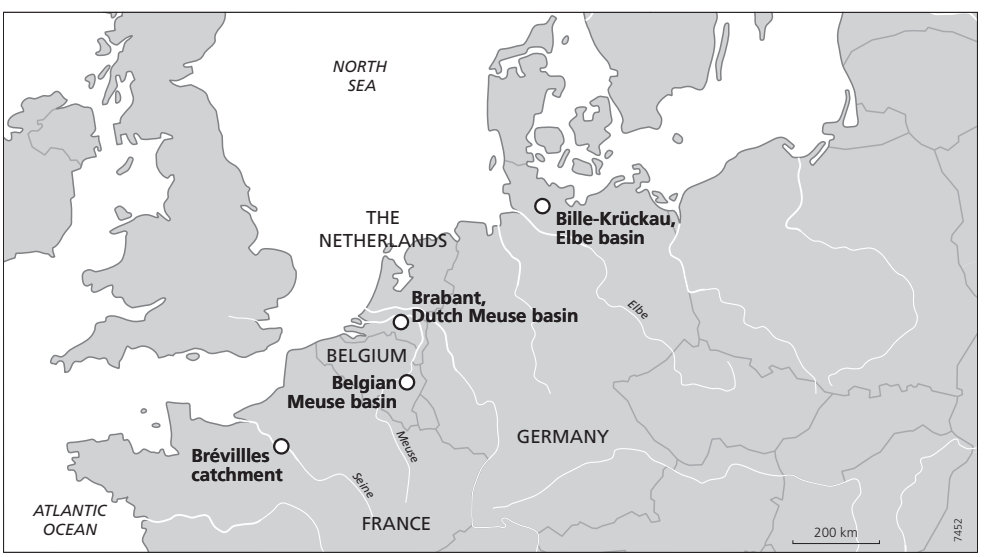

Figure 4.2 Location of test sites within Europe.

groundwater quality can also be predicted using empirical, functional or deterministic models of varying complexity (Refsgaard *et al.* 1999; Almasri and Kaluarachchi 2007; Van der Grift and Griffioen 2008). The efficiency of these tools depends on several factors like the availability of groundwater quality data, the character of the groundwater flow system, and the available resources for trend assessment.

The aim of our work was to assess the capabilities and efficiency of various tools to detect and extrapolate of trends in groundwater quality in a variety of different groundwater systems, ranging from unconsolidated unconfined aquifers to fissured dual porosity systems. We compared four approaches for the detection and extrapolation of trends in groundwater quality: (1) statistical methods, (2) groundwater dating, (3) transfer functions, and (4) deterministic modeling. The comparison was based on the analysis of monitoring datasets at four different locations representing different hydrogeological settings

4.2 Test sites and datasets

Groundwater bodies were selected at four locations to evaluate trend detection methods: the Dutch part of the Meuse basin, a number of catchments in the Belgian part of the Meuse basin, the Brévilles catchment in France and the German Bille-Krückau watershed in the Elbe basin

Table 4.1 Selected characteristics of the four test sites

Sub-basin	Hydrogeological characteristics	Spatial scale	Contaminants	Methods used
Dutch part of Meuse basin (Brabant/ Kempen)	Unconsolidated Pleistocene deposits; fine to medium coarse sands, loam	5000/500 km^2	Nitrate, sulfate, Ni, Cu, Zn, Cd	Statistical, groundwater dating and deterministic modeling
Belgian part of Meuse basin				
Hesbaye	Cretaceous chalk, fissured, dual porosity aquifer	440 km^2	Nitrate	Statistical, groundwater dating and deterministic modeling
Pays de Herve	Cretaceous chalk and sands, fissured	285 km^2	Nitrate	Statistical
Néblon catchment	Carboniferous limestone, folded karstified	65 km^2	Nitrate	Statistical
Meuse alluvial plain	Unconsolidated deposits; gravels, sands and clays	125 km^2	Nitrate	Statistical
Brévilles	Lutecian limestone over Cuise sands, limestone fissured	2.5 km^2	Pesticides (Atrazine and deethylatrazine (DEA))	Groundwater dating, transfer functions and deterministic modeling
Elbe basin	unconsolidated glacial deposits of sand and gravel	1300 km^2	Nitrate	Statistical and groundwater dating

(Figure 4.2). The characteristics of each of the test sites are summarized in Table 4.1 and described in detail in the following sections. The test sites vary strongly in geohydrological characteristics and were studied in different contamination settings (nitrate, pesticides, heavy metals).

4.2.1 Dutch Meuse basin

The Dutch part of the Meuse basin almost entirely belongs to the groundwater body Sand Meuse, which covers most of the province of Noord-Brabant and part of Limburg (5000 km^2 in total) (Visser *et al.* 2004). The groundwater body consists of fluvial unconsolidated Pleistocene sands, covered by 2-30 meters of fluvio-periglacial and aeolian deposits of fine sands and loam. The history of intensive livestock farming on 62% of the area has produced a large surplus of manure contributing to widespread agricultural pollution (Broers *et al.* 2004b). The relatively flat area (0-30 m above mean sea level) is drained by a natural system of brooks, extended in the 20th century with drains and ditches to allow agricultural practices in the poorly drained areas. Groundwater tables are 1-5 m below surface as a result (Broers 2002). Net groundwater recharge is around 300 mm/y resulting in a downward groundwater flow velocity of about 1 m/y in recharge areas (Broers 2004a).

Time series of major cations, anions and trace metals are available since 1992 from the dedicated national and provincial monitoring network sampled annually from 2 m-long screens in multilevel wells at depths of 8 and 25 meters below the surface (Broers and Van der Grift 2004). ^{3}H/^{3}He groundwater ages were obtained from 34 screens of 14 wells in agricultural recharge areas (see Chapter 5). Thanks to the dedicated monitoring wells with short screens and the character of the aquifer, little mixing occurs between recharge and sampling and a groundwater sample is estimated to contain a mixture of water recharged within a period of less than 5 years.

4.2.2 Belgian Meuse basin

Four groundwater bodies were selected as test cases in the Walloon part of the Meuse basin in Belgium (Batlle-Aguilar and Brouyère 2004), which represent various hydrogeological settings: the cretaceous chalk of Hesbaye, the cretaceous chalk of Pays de Herve, the Néblon basin in the carboniferous limestone of the Dinant synclinorium, and the alluvial plain of the Meuse river.

The cretaceous chalk groundwater body of Hesbaye also referred as the Geer basin covers an area of 440 km^2 located north-west from Liège (Dassargues and Monjoie 1993). The groundwater body is drained by the Geer River, a tributary of the Meuse River. Twenty-five million m^3 of groundwater are pumped annually from the fissured dual porosity chalk aquifer to supply the city of Liège and surrounds. 85% of the area of the Hesbaye groundwater body is covered by agriculture, mostly crops. Time series of nitrate are available from 32 monitoring points in the groundwater body, varying from dedicated monitoring wells to pumping wells, traditional wells, springs and galleries.

The chalk groundwater body of Pays de Herve covers an area of 285 km^2 about 80% of which is covered by grassland. Groundwater is pumped at a rate of 12 million m^3 per year from the chalk aquifer. Nitrate concentrations of over 100 mg/l are observed in some of the 59 monitoring points which are distributed throughout the groundwater body.

The Néblon basin covers an area of 65 km^2 in the "Entre Sambre et Meuse" groundwater body, built of 500 m-thick folded and karstified Carboniferous limestone and sandstone. Around 10 millions of m^3 of groundwater are pumped annually from the limestone aquifers. Nitrate

concentrations have been monitored since 1979 at two of the six monitoring locations in the basin. Grassland covers most of the area: 50% permanently and 25% seasonally.

The alluvial plain of the Meuse groundwater body (125 km² along 80 km of the Meuse) consists of gravel bodies embedded in old meandering channels filled with clay, silt and sandy sediments. Land use is 40 % residential or industrial, and 60% natural land. Groundwater quality data are available from 47 monitoring points.

4.2.3 Brévilles catchment

The Brévilles catchment (2.8 km²), 75 km to the northwest of Paris, France, is built up out of a thick unsaturated zone (0-35 m) of dual porosity Lutecian limestone, overlying the Cuise sands, 8-20 m thick and outcropping in the west of the catchment (Dubus *et al.* 2004; Mouvet *et al.* 2004). There is no superficial drainage and the catchment is drained by the Brévilles spring, an outcrop of the Cuise sands. Land use is largely agricultural, with predominantly peas, wheat and maize (Baran *et al.* 2004). Monthly time series of concentrations of atrazine and its degradation product deethylatrazine (DEA) are available from seven piezometers and the Brévilles spring since 2001. The application of atrazine on the catchment was halted in 2000.

4.2.4 Elbe basin

The groundwater bodies in the Bille-Krückau watershed (1300 km²), located in Schleswig-Holstein, northern Germany, consist of unconsolidated glacial deposits of sand and gravel (Korcz *et al.* 2004). The sediments were deposited during the last and previous glaciations and subsequently denudated to a plateau-like landscape approximately 40 m above mean sea level. The area is drained by a dense network of natural streams, of which the Bille River is the largest draining 335 km². Groundwater is abstracted for drinking water purposes from the sandy and gravely deposits.

Two groundwater quality monitoring networks are in place, aimed at describing the natural conditions (baseline) and detecting trends in groundwater quality (trend). From these networks composed of 27 observation screens in total we selected 19 time series, sampled bi-annually from 8 shallow and 11 deep monitoring wells. The time series contain the concentrations of major cations and anions, from which we selected K, NO_3, Al and Cl, and constructed OXC and SUMCAT, for trend analysis

4.3 Approaches to trend analysis and their application

4.3.1 Statistical trend detection and estimation

The success of a statistical trend analysis largely depends on selecting the right statistical tools (Harris *et al.* 1987) considering various aspects of the available data: whether the data are normally distributed or contain seasonality (Hirsch *et al.* 1982), whether the trend is monotonic or abrupt (Hirsch *et al.* 1991), whether trends are expected to be univariate or multivariate (Loftis *et al.* 1991b). Loftis (1996) suggested that a clear definition of "trend" should be adopted before analyzing the data. Here we define a temporal "trend" as *a significant change in groundwater quality over a specific period of time, over a given region, which is related to land use or water quality management*.

The aim of the statistical methods deployed on three of the test sites was to detect and estimate statistically significant changes in the concentrations of contaminants over time.

The methods had to be robust and applicable to typical groundwater quality time series, with a limited amount of data, a rather short observation period with possibly missing data, often non-normally distributed, either annually sampled or containing seasonal trends. To meet these requirements, a three-step procedure was adopted (Batlle-Aguilar *et al.* 2005; Batlle-Aguilar *et al.* 2007) following Hirsch *et al.* (1991). First, time series were tested for normality; second, the presence of a trend was assessed; and third, the slope of the trend was estimated. The procedure (Figure 4.3) was applied to various time series from different study sites.

To test the data for normality, the Shapiro-Wilks test (Shapiro and Wilk 1965) was applied to datasets with less than 50 records, while the Shapiro-Francia test (Shapiro and Francia 1972) was applied to datasets containing 50 or more records. On time series which were normally distributed, a linear regression was performed. The correlation coefficient was used to assess the robustness of the trend (Carr 1995). On time series with a non-normal distribution, the non-parametric Mann-Kendall test (Mann 1945; Kendall 1948) was performed. This test is commonly used in hydrological sciences since its appearance in the paper by Hirsch *et al.* (1982) as it is rather insensitive to outliers (Helsel and Hirsch 1995) and has recently been proven as powerful as the Spearman's rho test (Yue *et al.* 2002). If a significant trend was detected, the slope of the trend was determined as the slope of the linear regression equation for normally distributed time series, or using Kendalls slope for non-normal time series (Hirsch *et al.* 1991). To aggregate the trend analysis over the entire groundwater body, the number of significant trends was expressed as a percentage. Additional analyses could include the determination of the median trend, or the spatial distribution of trends across groundwater bodies.

Application

Statistical trend analysis was applied to the dataset of 34 time series of concentrations from the Dutch part of the Meuse basin. Investigated solutes were nitrate (NO_3) and potassium (K), and two conservative chemical indicators: oxidation capacity (OXC) and sum of cations (SUMCAT). The time series from shallow (8 m below surface) and deep (25 m below surface) were analyzed separately. Non-parametric statistical trend analysis demonstrated significant trends for OXC and SUMCAT concentrations: increasing in deep screens and decreasing in shallow screens. No significant trends for NO_3 were detected (Visser *et al.* 2005b).

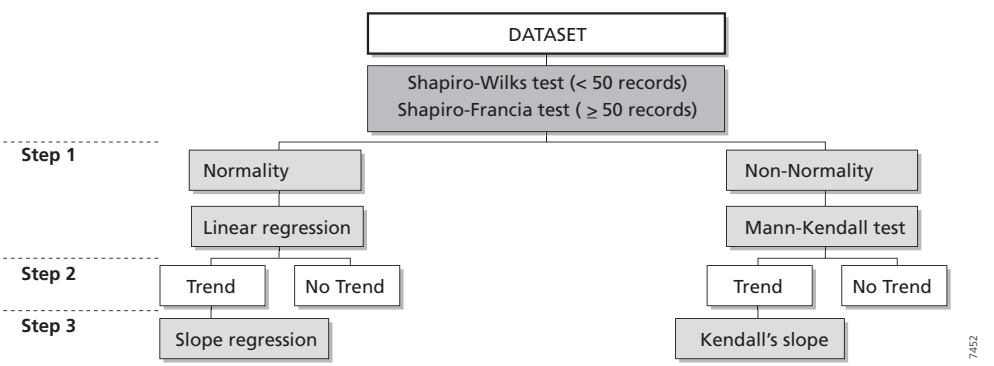

Figure 4.3 A three-step procedure is adopted for statistical trend analysis of contaminant concentrations in the selected groundwater bodies: 1) normal/non-normal distribution data; 2) trend detection; 3) trend estimation (Batlle-Aguilar *et al.* 2007).

Table 4.2 Summary of results for trend tests for each groundwater body in the Belgian part of the Meuse basin

Groundwater body	Number of nitrate sampling sites	Number of downward trends	Number of upward trends	Percent of significant trends
Geer basin	26	0	15	57.7%
Pays de Herve	12	2	6	66.6%
Néblon basin	6	1	4	83.3%
Alluvial plain	38	15	11	68.4%

Statistical trend analysis was applied to 97 nitrate time series from the Belgian part of the Meuse basin (Table 4.2). Significant trends were detected in 60% of the time series (Batlle-Aguilar *et al.* 2005). Most of the detected trends were increasing, except for the Meuse alluvial plain, where both increasing and downward trends were detected. For 36 time series in the Geer basin, the estimated slope was used to predict the year in which the concentration of nitrate would exceed the drinking water limit (50 mg/l). For most of the points, the drinking water limit is estimated to be exceeded within 10-70 years (Batlle-Aguilar *et al.* 2007). This estimate represents a worst-case scenario, as it does not assume changes in land use and agricultural practices to protect groundwater quality.

Finally, statistical trend analysis was applied to the time series of NO_3, K, Al, OXC, Cl and SUMCAT concentrations from the Bille-Krückau watershed in the Elbe basin (Table 4.3). Time series from shallow and deep screens were analyzed separately. For the conservative solutes Cl, OXC and SUMCAT, significant upward trends were detected in time series from deep monitoring screens, whereas significant decreasing concentrations were detected in time series from the shallow screens (Korcz *et al.* 2007). A further analysis of spatially weighted means indicated significant downward trend of potassium in shallow screens and significant upward trends of chloride and sum of negative ions. Significant trends were not detected in deep screens.

4.3.2 Groundwater dating

Groundwater dating as a tool to aid trend detection was applied on all four datasets. Groundwater dating requires the possibility to accurately sample a range of groundwater age tracers, preferably $^3H/^3He$ (Schlosser *et al.* 1988), or CFCs (Busenberg and Plummer 1992) and/or SF_6 (Busenberg and Plummer 2000). If these gaseous tracers are impractical, a qualitative approach based on ^3H measurements alone can be applied to distinguish between old (recharged prior to 1950) and young (recharged after 1950) groundwater (Orban and Brouyère 2007).

Table 4.3 Percentage of the individual time-series of the Bille-Krückau dataset showing a significant trend

	NO3	K	Al	OXC	Cl	SUMCAT
shallow	-	40% ↓	-	20% ↓	20% ↓	20% ↓
deep	-	11% ↓	-	33% ↑, 11% ↓	44% ↑	11% ↑

↑: significant upward trend, ↓: significant downward trend

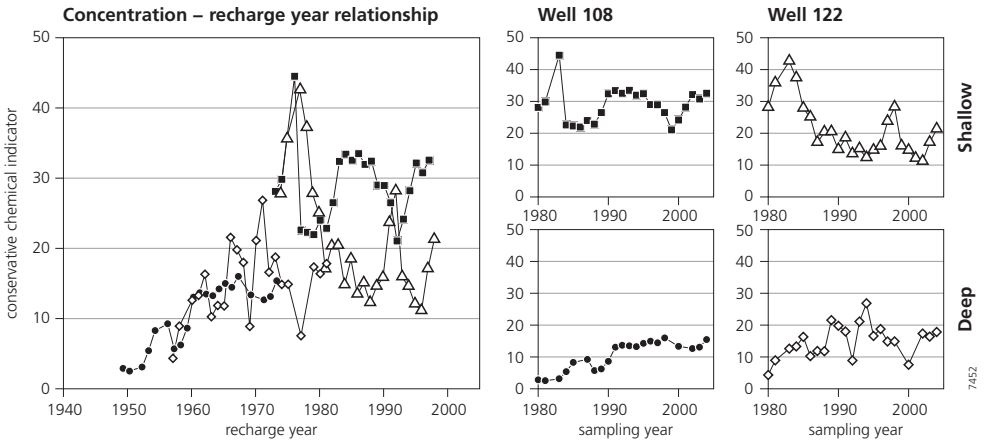

Figure 4.4 Example of the use of groundwater dating as a tool to aid trend detection. The concentrations of a conservative chemical indicator (OXC) sampled from the shallow (8m) and deep (24m) screens of two observation wells. Concentrations are plotted at the time of sampling (right) and plotted at the recharge year of the sampled groundwater (left). The result is the *concentration – recharge year relationship*, from which a clear trend can be observed that was not visible in the individual time series.

The aim of groundwater dating is to remove the travel time of groundwater as a complicating factor for trend analysis and aggregate monitoring data from wells across groundwater bodies. This was obtained by relating measured concentrations directly to the time of recharge (Figure 4.4). In the Dutch part of the Meuse basin, the aggregated data were analyzed using a LOWESS smooth (Helsel and Hirsch 1995) to indicate the general pattern of change and compare that to contamination history and trends in the aggregated data were detected using simple linear regression. Trends detected in this way could directly be related to changes in land use or contamination history.

Application

Samples from 34 monitoring screens in the Dutch part of the Meuse basin were analyzed for $^{3}H/^{3}He$, CFCs and SF_6, to determine groundwater travel time and recharge date. CFC samples showed irregularities attributed to degassing caused by denitrification (see Chapter 5) and contamination (Visser *et al.* 2005b). $^{3}H/^{3}He$ ages were considered more reliable following internal checks on degassing or contamination. $^{3}H/^{3}He$ ages were used to interpret the time series of concentrations, by relating concentrations to the estimated time of recharge and aggregating all data available for the entire groundwater body (Visser *et al.* 2005a). The aggregated data were analyzed using linear regression to detect trends in concentrations in groundwater recharged between 1960 and 1980, or between 1990 and 2000 (Figure 4.5). Significant upward trends were found in the concentrations of NO_3, K, OXC and SUMCAT in "old" groundwater (recharged between 1960 and 1980), but also significant downward trends in the concentrations of NO_3, OXC and SUMCAT in young groundwater (recharged between 1990 and 2000). These results (Chapter 2) demonstrated trend reversal in groundwater quality on the relevant scale of a groundwater body, as required by the EU Groundwater Directive (EU 2006).

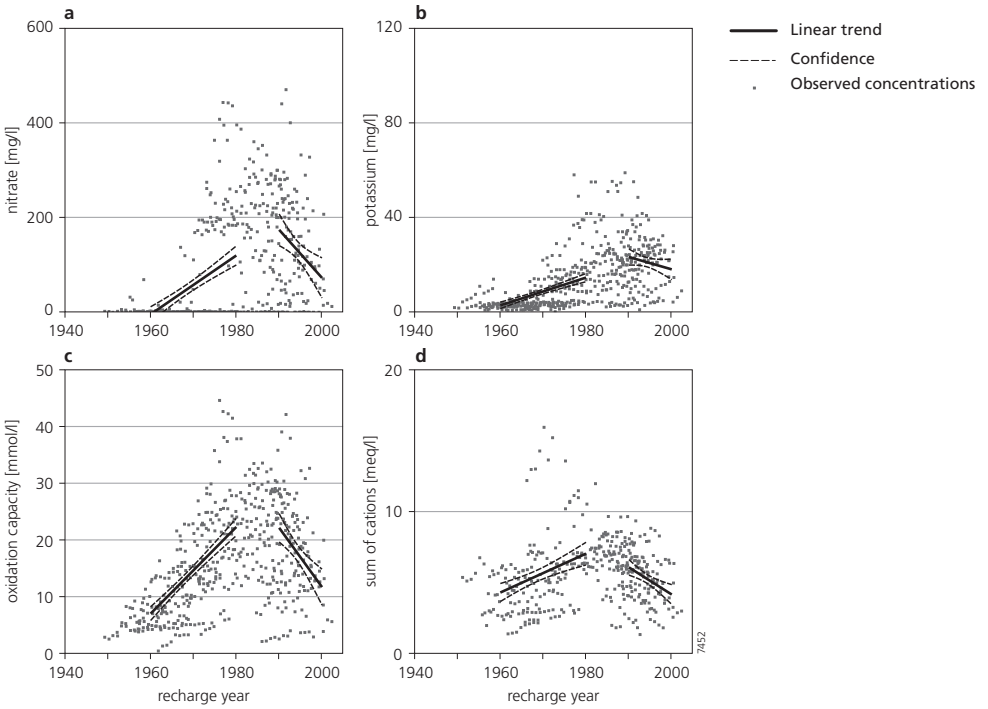

Figure 4.5 Linear trends through *concentration – recharge year* data from the Dutch part of the Meuse basin show significant trend reversal between 1980 and 1990 for nitrate (a), oxidation capacity (c) and sum of cations (d).

Tritium samples were taken from 33 monitoring points in the Geer basin. The distribution of tritium concentrations only shows a distinction between "old" (>50 years) and "young" groundwater (Figure 4.6), because travel times cannot be estimated accurately and univocally based on the tritium concentration only. High concentrations of tritium were observed in a large southwestern portion of the basin, where recharge is assumed to take place. Towards the downstream end of the basin, tritium concentrations decrease, indicating mixing of younger and older groundwater. No tritium is found in the northern confined part of the basin, indicating old (<1950) groundwater (Orban and Brouyère 2007). The presence of old groundwater explains the absence of nitrate in this part of the aquifer.

The interpretation of groundwater age tracers (^{3}H and CFCs) is not straightforward in hydrogeological complex systems like the Brévilles catchment. An experimental sampling campaign was performed to assess whether an extensive data set of groundwater age tracers would provide additional knowledge on the functioning of the system. Tritium and CFC were analyzed in samples taken from 8 piezometers and the Brévilles spring. The estimated ages showed a high variability within the small catchment with both old (<1960) and young (>1980) water in close proximity. The individual CFC ages (CFC-11, CFC-12, and CFC-113) were generally in good agreement, but some samples showed signs of degradation or contamination. Qualitative tritium groundwater age estimates were generally younger than the CFC age due to the dual porosity nature of the system. The tracers confirmed the complex hydrogeology of

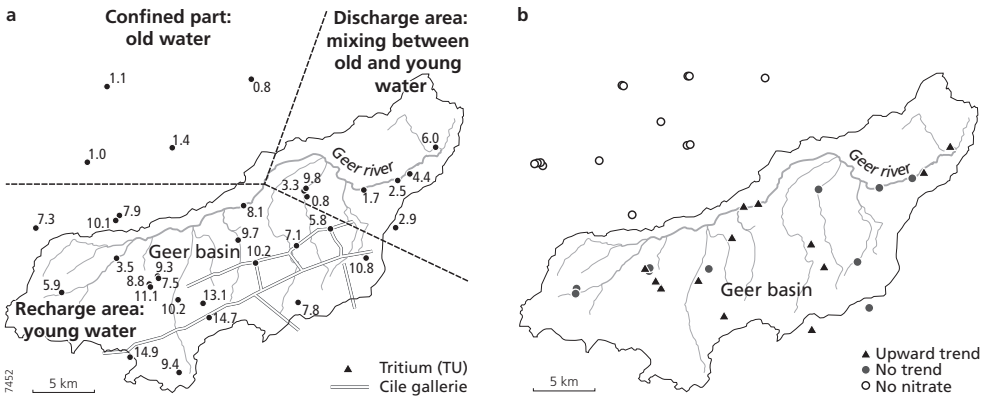

Figure 4.6 Spatial distribution of tritium (a) and trends in nitrate concentrations (b) in the Geer basin.

the system, but could not be used for reliable age dating and trend interpretation because of the likely mixing coccuring in the thick unsaturated zone (Gourcy *et al.* 2005).

For the Elbe dataset, an empirical exponential relationship between depth and groundwater age was assumed, instead of dating groundwater using tracers. Such an exponential increase in groundwater age with depth may be expected in unconsolidated unconfined aquifers like the Bille-Krückau catchment (Vogel 1967). Using the empirical relationship, the groundwater quality time series were related to the approximate time of recharge and analyzed again for trends using LOWESS smooth (Figure 4.7). The LOWESS smooth approach showed that the overall pattern in the measured concentration – recharge time relationship is similar to the historical surplus of N applied at the surface. Similar results were found in the Dutch part of the Meuse basin, probably due to the similarities in land use history and hydrogeology.

4.3.3 Transfer functions to predict future trends

The aim of the transfer function approach deployed in the dataset from the Brévilles catchment in France was to detect and extrapolate trends in the concentrations of agricultural contaminants in macro-porous or dual-porosity systems where concentrations are strongly correlated to other hydrological parameters, such as precipitation or stream flow. Transfer functions were identified

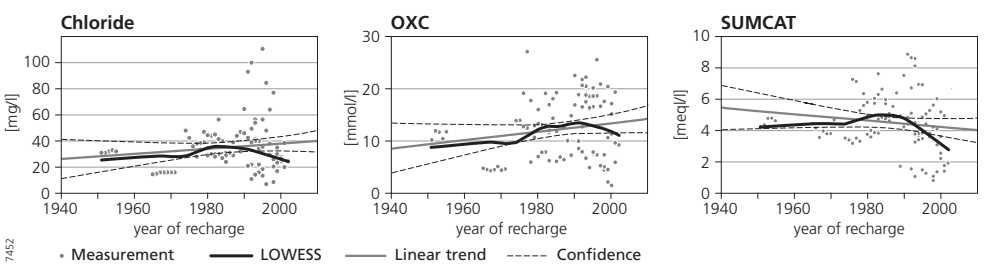

Figure 4.7 Linear trends and LOWESS smooth lines through concentrations of Cl, OXC, and SUMCAT in relation to time of recharge from the Elbe Basin.

and applied using the TEMPO tool (Pinault 2001) which is capable of modeling time series through iterative calibrations of combinations of transfer functions (Pinault *et al.* 2005).

Hydraulic heads were modeled as a function of effective rainfall using combined convolution functions for transport and dispersion, while effective rainfall was modeled as a function of the actual rainfall and of a threshold value representing the water storage in the soil (Pinault and Dubus 2008). The threshold value for soil water storage was related to the rainfall and potential evapotranspiration with trapezoid impulse response functions with four degrees of freedom. Concentrations of contaminants were modeled in a similar fashion, using the effective flux of the contaminant from the unsaturated soil instead of the effective rainfall, to predict the flux or concentrations in the Brévilles spring. To predict spring fluxes and concentrations, the impulse response functions were extended to include the contribution of various pathways of contaminants to the spring. Future concentrations were calculated based on 5-year long generated

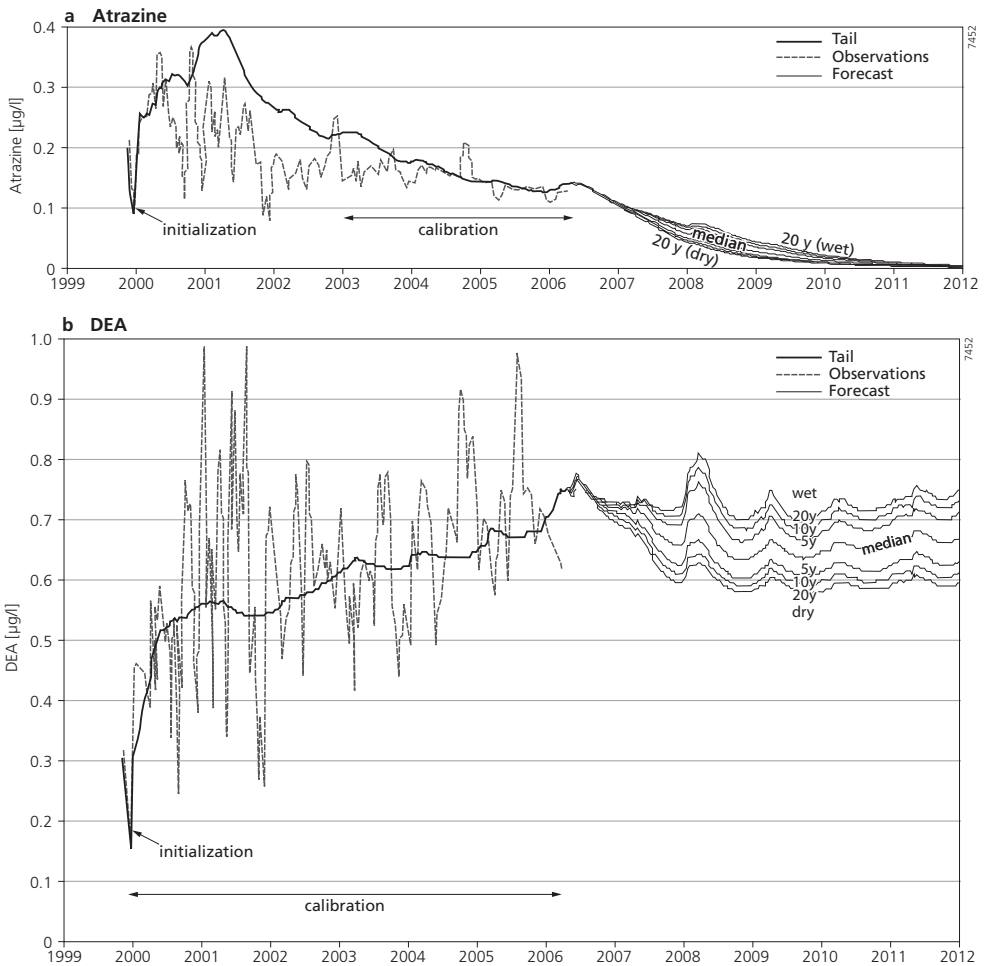

Figure 4.8 Predictions of the TEMPO software for concentrations of atrazine and the atrazine metabolite DEA (Deethylatrazine) at the Brévilles spring.

meteorological time series based on the median annual precipitation and the 5, 10 and 20 year extreme wet and dry years (Pinault and Dubus 2008).

Application

The transfer function approach was applied to time series of head, flux, and nitrate, atrazine and DEA concentrations from the piezometers and spring in the Brévilles catchment using the TEMPO tool (Pinault and Dubus 2008). The transfer function model was capable of reproducing the general trends in the time series, both in the monitoring wells and in the spring. The good fit is remarkable given the short monitoring period and the long travel times in the groundwater system, as indicated by impulse response functions of over 10 years long. Because of these long transfer times, it was possible to reconstruct the concentrations of the contaminants in the vadose zone (Pinault *et al.* 2005). Interestingly, the reconstructed inputs were in agreement with the historical application of atrazine in the catchment.

Future concentrations of atrazine and DEA at the Brévilles spring were predicted using the calibrated transfer function model and rainfall data generated by the TEMPO tool (Figure 4.8). The generated rainfall series contained either only wet or dry years, with historical recurrence intervals of 5, 10 or 20 years, to illustrate the response of atrazine concentrations to different future climates. Atrazine release was predicted to occur more during wet years than in dry years. While atrazine concentrations in the spring are predicted to decrease dramatically over the next 5 years, concentrations of its metabolite DEA are expected to remain constant over the next decade (Pinault and Dubus 2008).

4.3.4 Physical-deterministic modeling

The aim of using physical-deterministic models was to predict future trends in groundwater quality in systems of varying complexity. Distributed groundwater flow and transport models were developed separately and specifically for three sites. Transport models included advective transport, hydrodynamic dispersion and, where necessary, dual-porosity effects, sorption and degradation of contaminants. Predictions of future concentrations were based on scenarios of land use and agricultural application of fertilizer and pesticides, and climate scenarios.

For the Kempen region in the Dutch part of the Meuse basin, the physical-deterministic groundwater flow and transport model was a steady-state MODFLOW (Harbaugh *et al.* 2000) model for groundwater flow, and MT3DMS (Zheng and Wang 1999) for solute transport. Historical concentrations of contaminants at the land surface were reconstructed based on statistical records of atmospheric depositions and manure applications (Van der Grift and Van Beek 1996). Leaching of heavy metals from the unsaturated zone, sensitive to sorption and fluctuating water tables, was modeled with Hydrus-1D (Van der Grift and Griffioen 2008). The coupled transport model was used to predict concentrations of nitrate, potassium and heavy metals in groundwater at the monitoring locations within the model area (Visser *et al.* 2006).

For the Geer basin in the Walloon part of the Meuse basin, a physical-deterministic model was constructed (Orban *et al.* 2005) using the SUFT3D code (Carabin and Dassargues 1999). This model combines a new approach to model the solute transport (Hybrid Finite Element Mixing Cell) with a conventional finite element model for groundwater flow based on Darcy's law both in the saturated and partially saturated zones. The model was calibrated on groundwater levels, as well as measured tritium concentrations. The model was used to reproduce and to extrapolate observed nitrate concentrations in the Geer basin at the monitoring points.

For the Brévilles catchment in France, the physical deterministic model constructed consisted of the combination of a series of a 1D unsaturated zone models to simulate water flow and contaminant transport through the fissured dual porosity chalk, and a 2D groundwater flow and transport model for the Cuise sands (Dubus *et al.* 2005). The 1D pesticide fate model MACRO (Jarvis 1994) was used to simulate transport through the root zone, taking into account preferential flow phenomena, while transport through the unsaturated zone was modeled using MARTHE (Thiéry 1990). The combined model was used to reproduce observed groundwater levels, as well as nitrate, atrazine and DEA concentrations in piezometers and in the Brévilles spring. Thirteen regional climate model scenarios were used for predicting future trends in concentrations.

Application
The 3D model built for the Kempen area in the Dutch part of the Meuse basin predicted significant trends in the concentrations of nitrate and OXC for the period 1995-2005: upward in deep groundwater, downward in shallow groundwater (Visser *et al.* 2008). Due to variations in groundwater travel times and the constant recharge concentrations from 2005 onward, few significant trends are predicted for the future, except a decrease in OXC between 2010 and 2020. Between 2010 and 2020, the model also predicted a significant upward trend in the concentration of zinc in shallow groundwater. This trend is caused by a slow release of zinc accumulated in the unsaturated zone and the retarded transport of zinc through the groundwater system due to cation exchange (Broers and Van der Grift 2004; Van der Grift and Griffioen 2008).

The physical deterministic model of the Geer basin was capable of reproducing both groundwater levels and the distribution of tritium in the aquifer (Orban *et al.* 2008). The model also accurately reproduced the upward trends in nitrate concentrations in the Geer basin. The future evolution of nitrate trends in groundwater was computed for different scenarios of nitrate concentrations in the leaching water. The time before trend reversal is a function of the location of the monitoring points in the basin. In the Southern part of the basin, time before reversal is a function of the thickness of the unsaturated zone where the nitrates move slowly. In the Eastern part of the basin, due to the mixing between old and young water, trend reversal would not occur in the next fifty years and nitrate concentrations would still increase (Orban *et al.* 2008).

The physical deterministic model of the Brévilles catchment accurately reproduced the observed groundwater levels at the piezometers and also the discharge from the Brévilles spring (Amraoui *et al.* 2008). Predicted atrazine concentrations at the piezometers were in the same order of magnitude as the measurements, but predicted concentrations underestimated observations in the spring, probably due to the lack of accurate data on the application of atrazine on individual fields in the catchment. Similar to the predictions made using the transfer function approach, concentrations of atrazine in piezometers were predicted to decrease exponentially over the next 14 years. A slower decline in the concentrations was predicted for the spring.

4.4 Discussion of trend detection approaches

In this section, we discuss each of the methods applied in this study in terms of data requirement, additional monitoring costs, applicability in different geohydrological systems, and their power

Table 4.4 Summary table comparing the strengths and weaknesses of each of the trends analysis methodologies based on the experiences of their application to the four test sites and datasets.

	Purely statistical approaches	**Transfer function approaches**	**Age dating**	**Deterministic modeling with poor fit to the data**	**Deterministic modeling with good fit to the data**
Data requirements	monitoring data	monitoring data + information on the input flux (rainfall, and either inputs or land use)	monitoring data + analysis of tracers in samples	monitoring data + collection of additional information (other piezometers, pumping and tracer tests, geophysics, soil mapping)	monitoring data + collection of additional information (other piezometers, pumping and tracer tests, geophysics, soil mapping)
Associated cost magnitude (on top of the data collection effort)	0	1 (surveys if not already available – purchasing of meteo data)	10	100 (geophysics, additional piezometers, soil mapping)	100 (geophysics, additional piezometers, soil mapping)
Requirements on the understanding of the groundwater system	No understanding of the system	Functional understanding of the system (identification of the key factors and understanding of their influence)	Functional understanding of the system	Detailed data on the system, but lack of overall understanding of the functioning of the system	Detailed understanding of the system under study
Extrapolation potential	Poor	Good	Good	Poor	Very good
Potential universality to all systems	Potentially	Potentially	Limited, only applies to homogeneous systems.	Potentially	Potentially
Potential for operational use	-	+	+	-	+
Source of new knowledge about the functioning of the system	-	+	+	+	++

to extrapolate. Prerequisites, costs, and overall usefulness of all methods are summarized in Table 4.4.

4.4.1 Statistical trend detection and estimation

The three-step approach to detect trends in groundwater quality was applied at three test sites and proved to be a simple and easily applicable technique to existing time series of contaminant concentrations, having a normal distribution or not, making it universally applicable (Table 4.4). Statistical trend detection requires time-series that span several years to decades to detect a significant trend, depending on the hydrogeological system and monitoring network. If the quality of the available datasets is sufficient, it requires no additional costs for sampling. The approach provides an objective detection of trends.

Statistical trend analysis may be of limited operational use because no link to the driving forces (e.g. meteorological data, groundwater flow and travel times or historical agricultural practices) is incorporated in the analysis, and no knowledge about the functioning of the system will be gained by its application. Therefore the trends that are found in individual time series may be extrapolated over short periods of time only. Statistical trends cannot sensibly be extrapolated over longer periods of time, because they are incapable of dealing with changes in agricultural practices, meteorological conditions or the groundwater flow system. Statistical tend analysis is not capable of predicting trend reversal, which is a major disadvantage. In conclusion, statistical trend analysis provides a sound initial survey of possible changes in groundwater quality as required by the EU Groundwater Directive (EU 2006), but is little suited for operational use to analyze whether these changes will pose a threat for future groundwater quality.

4.4.2 Groundwater dating

Groundwater dating can be used to reinterpret groundwater quality time series and demonstrate trend reversal in groundwater quality. Monitoring wells with short and known location of the screens are of benefit, because groundwater is expected to have a distinct age, rather than to be a mixture of older and younger water. In single porosity aquifers with short-screened monitoring wells, groundwater dating greatly enhances the interpretation of groundwater quality data by eliminating variations in groundwater age as a complicating factor. Knowledge about the travel times in the groundwater system enhances the understanding of the flow system and may also explain the slow improvement of groundwater quality (Table 4.4).

In hydrogeologically complex systems such dual porosity aquifers, or under a variably or thick unsaturated zone, groundwater age tracers are difficult to interpret and may only confirm the complexity of the system and proper application is limited to more simple groundwater systems. Qualitative groundwater dating using tritium can be applied to detect the presence of "old" groundwater, which may for example explain the presence of nitrate at low concentrations due to old age rather than denitrification.

Groundwater dating requires a substantial financial investment for sampling and sample analysis, even if a proper monitoring network is in place. The benefit is that the existing groundwater quality data becomes more valuable as the re-analysis of this data may reveal trends that could not be demonstrated without knowledge of the recharge times of the groundwater samples. This makes groundwater dating suitable for operational use, where applicable.

4.4.3 Transfer functions to predict future trends

The transfer function approach is intermediate between statistical and deterministic models. If the available data are sufficient to calibrate a transfer function that expresses the delay in transfers of water and pollutants in the systems considered, transfer functions require no additional financial investment (Table 4.4). The main advantages of transfer functions are that they require little information about the physical functioning of the system, but rather rely on the available data, which makes them suitable for application in a wide variety of systems.

Transfer functions provide a good agreement with measured time series in the complex aquifer of the Brévilles catchment showing that they are capable of reproducing the non-linear behavior of dual porosity systems (Pinault and Dubus 2008), where other approaches failed. This makes them suitable for operational use in these systems. Transfer functions may be used for trend extrapolation, but only with great care to ensure that the predicted trends are within the range of the observations. In these systems, groundwater dating may serve to confirm the hydrological functioning and transfer times of the system.

4.4.4 Physical-deterministic modeling

Because of the geohydrological diversity among test sites, site-specific physical-deterministic models had to be built. One of the main issues associated with deterministic modelling is the need to have a detailed characterization of the system under study available in terms of meteorology, soils, subsoils, hydro(geo)logy and use of pollutants on the catchment. This typically requires very significant financial and time investments in the field, which usually spans over several years. On the other hand, one of the great advantages of undertaking deterministic modelling activities is that it brings together various sources of information collected in the field that allow the expansion of the understanding of the catchment functioning using both measured and predicted information. Although there is no dispute as to the usefulness of intensive catchment modelling activities from a research point of view, the 'return on investment' from an operational perspective is mainly dependent on whether a model can be successfully fitted to the data and whether the model has shown potential for supporting extrapolation and management activities. A distinction was therefore made in Table 4.4 between modelling efforts which provide successful fit to measured data and trends, and those where the fit to the data is considered to be below the standard for operational activities.

The very large financial, human resources and time investments associated with the collection of data and their integration into an overarching modeling exercise means that the deployment of deterministic models for operational analysis of trends across the EU is beyond reach, even if a good fit to the data would be obtained. Such modeling activities should concentrate on areas of high ecological, sustainability or economical importance within the context of the Water Framework Directive.

The main advantage of physically-deterministic models is their capability to predict trends in the future that are not yet observed in the monitoring data, for example due to the slow release of zinc from the unsaturated zone. They can provide estimates of the time scales at which trend reversal should be expected as a result of protective legislation, which may be several decades because of the long travel times of groundwater. Physical-deterministic models may also be used for scenario analysis to aid policy makers decide on the effectiveness of proposed regulations.

4.5 Conclusions

Trend detection as required by the GWD is dedicated to detect trends in the concentrations of pollutants resulting from anthropogenic sources and distinguish these from natural variation with an adequate level of confidence and precision (GWD, Annex V, art 2(a)(i)). To address the challenges of the WFD, a number of working groups were asked to design a common implementation strategy (CIS) and produce "guidance documents" for the implementation of the WFD. The mandate of the Groundwater Working Group (WGC) required the development of practical guidance and technical specifications for the derivation of threshold values, the assessment of status compliance (both quantitative and chemical) and the assessment of groundwater trends and trend reversal. The focus of the guidance document on "statistical aspects of the identification of groundwater pollution trends, and aggregation of monitoring results" (Grath *et al.* 2001) left little room to include conceptual understanding of the factors determining groundwater quality. In recent years, it was generally realized that a conceptual understanding of the groundwater systems is essential for the characterization of chemical status and the detection of trends (EU 2007). It is our conclusion that only for an initial survey to detect changes in groundwater quality, a classical statistical approach is most suitable, but more elaborate approaches to trend detection including more information about the groundwater body and contaminant transport may have a higher chance of determining and understanding significant and sustained upward trends or trend reversal.

The most important difference between groundwater bodies is whether the character of the subsurface or the monitoring system causes mixing of groundwater with different travel times. In single porous systems, groundwater at a specific location typically has a distinct groundwater age. In practice, the possibility of sampling groundwater with a distinct age also requires a monitoring network with short (< 5 m) monitoring screens or the use of packers in long screened wells to prevent mixing during sampling. In simple single-porosity groundwater bodies with access to monitoring wells with short screens, groundwater dating has been applied by various studies as a tool for aggregating groundwater quality data and analyzing trends therein by relating the measured concentrations of pollutants to the time of recharge of the sampled groundwater (Böhlke and Denver 1995; MacDonald *et al.* 2003; Wassenaar *et al.* 2006; Burow *et al.* 2007; Tesoriero *et al.* 2007, Chapter 2, this thesis). The resulting concentration – travel time relationship can be linked directly to historical records of land use or agricultural practices. Recent publications presenting studies from the U.S. Geological Survey National Water-Quality Assessment program (NAWQA) in which concentrations are directly related to recharge time of groundwater conclude that groundwater travel times are invaluable to the detection of trends in existing groundwater quality data (Burow *et al.* 2008; Debrewer *et al.* 2008; Rosen and Lapham 2008; Rupert 2008; Saad 2008).

In dual porosity systems, a groundwater sample is likely to be the result of a young fast component and an old slow component. In such cases the contributions of either component should be separated to properly analyze the trends in groundwater quality. In complex dual-porosity systems, possibly with seasonal influences, a transfer function approach is likely to be better suited for trend detection.

Large-scale 3D models are suitable to extrapolate long-term trends, but they are less capable of predicting short-term variations due in part to their coarse resolution and simplified aquifer characteristics. The quality of predicted future trends relies on the appropriate incorporation of

important processes into the model, the fit of the model to the existing data, and accuracy of future land use, agricultural practices, and contamination scenarios.

Their advantage is their capability to predict trends in the future that are not yet observed in the monitoring data and provide estimates of the time scales at which trend reversal should be expected as a result of protective legislation (Van der Grift and Griffioen 2008). Because of the large financial, human resources and time investments required to obtain a model that shows a good fit to the data, deterministic groundwater modeling should be applied in areas with high ecological, economical or sustainability importance.

There is no unique solution to detect trends in groundwater quality across widely differing catchments and monitoring systems. The choice of the method for trend detection and extrapolation should firstly be made on the basis of the specific goals of the study (only trend detection or also extrapolation), the system under study, and the available resources (Table 4.5). While statistical trend detection may be suitable for preliminary surveys of trends in groundwater quality, more elaborate studies aimed at detecting trends should apply groundwater dating in unconsolidated aquifers or transfer functions in complex aquifers. Only for short-term extrapolation of trends, statistical approaches or transfer functions are suitable, because no direct link with the driving forces of the trends is included in these methods. Long-term extrapolation requires the use of deterministic models with a good fit to the available data, which are capable of predicting the effects of land use changes and various management scenarios.

Regardless of the complexity of the model used, being transfer functions or deterministic models, trend detection and extrapolation is always associated with uncertainty. This means that groundwater quality monitoring should remain a priority. Additional data will improve the detection of trends and increase the knowledge of the functioning of the groundwater system. Better understanding of the system, possibly derived from deterministic modeling, can in turn provide feedback for the optimization of the groundwater quality monitoring networks.

Table 4.5 Recommended preliminary and elaborate methods for trend detection and extrapolation in simple and complex groundwater systems.

		Groundwater system	
		Simple	**Complex**
Trend detection	**Preliminary**	Statistics	Statistics
	Elaborate	Groundwater dating	Transfer functions
Trend extrapolation	**Preliminary**	Statistical methods for short term extrapolation	Transfer functions for short term extrapolation
	Elaborate	Deterministic model	Deterministic model

PART II

GROUNDWATER AGE

5 Dating degassed groundwater with $^{3}H/^{3}He$

This chapter has been published as:
Ate Visser, Hans Peter Broers, and Marc F. P. Bierkens (2007) *Dating degassed groundwater with $^{3}H/^{3}He$*, Water Resources Research, 43, W10434, doi:10.1029/2006WR005847.

Abstract

The production of gases in groundwater under contaminated locations by geochemical and biological processes is not uncommon. Degassing of these gases from groundwater and re-partitioning of noble gases between water and gas phase distorts groundwater dating by $^{3}H/^{3}He$. We observed noble gas concentrations below atmospheric equilibrium in 20 out of 34 groundwater samples from agriculturally polluted sandy areas in the Netherlands. From the absence of nitrate in degassed samples, we conclude that denitrification causes degassing. The $^{22}Ne/^{20}Ne$ ratios show that degassing had attained solubility equilibrium and had not caused isotopic fractionation by diffusion. To correct for the loss of tritiogenic ^{3}He due to degassing, we present a single-step equilibrium degassing model. We use the total dissolved gas pressure (TDG) at the monitoring screen to estimate the depth and timing of degassing, which is essential to estimate travel times from degassed samples. By propagating the uncertainties in the underlying measurements and assumptions through the travel time calculations, we found a travel time uncertainty of 3 years. We therefore conclude that $^{3}H/^{3}He$ dating can produce valuable information on groundwater flow even at sites with strong degassing.

5.1 Introduction

Groundwater resources valuable for drinking water and ecosystem functioning are threatened by nitrate pollution in most European and North American countries. To protect groundwater as a drinking water resource, a good understanding of the origin, transport and attenuation processes of pollutants (e.g. nitrate) in groundwater is needed. Knowledge of the travel time of groundwater can be used to estimate flow velocities, groundwater recharge rates, or to reconstruct past releases of contaminants into aquifers (Cook and Solomon 1997).

For travel times up to 50 years, $^{3}H/^{3}He$ is one of the most reliable groundwater dating methods today (Solomon *et al.* 1993; Ekwurzel *et al.* 1994; Cook and Solomon 1997; Kipfer *et al.* 2002). *Tolstikhin and Kamenski* (1969) suggested measuring the $^{3}H/^{3}He$ ratio to determine the travel time of groundwater. *Takaoka and Mizutani* (1987), *Poreda et al* (1988), *Schlosser et al* (1988) and *Solomon et al* (1992) were among the first to apply the method. Today it is commonly applied in groundwater studies aimed at aquifer characterization (Solomon *et al.* 1992; Solomon *et al.* 1995; Beyerle *et al.* 1999; Manning *et al.* 2005; Koh *et al.* 2006), assessing the susceptibility of

aquifers to contamination (Manning *et al.* 2005), contamination history reconstruction (Solomon *et al.* 1995; Shapiro *et al.* 1999) or to facilitate the demonstration of trends and trend reversal in groundwater quality (Chapter 2).

$^3H/^3He$ groundwater dating is based on the radioactive decay of tritium and the containment of the decay product ^3He in groundwater. It involves the sampling and measurement of dissolved noble gases and isotopes in groundwater (Cook and Solomon 1997): ^3He to calculate the $^3H/^3He$ ratio; helium, neon, argon, krypton and xenon to correct for excess air (Heaton and Vogel 1981; Stute *et al.* 1995; Aeschbach-Hertig *et al.* 2000) and possibly the neon isotope ratio to decide on the model to by used for excess air separation (Peeters *et al.* 2003). Only under completely saturated flow conditions can these noble gases be considered as perfectly conservative tracers (Gupta *et al.* 1994). The presence of a gas phase in the aquifer invalidates this prerequisite (Fry *et al.* 1995) because of gas re-partitioning between the water and gas phase.

The formation of a gas phase below the groundwater table by exsolution of gases from groundwater is not uncommon. This degassing process occurs when the total dissolved gas pressure exceeds the hydrostatic pressure (Fry *et al.* 1997). Degassing can be caused by a decrease of the hydrostatic pressure when groundwater flows upward (Thomas *et al.* 2003) or as a result of groundwater pumping (Fortuin and Willemsen 2005); or an increase of the total dissolved gas pressure by the production of gases like N_2, CO_2, H_2S or CH_4 by geochemical and biological processes in the aquifer. Degassing has been observed as a result of methane production under landfills (Solomon *et al.* 1992; Baedecker *et al.* 1993; Revesz *et al.* 1995; Van Breukelen *et al.* 2003; Purtschert *et al.* 2004) and in lake sediments (Holzner *et al.* 2004; Brennwald *et al.* 2005); under anaerobic conditions under rice fields (Klump *et al.* 2006) and as a result of N_2 production by denitrification under agricultural land (Blicher-Mathiesen *et al.* 1998). Because noble gases re-partition between the water and gas phase after gas formation, onward flowing groundwater can have noble gas concentrations below atmospheric equilibrium. Subsurface gas production at polluted sites may therefore lead to degassing of ^3He from the groundwater, complicating the $^3H/^3He$ dating method at polluted sites where groundwater dating is especially useful.

Degassing has been observed in $^3H/^3He$ samples before (Takaoka and Mizutani 1987; Solomon *et al.* 1992; Solomon *et al.* 1993; Ekwurzel *et al.* 1994; Purtschert *et al.* 2004; Klump *et al.* 2006). Solomon (1992) interpreted the $^3H/^3He$ measurements by assuming degassing near the water table, others assumed degassing during sampling (Solomon *et al.* 1993) or analysis (Takaoka and Mizutani 1987), or discarded the $^3H/^3He$ data completely. In Chapter 2, we applied $^3H/^3He$ to facilitate the demonstration of anthropogenic trends in groundwater quality in agriculturally polluted sandy recharge areas in the province of Noord-Brabant, the Netherlands. During analysis, we observed noble gas concentrations in groundwater below atmospheric equilibrium, indicating subsurface degassing.

In this paper we argue that the observed degassing in this case is caused by the production of considerable amounts of nitrogen gas by denitrification of agricultural pollution at a certain depth below the water table, and that the $^3H/^3He$ concentrations cannot be interpreted by assuming degassing at either recharge or sampling. Instead, we present a simple single-step degassing model to correct for ^3He loss to degassing using the total dissolved gas pressure in the sample to estimate the depth of degassing. We apply this correction to a data set of degassed $^3H/^3He$ samples to estimate the travel time of degassed groundwater. Finally, we use an error propagation method to assess the uncertainty of the travel times obtained from degassed groundwater samples.

5.2 Methods

5.2.1 Study area and data collection

The subsurface of the province of Noord-Brabant (5100 km^2), in the south of the Netherlands, consists of fluvial unconsolidated sand and gravel deposits from the Meuse River, overlain by a 2-30 m thick cover of Middle- and Upper-Pleistocene fluvio-periglacial and aeolian deposits consisting of fine sands and loam. Some sediments have a high organic matter content and in some areas pyrite occurs in the subsurface (Broers 2004b), both of which are capable of reducing nitrate.

Noord-Brabant is a flat area with altitudes ranging from mean sea level (MSL) in the north and west to 30 m above MSL in the southeast. Groundwater tables are generally shallow, usually

Table 5.1 Symbols and constants used in this chapter

Symbol	Description	Units
t_r	time of recharge	yr
t_d	time of degassing	yr
t_s	time of sampling	yr
h_0	depth of the water table	m
z_d	depth of degassing	m
z_s	screen depth	m
P_i	partial pressure of gas i	Pa
P_g	total pressure in gas phase	Pa
P_{hydr}	hydrostatic pressure	Pa
P_{cap}	capillary pressure	Pa
P_{TDG}	total dissolved gas pressure	Pa
ρ_w	density of water	kg/m^3
σ_w	surface tension of water (= 72.8×10^{-3} N/m at 293°C (Reid et al., 1987))	N/m
r	radius of bubble	m
λ	decay constant of ^{3}H	0.05626 y^{-1}
V_g	volume of exsolved gas per volume of water	cm^3/cm^3
$C_{w,i}$	concentration of (noble) gas i in water	cm^3 STP/cm^3
$C_{g,i}$	concentration of (noble) gas i in gas	cm^3 STP/cm^3
$R_{w,ij}$	ratio of isotopes i and j in water ($\equiv C_{w,i}/C_{w,j}$)	-
$R_{w,ij,0}$	ratio of isotopes i and j in water before degassing	-
$R_{g,ij}$	ratio of isotopes i and j in gas ($\equiv C_{g,i}/C_{g,j}$)	-
f_j	fraction of species j remaining in water after degassing ($\equiv C_{w,j}/C_{w,j,0}$)	-
$K_{H,i}$	Henry's law solubility coefficient ($\equiv C_{w,i}/P_i$)	(cm^3 STP/cm^3)/Pa
H_i	dimensionless Henry's law partitioning coefficient ($\equiv C_{g,i}/C_{w,i}$) $K_{H,i} = 1/(44.65\ R\ T\ H_i) = 9.513\times10^{-6}/H_i$ (at 10°C)	-
D_i	molecular diffusion coefficient of species i	m^2/s
$\alpha_{D,ij}$	diffusive fractionation parameter between isotopes i and j ($\equiv D_i/D_j$-1)	-
$\alpha_{M,ij}$	mass dependent fractionation factor between species i and j ($\equiv R_{w,ij}/R_{g,ij}$)	-
σ	standard deviation of measurement uncertainty	…
d_i	difference between duplicates of sample i	…
n	number of samples	-

1 cm^3 STP is 1 cm^3 gas under standard temperature and pressure (≡ 4.465×10^{-5} moles)
Here σ and d assume the units of the underlying variable

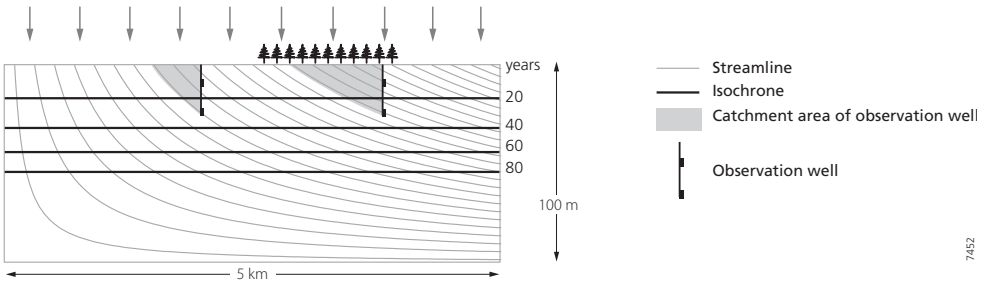

Figure 5.1 Schematic representation of groundwater flow in recharge areas. Groundwater flow is continuously downward in recharge areas and groundwater travel times increase with depth. Monitoring wells were placed such that the land use in the catchment area of the monitoring well was homogeneous.

within 1-5 m below the surface. A natural network of brooks, which developed in equilibrium with a shallow groundwater table, drained the area before 1900. To allow for agricultural use of the poorly drained areas, the natural drainage was artificially extended during the 20th century, resulting in a dense network of ditches, drains and small watercourses.

The geohydrological situation was mapped to identify homogeneous recharge areas for the design of the groundwater quality network of Noord-Brabant (Broers 2002). Homogeneous recharge areas lack a superficial drainage network, have relatively deep groundwater levels, permeable soils and high topographical position. Groundwater flow in these homogeneous recharge areas can be simplified to a two-dimensional model with impermeable left and bottom boundaries and a fully penetrating drain on the right (Figure 5.1). In this model, groundwater flows continually downward and groundwater travel times increase logarithmically with depth (Vogel 1967; Raats 1981). Monitoring wells were placed within the largest of the geohydrological homogeneous areas, using stratified sampling (Broers and Van der Grift 2004), such that the land use in the catchment area of the monitoring well was also homogeneous. The groundwater quality is monitored because Noord-Brabant is one of the areas in Europe which is most affected by agricultural pollution. Intensive livestock farming in the area produces a large surplus of nitrate rich manure. The agricultural recharge areas of the province of Noord-Brabant are vulnerable to diffuse groundwater pollution with nitrate because groundwater and contaminants can leach deep into the subsurface.

We selected 14 monitoring wells in recharge areas of several watersheds located throughout the province of Noord-Brabant (Figure 1.2) with intensive livestock farming in each of the catchments. These wells serve as a random sample that represents the groundwater quality in the areas with the highest risk to deeper groundwater, because of high pollutant loadings and vulnerable soils. The wells consist of nested piezometers with a diameter of 5.2 cm and a screen length of 2 m. Most wells had two piezometers, with screens at about 8 or 25 m below surface (Van Duijvenbooden 1993; Broers 2002).

We took tritium and noble gas samples from these wells with a submersible pump (MP1, Grundfos). Before sampling, the wells were purged for approximately 30 minutes until field parameters (temperature, pH, electric conductivity and dissolved oxygen concentration) measured in a flow-through cell showed constant values. Nitrate concentrations were determined as part of the annual groundwater quality monitoring effort (Van Duijvenbooden 1993). The Bremen

Mass Spectrometric Facility (Sültenfuß *et al.* 2004) determined the concentrations of tritium, helium and neon and the $^{3}He/^{4}He$ and $^{22}Ne/^{20}Ne$ ratios. We measured total dissolved gas (TDG) pressure (Manning *et al.* 2003) with a TDG probe (T300E, In-Situ Inc.) at screen depth during a second sampling campaign in 2006.

5.2.2 Denitrification and gas formation

Denitrification by organic C and pyrite is described by (Postma *et al.* 1991):

$$5\,C + 4\,NO_3^- + 2\,H_2O \rightarrow 4\,HCO_3^- + CO_2 + 2\,N_2 \tag{5.1}$$

$$5\,FeS_2 + 14\,NO_3^- + 4\,H^+ \rightarrow 5\,Fe^{2+} + 10\,SO_4^{2-} + 2\,H_2O + 7\,O_2 \tag{5.2}$$

An increase of the concentration of nitrogen gas in water ($C_{w,i}$; see Table 5.1) after denitrification increases the partial pressure (P_i) of nitrogen gas in solution, controlled by Henry's law solubility coefficient ($K_{H,i}$), and consequently the total dissolved gas pressure (P_{TDG}), defined as the sum of partial pressures of all gases in solution including water vapor (ΣP_i), increases:

$$\Sigma \frac{C_{w,i}}{K_{H,i}} = \Sigma\ P_i = P_{TDG} \tag{5.3}$$

Nitrogen gas produced by denitrification will remain dissolved when the total dissolved gas pressure does not exceed the sum of atmospheric and hydrostatic pressure. If it does, gases escape from solution into a gas phase when capillary forces can be overcome (Fry *et al.* 1997). The volume of the gas phase (per liter water) is related to the initial nitrate concentration and the depth of the reaction, decreasing with depth and increasing with the initial amount of nitrate (Figure 5.2).

The total amount of N_2 per liter in both the dissolved and the gas phase equals the initial amount of nitrate ($[NO_3]$) divided by two to correct for the stoichiometry of the reaction plus the atmospheric equilibrium concentration of N_2 in groundwater ($N_{2,eq}$ = 0.648 mmol/l at 10°C, neglecting excess air). The amount of N_2 in the water phase depends on the solubility of N_2 (K_H = 0.840 mmol/l/atm at 10°C) and the pressure under which the reaction takes place (P_g), which is a function of depth (Equation 5.5). The depth of denitrification is related to the presence of organic matter or pyrite in the subsurface and the location of the redoxcline. The amount of N_2 in the gas phase is the difference between the total and dissolved amount of N_2. The volume of the N_2 gas phase produced by denitrification at depth z is then, according to the gas law:

$$Vg = \frac{\left([NO_3]/2 + N_{2,eq} - K_H P_g\right) RT}{P_g} \tag{5.4}$$

Once a gas phase is formed, the gas pressure inside the gas phase (P_g) will equilibrate with the sum of atmospheric (P_{atm}), hydrostatic (P_{hydr}) and capillary (P_{cap}) pressures that are acting on the gas phase (Holocher *et al.* 2003):

$$P_g = P_{atm} + P_{hydr} + P_{cap} \approx P_{atm} + z_g \rho_w g = P_{TDG} \tag{5.5}$$

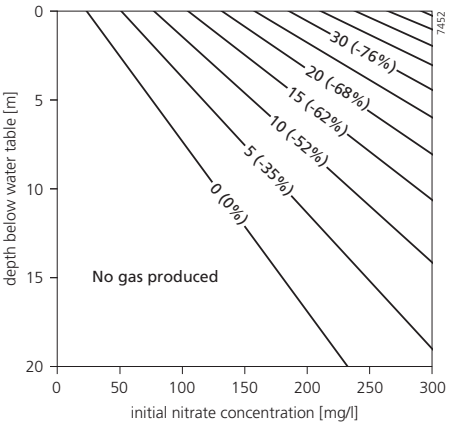

Figure 5.2 The volume of the gas phase (V_g) and amount of degassing (Δ^4He) depends on the initial concentration of nitrate and the depth of denitrification.

The capillary pressure inside a bubble is proportional to the surface tension of water (σ_w = 72.8×10^{-3} N/m at 293°C (Reid *et al.* 1987)) and the inverse of the radius of the bubble (r) as $P_{cap} = 2\sigma_w/r$. For bubbles with a radius of 10^{-4} m, capillary pressure is generally two orders of magnitude smaller than atmospheric pressure (Cirpka and Kitanidis 2001). We therefore neglected the capillary pressure in our calculations, but assessed the effect capillary pressures up to 0.1 atm in the uncertainty of the travel times by error propagation in section 4.5.

Neglecting capillary pressure and assuming a constant atmospheric pressure, the depth of the gas phase (z_g) below the water table controls the total gas pressure within the bubble (Equation 5.5). Because the partial pressures of gases within the bubble are related to the concentrations of dissolved gases outside the bubble (Equation 5.3), the depth below the water table is also one of the factors controlling the concentrations of dissolved gases, together with the composition of dissolved gases and their respective solubilities. Groundwater flow may separate the mobile aqueous phase and the immobile gas phase. If we assume no gas is formed or consumed after separation, the concentrations of dissolved gases at the monitoring screen are the same as at the location of degassing. Measuring the total dissolved gas pressure at the screen (P_{TDG}) then relates to the depth below the water table where degassing took place (z_d):

$$z_d = \frac{\left(P_{TDG} - P_{atm}\right)}{\rho_w g} \tag{5.6}$$

We used this relation as a constraint on the time of degassing in the correction of ^{3}He loss to degassing.

In our setting, the assumption that the total dissolved gas pressure at the screen is the same as at the depth of degassing is valid because:

1 The selected areas are recharge areas, where groundwater flows continually downward and depth below the water table – and thus hydrostatic pressure – increases with travel time. Degassing occurs where gas is produced and the total dissolved gas pressure exceeds the hydrostatic pressure. Further along the flow line, hydrostatic pressure increases and the total

dissolved gas pressure no longer exceeds the hydrostatic pressure. Therefore, degassing is not likely below the point where gas is produced.

2 Autotrophic denitrification by pyrite often results in a sharp redoxcline (Postma *et al.* 1991; Smith *et al.* 1991) where concentrations decrease to zero within a few meters across the redoxcline. At the same depths, sulfate concentrations increase sharply indicating denitrification by pyrite oxidation. Such a sharp redoxcline was observed in mini-screened wells in Vierlingsbeek (Van Beek *et al.* 1989) and Oostrum (Broers 2004b) in the same geological formations near wells 107 and 122.

3 Gas consumption or production after degassing is unlikely because oxygen is already consumed before denitrification and degassing takes place, and nitrogen gas is inert and can only be consumed by nitrogen fixing bacteria in the aerobic root zone. High concentrations of sulfate in denitrified samples indicate that extensive sulfate reduction is not taking place.

5.2.3 Degassing of noble gases

Re-partitioning of noble gases between the water and gas phase removes noble gases from solution when a gas phase is formed (Gupta *et al.* 1994; Fry *et al.* 1995; Donaldson *et al.* 1997; Donaldson *et al.* 1998). The transport of noble gases across the gas-water interface is initially controlled by diffusion, until solubility equilibrium is reached between the concentrations in water and gas (Equation 5.3). Diffusive transport causes isotopic fractionation of noble gases, which would seriously affect the interpretation and correction of ^{3}He measurements. Light noble gas isotopes (^{3}He, ^{20}Ne) diffuse faster into the gas phase and, as long as equilibrium is not attained, groundwater is enriched in heavy noble gas isotopes (^{4}He, ^{22}Ne). The fractionation between isotopes *i* and *j* caused by diffusion is related to the amount of degassing of isotope *j* (fraction of isotope *j* present in water after degassing: f_j) and the quotient of the diffusion coefficients of the isotopes *i* and *j* (α_{ij}, Table 5.2), according to the Rayleigh equation (Brennwald *et al.* 2005), relating the ratio of the isotopes *i* and *j* before ($R_{ij,o}$) and after (R_{ij}) degassing:

$$R_{ij} = R_{ij,0} f_j^{\alpha ij} \tag{5.7}$$

Table 5.2 Properties of helium and neon (at 10°C and zero salinity)

	atmospheric volume fraction	H [a] [-]	$K_{H,i}$ [a] ×10^{-8} [(cm^3 STP/cm^3)/Pa]	$\alpha_{M,ij}$ [-]	D [b] ×10^{-9} [m^2/s]	atmospheric isotopic ratio	atmospheric solubility ratio
^{3}He	5.24×10^{-6}	107.4	8.85	0.983[c]	6.56	1.399×10^{-6}	1.375×10^{-6}
^{4}He				-	5.68	≡1	≡1
^{20}Ne	1.818×10^{-5}	85.8	11.1	-	2.81	≡1	≡1
^{22}Ne				1.002[d]	2.94	0.1020	0.1022

a From *Ozima and Podosek* (2002)

b From *Jähne et al* (1987). Diffusivities of ^{3}He and ^{22}Ne were calculated assuming an inverse proportional relationship of *D* to the square root of the atomic mass. ($D_j = D_i \times (M_j/M_i)^{0.5}$) (Jähne et al., 1987) A recent molecular dynamics simulations study (Bourg and Sposito, 2008) suggests that the diffusivity of ^{22}Ne is more accurately approximated by $D_j = D_i \times (M_j/M_i)^{0.15}$.

c From *Benson and Krause* (1980)

d From *Beyerle et al* (2000).

Because the $^{3}He/^{4}He$ ratio may be affected by tritium decay and radiogenic or terrigenic ^{4}He production, we used the $^{22}Ne/^{20}Ne$ ratio to assess whether degassing had reached solubility equilibrium ("equilibrium degassing") or not ("diffusive degassing"). If the measured $^{22}Ne/^{20}Ne$ ratio resembled the atmospheric solubility equilibrium ratio (Table 5.2) we concluded that degassing had reached solubility equilibrium.

When equilibrium is reached between the concentrations in water and gas, the amount of noble gas that is removed from solution depends on the volume of the gas phase and the solubility of the noble gas (Table 5.2). Less soluble noble gases prefer the gas phase and are more depleted. We used this relation to calculate the volume of the gas phase from the depletion of ^{4}He. Because the solubility and diffusivity of ^{3}He and ^{4}He are nearly the same, we think that using the ^{4}He concentration to correct the ^{3}He loss to degassing is more accurate than using the Ne concentration. (In situations where measurements indicate a radiogenic ^{4}He component, correcting ^{3}He for degassing has to be based on the Ne concentration.) We assumed a single-step degassing process into one gas phase with volume V_g. By expressing the volume V_g per volume of water, we can use a simple mass balance to relate the concentration of ^{4}He in water before degassing ($^{4}He_{w,o}$) to the concentrations of ^{4}He in water ($^{4}He_{w}$) and gas ($^{4}He_{g}$) after degassing according to:

$$^{4}He_{w,0} = {}^{4}He_{w} + {}^{4}He_{g}\, V_g = {}^{4}He_{w}\left(1 + H_{He} V_g\right) \tag{5.8}$$

We related the ^{4}He concentration in gas to the concentration in water in Equation 5.8 using the dimensionless Henry's law partitioning coefficient (H_{He}). We further assumed that the concentration of ^{4}He before degassing ($^{4}He_{w,o}$) was the atmospheric equilibrium concentration ($^{4}He_{eq}$). Thereby we neglected the presence of excess air in the groundwater before degassing. From Equation 5.8 we can calculate the degassing volume from the ^{4}He concentration in the sample ($^{4}He_{s}$) according to:

$$V_g = \frac{{}^{4}He_{eq} - {}^{4}He_{s}}{{}^{4}He_{s} \bullet H_{He}} \tag{5.9}$$

If excess air was present before degassing, the calculated gas volume is an underestimation of the actual gas volume. As a result, we would underestimate the degassing of ^{3}He as well. We assessed the effect of this assumption by error propagation in section 4.5.

Conversely, one can calculate the expected depletion of noble gases from solution ($\Delta^{4}He$ and ΔNe, expressed as a percent deviation from the initial atmospheric equilibrium concentration) from the gas phase volume which is related to the depth and initial amount of nitrate according to (Figure 5.2):

$$^{4}He = \left(\frac{{}^{4}He_{w}}{{}^{4}He_{w,0}}\right) 1 \times 100\% = \left(\frac{1}{1 + H_{He} V_g} - 1\right) \times 100\% \tag{5.10}$$

$$Ne = \left(\frac{Ne_{w}}{Ne_{w,0}} - 1\right) \times 100\% = \left(\frac{1}{1 + H_{Ne} V_g} - 1\right) \times 100\% \tag{5.11}$$

For example, an initial concentration of 100 mg/l nitrate is sufficient to cause a depletion of ^{4}He of 24% (Δ^4He = -24%) when denitrification takes place at 5 m below the water table. With the gas volume calculated from the depletion of ^{4}He, we then calculated the fraction of ^{3}He present in solution after degassing ($f_{^3\mathrm{He}}$) as the concentration of ^{3}He after degassing ($^3\mathrm{He}_w$) divided by the concentration of ^{3}He before degassing ($^3\mathrm{He}_{w,0}$):

$$f_{^3\mathrm{He}} = \frac{^3\mathrm{He}_w}{^3\mathrm{He}_{w,0}} = \frac{1}{1 + H_{\mathrm{He}}\alpha_M V_g} \tag{5.12}$$

We considered the mass dependent isotopic fractionation between ^{3}He and ^{4}He (Benson and Krause 1980) by incorporating the fractionation factor α_M in Equation 5.12. Once we have the fraction of ^{3}He present in solution after degassing, we can use this together with the atmospheric equilibrium ^{3}He concentration ($^3\mathrm{He}_{eq}$) to estimate the amount of tritiogenic ^{3}He (produced by tritium decay) in the sampled solution ($^3\mathrm{He}^*_s$):

$$^3\mathrm{He}^*_s = {}^3\mathrm{He}_s - {}^3\mathrm{He}_{eq} \bullet f_{^3\mathrm{He}} \tag{5.13}$$

Again we neglected a possible excess air component and used the atmospheric equilibrium concentration ($^3\mathrm{He}_{eq}$).

Correcting the tritiogenic component of ^{3}He ($^3\mathrm{He}^*$) for degassing is more complicated because degassing only affects $^3\mathrm{He}^*$ that is produced before degassing; $^3\mathrm{He}^*$ that is produced after degassing is not affected. Therefore, the groundwater sample contains a 'mixture' of degassed $^3\mathrm{He}^*$ (produced before degassing) and undisturbed $^3\mathrm{He}^*$ (produced after degassing) (Figure 5.3B). Extreme cases are degassing at recharge (Figure 5.3A) and degassing at sampling (Figure 5.3C), when either none or all tritiogenic ^{3}He is degassed. Either of these cases is equally probable if no additional information is available. In that situation, correcting none or all tritiogenic helium for degassing yields minimum and maximum travel time estimates.

To properly correct for the degassing of the tritiogenic ^{3}He, we considered the continuous production of $^3\mathrm{He}^*$ by tritium decay and the single-step degassing of $^3\mathrm{He}^*$ at one point along the flow path. In an undisturbed sample the concentration tritiogenic ^{3}He ($^3\mathrm{He}^*_s$) is related to the sampled concentration of ^{3}H ($^3\mathrm{H}_s$), and the travel time from recharge to sampling (t_{rs}) and the tritium decay constant (λ):

$$^3\mathrm{He}^*_s = {}^3\mathrm{H}_s\left(e^{\lambda t_{rs}} - 1\right) \tag{5.14}$$

In a degassed sample, the concentration of tritiogenic ^{3}He is the amount of tritiogenic ^{3}He produced before degassing ($^3\mathrm{He}^*_{before}$) times the fraction of ^{3}He present in solution after degassing ($f_{^3\mathrm{He}}$), plus the amount of tritiogenic ^{3}He produced after degassing ($^3\mathrm{He}^*_{after}$). Similar to an undisturbed sample, the concentration of tritiogenic ^{3}He in a degassed sample is related to the measured concentration of tritium, the total travel time and the travel time between degassing and sampling (t_{ds}) as follows:

$$^3\mathrm{He}^*_s = f_{^3\mathrm{He}} \bullet {}^3\mathrm{He}^*_{before} + {}^3\mathrm{He}^*_{after} = f_{^3\mathrm{He}} \bullet {}^3\mathrm{H}_s\left(e^{\lambda t_{rs}} - e^{\lambda t_{ds}}\right) + {}^3\mathrm{H}_s\left(e^{\lambda t_{ds}} - 1\right) \tag{5.15}$$

5.2.4 Total dissolved gas pressure as a constraint on the moment of degassing

To solve Equation 5.15, we need to know the moment between recharge and sampling at which degassing took place. In a simple flow system, the travel time at a certain depth is a logarithmic function of recharge rate and aquifer thickness (Figure 5.1) (Vogel 1967; Raats 1981), which may be approximated by a linear increase of travel time with depth, if the depth is small compared to the thickness of the aquifer. The ratio between the travel time from degassing to sampling (t_{ds}) and from recharge to sampling (t_{rs}) is then proportional to the ratio between vertical distance between degassing and sampling ($z_d - z_s$) and the sampling depth (z_s) below the water table. For each sample, the travel time from degassing to sampling can be written as:

$$t_{ds} = t_{rs} \frac{z_s - z_d}{z_s} \tag{5.16}$$

Using the depth of degassing derived from the total dissolved gas pressure at the monitoring screen according to Equation 5.6 and substituting Equation 5.16 into 5.15, we obtained the following equation relating the total travel time from recharge to sampling (t_{rs}) to the measured concentrations of ^{3}H and tritiogenic ^{3}He and the depth of degassing (z_d) and sampling (z_s):

$$^3\mathrm{He}^*_s = f_{^3\mathrm{He}} \bullet {}^3\mathrm{H}_s \left(e^{\lambda t_{rs}} - e^{\lambda t_{rs} \frac{z_s - z_d}{z_s}} \right) + {}^3\mathrm{H}_s \left(e^{\lambda t_{rs} \frac{z_s - z_d}{z_s}} - 1 \right) \tag{5.17}$$

Equation 17 cannot be solved analytically and was solved numerically for t_{rs} by minimizing the difference between the observed tritiogenic ^{3}He concentration in the sample and that predicted by equation 17.

5.2.5 Summary of correction method

The method to estimate travel times from degassed groundwater by ^{3}H/^{3}He can be summarized in five steps. The first step is the analysis of the ^{22}Ne/^{20}Ne ratio to see whether degassing had led to fractionation. Fractionated samples cannot be corrected by the method we present here. If fractionation is not observed, the second step is to use Equation 5.9 to calculate the volume of gas that caused the degassing of the noble gases and Equation 5.12 for the fraction of ^{3}He left in solution after degassing. The third step is to separate the tritiogenic ^{3}He from the atmospheric ^{3}He using Equation 5.13. If the assumption that no gas is produced or consumed after degassing is valid, the fourth step is to estimate the place and time of degassing between recharge and sampling, e.g. using the total dissolved gas pressure measured at the screen (Equation 5.6 and 5.16). The fifth and last step is to solve the total travel time from recharge to sampling in Equation 5.17. Optionally, the uncertainty of the estimated travel times can be assessed by propagating the uncertainty of the underlying measurements through the travel time calculations.

5.2.6 Uncertainty of the travel time estimate

The lack of an analytical solution to Equation 5.17 precludes an analytical uncertainty analysis of ^{3}H/^{3}He travel times (Solomon *et al.* 1993). Instead, we used a Monte-Carlo type approach to analyze the sensitivity of the estimated travel times to uncertainties in the underlying measurements and assumptions, by propagating these uncertainties through the travel time calculations. We considered four types of uncertainty: (i) analytical error of tritium and noble gas concentrations, (ii) uncertainty in depth of degassing caused by groundwater level fluctuations,

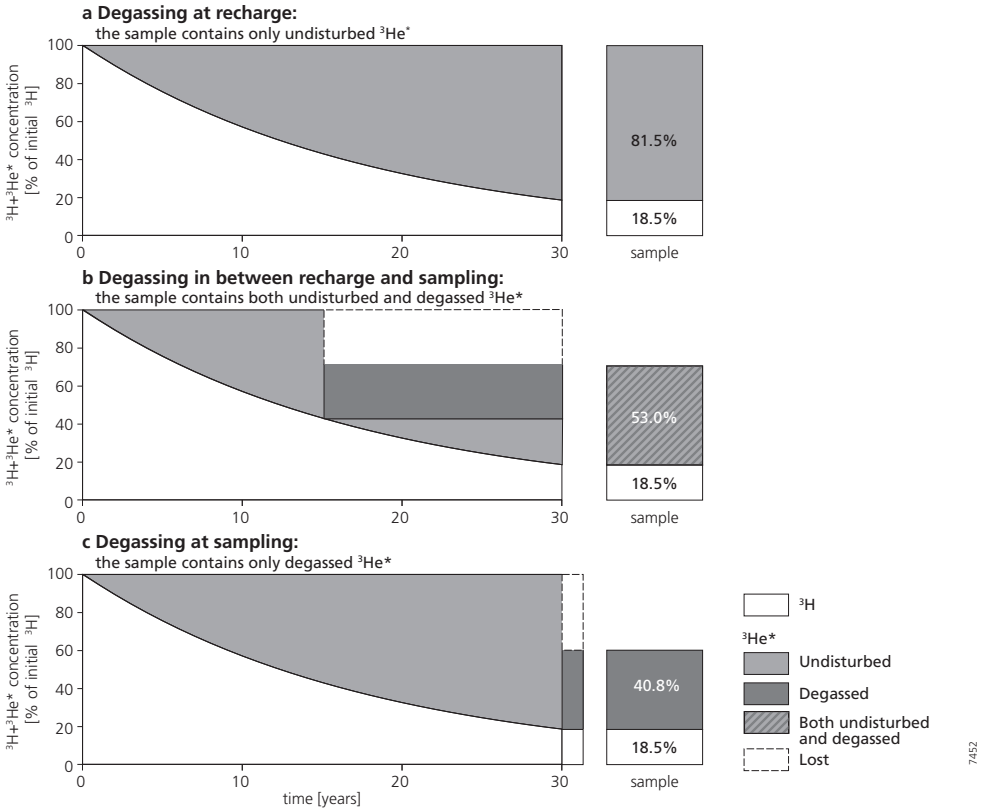

Figure 5.3 Evolution of ^{3}H and tritiogenic ^{3}He (^{3}He*) concentrations in groundwater for different degassing scenario's.

(iii) uncertainty about the presence of excess air before degassing, (iv) uncertainty about the effect of capillary pressure on the estimated depth of degassing by total dissolved gas pressure.

We propagated the uncertainty of these four sources one-by-one through the travel time calculation of each sample. To do so, we added 1000 realizations of noise to one underlying measurement and calculated the 95% percentile of the 1000 travel time estimates, which indicates the 95% confidence interval around the travel time caused by that particular source of uncertainty. Finally, we added all types of uncertainty to the measurements, to assess the overall uncertainty of the travel time estimate. We compared the resulting uncertainty of the travel time estimate with the uncertainty resulting from not knowing the time of degassing, as well as the uncertainty of the travel times of undisturbed samples as a result of tritium and noble gas measurement uncertainty alone.

We obtained the statistics of the measurement uncertainty from duplicate differences and used this to simulate noise. We calculated the standard deviation of the measurements uncertainty (σ) from the duplicate differences (d) and total number of samples (n) as follows

$$\sigma = \sqrt{\frac{\Sigma\, d_i^2}{2n}} \tag{5.18}$$

Table 5.3 Tritium and Noble Gas Measurements

Well Number	Screen Number	Depth [m]	Date d-m-yr	^3H [TU][a]	$^3He \times 10^{-13}$ [cm^3STP/cm^3]	$^4He \times 10^{-7}$ [cm^3STP/cm^3]	$Ne \times 10^{-7}$ [cm^3STP/cm^3]	$\Delta^{22}Ne$[b] [%]	Δ^4He[c] [%]	ΔNe[c] [%]
107	1	8	17-03-2005	7.92	0.894	0.552	2.41	0.102	18.8	19.5
107	3	24	17-03-2005	11.2	1.59	0.502	2.15	0.245	8.1	6.6
108	1	8	4-12-2001	10.1	0.773	0.481	2.12	0.125	3.5	5.1
108[d]	3	24	14-04-2005	14.3	1.89	0.361	1.66	0.266	-22.3	-17.7
122	1	9	9-12-2001	9.15	0.900	0.592	2.53	-0.315	27.4	25.4
122	3	24	17-03-2005	8.50	1.20	0.474	2.16	0.428	2.0	7.1
124[d]	1	9	2-03-2005	8.57	0.586	0.358	1.72	0.299	-22.9	-14.7
124	3	26	2-03-2005	8.39	0.872	0.502	2.19	0.342	8.1	8.6
125	1	12	16-12-2001	9.72	0.983	0.530	2.26	0.042	14.1	12.0
125[d]	3	23	3-03-2005	10.6	1.18	0.370	1.69	0.073	-20.3	-16.2
1806[d]	1	5	12-11-2001	9.08	0.188	0.129	0.560	-0.538	-72.2	-72.2
1806[d]	3	23	24-01-2005	12.4	0.623	0.039	0.254	-0.093	-91.6	-87.4
1810[d]	1	4	18-11-2001	9.79	0.521	0.274	1.36	0.362	-41.0	-32.6
1823[d]	1	8	18-11-2001	8.81	0.368	0.200	0.978	-0.261	-56.9	-51.5
1823[d]	3	18	14-04-2005	10.4	0.413	0.116	0.542	-0.043	-75.0	-73.1
1833[d]	1	8	20-11-2001	9.60	0.299	0.109	0.425	-0.615	-76.5	-78.9
1833[d]	3	19	21-02-2005	14.2	2.48	0.181	0.896	0.004	-61.0	-55.6
1840[d]	2	10	4-12-2001	9.62	0.122	0.048	0.155	1.847	-89.7	-92.3
1840[d]	4	25	29-03-2005	8.92	1.37	0.364	1.51	0.064	-21.6	-25.2
1843	1	4	9-03-2005	8.63	0.770	0.553	2.40	0.158	19.0	19.0
1843	2	8	4-12-2001	9.81	0.819	0.560	2.41	0.049	20.6	19.5
1843	4	23	9-03-2005	10.9	2.38	0.498	2.21	0.517	7.2	9.5
1844	1	5	2-03-2005	9.25	0.842	0.594	2.56	0.399	27.9	26.9
1844	2	8	2-03-2005	9.21	0.889	0.614	2.64	0.280	32.2	30.9
1844[d]	4	23	2-03-2005	12.6	0.957	0.244	1.12	0.183	-47.5	-44.5
1847[d]	1	8	9-03-2005	8.26	0.414	0.278	1.37	0.257	-40.2	-32.1
1847[d]	3	24	9-03-2005	15.4	1.46	0.184	0.739	-0.234	-60.4	-63.4
1851[d]	1	9	29-11-2001	10.0	0.198	0.028	0.126	-0.261	-94.0	-93.8
1851[d]	3	23	22-02-2005	21.6	2.64	0.246	1.13	0.211	-47.0	-44.0
1853[d]	2	10	29-11-2001	10.1	0.143	0.019	0.072	-2.970	-95.9	-96.5
1863	1	3	20-11-2001	10.2	1.25	0.873	3.55	-0.190	87.9	76.0
1863[d]	2	10	20-11-2001	15.7	1.44	0.253	1.16	-0.036	-45.5	-42.5
1863	4	22	16-03-2005	11.3	2.47	0.492	2.16	0.419	5.9	7.1
1866[d]	1	9	20-11-2001	8.95	0.602	0.383	1.81	0.308	-17.6	-10.3

a TU, tritium unit (1 TU represents a ratio of 1 atom of tritium per 10^{18} atoms of hydrogen and corresponds to 2.488×10^{-15} cm^3 STP ^3He per cm^3 water: 1 TU of ^3H will decay to 1 TU of ^3He).

b $\Delta^{22}Ne$ is the deviation of the sampled $^{22}Ne/^{20}Ne$ isotope ratio from the atmospheric ratio ($\Delta^{22}Ne = ([^{22}Ne/^{20}Ne]_s / [^{22}Ne/^{20}Ne]_{atm} - 1) \times 100\%$).

c Δ^4He and ΔNe refer to the deviation of the sampled concentration from atmospheric equilibrium (e.g.: $\Delta^4He = (^4He_s/^4He_{eq} - 1) \times 100\%$).

d Degassed samples.

We calculated the standard deviation of the tritium and noble gas measurement uncertainty based on 24 duplicates of ^{3}H, ^{3}He and ^{4}He. We also analyzed the correlation between the duplicate differences of ^{3}He and ^{4}He to construct Gaussian noise with the correct noise correlation statistics. To compare the uncertainty of degassed samples to that of undisturbed samples, we also propagated the sampling error through the calculations of the undisturbed samples separately. For the uncertainty of the groundwater level we used the difference between the head measurement at the time of $^{3}H/^{3}He$ sampling and the head measurement at the time of total dissolved gas pressure sampling. To assess the sensitivity to the assumption that no excess air was present, we added a random amount of unfractionated excess air (uniformly distributed between 0 and 0.3 times the atmospheric equilibrium concentration) to the measured ^{3}He and ^{4}He concentrations. To simulate the effect of capillary pressure, we subtracted a random capillary pressure (uniformly distributed between 0 and 0.1 atm) from the TDG measurement. The value wof 0.1 atm capillary pressure corresponds to the air-entry value of moderate to heavy clay (Brooks and Corey 1964). The air entry value is the highest pressure of a gas phase that capillary forces can resist from entering the pores and we assume it is also the highest supersaturation of dissolved gases that capillary forces can resist to form a bubble in moderate heavy clays.

5.3 Results

We collected 34 $^{3}H/^{3}He$ samples in 2001 and 2005. Twenty of the 34 samples showed noble gas concentrations below atmospheric equilibrium (see footnote d, Table 5.3) indicating that degassing had removed noble gases from this groundwater. The other 14 samples showed noble gas concentrations above atmospheric equilibrium because of an excess air component.

Figure 5.4a shows a box plot of the distribution of the nitrate concentration in degassed (n = 20) and normal (n = 14) samples. The nitrate concentration in degassed samples ranged from below detection limit to only 21 mg/l with 4 outliers, but in normal samples from the detection limit to 330 mg/l. We used a t-test to analyze the difference in nitrate concentration in normal and degassed samples. The mean concentration of all degassed samples was significantly (t-test: $p < 0.01$) lower than that of normal samples.

We plotted the nitrate concentration against the neon concentration to further analyze the relationship (Figure 5.4b). The nitrate concentration was below the detection limit in 15 of the 20 degassed samples, confirming our hypothesis that denitrification causes degassing. In contrast to the absence of nitrate in degassed samples, 10 of the 14 samples with noble gas concentrations above atmospheric equilibrium (excess air) contained substantial amounts of nitrate. The samples with excess air and no nitrate were taken from deep screens and may have been denitrified at greater depth where higher hydrostatic pressures prevented degassing and all noble gases remained dissolved in the groundwater. Mixing of groundwater during sampling may have resulted in the five degassed samples with nitrate.

Using Equation 5.4 and assuming a degassing depth of 5 m below the water table, we drew dashed lines from initial concentrations of nitrate (with increments of 50 mg/l) to the corresponding (degassed) Ne concentrations below atmospheric equilibrium. Figure 5.4b shows again (bold dashed line) that denitrification of an initial nitrate concentration of 100 mg/l leads to a neon concentration of 1.6×10^{-7} cm^3 STP/cm^3 which is the equivalent of a neon depletion of 23% ($\Delta Ne = -23\%$).

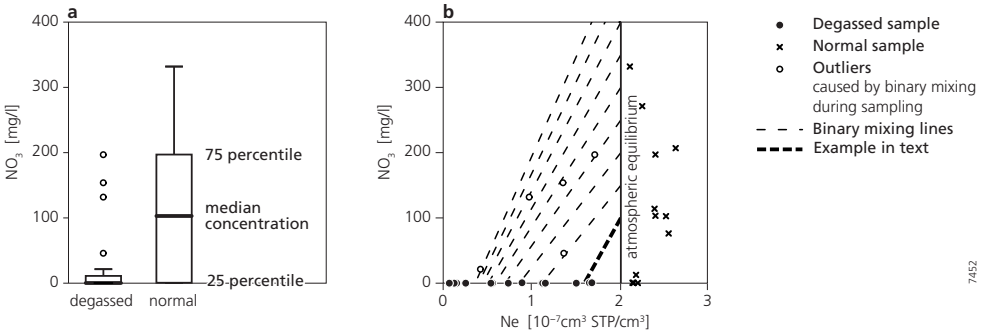

Figure 5.4 Nitrate concentrations in degassed and normal samples. Box plots of nitrate concentrations in degassed and normal samples (a). Thick line represents the median concentration, upper and lower end of the boxes indicate the 25 and 75 percentiles respectively. The mean nitrate concentration of all degassed samples was significantly lower than that of undisturbed samples. The nitrate concentrations in individual samples (b) are below the detection limit in most degassed samples with neon concentrations below atmospheric equilibrium (•) and present in most normal samples (×). Dashed lines link nitrate rich and degassed end-members (Equation 5.4), for a degassing depth of 5 m below the groundwater table. Open circles denote outliers, caused by binary mixing during sampling.

These lines can also be interpreted as binary mixing lines between an oxic end-member (containing between 100 and 500 mg/l nitrate and an atmospheric Ne concentration) and an anoxic end-member (with no nitrate and a Ne concentration calculated from Equation 5.4 using the initial nitrate concentration of the oxic end-member). Because all degassed samples with nitrate are along one of the mixing lines, we assume that binary mixing of oxic and anoxic water during sampling explains the nitrate concentration in these samples. We observed that the redoxcline is often found between 5 and 7 m below surface (Table 5.4) which is at or near the depth of the 2 m long sampling screens (between 7 and 9 m below surface, Table 5.3). This supports our assumption that some of our samples contained a mixture of oxic water from above the redoxcline and anoxic water from below the redoxcline. These samples were excluded from further analysis, because analyzing mixed degassed samples is beyond the scope of this paper.
We studied the $^{22}Ne/^{20}Ne$ ratio to decide whether degassing had caused isotopic fractionation by diffusion. We found that all $^{22}Ne/^{20}Ne$ ratios were close to the solubility equilibrium, within the analytical uncertainty range, and none of them was consistent with isotopic fractionation by Rayleigh diffusion (Figure 5.5). Two samples with very low noble gas concentrations had neon isotope ratios far from atmospheric equilibrium and were left out of subsequent analyses.
Differences in solubility cause slight fractionation between ^{4}He and Ne concentration by degassing, even if degassing attains equilibrium, and the "solubility equilibrium degassing" path between the atmospheric equilibrium and complete degassing is slightly curved. Diffusive degassing would cause even greater fractionation and the "diffusive degassing" path is more curved (Figure 5.6). Plotting ^{4}He concentration against Ne concentration (Figure 5.6b) shows that all samples correspond to the "solubility equilibrium degassing" path. Plotting ^{3}He concentration against Ne concentration (Figure 5.6a) shows the tritiogenic ^{3}He component causing a vertical deviation from the "solubility equilibrium degassing" path. Note that this tritiogenic ^{3}He may be

Table 5.4 Degassing volume, total dissolved gas pressure measurements, depth of degassing and estimated travel times without (min and max) and with information on the timing of degassing (TDG).

Well Number	Screen Number	Δ^4He	V_g	f^3_{He}	TDG	depth			^3H	$^3He^*$			travel time		
						ground-water	degassing	screen		min[a]	max[b]	TDG[c]	min[a]	max[b]	TDG[c]
				[-]	[atm]	[m]	[m]	[m]	[TU]	[TU]	[TU]	[TU]	[years]	[years]	[years]
108	3	-22%	0.3%	0.78	>2	2.4	>12.4	24	14	56	72	66.1 – 72.4	28	32	30.7 – 32.0
125	3	-20%	0.2%	0.80	>2	5.5	>15.5	23	11	27	34	32.0 – 34.2	23	26	24.7 – 25.7
1806	1	-72%	2.4%	0.28	1.14	2.6	4.0	5	9.1	0.5	1.9	0.92	1.0	3.3	1.7
1806	3	-92%	10.2%	0.09	1.29	3.5	6.4	23	12	23	274	29.1	19	56	21.5
1823	3	-75%	2.8%	0.25				18	10	10	41	10.3 – 41.1	12	28	-
1833	3	-61%	1.5%	0.39	1.35	1.2	4.7	19	14	90	230	119	35	51	39.8
1840	4	-22%	0.3%	0.79	1.28	4.1	6.8	25	8.9	35	45	37.2	28	32	29.2
1844	4	-47%	0.8%	0.53	>2	2.7	>12.7	23	13	25	48	36.6 – 47.9	19	28	24.2 – 27.8
1847	3	-60%	1.4%	0.40	1.50	2.6	7.7	24	15	49	123	64.0	25	39	29.2
1851	1	-94%	14.5%	0.06	1.54	1.3	6.7	9	10	6.4	107	29.1	8.8	44	24.2
1851	3	-47%	0.8%	0.53	1.83	0.9	9.2	23	22	93	175	129	30	39	34.6
1863	2	-46%	0.8%	0.55	1.48	1.4	6.2	10	16	44	81	66.8	24	32	29.5
1866	1	-18%	0.2%	0.83	1.31	1.5	4.6	9	8.9	3.3	4.0	3.59	5.6	6.6	6.0

a Corrected for degassing at time of recharge, yielding minimum $^3He^*$ and travel time estimate
b Corrected for degassing at time of sampling, yielding maximum $^3He^*$ and travel time estimate
c Corrected for degassing using the Total Dissolved Gas pressure (TDG) to estimate the depth of degassing, yielding most accurate $^3He^*$ and travel time estimate

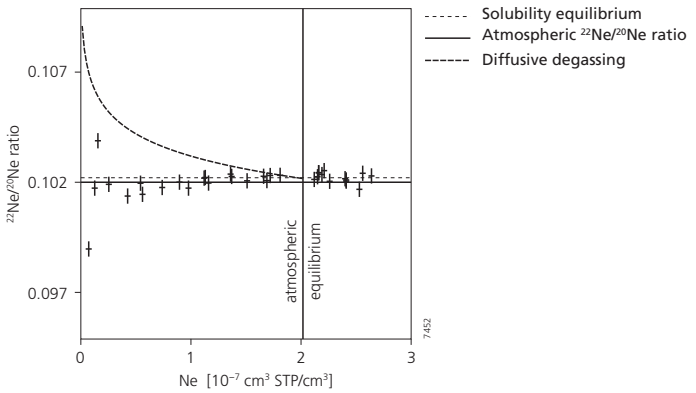

Figure 5.5 The $^{22}Ne/^{20}Ne$ ratios plotted against the Ne concentrations were within the analytical uncertainty range of the solubility equilibrium (Table 5.2). Diffusive degassing line calculated with ^{22}Ne diffusivity of Bourg and Sposito (2008).

completely degassed, partially degassed or undisturbed and cannot directly be used to calculate the travel time.

Assuming that degassing took place at either time of recharge or time of sampling, we corrected none or all of the tritiogenic ^{3}He for degassing and calculated the range of ages that are possible without a constraint on the location of degassing (Table 5.4). The uncertainty of the travel time was as high as 37 years for a sample with a Ne concentration of 13% of the atmospheric equilibrium (87% degassed). The uncertainty was larger for the samples with a high degree of degassing and longer travel times (Figure 5.7).

All total dissolved gas pressure (TDG) measurements showed elevated gas concentrations, but none were supersaturated with respect to the hydrostatic pressure at screen depth (Table 5.4).

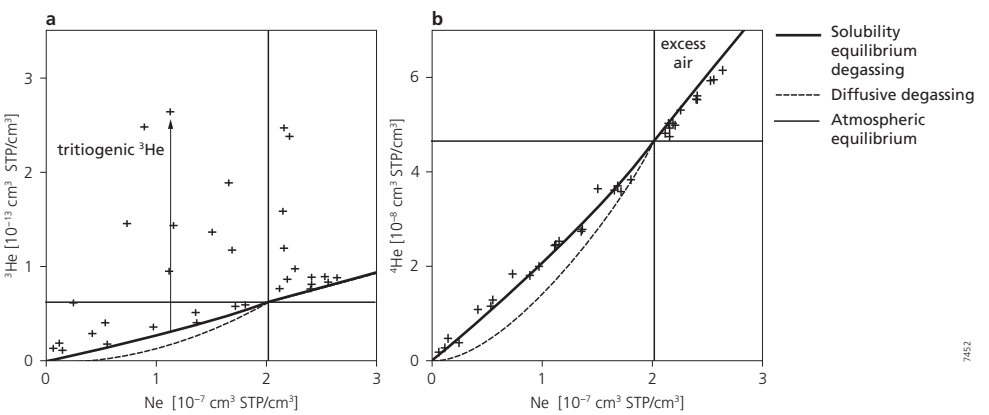

Figure 5.6 Concentrations of ^{3}He (a) and ^{4}He (b) against Ne. All degassed samples, with concentrations below atmospheric equilibrium, are along the "solubility equilibrium degassing" path (b). Tritiogenic ^{3}He causes a vertical deviation from this path (a).

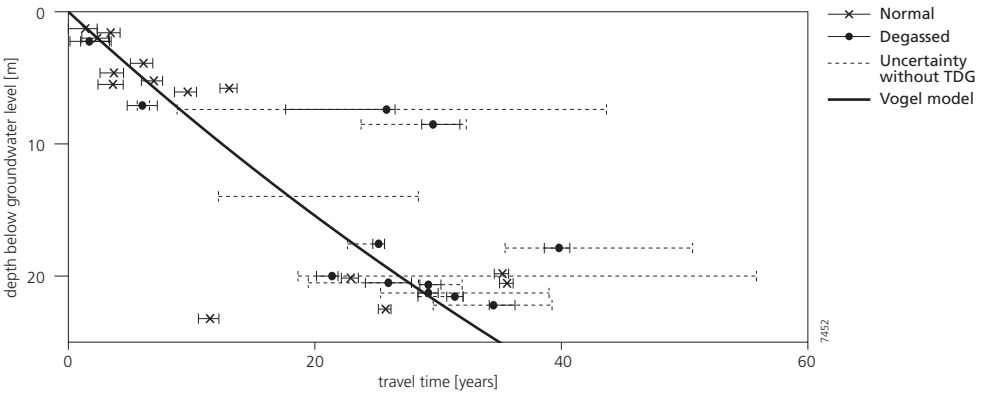

Figure 5.7 Travel times plotted against depth below the water table. Travel time uncertainties of normal samples (×, solid error bars) and degassed samples using TDG to estimate the depth of degassing (•, solid error bars) and without TDG information (dashed error bars). Estimated travel times deviate significantly from the Vogel model (with a porosity of 0.35, a recharge rate of 0.3 and an aquifer thickness of 80 m).

The total dissolved gas pressure in some wells exceeded the limitations of the total dissolved gas pressure probe (2 atm), indicating that this groundwater was degassed below 10 m below the groundwater level. One well was inaccessible in 2006 and no total dissolved gas measurement could be taken. We calculated the depth of degassing using the total dissolved gas pressure according to Equation 5.6. Then we solved Equation 5.14 and estimated the travel times of the degassed groundwater samples (Table 5.4). Even when the total dissolved gas pressure exceeded the limitations of the probe, knowing that degassing took place below 10 m below the groundwater table strongly reduced the range of possible travel times towards the maximum estimate.

To show the large variation in travel times, especially in the deep screens, we plotted the travel times of the groundwater samples, using the TDG to estimate the depth of degassing, against the depth of sampling below the water table (Figure 5.7). This variation shows that assuming a single travel time – depth relation (e.g. the Vogel model) is invalid and that there is a great need for groundwater dating. Figure 5.7 also shows the confidence intervals of the estimated travel times, based on the 95% percentile of the ensemble for each sample using all sources of noise. The confidence intervals of the travel time of degassed samples (using the TDG) are much smaller than without using TDG, showing the benefit of the TDG method.
In Figure 5.8 we plotted the sum of measured tritium and estimated tritiogenic ^{3}He against the estimated time of recharge together with measurements of tritium in precipitation at Groningen, the Netherlands (IAEA/WMO 2004). Figure 5.8 shows that the estimated travel times are consistent with the known history of tritium in precipitation.

The standard deviations of the duplicate differences of the noble gas measurement were in the order of 1% of the atmospheric equilibrium concentrations (Table 5.5) and the duplicate differences of the noble gas measurements were highly correlated. The standard deviation derived from the differences between the groundwater level measurements at two moments was 0.34 m. These statistics were used to generate the noise for the error propagation analysis.

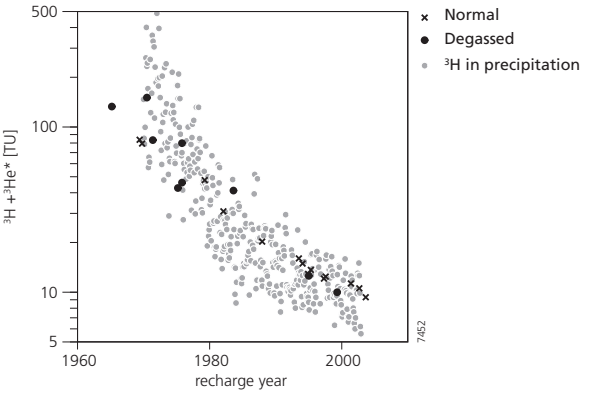

Figure 5.8 Sum of tritium and tritiogenic ^{3}He plotted against recharge year.

Sixteen degassed samples showed no neon isotope fractionation and had a total dissolved gas pressure measurement available and were suitable for the error propagation analysis. The propagation of each source of uncertainty produced a distribution of 1000 travel time estimates for each of the 16 samples. From each distribution we derived the 95% confidence interval of the travel time. To present the overall uncertainty of the travel time estimates, we plotted the median and maximum 95% confidence interval of all 16 samples in Figure 5.9. We also plotted the median uncertainty of the travel time estimates caused by not knowing the depth and timing of degassing, as well as the uncertainty of the travel times estimates of undisturbed samples.
The largest median uncertainty is caused by not knowing the time of degassing (6 years), with maximum values of over 30 years for some samples. Noble gas measurement uncertainty caused a median 95% confidence interval of 2 years. Neglecting a possible presence of excess air up to 30% before degassing causes an uncertainty of 1 year. If excess air was present before degassing, the actual travel time is larger. If capillary pressures of up to 0.1 atm distorted the estimate of the depth of degassing by total dissolved gas pressure, the actual travel time would be slightly smaller than estimated. The median uncertainty of the travel times is 3 years, considering all four sources of uncertainty. The largest uncertainty of the estimated travel time is 9 years, for a sample which has been 94% degassed (well 1851, screen 1). The median uncertainty of the estimated travel time of degassed groundwater samples is comparable to the uncertainty of undisturbed samples (2 years), which we determined by propagating the sampling error alone through the calculations of the undisturbed samples.

Table 5.5 Statistics of duplicate differences.

	standard deviation	**correlation matrix**			
		^{3}H	**^{3}He**	**^{4}He**	**Ne**
^{3}H [TU]	0.23	1	0.05	0.00	-0.22
^{3}He [cm^3 STP/cm^3]	1.21×10^{-15}	0.05	1	0.64	0.62
^{4}He [cm^3 STP/cm^3]	4.67×10^{-10}	0.00	0.64	1	0.86
Ne [cm^3 STP/cm^3]	1.87×10^{-9}	-0.22	0.62	0.86	1
Δ^{22}Ne [%]	0.24				
groundwater level [m]	0.34				

5.4 Discussion and conclusions

Nitrogen gas produced by denitrification of nitrate from agricultural pollution causes degassing of noble gases at specific depths below the groundwater table throughout the province of Noord-Brabant, the Netherlands. Because degassing takes place at some depth below the water table, $^{3}H/^{3}He$ concentrations cannot be interpreted by assuming degassing at either at the point of recharge or during sampling as was done in previous studies. Therefore we presented a method to interpret degassed groundwater samples by using the total dissolved gas pressure to estimate the depth and relative timing of degassing. This method can provide reliable groundwater travel times from degassed $^{3}H/^{3}He$ samples, if the following requirements are met. (1) Degassing has reached solubility equilibrium. Analysing the neon isotope ratio can easily confirm that degassing has reached solubility equilibrium. (2) Degassing of ^{3}He and other noble gases can be described by a single-step degassing model.

Single-step degassing is likely if the gas-producing geochemical reaction is caused by changes in sediment chemistry, for example with autotrophic denitrification (Korom 1992) where an abrupt change of geochemistry causes a sharp redoxcline at which point nitrate is reduced to nitrogen gas (Van Beek *et al.* 1989; Frind *et al.* 1990; Postma *et al.* 1991; Smith *et al.* 1991; Robertson *et al.* 1996; Broers 2004b). In these studies, pyrite in the unconsolidated sedimentary aquifers acted as electron donor and caused the drop in the redox potential across the redoxcline. Degassing of groundwater by denitrification as observed in this study has been reported before (Dunkle *et al.* 1993; Ekwurzel *et al.* 1994; Blicher-Mathiesen *et al.* 1998). Similar degassing is likely to occur in other unconsolidated sedimentary aquifers which contain organic matter or ironsulfides (i.e. pyrite) and receive high inputs of nitrate from agriculture.

In recharge areas, with continuous downward flow, the total dissolved gas pressure in the sample can provide the depth and relative timing of degassing. One additional requirement for the use of total dissolved gas pressure to estimate the depth of degassing is that no gas may be produced or consumed after degassing has taken place. If the reaction products causing the degassing in the first place are stable, like nitrogen gas, and no new changes in redox potential or acidity occur, the total dissolved gas pressure at the well screen will be the same as at the depth of degassing. Downward flow in recharge areas, where hydrostatic pressure increases with depth, will ensure that after degassing all dissolved gases will remain dissolved. These assumptions

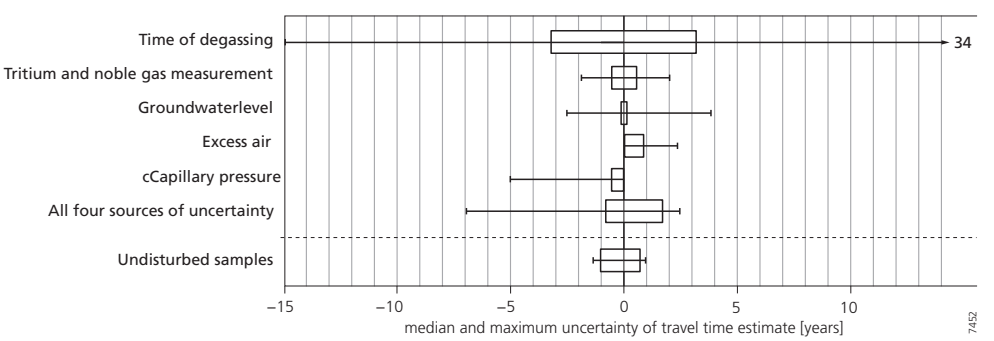

Figure 5.9 Median (box) and maximum (error bar) 95% confidence intervals of travel time estimates from 4 sources of uncertainty.

may not always be valid and should be substantiated when this method is applied. If reactions are slow compared to the vertical groundwater velocity because no sharp redoxcline exists or if a second redoxcline causes gas to be formed or consumed below the depth of degassing, concentrations of dissolved gases change between degassing and sampling, and using the total dissolved gas pressure does not give a valid estimate about the depth of degassing. In those situations, geochemical mapping to identify sediments capable of nitrate reduction or other reactions producing a gas may approximate the timing of degassing.

Unconsolidated sedimentary aquifers in deltas or alluvial plains are often used for intensive agricultural production, making nitrate pollution a common problem in the US (Kelly 1997; Hudak 2000; Harter *et al.* 2002; Katz *et al.* 2004), Europe (Postma et al. 1991; Wendland et al. 1994; Pauwels et al. 2001; Van Maanen et al. 2001; Molénat et al. 2002; Broers and Van der Grift 2004), China (Zhang *et al.* 1996), Japan (Kumazawa 2002) and increasingly in developing countries like India (Bijay-Singh *et al.* 1995). Groundwater dating may be essential in studies of nitrate contamination in which, for example, measured concentrations must be related to historic input so that a trend reversal in agricultural pollution can be demonstrated (Chapter 2) as required by the new EU regulations (EU 2006) or that the effects of regulatory measures aimed at reducing the nitrate load to the groundwater system can be assessed. Therefore the need for a reliable tool to date degassed groundwater certainly exists.

None of the other readily available groundwater age tracers (CFCs (Busenberg and Plummer 1992), SF_6 (Busenberg and Plummer 2000)) will likely provide reliable groundwater travel time estimates when degassing has taken place. SF_6 has a very low solubility and it is therefore very susceptible to degassing. SF_6 also provides no internal consistency check, like the historical tritium concentration in precipitation for $^3H/^3He$ (Figure 5.8). Although CFCs are less susceptible to degassing because of their higher solubility, they often suffer from local contamination in industrially developed areas (Oster *et al.* 1996) or degradation in anaerobic environments (Lovley and Woodward 1992) which are related to denitrification. Hence, $^3H/^3He$ is more reliable then both SF_6 and CFCs for anoxic degassed samples. ^{85}Kr (Smethie *et al.* 1992) is based on an isotope ratio of a noble gas and it is therefore much less sensitive to degassing (Purtschert *et al.* 2004) and would be an interesting alternative. Its widespread application however is limited due to the labour-intensive sampling and analysis (Zuber *et al.* 2005). Therefore we conclude that $^3H/^3He$ is the most readily available and promising method to date degassed groundwater, using the method we presented to estimate the timing of degassing from the measured total dissolved gas pressure.

6 Degassing of $^3H/^3He$, CFCs and SF_6 by denitrification: measurements and two-phase transport simulations

This chapter has been published as:
Ate Visser, Joris D. Schaap, Hans Peter Broers, and Marc F.P. Bierkens (2008) *Degassing of $^3H/^3He$, CFCs and SF_6 by denitrification: Measurements and two-phase transport simulations*, Journal of Contaminant Hydrology 103(3-4):206-218, doi:10.1016/j.jconhyd.2008.10.013

Abstract

The production of N_2 gas by denitrification may lead to the appearance of a gas phase below the water table prohibiting the conservative transport of tracer gases required for groundwater dating. We used a two-phase flow and transport model (STOMP) to study the reliability of $^3H/^3He$, CFCs and SF6 as groundwater age tracers under agricultural land where denitrification causes degassing. We were able to reproduce the amount of degassing (R^2 = 69%), as well as the ^3H (R^2 = 79%) and $^3He^*$ (R^2 = 76%) concentrations observed in a $^3H/^3He$ data set using simple 2D models. We found that the TDG correction of the $^3H/^3He$ age overestimated the control $^3H/^3He$ age by 2.1 years, due to the accumulation of $^3He^*$ in the gas phase. The total uncertainty of degassed $^3H/^3He$ ages of 6 years (± 2 σ) is due to the correction of degassed $^3He^*$ using the TDG method, but also due to the travel time in the unsaturated zone and the diffusion of bomb peak $^3He^*$. CFCs appear to be subject to significant degradation in anoxic groundwater and SF_6 is highly susceptible to degassing. We conclude that $^3H/^3He$ is the most reliable method to date degassed groundwater and that two-phase flow models such as STOMP are useful tools to assist in the interpretation of degassed groundwater age tracer data.

6.1 Introduction

Groundwater dating has proven to be an excellent research tool to gain understanding of groundwater flow and transport processes of contaminants. Several methods are available today: $^3H/^3He$, CFCs, ^{85}Kr (Cook and Solomon 1997) and SF_6 (Busenberg and Plummer 2000). $^3H/^3He$ groundwater ages are based on the radioactive decay of ^3H (tritium) and are calculated from the ratio between the concentrations of ^3H and its decay product ^3He in groundwater. To mathematically separate the ^3He produced by ^3H decay from other sources of ^3He in groundwater (e.g. atmospheric, excess air, radiogenic), the concentrations of ^4He and Ne are measured simultaneously. Groundwater ages can also be derived by comparing the concentrations of CFCs

or SF_6 in groundwater to the known time-varying historical concentrations in the atmosphere or by comparing the $^{85}Kr/Kr$ ratio in groundwater to the historical time-varying $^{85}Kr/Kr$ ratios in the atmosphere. All these groundwater dating methods rely on the conservative transport of these trace gases (He, Ne, CFCs, SF_6, or Kr) in groundwater.

These gases are only transported conservatively when groundwater does not come in contact with a gas phase below the groundwater table (Fry *et al.* 1995). The production of gases and subsequent appearance of a gas phase causes re-partitioning of tracers between the gas and water phase and decreases the dissolved concentration in on-flowing groundwater.

Gases (such as N_2, CH_4, CO_2 and H_2S) can be produced below the groundwater table by biogeochemical reactions between the solutes and the subsurface. Especially at polluted sites – where groundwater dating is particularly useful – the formation of a gas phase is not unlikely because of the high concentrations of reactive solutes. For example, the formation of a gas phase and subsequent degassing of tracer gases has been observed several times as a result of methane production in deep groundwater (Fortuin and Willemsen 2005), under landfills (Solomon *et al.* 1992; Van Breukelen *et al.* 2003; Purtschert *et al.* 2004) or oil spills (Baedecker *et al.* 1993; Revesz *et al.* 1995; Amos *et al.* 2005). In agricultural areas with high input of nitrate and reactive sediments in the subsurface, the production of N_2 gas by denitrification has led to the formation of a gas phase, observed as noble gas concentrations below atmospheric equilibrium (Chapter 5, and Blicher-Mathiesen *et al.* 1998). These findings are supported by laboratory experiments investigating degassing by methanogenesis (Amos and Mayer 2006b) or denitrification (Istok *et al.* 2007).

Standard interpretation of tracer gases is not valid when degassing has occurred because tracer gases are no longer transported conservatively. Therefore we need a better understanding of the fate of the appearing gas phase and the advective and diffusive transport of tracer gases in both the water and gas phase. This can be achieved by numerical multiphase modeling of groundwater flow and solute transport. For example, two-phase flow and transport models have yielded insight in the oxygenation of anoxic water by entrapped air (Williams and Oostrom 2000), the transport of dissolved gases in the presence of a trapped gas phase (Cirpka and Kitanidis 2001) and the role of gas bubbles in contaminated aquifers (Amos and Mayer 2006a).
We used a two-phase groundwater flow and solute transport model (STOMP, White and Oostrom 2000) to study the appearance and fate of a gas phase that is produced by the denitrification of large amounts of nitrate under agricultural land in the south of the Netherlands. To study how the appearing gas phase affects the tracer gas transport, we also simulated the transport of groundwater age tracers (^3H, ^3He, ^4He, Ne, CFCs and SF_6) both dissolved by groundwater flow and in the gas phase. Firstly, we used a simple one-dimensional column to illustrate the formation of a gas phase and the behavior of noble gases in this situation. Secondly, we attempted to reproduce a set of $^3H/^3He$, CFCs and SF_6 measurements taken at 14 different locations in agriculturally polluted areas in the south of the Netherlands. For each location, we constructed and calibrated a two-dimensional model to fit measurement of head, total dissolved gas pressure and tracer concentrations. By comparing the modeled results to groundwater age tracer measurements, we assessed the usefulness of tracers in situations where degassing occurs and the capability of a two-phase flow and transport model to assist in the interpretation of degassed groundwater age tracer measurements. Finally, we used modeled $^3H/^3He$ and model ages to assess the accuracy of $^3H/^3He$ dating under normal and degassed conditions.

6.2 Study area

The province of Noord-Brabant, in the south of the Netherlands, is one of the areas in Europe which is most affected by agricultural pollution. Intensive livestock farming in the area produces a large surplus of nitrate-rich manure. The subsurface of Noord-Brabant consists of fluvial unconsolidated deposits from the Meuse River, with textures ranging from coarse sand to clay. Some sediments have a high organic matter content and in some areas pyrite occurs in the subsurface (Broers 2004b), both of which are capable of reducing nitrate.

Because of the vulnerability of Noord-Brabant to agricultural pollution, a groundwater quality monitoring network was installed (Van Duijvenbooden 1993). As part of the groundwater quality network, observation wells were placed in groundwater recharge areas (Broers and Van der Grift 2004). These recharge areas lack a superficial drainage network; have groundwater levels between 1 and 5 m below the surface, permeable soils and a relatively high topographical elevation (0 – 30 m above mean sea level).

The wells of the groundwater quality monitoring network consist of nested piezometers with a diameter of approximately 5 cm and a screen length of 2 meters. Most wells have two piezometers, with screens at about 8 or 25 meters below surface (Figure 6.1) (Van Duijvenbooden 1993; Broers 2002).

In this study we attempted to reproduce the data set of $^{3}H/^{3}He$ measurements from 14 wells in recharge areas with intensive livestock farming presented in Chapter 5. The data set consisted of tritium and noble gas samples taken with a submersible pump (MP1, Grundfos) in pinch-clamped copper tubes and measurements of total dissolved gas (TDG) pressure (Manning *et al.* 2003) taken with a TDG probe (T300E, In-Situ Inc.) at screen depth. We also used

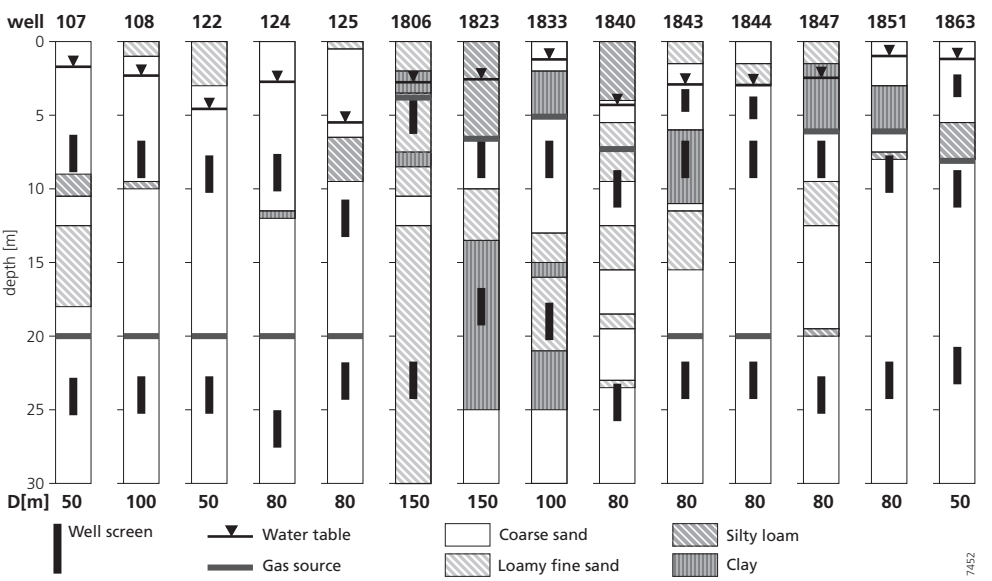

Figure 6.1 Soil texture profiles of the 14 well locations, showing the depth of the well screens, the water table and the depth of the gas source. D stands for aquifer thickness.

measurements of CFC-11, CFC-12 and CFC-113 and SF_6 concentrations in samples collected from these wells in 2005. These samples were collected in 500 ml glass bottles, submerged in a container filled with groundwater, to prevent contact of the sample with the atmosphere (Bauer *et al.* 2001) and analyzed by Spurenstofflabor Dr. Harald Oster, Wachenheim, Germany.

6.3 Model

6.3.1 Model description

We used the numerical model STOMP (Subsurface Transport over Multiple Phases) Version 2.0 (White and Oostrom 2000) to simulate the flow of groundwater and N_2 gas in the saturated zone, as well as the transport of groundwater age tracers. Several other models are also capable of simulating the exchange of tracer gases between groundwater and a gas phase (PHREEQC, (Parkhurst and Appelo 1999), Kinetic Bubble Dissolution model (Holocher *et al.* 2003), MIN3P (Mayer *et al.* 2002)), but all these simulate a trapped gas phase. Because we were interested in the mobility of the gas phase, we chose the true two-phase flow model STOMP. Recently, the MIN3P model was extended with an empirical formulation for gas ebullition (Amos and Mayer 2006b) and this model could have been used as an alternative.

Table 6.1 Properties of solutes at 10°C and zero salinity and of "air" at 20°C

	H [-]	D [$\times 10^{-9}$ m^2/s]	C_{eq} [mol/l]
"air" [a]	51.1	1.9	8.14×10^{-4}
N_2	51.2[b]	1.3[c]	6.47×10^{-4}
^{3}H	0	1.4[h]	-
^{3}He	109.3[b,f]	6.56[i]	2.85×10^{-15}
^{4}He	107.4[b]	5.68[i]	2.07×10^{-9}
^{20}Ne	85.8[b]	2.81[i]	8.17×10^{-9}
^{22}Ne	85.7[b,g]	2.94[i]	8.35×10^{-10}
CFC-11	2.0[d]	0.7[j]	-
CFC-12	7.8[d]	0.7[j]	-
CFC-113	6.6[d]	0.7[j]	-
SF_6	105.7[e]	0.8[k]	-
fictional decaying tracer	0	0	1
tracer decay product	0	0	0

H: Henry's law partitioning coefficient
D: molecular diffusion coefficient
C_{eq}: atmospheric equilibrium concentration
a *White and Oostrom* (2000)
b *Ozima and Podosek* (2002)
c *Geistlinger et al.* (2005)
d *Busenberg and Plummer* (1992)
e *Busenberg and Plummer* (2000)
f *Benson and Krause* (1980)
g *Beyerle et al* (2000)
h *Solomon et al* (1993)
i *Jähne et al* (1987). Diffusivities of ^{3}He and ^{22}Ne were calculated assuming an inverse proportional relationship of D to the square root of the atomic mass. ($D_j = D_1 \times (M_j/M_j)^{0.5}$) (Jähne et al., 1987)
j *Zheng et al(1998)*
k *King and Saltzman* (1995)

Table 6.2 Soil hydraulic parameters

Soil	*M50* [μm]	*n*	K_s [cm/d]	H_{ea} [m]	λ	θ_r
Coarse sand	310	0.34	25	0.12	0.959	0.01
Loamy sand	143	0.32	10.87	0.36	0.581	0.01
Silty loam	-	0.56	3.7	1.10	0.283	0.01
Clay	-	0.41	1.02	0.99	0.157	0.01

M50: median grain size of sand fraction, *n*: porosity; K_s: saturated hydraulic conductivity; H_{ea}: Brooks and Corey air entry head; λ: Brooks and Corey λ parameter; θ_r: residual water content

In the Water-Air operational mode, STOMP simulates two phases in a porous medium, each consisting of a single component. The gas phase is composed of the component "air", which has the average properties of the atmospheric mixture of gases at 20°C. This is conceptually not fully correct if a process take place that alters the composition of the gas phase. However, the focus of this study was the appearance of a gas phase as a result of N_2 produced by denitrification in anoxic parts of the aquifer. In anoxic parts of the aquifer, only N_2 gas plays a significant role because the production of significant amounts of CO_2 or CH_4 is not observed in these study areas. Therefore it is justified to use a single component gas phase. The properties of N_2 at the aquifer temperature (10°C) are close to those used for "air" in STOMP and it was legitimate to use the model unaltered to simulate the transport of N_2.

The STOMP model first solves the coupled mass conservation equations for water and N_2, assuming isothermal conditions and local thermodynamic equilibrium, and sequentially the mass conservation equations for solute transport over both phases. A third-order Total Variation Diminishing (TVD) scheme is used for advective transport to reduce numerical dispersion (Datta Gupta *et al.* 1991). We did not model dispersion because it is probably smaller than the numerical dispersion introduced by the cell sizes. Time steps were limited to ensure the local Courant number did not exceed 0.2. Diffusion coefficients and Henry's law coefficients, controlling the partitioning between the gas and water phase, were specified for each tracer (Table 6.1). Diffusion coefficients in the gas phase were 10^4 times those in the water phase. Tritium has a half-life of 12.32 years. The isotopes of He and Ne were simulated as separate solutes, with each their own partitioning and diffusion coefficients. References to the Ne concentration in this paper are in fact to the sum of ^{20}Ne and ^{22}Ne concentrations.

Borehole descriptions were made during well installation and texture classifications are available from the geological database of the Netherlands (TNO 2007). We classified all layers of the core descriptions into four distinct subsoil types of the Dutch soil classification system "Staring series" (Wösten 1994): coarse sand, loamy fine sand, silty loam and clay (Figure 6.1). The median grain size of the sand fraction (*M50*) of coarse sand ranges from 220 to only 400 μm; that of loamy sand from 114 to 172 μm (Wösten 1994). The subsoil types are defined by their porosity, saturated conductivity and capillary pressure-saturation function. We used the hydraulic properties porosity *n* and saturated hydraulic conductivity K_s as reported by the Staring series (Table 6.2). We converted the Van Genuchten (Van Genuchten 1980) saturation function parameters reported by the Staring series to Brooks and Corey parameters (Brooks and Corey 1964) according to Lenhard (1989), because the Brooks and Corey function is more stable near water saturation. We used the Mualem pore distribution model (Mualem 1976) to compute the aqueous-phase relative permeability from the aqueous saturation as described by the Brooks and

Corey function. For the gas phase, we used the Corey relative permeability function (Corey 1977) because it provides the possibility to define an irreducible trapped gas saturation below which the relative permeability is zero. We set the trapped gas saturation for the sands to 0.15 according to observations of trapped gas by Fry *et al.* (1997) and to 0.30 for the loam and clay sediments following observations by Amos and Mayer (2006b).

To simulate the production of nitrogen gas by denitrification, we modeled a source that injected N_2 into a cell or a horizontal layer of cells of the model. We did not model the denitrification of nitrate to N_2 because it was not the aim of this paper. Instead, the depth of the production of N_2 was calibrated and the rate was related to the expected concentration of nitrate arriving at the redoxcline. Because of the downward flow of nitrate-rich groundwater across the redoxcline, N_2 is continuously produced.

Simultaneously or prior to denitrification, oxygen is consumed and removed from solution (Appelo and Postma 2005). Here we assumed that oxygen consumption occurs in the saturated zone and effectively lowers the total dissolved gas pressure, rather than in the unsaturated zone. Removing all oxygen from solution reduces the initial total dissolved gas pressure by 21%. We adjusted the rate of N_2 production to compensate for the consumption of oxygen.

6.3.2 Model limitations

The STOMP model code has certain limitations that should be discussed before describing the model setup.

First, STOMP-WA is a single component gas phase model code. Because we focused on N_2 production in the anoxic zone, using a single component gas phase is valid. N_2 is the only gas that plays a significant physical role in the gas phase, because oxygen is reduced before nitrate. The tracer gases are only present at trace concentrations and their presence does not significantly contribute to the volume of the gas phase. For other applications where more gases play a significant role, STOMP-WA may not be a suitable model code.

Second, STOMP is not capable of simulating the process of denitrification. Instead we injected the reaction product N_2 at the depth at which denitrification takes place. This is valid because denitrification takes place at a sharp redoxcline in these systems (Van Beek *et al.* 1989; Postma *et al.* 1991; Broers 2004b).

Third, STOMP is a continuum model that simulates continuous coherent gas flow. There is ample evidence for incoherent or intermittent flow of gas through saturated porous media depending on sediment type and flow rate. In very coarse sediments (particle diameter > 2mm), gas flow is mostly incoherent (Brooks *et al.* 1999; Geistlinger *et al.* 2006; Istok *et al.* 2007) in the form of single separate gas bubbles or "bubble trains". In finer sediments (< 1 mm) as found in our study area, gas flow was observed as channelized flow (Brooks *et al.* 1999) or chamber flow (Peterson *et al.* 2001). Incoherent or intermittent flow was observed in a macro-heterogeneous fine sediment experiment (Glass *et al.* 2000). The low gas flow rate in this study does not meet the stability criterion defined by Geistlinger *et al.* (2006, eq. 12) and gas flow is likely to be instable. Glass *et al.* (2000) questioned whether two-phase, porous continuum-scale modeling (like STOMP) would be able to capture the unstable, lithology-driven migration behavior found in their experiments. In this study, we used the STOMP model in combination with a trapped gas saturation in the relative permeability function of Brooks. Upward gas flow is then controlled by the exceedence of the trapped gas saturation, rather than gas pressure differences between cells. Simulation of gas flow is reduced to an overflowing bucket-model and the model

is no longer a real continuum model. Despite this strong simplification of the complex behavior of gas in a saturated porous medium, we are confident that the results of the tracer transport simulations are reliable.

Fourth, the connectivity of the gas-filled pore space is very important to correctly simulate the diffusive transport of tracer gases. If the gas is present in individual separated bubbles, no diffusion through the gas phase is possible. The observations of channelized and chamber flow indicate that the gas phase trapped in fine sediments is rather connected and diffusion through the gas phase is possible. Therefore, we assumed that the tortuosity relation defined by Millington and Quirk (1959) can be applied to simulated diffusive transport through the gas phase.

6.3.3 1D simulation

To illustrate the formation of a gas phase and the effect on tracer transport, we first simulated the denitrification of 200 mg/l nitrate at 5 m depth in a one-dimensional column simulation (Figure 6.2a). The initial conditions of the 1D simulation were a saturated loamy fine sand soil column of 10 m (100 cells × 0.1×0.1×0.1 m) with concentrations of dissolved N_2 and solutes (He and Ne) at atmospheric equilibrium. The top boundary condition was a constant pressure of 1 atm for the gas phase (Dirichlet) and a constant downward flux of 0.4 m/yr for the aqueous phase (Neumann). The concentrations of tracer gases in inflowing water at the top boundary were at atmospheric equilibrium. The bottom boundary conditions were a zero flux for the gas phase (Neumann) and a constant pressure of approximately 2 atm (1 atm plus the weight of the water in the column) for the water phase (Dirichlet). The bottom boundary for solutes was transport by advection in the aqueous phase alone. We injected N_2 into the 51st cell (between 4.9 and 5 m from the top) at a rate of 577 mmol/m^2/year, corresponding to the denitrification of a nitrate input concentration of 200 mg/l, the consumption of all dissolved oxygen and a recharge rate of 0.4 m/yr.

6.3.4 2D simulations

To reproduce the data set of total dissolved gas pressure and groundwater age tracer concentrations, we calibrated the hydrogeochemical parameters of a simple two-dimensional model for each location (Figure 6.2b).

Groundwater flow in homogeneous recharge areas can be simplified to a two-dimensional model with impermeable west and bottom boundaries and a fully penetrating drain at the east boundary (Vogel 1967). In this two-dimensional model, groundwater flows continually downward and groundwater travel times increase with depth. This conceptual model was used to study groundwater age variation and groundwater quality (Broers 2004a; Broers and Van der Grift 2004). We used this geometry for the two-phase flow model, because it allowed for lateral flow of gas and separation of the water and gas phase by clay layers. The difference from the Vogel model was that we allowed an unsaturated zone to develop in the top layers of our numerical model to realistically simulate the head and pressure profile in the model.

The width of the model domain was 100m and the height was set to the thickness of the aquifer as reported by Broers (2004a). The dimensions (x×y×z) of each model cell were 10×0.1×0.5 m. The west and bottom boundaries of the 2D model plane were closed, and water recharging at the surface discharged through the entire east boundary. The top boundary condition was a constant pressure of 1 atm for the gas phase and a constant downward flux equal to the recharge rate N for the aqueous phase. We used the recharge rate as one of the calibration parameters.

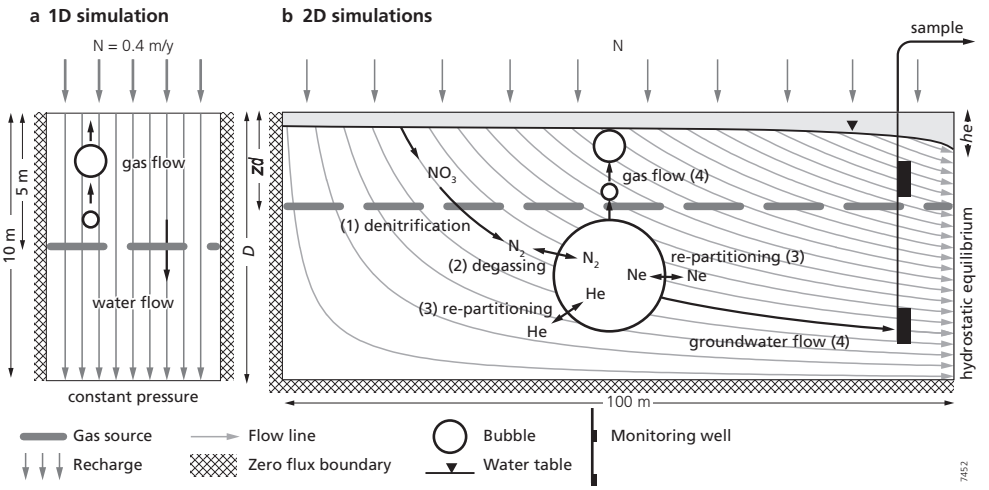

Figure 6.2 Schematic representation of the 1D (a) and 2D (b) model.

The top boundary conditions for noble gases were atmospheric equilibrium concentrations. The tritium concentration in recharging water varied according to the historical concentrations of tritium in precipitation (Meinardi 1994). The concentrations of CFCs and SF_6 in recharging water varied according to the atmospheric mixing ratios reported by Walker (2000) and Maiss and Brenninkmeijer (1998). The east boundary condition was a time-constant pressure profile with a hydrostatic gradient for the aqueous phase to simulate a fully penetrating drain. By lowering the east boundary pressure, we are able to let an unsaturated zone and a free water table develop in the top layers of the model. The east boundary water pressure was used as one of the calibration parameters, to reproduce the head measurements. The east boundary for the gas phase was a constant pressure gradient, equal to the aqueous pressure. This boundary allowed both water and gas to leave the model at the east boundary.

In the 2D model, we based the annual source rate on a historical reconstruction of nitrate concentrations in recharging groundwater (Chapter 2, Appendix). The concentrations of nitrate in recharging groundwater increased from 30 mg/l in 1940 to 255 mg/l in 1988 and decreased afterwards to 132 mg/l in 2005. Because nitrate is transported conservatively until denitrification takes place, we simply delayed the arrival of the nitrate concentrations at depth of the gas source by the modeled travel time towards this depth and compensated for the consumption of oxygen. As the result of the arrival of this nitrate-rich groundwater at the redoxcline, the injection rate of N_2 in the 2D simulations varied between 24 and 660 mmol/m^2/yr.

We calibrated each model to measurements of head, total dissolved gas pressure (TDG), ^{4}He and Ne concentrations (indicating degassing), ^{3}H and tritiogenic ^{3}He (^{3}He*) concentrations and calculated ^{3}H/^{3}He age. We adjusted three parameters -the recharge rate N, the head at the east boundary h_e, and the depth of the gas source z_{src} – by optically comparing the profiles of modeled variables in the west-most column to the measured values in the screens of the well. (The well in Figure 6.2b was placed in the east for illustrative reasons). East boundary head h_e and recharge rate N both affect the modeled head at the screen locations. Source depth z_{src} affects the modeled TDG, and can be calculated accurately beforehand if the groundwater table is modeled correctly. Because recharge rate N also affects the age profile, we calibrated N to the ^{3}H, ^{3}He* and age profiles.

The modeled CFC and SF_6 profiles were not used for calibrating the parameters of the model. They served as a consistency check and an evaluation of the reliability of CFCs and SF_6 as groundwater age tracers.

To quantify the performance, we studied the variance of the residuals between modeled and measured values, in relation to the variance of the measurements. We expressed the model performance as the measurement variance explained by the model (R^2).

We studied the effect of changing flow patterns as a result of gas production on groundwater age by comparing the groundwater ages of a degassed model run with a control run having the same hydrological parameters but without injecting N_2. We call this the hydrological effect of gas production. We calculated the model age from the ratio of concentrations of a fictional decaying tracer and its decay product. Both the fictional tracer and the decay product had a partitioning coefficient and a diffusion constant of zero so that they could only dissolve in water and not escape into the gas phase and transport was by advection alone.

6.3.5 Model summary

In summary, we modeled the following processes with the two-phase flow and transport model (Figure 6.2b):

1. Production of N_2 below the groundwater table as the result of denitrification of agricultural pollution.
2. Formation of an N_2 gas phase and degassing of the groundwater.
3. Re-partitioning of groundwater age tracers between the aqueous and gas phases.
4. Conservative transport of the dissolved gases by the groundwater from the degassing site to the monitoring screen.

6.4 Accuracy of $^3H/^3He$ groundwater ages

Three factors influence the accuracy of the modeled $^3H/^3He$ age of degassed groundwater: 1) $^3He^*$ escapes from water in the unsaturated zone into the atmosphere effectively starting the $^3H/^3He$ clock at the water table, 2) bomb peak $^3He^*$ diffuses faster into younger water than ^3H itself making groundwater of the late 1960s and early 1970s appear older, and 3) the concentration of $^3He^*$ is corrected for degassing by assuming degassing took place in a single step according to Chapter 5, while degassing may occur in multiple stages. To study the importance of these factors, we first compared the modeled $^3H/^3He$ ages with model ages of control runs to study the effect of the unsaturated zone and bomb peak diffusion and then compared the modeled $^3H/^3He$ ages of degassed runs to the modeled $^3H/^3He$ ages of control runs to study the effect of the $^3He^*$ correction.

6.5 Results

6.5.1 1D model

During the first 12 days of the 1D simulation, the N_2 injected into cell 51 completely dissolved and the dissolved N_2 concentration rose from the atmospheric equilibrium concentration of 23.6 mg/l to 36.1 mg/l (Figure 6.3). On the 13^{th} day of the simulation, the dissolved gas pressure

exceeded the hydrostatic pressure plus the air entry value and a gas phase formed in cell 51. Before the gas phase extended upward into cell 52, the gas saturation increased over the next 325 days up to the maximum trapped gas saturation. Due to the higher capillary pressure needed to support the larger gas saturation, the dissolved N_2 concentration also increased. The dissolved N_2 concentration in cell 52 increased to 26.5 mg/l due to upward diffusion of N_2 from cell 51, counteracted by downward advection of atmospheric equilibrium concentrations from cell 53. The increasing gas saturation in cell 51 reduced the upward diffusive flux through the water phase (due to increased tortuosity) while the advective downward flux remained constant and as a result the concentration dissolved N_2 in cell 52 decreased slightly after 125 days.
After the maximum trapped gas saturation was reached in cell 51, the gas phase extended upward into cell 52 and the dissolved N_2 concentration remained constant and in equilibrium with the hydrostatic pressure (hydrostatic equilibrium concentration). Note that because the hydrostatic pressure in cell 52 is lower than in cell 51, the dissolved gas concentration in equilibrium with the hydrostatic pressure is also lower. The gas phase extended upward at a rate of 0.1 m/yr while gas was injected (Figure 6.4a).

In the cells with a gas phase, the dissolved N_2 concentration was in equilibrium with the hydrostatic pressure (Figure 6.4b). Below the injection point, the dissolved N_2 concentration remained constant because no N_2 was added to or removed from downward flowing water. As a consequence, the total dissolved gas concentration below a degassing zone is related to the depth below the water table at which degassing took place. This relation was used to estimate the depth of degassing from measurements of total dissolved gas pressure (Equation 5.6).

Profiles of noble gas concentrations show that the gas phase removed a part of the noble gases from solution as a result of repartitioning of noble gases between the gas and water phase (Figure 6.4c and 6.4d). ^{4}He was more degassed than Ne, because it is slightly less soluble and prefers the gas phase more. Initially, degassing of noble gases only occurs at the injection point, but upward

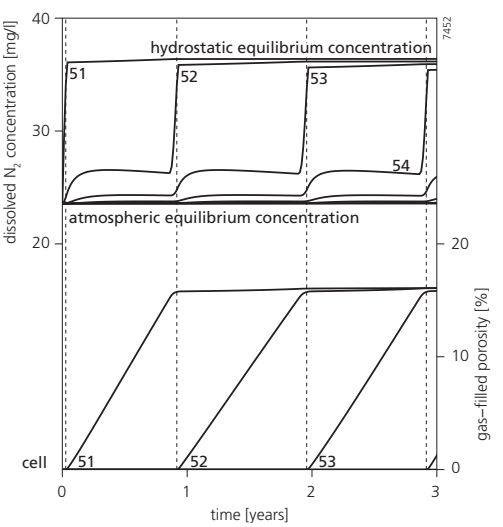

Figure 6.3 Dissolved N_2 concentration and gas saturation in model cells 51 through 55 for 3 years after the start of N_2 injection in cell 51. The gas phase extends upward if the maximum trapped gas saturation (15%) is exceeded.

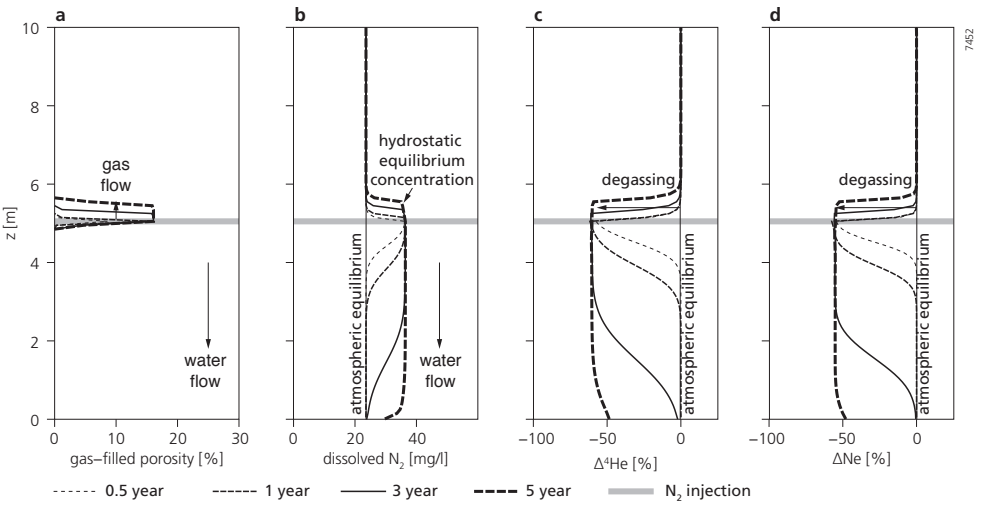

Figure 6.4 Profiles of gas-filled porosity (a), dissolved N_2 concentration (b) and ^{4}He (c) and Ne (d) concentrations in 1D model at 4 times after the start of gas injection.

moving gas also removes noble gases from solution above the injection point. In reality, upward flowing gas could cause the depletion of noble gases from nitrate-rich groundwater above the depth of denitrification but only within a limited area considering the slow upward migration of gas. Also, the total dissolved gas concentration is then also in equilibrium with the hydrostatic pressure and measuring TDG would tell whether this is the case. This example illustrates the limited mobility of a gas phase in a loamy sand column and its capability of removing noble gases from solution.

6.5.2 2D model calibration

To illustrate the calibration procedure and the 2D modeling results we plotted the profiles of modeled variables in the top 30 meters of location 1851 together with the measured values (Figure 6.5). Modeled profiles show both the results of degassing (solid line) as well as the result of the control run without degassing (dashed line). Because ^{3}H/^{3}He samples of shallow and deep groundwater were taken in 2001 and 2005 respectively, modeled profiles for both years were shown. Dashed areas illustrate the soil profile (see also Figure 6.1).

The modeled head shows steep gradients across clay layers, but the measured heads are nearly equal in the underlying sand (Figure 6.5a). The modeled TDG in this profile is close to the measured value in the shallow well screen but the TDG in the deep well screen is underestimated (Figure 6.5b). The gas source was placed at 6.1 m depth to match the TDG in the shallow screen and degassing took place just below the upper clay layer. Gas was obstructed by the clay layer from migrating upward and moved laterally to the east boundary. The modeled amount of degassing – observed as depletion of ^{4}He and Ne – was close to the measured values, although degassing of the shallow sample was slightly underestimated (Figure 6.5c and 6.5d). The modeled amount of degassing was not calibrated by adjusting any of the parameters.

The ^{3}H profile (Figure 6.5e) at the depth of shallow screens was nearly vertical and the shallow part of the ^{3}H profile alone could not be used to calibrate *N*. Because the amount

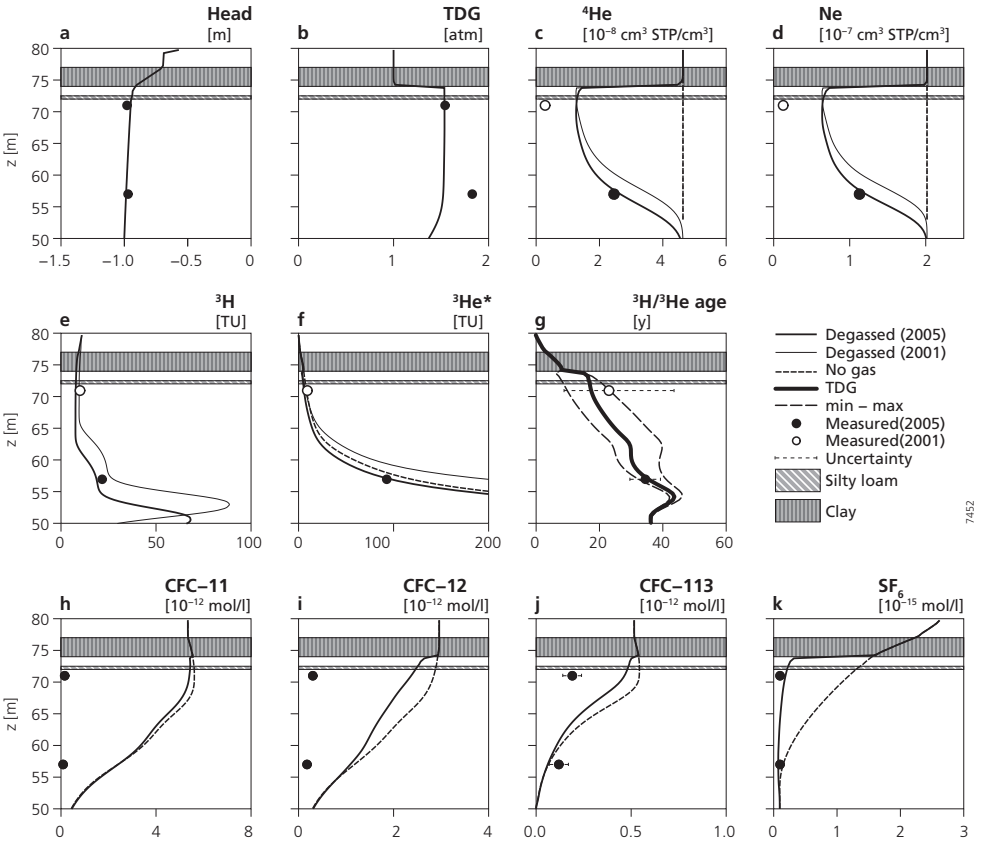

Figure 6.5 Profiles of modeled and measured variables in well 1851.

of degassing (^{4}He and Ne concentrations) was not modeled accurately, the degassed ^{3}He* concentration (Figure 6.5f) at the shallow screen could not be used to calibrate *N* either. Near the deep screens, the ^{3}H and ^{3}He* profiles both showed steep gradients and *N* was mostly calibrated to the ^{3}H and ^{3}He* measurements in the deep screen.

Without additional information, a range of groundwater ages can be estimated from a degassed ^{3}H/^{3}He sample, depending on when and where degassing took place (Chapter 5). The range of possible groundwater ages based on the modeled and measured ^{3}H and ^{3}He* concentrations is plotted in Figure 6.5g (min-max). For the shallow screen the possible range of modeled ^{3}H/^{3}He ages is smaller than the measured ^{3}H/^{3}He range, because the model underestimated the amount of degassing. The modeled age range matched the observed age range at the deep screen, because the amount of degassing was modeled accurately. Using the TDG to estimate the depth of degassing, we also calculated the most likely groundwater age based on the modeled and measured ^{3}H, ^{3}He*, ^{4}He and TDG values following the method presented in Chapter 5. The model underestimates the shallow TDG age, probably because the model is incapable of simulating three-dimensional heterogeneous flow patterns near clay layers. The TDG age in the deep well screen is modeled accurately. Because the modeled ^{3}H and ^{3}He*

concentrations are also consistent with the measurements, we are confident that the estimated recharge rate is reliable.

We found that neither CFCs nor SF_6 was a reliable age tracer at this location. Measured CFC-11 concentrations were near zero indicating that CFC-11 had been degraded in the anoxic environment. Measured CFC-12 concentrations were also below modeled profile indicating degradation of CFC-12 as well. CFC-11, CFC-12 and CFC-113 are hardly affected by degassing, indicated by the small difference between the modeled control and degassed profile. The modeled CFC-113 concentration also overestimated the measurement in the shallow screen. This overestimation was probably caused by underestimating the groundwater age at the shallow screen, as had become apparent by the $^3H/^3He$ age profile. Both the observed $^3H/^3He$ age and the CFC-113 concentration matched a groundwater age of about 30 years, found at 15 m below the surface in the modeled profile. In this case the model failed to simulate relatively older water at shallow depths and here the $^3H/^3He$ and CFC-113 measurements are consistent.

The modeled SF_6 concentration slightly exceeded the measurement at the shallow screen and matched the measurement at the deep screen. The low measured SF_6 concentration in the shallow sample in itself did not indicate that degassing had taken place. This may have been older groundwater that had recharged with a low SF_6 concentration. If no information about degassing had been available, simply comparing the measured concentration in this sample to the input curve would have led to an erroneously high age estimate. The SF_6 concentration in the deep screen is near the detection limit and beyond the horizon for groundwater dating with SF_6. This shows that both old groundwater as well as young degassed groundwater may have low SF_6 concentrations and that it is difficult to assign a reliable groundwater age to a sample with a low SF_6 concentration.

Using similar profiles, we calibrated 14 2D models to fit the measurements at each site. At 11 locations the model adequately simulated the amount of degassing. At three locations (107, 1843, 1863), we observed that the model strongly overestimated the amount of degassing. Measured time series of nitrate and other agricultural contaminants from these locations showed that the observed concentrations were systematically below the input curve of nitrate we used to model the production of N_2 gas. By lowering the input curve of nitrate to the observed levels, the modeled amount of degassing became close to the observed values (Table 6.3). At other locations, the model calculated that gas escaping to the unsaturated zone through a connected gas-filled porosity allowed tracer gases to diffuse back into the saturated zone. This led to fractionation between ^4He and Ne in the model results, which was not present in the observations. Istok *et al.* (2007) and Williams *et al.* (2007) observed that flow of gas across the groundwater table was intermittent – "burping" – which prevents back-diffusion of tracer gases. Because the model was not constructed to simulate intermittent gas flow, we forced the gas to leave the system at the east boundary by changing the uppermost fine sand layers in wells 1823, 1840 and 1863 into silty loam. By using this conceptual escape fractionation between Ne and He was avoided.

The estimated recharge rate varied from 0.29 m/yr to 0.4 m/yr with an average value of 0.32 m/yr (Table 6.3). Broers and van der Grift (2004) estimated the recharge rates for these wells between 0.17 m/yr and 0.41 m/yr with an average of 0.27 m/yr, by fitting the Vogel model to tritium measurements from the shallow and deep screens. The smaller range of estimates indicates that calibrating the recharge rate to both ^3H and $^3He^*$ measurements is better constrained, and that the resulting range is closer to the actual variation in net groundwater recharge. The modeled east boundary head ranged between 1.45 and 6.0 m below surface. At six

Table 6.3 Aquifer thickness, estimated parameters and source rate adjustment.

well	aquifer thickness (*D*) [m]	recharge rate (*N*) [m/yr]	east boundary head (h_e) [m]	degassing depth (z_{src}) [m]	source rate adjustment
107	50	0.39	-2.5	20	25%
108	100	0.31	-2.8	20	100%
122	50	0.37	-5.30	20	100%
124	80	0.40	-3.5	11	100%
125	80	0.29	-6.0	20	100%
1806	150	0.33	-3.6	3.8	100%
1823	150	0.29	-4.0	6.6	100%
1833	100	0.30	-1.90	5.1	100%
1840	80	0.37	-4.9	7.3	100%
1843	80	0.31	-3.55	20	25%
1844	80	0.31	-3.5	20	150%
1847	80	0.34	-3.1	6.1	100%
1851	80	0.29	-1.45	6.1	100%
1863	50	0.34	-1.95	8.1	50%
mean		0.32			

locations, the depth of the gas source was arbitrarily set to 20 m because the limitations of the TDG probe were exceeded in the field and the depth of the gas source could not be calibrated to the measured TDG. For the other locations the depth of the gas source ranged between 3.8 and 11 m below surface.

6.5.3 Model performance at all 14 locations

To evaluate the performance of the model at all 14 sites, we plotted the measured values against the modeled values of 11 variables (Figure 6.6): head, TDG, ^{4}He and Ne concentration, ^{3}H and ^{3}He* concentration, age, and CFC-11, CFC-12, CFC-113 and SF_6 concentrations. The axes of each plot are equal and the 1:1 line is diagonal. Degassed samples, with measured concentrations of ^{4}He and Ne below atmospheric equilibrium, are plotted with dots and normal samples with crosses to indicate the differences. The explained variances of all measured variables for the entire data set as well as subsets of normal and degassed samples are in Table 6.4.

The calibration parameters allowed us to accurately model the head at the well screen (Figure 6.6a), with a few exceptions where clay layers probably caused a steeper gradient than the model could reproduce and the explained variance is 98%. The modeled TDG (Figure 6.6b) generally captures the spread of the measured values, although the explained variance is only 33%. The measured TDG pressure of normal samples shows some variation due to the formation of excess air during infiltration (Heaton and Vogel 1981; Holocher *et al.* 2002). Because we did not model the formation of excess air, the simulated TDG pressure of normal samples was always 1 atm (along the dashed vertical atmospheric equilibrium line). The upper limit of the TDG probe was 2 atm. In these cases we allowed the modeled TDG pressure to exceed this value in order to obtain a more accurate amount of degassing (^{4}He and Ne). As a result, the R^2 of TDG dropped to 1% for degassed samples. Omitting the samples with a measured TDG of 2 atm resulted in an R^2 of 30% for the rest of the degassed samples.

The model reproduced 69% of the measured variability of ^{4}He (Figure 6.6c) and Ne (Figure 6.6d) measurements. The ^{4}He and Ne concentration in normal samples were modeled at their respective atmospheric equilibrium concentrations, again because the formation of excess air is not incorporated into the model. Within the subset of degassed samples, the model explained 43% and 48% of the measured variability (Table 6.4). This indicates that the model was not just capable of reproducing the process of degassing, but also the amount of degassing, with just the average concentrations of nitrate in recharging groundwater in the entire province as input.

The concentrations of ^{3}H (Figure 6.6e) and $^{3}He^{*}$ (Figure 6.6f) were accurately reproduced by the model (R^2 of 79% and 76% respectively), considering that it was a rather homogeneous 2D simplification of a probably heterogeneous 3D flow pattern. Modeled ages could explain 81% of the observed variance in $^{3}H/^{3}He$ ages in both normal and degassed groundwater (Figure 6.6g). Deviations from the 1:1 line were the result of either the inability of the 2D model to reproduce the variability of groundwater ages or improper correction of degassed $^{3}He^{*}$ concentrations. We studied the latter by comparing the $^{3}H/^{3}He$ ages of degassed runs with $^{3}H/^{3}He$ ages of control runs (see hereafter).

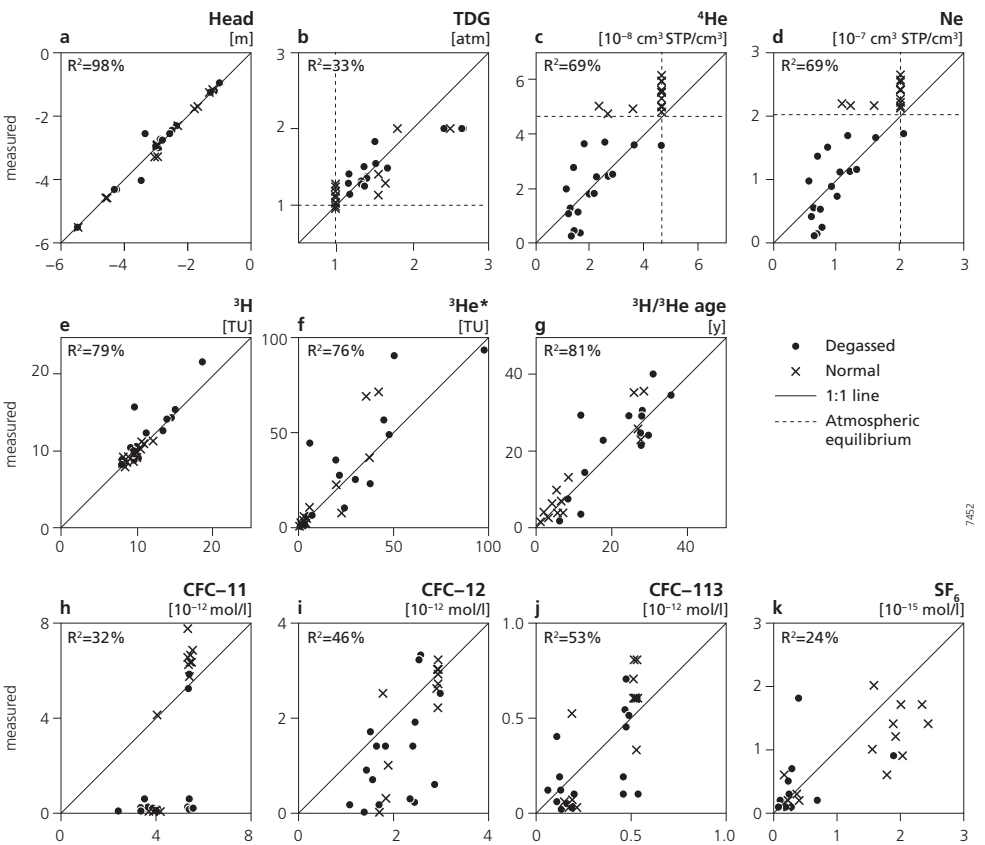

Figure 6.6 Scatter plots of modeled and measured variables of all 14 wells. R^2 indicates the explained variance by the model.

Table 6.4 Measurement variances explained by the model.

	head	TDG	^{4}He	Ne	^{3}H	^{3}He*	age	CFC-11	CFC-12	CFC-113	SF_6
all	98%	33%	69%	69%	79%	76%	81%	32%	46%	53%	24%
normal	99%	42%	-8%	-18%	71%	75%	89%	40%	58%	63%	32%
degassed	96%	1%	43%	48%	78%	75%	65%	24%	24%	31%	-12%

The discrepancy between modeled and measured CFC-11 concentrations indicated that CFC-11 is degraded in reducing environments (Figure 6.6h). Almost all degassed and thus anoxic samples were completely depleted from CFC-11 whereas the model predicted a normal range of concentrations because degradation was not simulated. The normal samples often contained CFC-11 concentrations above the modeled values. This may indicate the presence of excess air in the samples, which was not modeled, or regionally elevated atmospheric CFC-11 mixing ratios which is likely in highly industrial, densely populated areas of Western Europe. Degradation of CFC-12 is less obvious, but almost all degassed samples have measured concentrations below the modeled concentration (Figure 6.6i). CFC-113 concentrations showed large scatter, and both contamination and degradation may have occurred (Figure 6.6j). SF_6 is very sensitive to degassing because of its low solubility. Low concentrations are often largely caused by degassing, while high concentrations are only found in normal samples. The range of SF_6 values is therefore largely the result of the degree of degassing, rather than an indication of groundwater age (Figure 6.6k). The model overestimated the measured SF_6 concentration of normal samples several times, mostly because it underestimated the groundwater age.

6.5.4 Hydrological effect of degassing on groundwater age

We studied the effect of the presence of a gas phase below the water table on groundwater age by comparing model ages calculated at the sampling locations of degassed runs with model ages of control runs (Figure 6.7b, Table 6.5). We found that model ages in degassed runs were slightly younger (with mean μ = -0.27 year and standard deviation σ = 0.21 year) than in control runs. This was the effect of the gas phase reducing the water-filled porosity and increasing the flow velocity under constant recharge rates. This effect is hydrological, regardless of groundwater tracer and – under these gas flow rates – negligible compared with the uncertainties regarding modeled ^{3}H/^{3}He ages.

6.5.5 Accuracy of ^{3}H/^{3}He ages of degassed groundwater

Several factors determined the accuracy of modeled ^{3}H/^{3}He ages of degassed groundwater. First we analyzed the two factors that affect the accuracy of ^{3}H/^{3}He ages in general – ^{3}He* escape in unsaturated zone and faster diffusion of bomb peak ^{3}He* – before analyzing the effect of the correction of degassed ^{3}He*.

Because the "^{3}H/^{3}He clock" is set at the groundwater table where water is isolated from gas exchange with the atmosphere (Schlosser *et al.* 1988), the travel time in the unsaturated zone is not observed by ^{3}H/^{3}He. As a result, the modeled ^{3}H/^{3}He ages at the sampling depths (in normal runs) systematically underestimated the model ages (Figure 6.7a). To calculate the travel time in the unsaturated zone we compared the ^{3}H/^{3}He age in the topmost entirely saturated model cell of the control run to the model age (calculated from the fictional decaying tracer). This apparent age difference between the ^{3}H/^{3}He and model age was the travel time in the unsaturated zone.

In this case, the travel time in the unsaturated zone was 1.04 years on average, with a standard deviation of 0.87 year.

To study the diffusion of ^{3}He* around the bomb peak, we analyzed the residual between the modeled ^{3}H/^{3}He ages (of normal runs) and the model ages, after adding the travel time in the unsaturated zone to the modeled ^{3}H/^{3}He ages to remove the systematic underestimation. The ^{3}H/^{3}He ages (corrected for the travel time in the unsaturated zone) are accurate in shallow screens but generally overestimate the groundwater age in deep screens with water of about 30 years old (μ = 1.36 years and σ = 1.36 years) (Figure 6.7c). This overestimation is the result of faster diffusion of bomb peak ^{3}He* and similar to dispersive mixing around the bomb peak, which has already been discussed qualitatively by Tolstikhin and Kamenski (1969) and quantified by Schlosser (1989) and Ekwurzel (1994).

The uncertainty of modeled ^{3}H/^{3}He ages of control runs (Figure 6.7e) is the net effect of the travel time in the unsaturated zone and the diffusion of bomb peak ^{3}He* and has a mean of 0.32 year and a standard deviation of 1.56 years.

We assessed the accuracy of ^{3}H/^{3}He ages of degassed groundwater (using the modeled TDG to estimate the depth of degassing) by comparing the ^{3}H/^{3}He ages of degassed runs to the ^{3}H/^{3}He ages of control runs to avoid including the other sources of inaccuracy into the assessment (Figure 6.7d). We first corrected the modeled ^{3}H/^{3}He ages of the control run for the hydrological effect of the gas phase (Figure 6.7b). In this case, the error made by using ^{3}H/^{3}He on degassed groundwater had a mean of -2.09 years and a standard deviation of 1.11 years. All

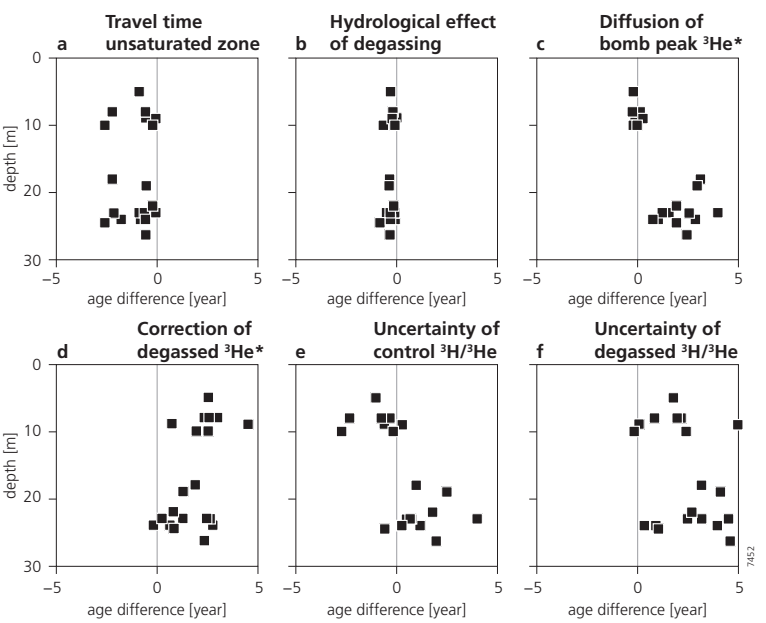

Figure 6.7 Age deviations as a result of various factors for all 14 wells.

The hydrological effect of the presence of the gas phase (b) is negligible. Uncertainty of the control ^{3}H/^{3}H age (e) is the net effect of the unobserved travel time in the unsaturated zone (a) and the diffusion of bomb peak ^{3}He* (c). Uncertainty of degassed ^{3}H/^{3}He age (f) is the net effect of (a), (b), (c) and the correction of degassed ^{3}He* (d).

Table 6.5 Statistics of uncertainties of control and degassed $^3H/^3He$ modeled groundwater ages.

Source of uncertainty	μ	σ
Travel time unsaturated zone (Figure 6.7a)	-1.04	0.87
Diffusion of bomb peak $^3He^*$ (Figure 6.7c)	1.36	1.36
Uncertainty of control $^3H/^3He$ ages (Figure 6.7e)	0.32	1.56
Hydrological effect of degassing (Figure 6.7b)	-0.27	0.21
Correction of degassed $^3He^*$ (Figure 6.7d)	2.09	1.11
Uncertainty of degassed $^3H/^3He$ ages (Figure 6.7f)	2.41	1.56

$^3H/^3He$ age estimates of degassed groundwater (except one) overestimated the model age, with an error of up to 5 years. The overestimated ages are caused by the accumulation of $^3He^*$ in the trapped gas phase. Once a gas phase has formed, the $^3He^*$ concentration equilibrates with the surrounding groundwater. Because the concentrations of tritium in precipitation are decreasing, the concentrations of $^3He^*$ arriving at the depth of degassing are also decreasing. Groundwater arriving at the depth of degassing now encounters a previously formed gas phase that has equilibrated to a higher $^3He^*$ concentration. As a result, the gas phase effectively releases $^3He^*$ to the groundwater and increases the apparent $^3H/^3He$ age, causing the overestimation.

We calculated the uncertainty of $^3H/^3He$ ages of degassed groundwater – the net effect of the travel time in the unsaturated zone, the diffusion of bomb peak $^3He^*$ and the correction of degassed $^3He^*$ – as the difference between the modeled TDG corrected $^3H/^3He$ ages of degassed groundwater and model ages of the degassed model runs. The uncertainty of $^3H/^3He$ ages of degassed groundwater had a mean of 2.41 years and a standard deviation of 1.56 years (Figure 6.7f). In this case, the TDG corrected groundwater age overestimated the true age with a bias of 2.41 years and had a 95% uncertainty interval of 6 years ($\pm 2\ \sigma$).

6.6 Discussion and conclusions

Simulating the denitrification of the historical deposition of nitrate on agricultural land in the Netherlands with a two-phase flow and transport model shows that the production of N_2 gas can cause a gas phase to form below the water table and noble gases to be depleted from groundwater. Using a simple two-dimensional model with the historical deposition of nitrate as input, we were able to reproduce the amount degassing of He and Ne. This demonstrates that degassing is most likely caused by exsolution of N_2 gas produced by denitrification.

The model was set up to trap gas until the saturation exceeded 0.15 in the sandy sediments, according to experimental observations by Fry *et al* (1997). With this setting, the gas phase only slowly extends upward, due to its immobility and the slow production of N_2 gas.

Comparing modeled CFC-11 and CFC-12 concentrations to measurements indicated that CFC-11 and CFC-12 are subject to degradation in anoxic environments. CFC-113 showed both the effect of degradation and contamination. Degradation of CFCs has also been observed in the pyritic aquifers in Canada, the US and Denmark (Tesoriero *et al.* 2000; Hinsby *et al.* 2007; Sebol *et al.* 2007). SF_6 is very susceptible to degassing because of its low solubility and therefore not reliable as an age tracer when degassing takes place. When degassing takes place under anoxic

conditions, none of the transient tracers (CFCs or SF_6) can produce reliable groundwater age estimates.

By comparing modeled $^3H/^3He$ ages of degassed runs and control runs to the model age calculated from a fictional tracer, we used the model to assess the accuracy of modeled $^3H/^3He$ ages. We found that the TDG correction of the $^3H/^3He$ age overestimated the control $^3He/^3He$ age by 2.41 years, due to the accumulation of $^3He^*$ in the gas phase. The total uncertainty of degassed $^3H/^3He$ ages of 6 years ($\pm$ 2 σ) is larger than the propagated errors in underlying measurements resulting in an uncertainty of 3 years as reported in Chapter 5. The larger uncertainty is due to the accumulation of $^3He^*$ in the gas phase and the correction of degassed $^3He^*$ using the TDG method, but also due to the travel time in the unsaturated zone and the diffusion of bomb peak $^3He^*$.

We used a simple two-dimensional two-phase flow model to study the effect of degassing on groundwater age tracers. The use of continuum two-phase flow models to simulate the very slow production of gases by geochemical reactions in the subsurface is still questioned because of the intermittent and incoherent gas flow observed in air sparging experiments (Frette *et al.* 1994; Brooks *et al.* 1999; Glass *et al.* 2000; Geistlinger *et al.* 2006; Istok *et al.* 2007). Comparing benchmark experiments of very slow gas injection in fine-grained sediments over long time scales with model results of gas and tracer transport should confirm whether this approach to modeling gas flow is justified. If so, two-phase flow models and similar models, such as MIN3P-bubble (Amos and Mayer 2006b), can provide valuable insight in the process of degassing or the formation of excess air. On the other hand, studying the transport of noble gases by ebullition in laboratory experiments will yield more knowledge about the behavior of gas in porous media. Eventually, a better understanding of groundwater degassing opens possibilities for a wider application of groundwater age tracers that yield valuable information to groundwater hydrology and environmental impact studies.

7 Travel time distributions derived from particle tracking in models with weak sinks

This chapter has been published as:
Ate Visser, Ruth Heerdink, Hans Peter Broers, and Marc F.P. Bierkens (2009) *Travel time distributions derived from particle tracking in models with weak sinks*, Ground Water 47(2): 237-245, doi: 10.1111/j.1745-6584.2008.00542.x.

Abstract

A travel time distribution based on a particle tracking analysis in a groundwater model containing weak sinks is often uncertain, because whether a particle is discharged or allowed to pass through a weak sink is unresolved by particle tracking theory. We present a probability-based method to derive an objective travel time distribution in models containing weak sinks. The method discharges a fraction of the particle at the weak sink and allows the remaining fraction to pass through the weak sink. The weight of the discharged fraction depends on the ratio of the sink flux to the influx into the weak sink cell. We tested this approach on a coarse (100×100 m) and a fine (25×25 m) horizontal resolution regional scale groundwater model (34.5×24 km). We compared the travel time distributions in a small sub-catchment derived from particle tracking analysis with one derived from a transport model. We found that the particle tracking analysis with the coarse model underestimated the travel time distribution of the catchment compared to the transport solution or a particle tracking analysis with the fine model. The underestimation of travel times with the coarse model was a result of a large area covered by sink cells in this model and the more accurate flow patterns simulated by the fine model. The probability-based method presented here compares favorably with a solute transport solution and provides an accurate travel time distribution when used with a fine-resolution groundwater model.

7.1 Introduction

Knowledge of the travel time of groundwater is essential to understanding the transport of contaminants through the groundwater system. For example, the breakthrough of spatially diffuse contamination into the surface water is strongly related to the travel time cumulative frequency distribution of discharging groundwater (Raats 1977; Van Ommen 1986; Duffy and Lee 1992; Broers *et al.* 2007).

In finite difference models such as MODFLOW (Harbaugh *et al.* 2000), the travel time of groundwater can be determined by either particle tracking (Pollock 1988) or solute transport simulations. The cumulative frequency distribution of travel times of discharging groundwater

can be calculated using particle tracking by analyzing the arrival times of particles uniformly released at the surface of the catchment using a particle tracking model such as MODPATH (Pollock 1994). The cumulative frequency distribution can also be calculated by simulating the breakthrough curve of a tracer in surface water using a transport model such as MT3DMS (Zheng and Wang 1999).

Although transport simulations are computationally more demanding than particle tracking and sometimes impractical for large groundwater models, they have the advantage of also considering diffusion and dispersion mechanisms. Particle tracking on the other hand requires less computational effort, but only considers advective transport

Particle tracking relies on an analytical approximation of the flow pattern within the model cells. Such an analytical flow pattern is only defined if all flow terms of water entering or leaving the finite difference model cell can be assigned to one of the cell faces. If a sink, such as a well, river or drain discharges water from a model cell, the flow pattern within the cell cannot be approximated analytically.

Particles reaching a sink that discharges all water entering the cell – strong sinks – are stopped when they enter the cell. Weak sinks are cells that do not discharge all water entering the cell. The problem of a weak sink is that there is no explicit way to determine whether the weak sink should discharge the particle or allow it to pass through the model cell (Pollock 1994, p. 33). MODPATH offers three options to deal with weak sinks. First, particles are stopped when they enter a cell containing a weak sink. Second, particles can pass through the cell containing a weak sink. Third, particles are stopped only if the sink discharges more than a specified fraction of the total flux into the cell, and are allowed to pass if the sink discharges less. The first two weak sink stop options are essentially special cases of the last, stopping particles if the fraction of water discharged by the sink – referred to hereafter as the *weak sink stop fraction* – equals 0 or 1, respectively.

These options can produce entirely different results for the calculation of travel times or delineation of catchment areas. This introduces an undesired subjectivity in the particle tracking analysis, because no rationale exists for determining the appropriate weak sink stop fraction (Shoemaker *et al.* 2004). Experienced modelers will look for additional information to choose the most appropriate weak sink option, but the choice will often be model and site specific. Therefore it is impossible to recommend a weak sink stop fraction that applies to all particle tracking scenarios.

This problem has been recognized by many authors (Clarke and West 1998; Hinaman and Tenbus 2000; Kelly 2004; Cherry 2006; Barlow and Ostiguy 2007; Cherry and Clarke 2007) studying the capture area of wells and/or the travel times towards them (Barlow and Dickerman 2001; Kauffman *et al.* 2001; Renken *et al.* 2001; Walter and Whealan 2005) or the travel time distribution of a catchment (Shoemaker *et al.* 2004). Most authors made a substantiated choice on the weak sink stop fraction, but few analyzed the results obtained using several weak sink stop options (Barlow 1995; Paschke 2007). A particle tracking study to estimate the fractions of the underflow into Mexico by the US Bureau of Reclamation (2001, Attachment 5) showed that the chosen weak sink stop option can result in entirely different estimates of cross-border groundwater flow.

The weak sink problem was solved for some cases of weak sinks. Most of the published solutions focused on weak sinks represented by wells. The flow pattern within a weak sink cell containing one vertical well can be approximated by an analytical solution (Zheng 1994) or by using an automated rediscretization to locally refine the flow model (Spitz *et al.* 2001). Walter

and Whealan (2005) used a sub-regional model with such a fine resolution that all wells were represented as strong sinks. Walter and Masterson (2003) investigated the effect of cell sizes in regional and subregional models on the catchment areas of (proposed) municipal drinking water wells derived from particle tracking. MODFLOW-2000 (Harbaugh *et al.* 2000) and later versions offer the option to assign the flux of a sink to one of the cell faces, but only if the face is a boundary face. This may remove the weak sinks represented by rivers or drains, but only if the weak sinks are in a cell at the surface of the model.

The analytical solution by Zheng (1994) and the rediscretization method by Spitz *et al.* (2001) were designed for wells but may be extended to other types of weak sinks. However, these methods require accurate knowledge about the location of the sink feature. This information may be available for wells, but is often unknown for tile drainage systems. Furthermore, rediscretization requires more detailed geological information which is often not available, while small heterogeneities may strongly influence the flow pattern around sinks. More importantly, a large number of watercourses, tile-drains, or small wells would make it impractical to build a fine grid model for every weak sink cell. Therefore there is a need for a practical solution to deal with weak sinks in large-scale coarse-resolution groundwater models.

In this paper we present a probability-based solution to the weak sink problem for the calculation of the cumulative frequency distribution of travel times of discharging groundwater. We use the term *travel time distribution* to indicate a cumulative frequency analysis of travel times of discharging groundwater, rather than a spatial analysis of travel times. We tested this method on two MODFLOW models of the same area, one with a coarse and one with a fine horizontal resolution. To study whether this method provides reliable travel time distributions, we compared the results to the travel time distribution calculated with a transport model based on the coarse groundwater model.

7.2 Methods

7.2.1 Splitting particles at weak sinks

Because the fate of particles arriving at weak sinks is unknown in a deterministic sense, we propose to consider the fate of a particle arriving at a weak sink cell as a random process. We can then assume that the probability of a particle to either discharge or pass the cell is related to the fraction of water that is discharged by the weak sink. Under this assumption, the probability that the particle will discharge at the weak sink cell (P_{stop}) equals the amount of water discharged by the sink (Q_{sink}) as a fraction of the total influx through the cell faces (Q_{in}):

$$P_{stop} = \frac{Q_{sink}}{Q_{in}} \tag{7.1}$$

Similarly, the probability that the particle will pass through the weak sink cell (P_{pass}) equals the amount of water leaving the cell through one or more of the cell faces (Q_{out}) as a fraction of the total influx through the other cell faces:

$$P_{pass} = \frac{Q_{out}}{Q_{in}} \tag{7.2}$$

These probabilities are complementary and sum to one. If the weak sink cell can be regarded as a perfectly mixed reservoir, these probabilities are mathematically correct. In groundwater flow models, the probability that a particle will be discharged is also related to the exact flow pattern within the cell, which is generally unknown.

If the probability of a particle to either stop or pass is known, we can evaluate both possibilities and use the probability to weigh their effect on the travel time distribution. Instead of deciding upon a single fate of the particle during particle tracking, we now split the particle at the weak sink into two fractions. One fraction of the particle is discharged and the travel time (t_i) is recorded, the other fraction passes the cell and particle tracking continues. The probabilities of the particle stopping at or passing the cell determine the weight of each fraction.

To record the probabilities of particle fractions passing through a weak sink, we assigned a weight of one to each particle (i) at the start of the simulation. The weight of the particle fractions after splitting (W_i^+) equals the weight of the particle (or particle fraction) before splitting (W_i^-) times the probability of the entire particle either discharging P_{stop} (Equation 7.3) or passing P_{pass} (Equation 7.4):

$$W_{i,stop}^{+} = W_i^{-} \bullet P_{stop} = W_i^{-} \bullet \frac{Q_{sink}}{Q_{in}} \tag{7.3}$$

$$W_{i,pass}^{+} = W_i^{-} \bullet P_{pass} = W_i^{-} \bullet \frac{Q_{out}}{Q_{in}} \tag{7.4}$$

If the particle fraction subsequently passes through another weak sink cell, the weight of the particle fraction that passed the first weak sink cell ($W_{i,\ pass}^{+}$) is used again as the weight before the next split (W_i^-). If the weight of the particle fraction that would pass the cell is less than 0.001 after multiplication, this particle fraction is discharged as well, because its contribution to the travel time distribution would be negligible.

After particle tracking, the cumulative travel time distribution (D) of a catchment can be calculated as the travel time distribution of the discharging particle fractions. Usually, this is the number of forward-tracked particles released uniformly at the surface that discharges before a specified time. In this case, it equals the sum of the weights of all N particle fractions that discharged before a specified time (T) divided by the total weight of all particle fractions. Particle fractions with a weight smaller than one contributed to the travel time distribution according to their weight:

$$D(T) = \sum_{i=1}^{N} \begin{pmatrix} W_{i,stop}^{+} & if\ t_i \le T \\ 0 & if\ t_i > T \end{pmatrix} \Big/ \sum_{i=1}^{N} \left(W_{i,stop}^{+} \right) \tag{7.5}$$

with t_i the time of discharge of particle fraction i.

To test this approach, we inserted extra code into version 4.3 of MODPATH. The extra code only recorded the weight of the particle fractions. Particles were tracked by the original code of MODPATH using the "pass through weak sinks" option. The extra code was designed for forward particle tracking, but could also be developed for backward particle tracking. The weights of the discharging particles were recorded in the path line file, from which we derived when and where particles were partially discharged by weak sinks. We will refer to this method as the *split at weak sinks* option and the adapted MODPATH code was named SplitPath.

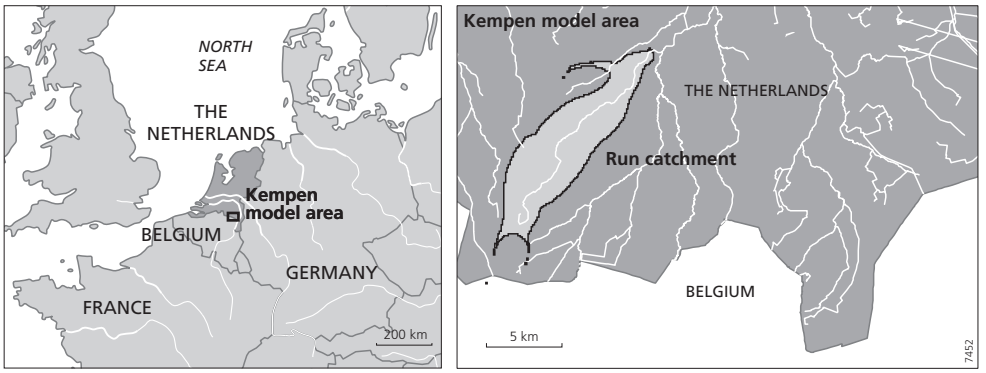

Figure 7.1 Study area and model extent.

Two weak points of this approach should be mentioned here, which are also true for other weak sink options. First, particles are discharged at the time they enter a sink cell, disregarding the travel time within the cell. Second, the calculation of the travel time through a weak sink cell may not be reliable because path lines through a weak sink cell may not accurately represent path lines of the actual groundwater flow system (Pollock 1994, p. 35).

7.2.2 Study area

We tested the probability-based method on a regional groundwater model of the Kempen area, in the south of the Netherlands, in which many river and drainage features act as weak sinks. The Kempen area (Figure 7.1) is flat lowland with surface levels increasing from about 20 m above sea level in the north to about 40 m above sea level in the south. Brook valleys are 10

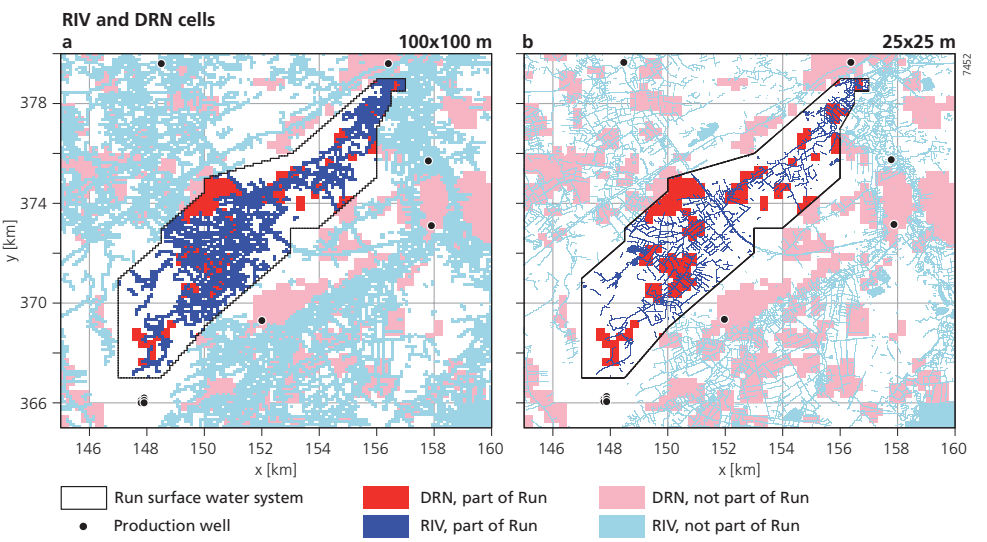

Figure 7.2 Maps of cells with RIV and/or DRN features in the second model layer of the coarse (a) and fine (b) models. Dark colors indicate cells that were assigned to the Run surface water system.

m below the surrounding area at most. Annual precipitation is 700 mm on average and net annual groundwater recharge is about 280 mm. Geologically, the area can be divided into two subareas: the Kempen High in the southwest and the Roer Valley Graben in the northeast of the model area. The Late Pleistocene sediments that cover the Roer Valley Graben are fine-grained fluvial and aeolian sandy deposits intercalated with heterogeneous layers of loam and peat. These sediments have a maximum thickness of 35 m. On the Kempen High, the top sediments consist mainly of medium and coarse sand and some gravel deposits from the rivers Rhine and Meuse. Deeper geological formations in the area are of aeolian origin or deposits from precursors of the river Rhine (Van der Grift and Griffioen 2008). The area was originally drained by a natural system of brooks and streams. In the 19th century, this natural system was extended with a fine network of ditches to form an interconnected surface water system and make agricultural land use possible. In the 20th century, tile drainage was installed in large parts of the agricultural land. More than half of the model area is used for agriculture, most of which is drained by ditches and/or tile drainage.

7.2.3 Groundwater flow models

The groundwater model was initially developed in combination with a transport model to study the transport of agricultural contaminants as well as heavy metal contamination from nearby zinc smelters in the Kempen area (Van der Grift and Griffioen 2008). This model was clipped from a larger regional groundwater model (Buma *et al.* 2002) and had a horizontal resolution of 100×100 m. We refer to this model as the *coarse* model. The horizontal resolution of this model was refined to 25×25 m to make the *fine* model. The models covered an area of 34.5×24 km. Both models had a thickness of 56.5 m distributed over 18 layers of which the thickness increased from 0.5 m for the top layer to 10 m for the bottom layer. The top of the model followed the surface elevation.

The north and south boundaries of the two models were constant head boundaries, derived from the larger regional model. The east and west boundaries were zero-flux boundaries because the regional groundwater flow direction is generally south-to-north. Recharge in the model area (283 mm/y) was modeled with the Recharge (RCH) Package. All features of the interconnected surface water system in the model area were modeled using the River (RIV) Package (Figure 7.2). RIV features were based on topographical maps for each model resolution separately, resulting in a more accurately defined river surface water system in the fine model. The Drain (DRN) Package was used to model tile drains, which were based on field scale information on tile drainage. The same DRN definition was used for the coarse model and the fine model because the exact location of individual tile drains is unknown and information on the presence of tile drains is not available at the fine model resolution. All river and drain features were located in the second model layer (0.5 – 2.5 m below surface), because the level of most streams, ditches, and especially drains is often more than 0.5 m below the average surface elevation. Also, placing them in the thin top layer resulted in numerical convergence problems (Buma *et al.* 2002). Production wells were modeled with the Well (WEL) Package and were located 31.5 to 56.5 m below land surface in layers 15, 16 or 17.

For this study, we focused on the catchment of the Run stream and its tributaries. The catchment of the Run is located on the Kempen High and has an area of 45 km^2. The Run stream discharges 12×10^6 m^3 of water annually. We specified cells containing RIV and/or DRN features based on the 1:10,000 topographical map, which were considered to represent the Run surface water system (Figure 7.2).

7.2.4 Transport model

To derive the travel time distribution of the Run, we simulated the transport of a fictional conservative tracer using a solute transport model (MT_3DMS, version 5.0) based on the coarse scale model. The initial concentration of the tracer was set to zero, and the concentration of the tracer in recharge was set to one. The concentration of the tracer in groundwater discharging into the stream increased from zero (at model time zero) to one at the maximum advective travel time in the catchment, when the entire groundwater flow system was flushed. The breakthrough curve of the tracer in the stream is analogous to the travel time cumulative frequency distribution of discharging groundwater (Van Ommen 1986). We used the TVD option in MT_3DMS to simulate advective transport of the tracer (Datta Gupta *et al.* 1991) and did not simulate diffusion and dispersion.

7.2.5 Analysis

First, we delineated the catchment area of the Run surface water system by a forward particle tracking analysis. A single particle was placed at the center of each model cell at the surface of the model and tracked to its discharge point. We repeated the forward particle tracking analyses for all possible weak sink stop options: stop at weak sinks, pass through weak sinks, as well as 10 values for the weak sink stop fraction. All cells from which a particle discharged into a RIV or DRN cell assigned to the Run surface water system (when using any of the stop options) were considered to be part of the catchment area of the Run surface water system. This resulted in the maximum extent of the catchment area.

Second, we mapped the weak sinks in the catchment area by analyzing the MODFLOW cell-to-cell flux files of both the coarse and fine models. We also studied the histograms of the strength of weak sinks (the fraction of water entering the cell that is discharged by the sink) within the Run catchment area. The histograms of sink strength may assist in determining the appropriate weak sink stop fraction or justify one of the weak sink stop options.

Third, we analyzed the travel time distribution of the Run catchment calculated from all possible weak sink stop options for the coarse and fine model. Finally, we applied the particle splitting approach and compared the results of all weak sink stop options with the transport model travel time distribution.

7.3 Results

7.3.1 Delineation of catchment area

To delineate the catchment area of the Run surface water system by means of a forward particle tracking analysis, we included all cells from which particles started that eventually discharged into the Run surface water system for at least one of the weak sink stop options (Figure 7.3). Most of these particles discharged in the Run regardless of the chosen weak sink stop fraction, but some only discharged in the Run for a few of the weak sink stop fractions. In the coarse model, particles originating in 119 cells (representing 2.5% of the catchment area) discharged in the Run for some stop fractions, but discharged to a different surface water system in the model when other stop fractions were used. Whether this area actually contributed to the Run is therefore uncertain. Moreover, each chosen weak sink stop fraction excluded some cells that were included in the Run catchment by other stop fractions. This indicates there was no single

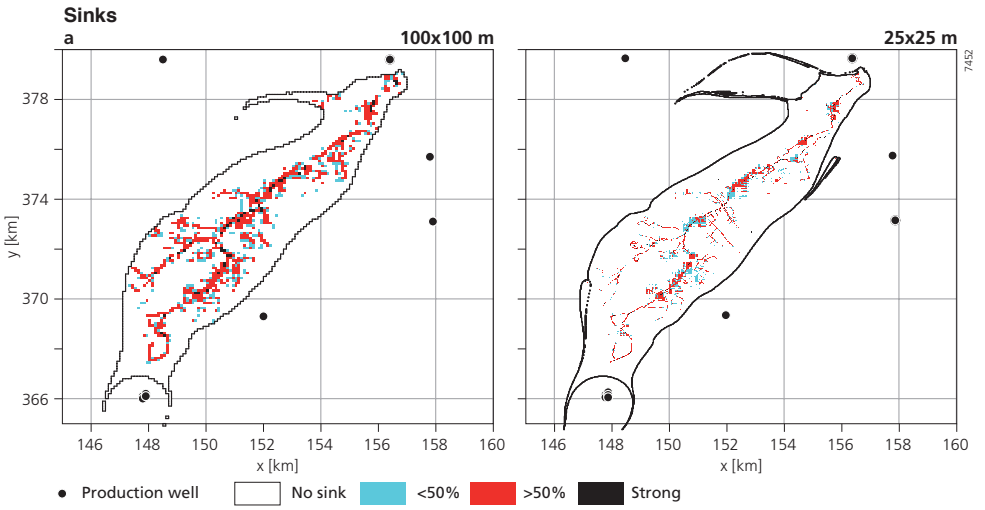

Figure 7.3 Delineation of the Run catchment in the coarse (a) and fine (b) models. Colors represent the "strength" of sinks in the model area: the fraction of water entering the cell that is discharged by the sink.

weak sink stop fraction that delineated the entire catchment area. This problem occurred to only 730 particles in the fine model (representing 0.08% of the catchment area), thus refining the horizontal model resolution practically solved the uncertainty in delineating the catchment area. The Run catchment delineated from the fine model shows some narrow disconnected bands in the northwestern part of the catchment (Figure 7.3b). The areas to the northwest and east of the Run catchment have complex local groundwater flow systems. To the south of the Run catchment is the capture area of a production well. The differences in the extent of the catchment area that is estimated with different weak sink stop options and horizontal discretizations illustrate the uncertainty in the estimated catchment area related to the model design.

7.3.2 Spatial distribution of weak sinks

We mapped the location and strength of the sinks in each model to illustrate the differences between the coarse and fine models (Figure 7.3). Not all RIV or DRN features were active, because the modeled head in these cells was below the RIV or DRN level. Although the number of RIV and DRN cells was much higher in the fine model, each of these cells covered an area of only 25×25 m. In contrast, each RIV or DRN cell in the coarse model covered an area of 100×100 m. As a result, sink cells covered a larger area in the coarse model (22%) compared to the fine model (8%). Figure 7.3 also shows that most weak sinks in the coarse model were rather strong (Q_{sink}/Q_{in} > 50%).

7.3.3 Histograms of sink strength

Because we assumed that the probability of a particle to discharge at a weak sink depends on the fraction of water discharged by the sink, it is interesting to know how "strong" the weak sinks are. To analyze the sinks in the model area, we plotted for each model the histogram of sink strengths (Figure 7.4) with respect to the area covered by the sink cells and the flux of water

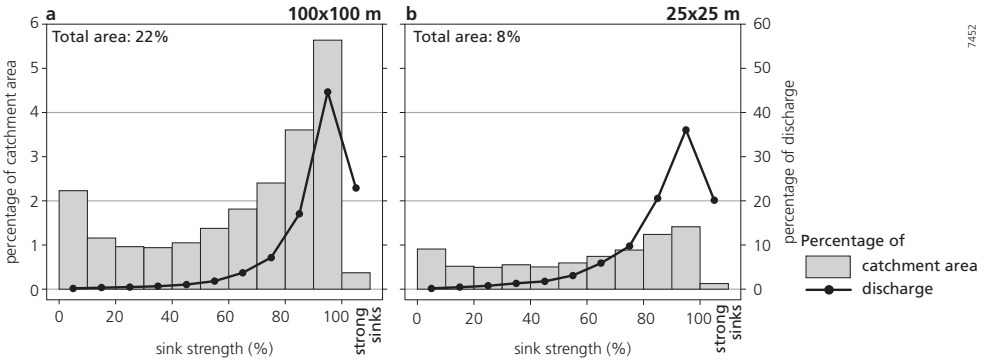

Figure 7.4 Histograms of sink strength (fraction of water entering the cell that is discharged by the sink) expressed as a percentage of the catchment area or discharge volume.

discharged by the sinks. Especially stronger weak sink cells (Q_{sink}/Q_{in} > 50%) covered a larger area of the coarse model than in the fine model. The fine model showed an almost uniform histogram of sink strength with respect to the model area, with only slightly more stronger weak sinks. The histogram of the amount of water discharged through weak sinks was quite similar for both models. The exponential shapes of the histograms of discharge indicate that stronger weak sinks also discharged at higher rates.

The histogram of sink strength could be used to choose an appropriate weak sink option or reject an inappropriate option. For example, letting particles pass through all weak sinks would fail to discharge the particles at many rather strong (Q_{sink}/Q_{in} > 80%) weak sinks in the coarse model, together responsible for producing about 50% of the discharge.

7.3.4 Travel time distributions with different weak sink options

The different weak sink stop options produced a wide range of travel time distributions (Figure 7.5). The envelope of possible travel time distributions is larger for the coarse model due to the larger number of stronger weak sinks. The choice between a weak sink stop fraction of 0.8, 0.9 or

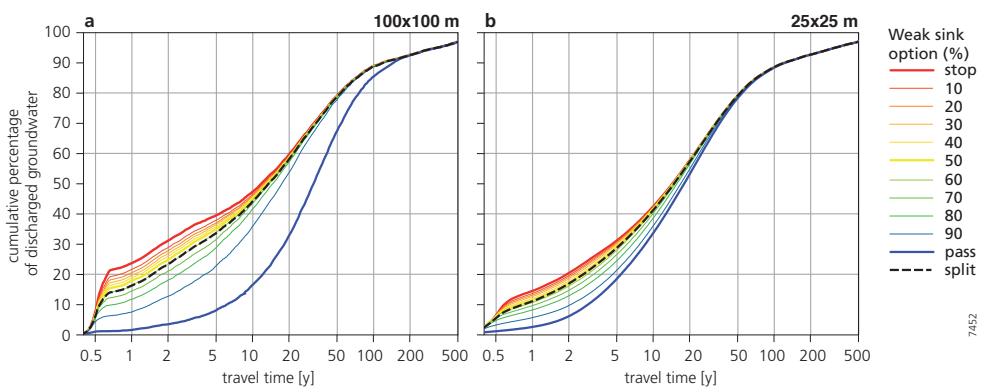

Figure 7.5 Travel time distributions of the Run catchment in the coarse (a) and fine (b) models calculated with several weak sink stop options.

1.0 (pass through weak sinks) had a profound effect on the shape of the travel time distribution of the coarse model, because these stronger weak sinks produced a large portion of the total discharge. The horizontal model refinement improved the accuracy of the travel time distribution: the envelope of possible travel times became narrower indicating that weak sinks were less important. However, the envelope was not reduced to a single unique travel time distribution.

The travel time distribution of the coarse model had a steep jump up to 20% within the first year, indicating that about 20% of recharging groundwater discharges within one year. This jump was the result of the arrival time of particles that recharged directly above sink cells, which covered an area of 22% of the coarse model. This effect was smaller for the fine model, because a smaller area was covered with sink cells. This part of the travel time distribution is also not very accurate because the steady-state model does not simulate seasonal fluctuations.

Under most weak sink stop options, the fine model predicted longer travel times than the coarse model: the travel time distribution of the fine model is lower than that of the coarse model. This was the result of two factors: First, fewer particles could discharge in the cell directly below the starting point because the drained area of the fine model was smaller. Second, the travel time is recorded as particles enter a sink cell. The fine sink features in the fine model were further apart and the fine model was able to calculate the flow path and travel time towards the actual sink feature within the space of the cells of the coarse model. Only if particles were allowed to pass weak sinks, the coarse model predicted longer travel times due to the large number of stronger (Q_{sink}/Q_{in} > 80%) weak sinks.

The travel time distributions using the split at weak sinks option closely resembled the travel time distributions calculated with a weak sink stop fraction of 50% (Figure 7.5). The travel time distributions of the coarse and fine model calculated with SplitPath were still quite different, due to differences in the flow pattern, but the uncertainty as a result of a subjective choice for any of the weak sink stop options is removed.

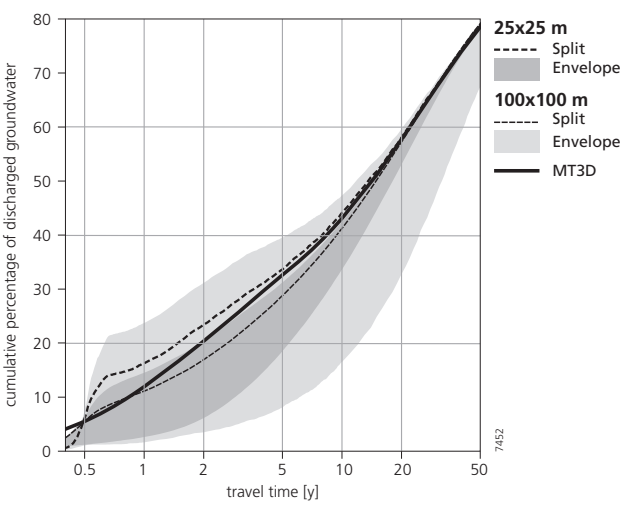

Figure 7.6 Travel time distributions derived from particle tracking compared to transport solution (MT3D).

7.3.5 Comparison with transport model

The travel time distribution of the transport model (Figure 7.6) was mostly in between the travel time distributions of the coarse and fine model calculated with SplitPath. The transport model estimated longer travel times than the particle tracking analysis with the coarse model. Rather than recording the travel time when a particle enters a sink cell, the transport model calculated the concentration of the tracer at the center of the model cell. This way, the transport model implicitly considered the travel time of solutes within the sink cell. Numerical dispersion in the transport model solution smoothed the arrival of the block-front in the second model layer containing the drainage features, resulting in a higher estimate of discharging groundwater younger than 0.5 year.

7.4 Discussion and conclusions

We present a probability-based method to calculate an objective cumulative frequency distribution of travel times of discharging groundwater that is based on a particle tracking analysis in a groundwater model containing weak sinks. This method splits a particle in two when it reaches a weak sink, discharging one fraction and allowing the other to pass through the weak sink cell. The contribution of either fraction to the travel time distribution depends on the fraction of groundwater discharged by the weak sink. This method – SplitPath – provides the most likely objective travel time distribution given the modeled groundwater flow field.

Having removed the uncertainty in the particle tracking analysis associated with weak sinks, it is possible to analyze the effect of refining horizontal model resolution on the travel time distribution of a small catchment. Particle tracking analysis in a coarse model underestimates travel times of discharging groundwater for two reasons. First, travel times are recorded when a particle enters a sink cell. A finer resolution model is capable of recording the travel time of particles towards a drainage feature within the space of the coarse model cells, resulting in longer travel times. Because a transport model calculates concentrations for the center of the model cell, it implicitly considers the travel time within the cells of a coarse-resolution model. Second, RIV and DRN cells cover a larger area of the catchment in a coarse model. All precipitation on this area is discharged almost immediately and has a very short travel time. Discharge features in a fine-resolution model cover a smaller area and the horizontal flow towards these features is more accurately considered.

A transport model is a more reliable method to calculate the travel time distribution of a catchment. However, a transport model based on a fine-resolution groundwater model may not be feasible. In that case, the most accurate travel time distribution is based on a SplitPath particle tracking analysis on a fine-resolution groundwater model.

The travel time distribution of a catchment calculated from particle tracking analysis can be combined with land use and contamination history to produce a breakthrough curve of conservative contaminants (Broers *et al.* 2007). If land use is not uniform within the catchment, this approach also requires a spatial analysis of travel times. A travel time distribution must then be derived for each land use type within the catchment, to be combined with the land use specific contamination history. These combinations provide land use specific contributions to the breakthrough curve (Broers and Van Geer 2005). The sum of these contributions produces a quick and reliable prediction of future surface water quality. This approach requires less

computational effort than transport simulations and can also be performed on a finer resolution groundwater model.

The SplitPath approach presented in this paper can be used to produce an accurate and objective cumulative frequency distribution of travel times in a groundwater model with many weak sinks, independent of the weak sink stop option and without the need for (local) model refinement.

8 Conclusions and New Research Questions

8.1 Summary of chapter conclusions

Each of the previous six chapters has provided an answer to one of the sub-questions. In this chapter, these conclusions are summarized to form the basis for the overall conclusion of the thesis and the formulation of new research questions, discussed in section 8.3.

PART I: TRENDS IN GROUNDWATER QUALITY

Can we detect trends and demonstrate trend reversal in groundwater quality using groundwater age?
Chapter 2 discussed the potential of relating concentrations of pollutants in groundwater to the time of recharge, instead of the time of sampling, to demonstrate trend reversal. Concentrations of conservative pollutants related to time of recharge showed an increase in groundwater recharged before 1985 and a decrease after 1990. Thereby, trend reversal of groundwater quality was demonstrated. This showed that $^{3}H/^{3}He$ dating is particularly useful to facilitate (re) interpretation of existing groundwater quality data. Additionally, the measured concentrations related to time of recharge showed a strong correlation to a reconstruction of the contamination history that was based on historical records of the application of fertilizer and manure.

Can we understand the trends of concentrations of reactive solutes using groundwater age?
The purpose of Chapter 3 was to identify solute specific trends in concentrations that are influenced by reactions with sediment geochemistry. Three types of trends were distinguished: (1) trends that are caused solely by changes in land use practices for conservative solutes, (2) trends that the result of changing recharge concentrations but that are affected directly by reactions with the subsurface, like retardation of K by cation exchange or nitrate reduction by pyrite oxidation, and (3) trends that the result of reactions between solutes and the subsurface, triggered by changing recharge concentrations of other pollutants, such as the release of heavy metals by nitrate induced pyrite oxidation. A combination of reactive transport modeling and the analysis of concentrations related to groundwater age provides an effective tool for revealing the appropriate hydrogeochemical processes that are responsible for trends in groundwater quality.

Which method is best suitable for the detection of trends in groundwater quality given a variety of available data, hydrogeological settings, and objectives?
Four methods for the detection and extrapolation of trends in groundwater quality were compared in Chapter 4: (1) statistical methods, (2) groundwater dating, (3) transfer functions, and (4) deterministic models. This chapter showed that there is no single optimal method to detect trends in groundwater quality across widely differing catchments. The selection of the method should firstly be made on the basis of the specific goals of the study (only trend detection or also

extrapolation), and secondly on the system under study, and the available resources. For trend detection in groundwater quality, the most important difference between groundwater bodies is whether the character of the subsurface or the monitoring system causes mixing of groundwater with different travel times.

PART II: GROUNDWATER AGE

Can we date groundwater that is affected by geochemical reactions and subsequent degassing?
The production of gases in groundwater under contaminated locations by geochemical reactions is not uncommon. Degassing of these gases from groundwater and re-partitioning of noble gases between water and gas phase distorts groundwater dating by $^{3}H/^{3}He$.

To correct for the loss of tritiogenic ^{3}He due to degassing, a single-step equilibrium degassing model was presented in Chapter 5. The total dissolved gas pressure (TDG) at the monitoring screen was used to estimate the depth and timing of degassing, which is essential to estimate travel times from degassed samples. By propagating the uncertainties in the underlying measurements and assumptions through the travel time calculations, we found a travel time uncertainty of 3 years. This showed that $^{3}H/^{3}He$ dating provides valuable information on groundwater flow even at sites with strong degassing.

What is the fate of N_2 bubbles in the subsurface and how accurate are tracer ages of degassed groundwater?
Chapter 6 discussed the use of a two-phase flow and transport model (STOMP) to study the reliability of $^{3}H/^{3}He$, CFCs and SF_6 as groundwater age tracers under agricultural land where denitrification causes degassing. The TDG correction of the $^{3}H/^{3}He$ age presented in Chapter 5 overestimated the groundwater age by 2.1 years, due to the accumulation of $^{3}He^*$ in the gas phase. The total uncertainty of degassed $^{3}H/^{3}He$ ages of 6 years ($\pm$ 2 σ) is due to the correction of degassed $^{3}He^*$ using the TDG method, but also due to the travel time in the unsaturated zone and the diffusion of bomb peak $^{3}He^*$. CFCs appear to be subject to significant degradation in anoxic groundwater and SF_6 is highly susceptible to degassing. Based on the two-phase flow model results, $^{3}H/^{3}He$ appears to be the most reliable method to date degassed groundwater in the anoxic parts of an aquifer.

How can we derive accurate travel time distributions in regional scale models in order to predict trends in surface water quality?
The breakthrough of spatially diffuse contamination into the surface water is strongly related to the travel time distribution of discharging ground water. However, a travel time distribution based on a particle tracking analysis in a ground water model containing weak sinks is often uncertain, because weak sinks in the flow model pose a problem to the particle tracking theory. The probability-based method presented in Chapter 7 compares favorably with the solute transport solution and provides the most accurate travel time distribution that is based on a fine-resolution ground water model.

8.2 Main conclusion

What is the value of groundwater age in the detection of trends in groundwater quality?
Groundwater age is of utmost importance in the detection of trends in groundwater quality. In general, a conceptual understanding of the groundwater system is essential for the characterization of chemical status and the detection of trends. Groundwater age is in particular valuable for two reasons. First, the possibility to aggregate groundwater quality data from several independent monitoring locations across a groundwater body, with similar land use in their catchment area; and second, the possibility to link measurements of groundwater quality, and trends therein, related to time of recharge, directly to the contamination history. The value of groundwater age is demonstrated, apart from this thesis, by a growing number of studies using groundwater age in the detection of trends (Laier 2004; Daughney and Reeves 2006; Wassenaar *et al.* 2006; Tesoriero *et al.* 2007; Burow *et al.* 2008; Debrewer *et al.* 2008; Rupert 2008; Saad 2008). These studies agree that groundwater age is invaluable to the interpretation of existing time-series (Rosen and Lapham 2008).

Given the importance of travel times, they may be used to optimize the monitoring program or aid in the extension or improvement of the existing network. Although groundwater ages can only be determined after the installation of a monitoring location, groundwater age distributions estimated from simple analytical equations or complex models are practically essential for the design of a monitoring network (Van Duijvenbooden *et al.* 1985; Broers 2004a; Janssen *et al.* 2006).

8.3 New research questions

8.3.1 Monitoring and trend detection

Twenty years after the first manure acts were implemented in the Netherlands, the improvement of groundwater quality has been demonstrated. This achievement was possible thanks to accurate groundwater dating allowing the existing groundwater quality time-series to be interpreted in a new way. The question is whether these time series are still necessary, if groundwater ages are available. This approach of trend detection relies on groundwater data to be related to the time of recharge. The range of groundwater ages at the screens of the monitoring network provides measurements of pollutant concentrations that represent the entire period of agricultural history. With this approach, existing poor quality time-series of groundwater quality data may no longer be required to show trends, but rather provide sufficient data to overcome the natural variations that obscure the anthropogenic trends. Instead of using time-series, trend detection is now feasible on a limited number of high quality measurements, combined with groundwater ages. This approach is most useful for the detection of existing trends in groundwater quality and to appoint areas at risk of failing to reach good chemical status. To demonstrate trend reversal in response to new measures or action programs, groundwater quality monitoring is still needed; preferable in shallow screens where young groundwater is found.

Present day concentrations of nitrate in groundwater in Noord-Brabant are still above the EU Quality Standard of 50 mg NO_3 per liter. The downward trends demonstrated in this thesis decrease the concentrations of nitrate towards the Quality Standard. These trends, linked to fertilizing practices through regression analysis, are particularly useful to predict the moment of compliance with the threshold values by extrapolation. The next challenge is to demonstrate

that good chemical status will be achieved by 2015. This also requires continued monitoring the shallow screens. If present day limitations on the application of fertilizers appear to be insufficient, stricter rules must be enforced. Legislation is often evaluated within a few years after its implementation, but the question is when it will be possible to reliably detect the effect of such measures. In principle, the ages of groundwater in the shallow screens represent the shortest response time of the monitoring network to detect changes water quality resulting from changing agricultural practices.

Groundwater ages provide a direct link between groundwater quality and past land use changes. This direct link between the input of pollutants and the response of groundwater quality forms a simple empirical model for predicting future groundwater quality. In contrast to simple linear regression through groundwater quality time-series, this approach is capable of predicting future trends – as well as trend reversal – in groundwater quality due to land use changes. Directly linking groundwater quality and historical land use changes implicitly assumes that the leaching processes remain the same. The question is whether changing agricultural practices, such as the direct injection of manure into the soil, have an effect on the net leaching of pollutants to groundwater.

Reactive pollutants and transport modeling

Trends in reactive pollutants in relation to groundwater age are better understood with the aid of a stream-tube reactive transport model. In this study the stream tube model was only used for the analysis of trends in reactive solutes, and intentionally not calibrated. However, such a calibration is in principle possible with the available data. Additional measurements of different geochemical variables will provide even more insight in the geochemical reactions. For example, the complete composition of all dissolved gases, including N_2 produced by denitrification, would be extremely helpful. Isotope ratios of NO_3-N and N_2-N have been used to distinguish between atmospheric and nitrate-derived N_2 (e.g. Wassenaar *et al.* 2006; e.g. Singleton *et al.* 2007), while the different sources of SO_4 (i.e. pollution and pyrite) have been distinguished by S isotopes (e.g. Moncaster *et al.* 1992; e.g. Schwientek *et al.* 2008). Additionally, O-isotopes of NO_3 and SO_4 provide even more insight into the sources of these solutes.

The non-linear behavior of reactive pollutants requires the use of reactive transport models for the extrapolation of trends in groundwater quality. Calibrating a reactive stream tube model against a large data set of concentration measurements makes it possible to estimate an effective geochemical parameterization of subsurface and build a representative 1D stream tube model. The dimension of this effective parameterization of the subsurface (1D) would match the dimension of point data available to calibrate the model. In contrast, the parameterization of a 3D reactive transport model strongly relies on generalizations of the subsurface and its properties. A different stream tube model is needed for each land use type and hydrological setting. Each of the stream tube models requires a separate data set for calibration.

The contribution of reactive solutes in groundwater to the surface water quality depends on the concentrations of reactive solutes along the groundwater flow path, and the distribution of groundwater travel times of discharging groundwater. The profiles of concentrations of pollutants along representative stream tubes in relation to travel time combined with particle tracking travel time distributions provide quick and reliable predictions of surface water quality for base flow conditions. Because of the computational demand of fully reactive 3D flow and transport models, such reactive stream tube models are very practical.

8.3.2 Groundwater age and tracers

$^{3}H/^{3}He$ ages show that heterogeneities in flow patterns cause quite some spatial variation in groundwater ages. The question is whether groundwater ages are also temporarily variable. In this thesis, groundwater ages are assumed to be constant in time at a certain location: a monitoring well always samples water with the same age. Time series of $^{3}H/^{3}He$ ages at monitoring location are needed to confirm the assumption. Time series of CFC concentrations from a granular unconsolidated aquifer in Denmark showed temporal variations (Laier 2004), which were attributed to varying groundwater ages at the monitoring screen. The variations of CFC concentrations may also have been the result of local variation of the recharge concentrations or the non-linearity of the leaching of CFC through the unsaturated zone. Variations in apparent $^{3}H/^{3}He$ groundwater age may have been caused by actual age fluctuations as the result of transient groundwater flow conditions, or by temporal variations in the entrapment of ^{3}He at the groundwater table.

Dating mixed groundwater ages and age spread

The new challenges in the field of groundwater dating are the application of age tracers in more complex systems. The first challenge is dating mixed groundwater (Rueedi *et al.* 2005) from production wells (Osenbrück *et al.* 2006; Zinn and Konikow 2007a, 2007b), springs (Plummer *et al.* 2001; Hendrix and Meinardi 2004) or highly dispersive aquifers (Weissmann *et al.* 2002; LaBolle *et al.* 2006). For this goal, time-series of age tracer concentrations should be analyzed with deconvolution techniques developed for the interpretation of ^{3}H data (Maloszewski and Zuber 1993, 1998). The use of multiple tracers will yield additional information on the distribution of groundwater ages – or age spread – in sampled groundwater (Castro *et al.* 1998). Furthermore, a combination of groundwater age tracers provide more insight into the contribution of groundwater to surface water (Ojiambo *et al.* 2001; Rose 2007; Koeniger *et al.* 2008) or the water balance and transit time of entire catchments (McGuire and McDonnell 2006).

Groundwater age and modeling

Comparing modeled groundwater ages with tracer ages is a challenging task. Groundwater ages are determined most reliably on point samples, and a direct comparison to a single point in the modeled 3D groundwater age field seems logical. But small local heterogeneities (e.g. clay lenses) may have dramatic effects on the groundwater age at the specific location (Weissmann *et al.* 2002). The question is whether the differences between model and tracer age, which are possibly only due to local discrepancies, can effectively be used to improve groundwater flow models, if these differences are not systematically biased. Even the use of groundwater ages to estimate recharge rates suffers from this dilemma. Both groundwater ages and recharge rates may be spatially very variable. To improve the understanding of the discrepancies between modeled and measured ages, groundwater age spread should be modeled simultaneously (Varni and Carrera 1998). A wide simulated groundwater age distribution will then keep us from rejecting the groundwater model if the measured age is a little off.

Simulating groundwater age spread provides a new approach to study and possibly quantify the numerical dispersion in groundwater transport models. The sensitivity of the simulated groundwater age spread to the model parameters describing hydrodynamic dispersion will reveal the numerical dispersion of the model. The results of such an analysis provides a substitute or

effective numerical dispersion length, that is characteristic to the groundwater transport model, or sub-domains of the model space.

Despite the uncertainties characteristic of groundwater ages derived from particle tracking in coarse models, these quick and easy groundwater ages are very valuable. Because groundwater ages represent fluxes, rather then pressures, a few modeled ages are likely to be more restrictive calibration targets than a large number of additional head measurements. So far, most work has focused on the simulation of groundwater age in stationary models. However, especially if travel times of a few years are studied, seasonal and transient effects are expected to play an important role. These short travel times require a very fine and accurate representation of the surface water system in the model. Current developments to implement drains and watercourses as line elements in models are promising; to facilitate the (automatic) model refinement needed for accurate groundwater age simulations. At such a fine scale, the simulated arrival time of particles at (weak) sinks is very accurate and the travel time within the sink cells – which is neglected by particle tracking algorithms – is actually be negligible.

Dating groundwater in reactive two-phase systems

The application of age tracers in exactly the environments where they are most useful – heavily polluted and reactive sites – becomes a challenge, because of the possible formation of a gas phase at such sites. In such relevant environments, $^{3}H/^{3}He$ is the most reliable method to date degassed groundwater, if anoxic conditions prevent the use of CFCs. ^{85}Kr (Smethie *et al.* 1992) is an alternative, but it requires large volumes of groundwater to be sampled, in the order of tens of m^3. Collecting such sample volumes from near the water table will likely affect the local groundwater flow pattern, which is undesirable.

If degassed groundwater is to be dated with $^{3}H/^{3}He$, an estimate of the relative timing of degassing is necessary. Under the assumption of downward flow, the total dissolved gas (TDG) pressure yields the depth, and thereby relative timing, of degassing. In other circumstances, detailed geochemical information on the reactivity of the aquifer or high-resolution vertical profiles of the concentrations of reactive solutes is needed to provide the relative timing of degassing. Such detailed information should also confirm the use of the TDG pressure to estimate the depth of degassing. In this study, the TDG pressure was assumed to equal the dissolved N_2 pressure because other sources of gas were unlikely. Measurements of the concentrations of all dissolved gases are needed to confirm this. In any case, a TDG probe is a highly recommended piece of field equipment in areas where gas production is possible, because it provides the minimum pressure to be maintained in the noble gas sampling line to prevent degassing during sampling.

Noble gases to study gas-water interactions

While the production of gases may pose a problem for the straightforward analysis of groundwater age tracers, these tracers are valuable to studies in gas-water phase interactions. The analysis of noble gas concentrations and isotope ratios yield valuable information on the pore-scale processes acting on gases in semi-saturated porous media. One important aspect of fluid flow in porous media is the area of contact or interfacial area between the gas and the water phase (Joekar-Niasar *et al.* 2008; Niessner and Hassanizadeh 2008). Laboratory studies analyzing the transport behavior of partitioning tracers (Gupta *et al.* 1994) provide new insight into the contact area between the water and gas phase in semi-saturated porous media (Holocher 2002; Holocher

et al. 2002; Holocher *et al.* 2003; Balcke *et al.* 2007). Upward movement of gas in semi-saturated porous media tends to be discontinuous. This burping behavior of gas movement may have a large impact on the transport of tracers and limit diffusion through the gas phase. Analyzing noble gas concentration in ebullition experiments (e.g. Geistlinger *et al.* 2005; Geistlinger *et al.* 2006) are likely to reveal the connectivity of a trapped gas phase. This information is essential to improve the two-phase flow and transport models available today (White and Oostrom 2000; Holocher *et al.* 2003; Amos and Mayer 2006b).

Depleted noble gas concentrations in natural waters reveal degassing has taken place and noble gas concentrations have been used to quantify degassing of N_2 (Blicher-Mathiesen *et al.* 1998). Noble gas analysis have great potential to be applied with that particular aim: to quantify the escape of gases from natural systems (Brennwald *et al.* 2002; Holzner *et al.* 2004; Brennwald *et al.* 2005; Holzner *et al.* 2008; Ma *et al.* 2009). Two systems would be very interesting in that context: peatlands and gas-hydrates (Winckler *et al.* 2002). Both systems represent an important but poorly quantified source of methane to the atmosphere. As a result, their contribution to the greenhouse effect is uncertain. The concentrations of noble gases, in combination with the $^{13}C/^{12}C$ ratio and pore water ages, are a promising approach to quantify the rate of escape of methane from peatlands. If noble gas concentrations appear to be a valid proxy for methane emissions, groundwater originating from peatlands forms a new environmental archive of a key climate variable.

Literature

(1986), Manure Act (Meststoffenwet). The Hague, the Netherlands, Staatsblad 133.

Ackermann, W.C., Harmeson, R.H. & Sinclair, R.A. (1970), Some long-term trends in water quality of rivers and lakes. Transactions, American Geophysical Union 51(6): 516-522.

Aeschbach-Hertig, W., et al. (1999), Interpretation of dissolved atmospheric noble gases in natural waters. Water Resources Research 35(9): 2779-2792.

Aeschbach-Hertig, W., et al. (2000), Palaeotemperature reconstruction from noble gases in ground water taking into account equilibration with entrapped air. Nature 405(6790): 1040-1044.

Alley, W.M., Ed. (1993), Regional Ground-Water Quality. New York, Van Nostrand Reinhold.

Almasri, M.N. & Kaluarachchi, J.J. (2005), Modular neural networks to predict the nitrate distribution in ground water using the on-ground nitrogen loading and recharge data. Environmental Modelling and Software 20(7): 851-871.

Almasri, M.N. & Kaluarachchi, J.J. (2007), Modeling nitrate contamination of groundwater in agricultural watersheds. Journal of Hydrology 343(3-4): 211-229.

Almasri, M.N. & Ghabayen, S.M.S. (2008), Analysis of nitrate contamination of Gaza Coastal Aquifer, Palestine. Journal of Hydrologic Engineering 13(3): 132-140.

Amos, R.T., et al. (2005), Use of dissolved and vapor-phase gases to investigate methanogenic degradation of petroleum hydrocarbon contamination in the subsurface. Water Resources Research 41(2): W02001.

Amos, R.T. & Mayer, K.U. (2006a), Investigating the role of gas bubble formation and entrapment in contaminated aquifers: Reactive transport modelling. Journal of Contaminant Hydrology 87(1-2): 123-154.

Amos, R.T. & Mayer, K.U. (2006b), Investigating ebullition in a sand column using dissolved gas analysis and reactive transport modeling. Environmental Science and Technology 40(17): 5361-5367.

Amraoui, N., Surdyk, N. & Dubus, I.G. (2008), Physically-deterministic determination and extrapolation of time trends at in the Brévilles' catchment (Chpt. 4). In Broers, H.P. and Visser, A., Report which describes the physically-deterministic determination and extrapolation of time trends at selected test locations in Dutch part of the Meuse basin, the Brévilles catchment and the Geer catchment (Deliverable T2.10). Utrecht, The Netherlands.

Appelo, C.A.J. & Postma, D. (2005), Geochemistry, groundwater and pollution. Leiden; London, Balkema.

Baedecker, M.J., et al. (1993), Crude oil in a shallow sand and gravel aquifer – III. Biogeochemical reactions and mass balance modeling in anoxic groundwater. Applied Geochemistry 8(6): 569-586.

Balcke, G.U., et al. (2007), Kinetic gas-water transfer and gas accumulation in porous media during pulsed oxygen sparging. Environmental Science and Technology 41(12): 4428-4434.

Baran, N., et al. (2004), Climatic and land use data for the Brévilles experimental catchment (Chpt. 4). In Broers, H.P. and Visser, A., Report with documentation of reconstructed land use around test sites (Deliverable T2.2). Utrecht, The Netherlands.

Barlow, P.M. (1995), Particle-Tracking Analysis of Contributing Areas of Public-Supply Wells in Simple and Complex Flow Systems, Cape Cod, Massachusetts. USGS Water-Supply Paper 2434.

Barlow, P.M. & Dickerman, D.C. (2001), Numerical-Simulation and Conjunctive-Management Models of the Hunt-Annaquatucket-Pettaquamscutt Stream-Aquifer System, Rhode Island. USGS Professional Paper 1636.

Barlow, P.M. & Ostiguy, L.J. (2007), Simulation of Hydrologic-System Responses to Ground-Water Withdrawals in the Hunt-Annaquatucket-Pettaquamscutt Stream-Aquifer System, Rhode Island. USGS Open-File Report 2006-1226.

Batlle-Aguilar, J. & Brouyère, S. (2004), Spatial dataset for Meuse BE (Chpt. 3). In Broers, H.P. and Visser, A., Documented spatial data set containing the subdivision of the basins into groundwater systems and subsystems, the selected locations per subsystem and a description of these sites, available data and projected additional measurements and equipment (Deliverable T2.1). Utrecht, The Netherlands.

Batlle-Aguilar, J., Orban, P. & Brouyère, S. (2005), Point by Point Statistical Trend Analysis and Extrapoled Time Trends at Test Sites in the Meuse BE (Chpt. 3). In Broers, H.P. and Visser, A., Report on extrapolated time trends at test sites (Deliverable T2.4). Utrecht, The Netherlands.

Batlle-Aguilar, J., et al. (2007), Identification of groundwater quality trends in a chalk aquifer threatened by intensive agriculture in Belgium. Hydrogeology Journal 15(8): 1615-1627.

Bauer, S., Fulda, C. & Schafer, W. (2001), A multi-tracer study in a shallow aquifer using age dating tracers ^{3}H, ^{85}Kr, CFC-113 and SF_6 – Indication for retarded transport of CFC-113. Journal of Hydrology 248(1-4): 14-34.

Beekman, W. (1998), Manual SPREAD: prediction of nitrate, hardness, chloride and sulphate in shallow groundwater (in Dutch). Kiwa Research and Consultancy, Nieuwegein, the Netherlands.

Behrendt, H., et al. (2003), Nutrient emissions into river basins of Germany on the basis of a harmonised procedure. Umweltbundesamt, Berlin, Germany.

Benson, B.B. & Krause, D. (1980), Isotopic fractionation of helium during solution: A probe for the liquid state. Journal of Solution Chemistry 9(12): 895-909.

Bethke, C.M. & Johnson, T.M. (2008), Groundwater age and groundwater age dating. Annual Review of Earth and Planetary Sciences. 36: 121-152.

Beyerle, U., et al. (1999), Infiltration of river water to a shallow aquifer investigated with $^{3}H/^{3}He$, noble gases and CFCs. Journal of Hydrology 220(3-4): 169-185.

Bijay-Singh, Yadvinder-Singh & Sekhon, G.S. (1995), Fertilizer-N use efficiency and nitrate pollution of groundwater in developing countries. Journal of Contaminant Hydrology 20(3-4): 167-184.

Bjerg, P.L. & Christensen, T.H. (1992), Spatial and temporal small-scale variation in groundwater quality of a shallow sandy aquifer. Journal of Hydrology 131(1-4): 133-149.

Bleeker, A. & Erisman, J.W. (1996), Deposition of acidifying components in the Netherlands in the period 1980-1995 (in Dutch) Report 722108018. National institute of public health and environment, RIVM, Bilthoven, the Netherlands.

Blicher-Mathiesen, G., McCarty, G.W. & Nielsen, L.P. (1998), Denitrification and degassing in groundwater estimated from dissolved dinitrogen and argon. Journal of Hydrology 208(1-2): 16-24.

Böhlke, J.K. & Denver, J.M. (1995), Combined use of groundwater dating, chemical, and isotopic analyses to resolve the history and fate of nitrate contamination in two agricultural watersheds, Atlantic coastal plain, Maryland. Water Resources Research 31(9): 2319-2339.

Böhlke, J.K. (2002), Groundwater recharge and agricultural contamination. Hydrogeology Journal 10(1): 153-179.

Böhlke, J.K., et al. (2002), Denitrification in the recharge area and discharge area of a transient agricultural nitrate plume in a glacial outwash sand aquifer, Minnesota. Water Resources Research 38(7): 1105.

Bourg, I.C. & Sposito, G. (2008), Isotopic fractionation of noble gases by diffusion in liquid water: Molecular dynamics simulations and hydrologic applications. Geochimica et Cosmochimica Acta 72(9): 2237-2247.

Brennwald, M.S., et al. (2002), Noble gases dissolved in porewater of lacustrine sediments. Geochimica et Cosmochimica Acta 66(15A): A104.

Brennwald, M.S., Kipfer, R. & Imboden, D.M. (2005), Release of gas bubbles from lake sediment traced by noble gas isotopes in the sediment pore water. Earth and Planetary Science Letters 235(1-2): 31-44.

Broers, H.P. & Buijs, E.A. (1997), Origin of trace metals and arsenic at the Oostrum well field. Netherlands Institute of Applied Geosciences TNO, The Netherlands.

Broers, H.P. (2002), Strategies for regional groundwater quality monitoring. PhD thesis. Fysische geografie. Utrecht University, Utrecht.

Broers, H.P. (2004a), The spatial distribution of groundwater age for different geohydrological situations in the Netherlands: implications for groundwater quality monitoring at the regional scale. Journal of Hydrology 299(1-2): 84-106.

Broers, H.P. (2004b), Nitrate Reduction and Pyrite Oxidation in the Netherlands. In Razowska-Jaworek, L. and Sadurski, A., Nitrate in groundwaters, IAH Selected papers on hydrogeology. Leiden, the Netherlands, A.A. Balkema: 141-149.

Broers, H.P., et al. (2004a), Groundwater quality trend detection at the regional scale: Effects of spatial and temporal variability. GQ2004, the 4th international Groundwater Quality Conference, Waterloo, Canada, IAHS-AISH Publication 297.

Broers, H.P. & Van der Grift, B. (2004), Regional monitoring of temporal changes in groundwater quality. Journal of Hydrology 296(1-4): 192-220.

Broers, H.P., Visser, A. & Van der Grift, B. (2004b), Land use history and the chemical load of recharging groundwater in agricultural recharge areas of the Dutch Meuse basin (Chpt. 2). In Broers, H.P. and Visser, A., Report with documentation of reconstructed land use around test sites (Deliverable T2.2). Utrecht, The Netherlands.

Broers, H.P. & Van Geer, F.C. (2005), Monitoring strategies at phreatic wellfields: A 3D travel time approach. Ground Water 43(6): 850-862.

Broers, H.P., et al. (2007), Modelling reactive transport of diffuse contaminants: identifying the groundwater contribution to surface water quality. In Quevauviller, P., Groundwater Science and Policy. London, UK, Royal Society of Chemistry: 630-644.

Broers, H.P., et al. (2008), Assessing and aggregating trends in groundwater bodies. Examples of the FP VI AquaTerra-project. EU Groundwater Policy Developments Conference, Paris, 13-15 November 2008, UNESCO, Paris, France.

Bronswijk, H. & Prins, H. (2001), Nitrogen fertilization and nitrate concentrations in deeper groundwater of the Netherlands (in Dutch). H2O 34: 27-29.

Brooks, M.C., Wise, W.R. & Annable, M.D. (1999), Fundamental Changes in In Situ Air Sparging Flow Patterns. Ground Water Monitoring and Remediation 19(2): 105-113.

Brooks, R.H. & Corey, A.T. (1964), Hydraulic properties of porous media. Hydrology Paper 3. Civil Engineering Department, Colorado State University, Fort Collins.

Buijsman, E. (1989), Extensive information about The Netherlands Air Quality Monitoring Network. I. The Netherlands National Precipitation Chemistry Network (in Dutch). National institute of public health and environment, RIVM, Bilthoven, the Netherlands.

Buma, J.T., et al. (2002), Watergoals: desired groundwater and surface water regime. Development of model instrument and exploring calculations of bottlenecks, measures and overall solutions (in Dutch). TNO – NITG report, Utrecht, the Netherlands.

Burow, K., Dubrovsky, N. & Shelton, J. (2007), Temporal trends in concentrations of DBCP and nitrate in groundwater in the eastern San Joaquin Valley, California, USA. Hydrogeology Journal 15(5): 991-1007.

Burow, K.R., Shelton, J.L. & Dubrovsky, N.M. (2008), Regional nitrate and pesticide trends in ground water in the eastern San Joaquin Valley, California. Journal of Environmental Quality 37(S5): 249-263.

Busenberg, E. & Plummer, L.N. (1992), Use of Chlorofluorocarbons (CCl_3F and CCl_2F_2) as Hydrologic Tracers and Age-Dating Tools: the Alluvium and Terrace System of Central Oklahoma. Water Resources Research 28(9): 2257-2283.

Busenberg, E. & Plummer, L.N. (2000), Dating young groundwater with sulfur hexafluoride: Natural and anthropogenic sources of sulfur hexafluoride. Water Resources Research 36(10): 3011-3030.

Busenberg, E. & Plummer, L.N. (2008), Dating groundwater with trifluoromethyl sulfurpentafluoride (SF_5CF_3), sulfur hexafluoride (SF_6), CF_3Cl (CFC-13), and CF_2Cl_2 (CFC-12). Water Resources Research 44(2): W02431.

Carabin, G. & Dassargues, A. (1999), Modeling groundwater with ocean and river Interaction. Water Resources Research 35(8): 2347-2358.

Carr, J.R. (1995), Numerical analysis for the geological sciences. Englewood Cliffs, NJ, Prentice Hall.

Castro, M.C., et al. (1998), Noble gases as natural tracers of water circulation in the Paris Basin 2. Calibration of a groundwater flow model using noble gas isotope data. Water Resources Research 34(10): 2467-2483.

Castro, M.C. & Goblet, P. (2005), Calculation of ground water ages – A comparative analysis. Ground Water 43(3): 368-380.

CBS (1976-1992), Manure production: 1950-1974 – 1992. Statistics Netherlands (CBS), The Hague, the Netherlands.

CBS (1987), Manure production 1986. Staatsuitgeverij, The Hague, the Netherlands.

CBS (2006), Statline electronic database (www.statline.nl). Statistics Netherlands (CBS), The Hague, the Netherlands.

Ceazan, M.L., Thurman, E.M. & Smith, R.L. (1989), Retardation of ammonium and potassium transport through a contaminated sand and gravel aquifer: The Role of cation exchange. Environmental Science and Technology 23(11): 1402-1408.

Cherry, G.S. (2006), Simulation and Particle-Tracking Analysis of Ground-Water Flow near the Savannah River Site, Georgia and South Carolina, 2002, and for Selected Ground-Water Management Scenarios, 2002 and 2020. USGS Scientific Investigations Report 2006-5195.

Cherry, G.S. & Clarke, J.S. (2007), Simulation and Particle-Tracking Analysis of Selected Ground-Water Pumping Scenarios at Vogtle Electric Generation Plant, Burke County, Georgia. USGS Open-File Report 2007-1363.

Cirpka, O.A. & Kitanidis, P.K. (2001), Transport of volatile compounds in porous media in the presence of a trapped gas phase. Journal of Contaminant Hydrology 49(3-4): 263-285.

Clarke, J.S. & West, C.T. (1998), Simulation of Ground-Water Flow and Stream-Aquifer Relations in the Vicinity of the Savannah River Site, Georgia and South Carolina, Predevelopment through 1992. USGS Water-Resources Investigations Report 98-4062.

Cleveland, W.S. (1979), Robust locally weighted regression and smoothing scatterplots. Journal of the American Statistical Association 74: 829-836.

Cook, P.G. & Solomon, D.K. (1997), Recent advances in dating young groundwater: Chlorofluorocarbons, $^3H/^3He$ and ^{85}Kr. Journal of Hydrology 191(1-4): 245-265.

Corey, A.T. (1977), Mechanics of heterogeneous fluids in porous media. Water Resources Publications. Fort Collins, Colorado.

Dassargues, A. & Monjoie, A. (1993), The chalk in Belgium. In Downing, R.A., Price, M. and Jones, G.P., The hydrogeology of the chalk of North-West Europe. Oxford, Oxford Science Publ.: 153-269.

Datta Gupta, A., et al. (1991), High-Resolution Monotonic Schemes for Reservoir Fluid-Flow Simulation. In Situ 15(3): 289-317.

Daughney, C.J. & Reeves, R.R. (2005), Definition of hydrochemical facies in the New Zealand National Groundwater Monitoring Programme. Journal of Hydrology New Zealand 44(2): 105-130.

Daughney, C.J. & Reeves, R.R. (2006), Analysis of temporal trends in New Zealand's groundwater quality based on data from the National Groundwater Monitoring Programme. Journal of Hydrology New Zealand 45(1): 41-62.

Debrewer, L.M., Ator, S.W. & Denver, J.M. (2008), Temporal trends in nitrate and selected pesticides in mid-atlantic ground water. Journal of Environmental Quality 37(S5): 296-308.

Di, H.J., et al. (2005), A pilot regional scale model of land use impacts on groundwater quality. Management of Environmental Quality 16(3): 220-234.

Donaldson, J.H., et al. (1997), Development and testing of a kinetic model for oxygen transport in porous media in the presence of trapped gas. Ground Water 35(2): 270-279.

Donaldson, J.H., Istok, J.D. & O'Reilly, K.T. (1998), Dissolved gas transport in the presence of a trapped gas phase: Experimental evaluation of a two-dimensional kinetic model. Ground Water 36(1): 133-142.

Dubus, I.G., et al. (2004), Spatial dataset for Brévilles (Chpt. 4). In Broers, H.P. and Visser, A., Documented spatial data set containing the subdivision of the basins into groundwater systems and subsystems, the selected locations per subsystem and a description of these sites, available data and projected additional measurements and equipment (Deliverable T2.1). Utrecht, The Netherlands.

Dubus, I.G., et al. (2005), Subsoil input data prepared for groundwater and reactive transport modelling in the French Brévilles catchment. In Broers, H.P. and Visser, A., Subsoil input data prepared for groundwater and reactive transport modelling in Dutch part of the Meuse basin (Deliverable T2.5). Utrecht, The Netherlands.

Duffy, C.J. & Lee, D.-H. (1992), Base flow response from nonpoint source contamination: simulated spatial variability in source, structure, and initial condition. Water Resources Research 28(3): 905-914.

Dunkle, S.A., et al. (1993), Chlorofluorocarbons (CCl_3F and CCl_2F_2) as dating tools and hydrologic tracers in shallow groundwater of the Delmarva Peninsula, Atlantic Coastal Plain, United-States. Water Resources Research 29(12): 3837-3860.

Eerens, H.C., et al. (2001), Large scale air pollution and deposition in the National Environmental survey 5. (in Dutch) Report 408129 016. National institute of public health and environment, RIVM, Bilthoven, the Netherlands.

Ekwurzel, B., et al. (1994), Dating of Shallow Groundwater: Comparison of the Transient Tracers $^3H/^3He$, Chlorofluorocarbons, and ^{85}Kr. Water Resources Research 30(6): 1693-1708.

Engesgaard, P., et al. (1996), Large-scale dispersion in a sandy aquifer: Simulation of subsurface transport of environmental tritium. Water Resources Research 32(11): 3253-3266.

Engesgaard, P. & Molson, J. (1998), Direct simulation of ground water age in the Rabis Creek Aquifer, Denmark. Ground Water 36(4): 577-582.

Esterby, S.R. (1996), Review of methods for the detection and estimation of trends with emphasis on water quality applications. Hydrological Processes 10(2): 127-149.

EU (1975), Council Directive 1975/440/EEC concerning the quality required of surface water intended for the abstraction of drinking water in the Member States.

EU (1991), Council Directive 1991/676/EEC concerning the protection of waters against pollution caused by nitrates from agricultural sources.

EU (2000), Directive of the European Parliament and of the Council 2000/60/EC establishing a framework for Community action in the field of water policy.

EU (2005), Common position adopted by the Council with a view to the adoption of a Directive of the European Parliament and of the Council on the protection of groundwater against pollution. Interinstitutional file 2003/0210 (COD), n. 12062/05, 9 November 2005.

EU (2006), Directive 2006/118/EC on the Protection of Groundwater against Pollution and Deterioration.

EU (2007), Common Implementation Strategy for the Water Framework Directive (2000/60/EC), Guidance Document No. 15, Guidance on Groundwater Monitoring. Technical Report – 002 – 2007. Office for Official Publications of the European Communities, Luxembourg.

Evers, M.A.A. (2000), Nutrient manual (in Dutch). Nutrient Management Institute, Wageningen, the Netherlands.

Fest, E.P.M.J., et al. (2007), Groundwater chemistry of Al under Dutch sandy soils: Effects of land use and depth. Applied Geochemistry 22(7): 1427-1438.

Fortuin, N.P.M. & Willemsen, A. (2005), Exsolution of nitrogen and argon by methanogenesis in Dutch ground water. Journal of Hydrology 301(1-4): 1-13.

Foster, S.S.D., Cripps, A.C. & Smith-Carington, A. (1982), Nitrate Leaching to Groundwater. Philosophical Transactions of the Royal Society of London. Series B, Biological Sciences 296(1082 The Nitrogen Cycle.): 477-489.

Frapporti, G., Vriend, S.P. & Van Gaans, P.F.M. (1993), Hydrogeochemistry of the shallow Dutch groundwater: interpretation of the national Groundwater Quality Monitoring Network. Water Resources Research 29(9): 2993-3004.

Frapporti, G. (1994), Geochemical and statistical interpretation of the Dutch national groundwater quality monitoring network. PhD thesis, Geologica Ultraiectina no. 115. University of Utrecht, Utrecht, the Netherlands.

Frapporti, G., Vriend, S.P. & Van Gaans, P.F.M. (1994), Qualitative time trend analysis of ground water monitoring networks. An example from the Netherlands. Environmental Monitoring and Assessment 30(1): 81-102.

Fraters, B., et al. (2004), Agricultural practice and water quality in the Netherlands in the 1992-2002 period: background information for the third EU Nitrates Directive Member States report. Report 500003002. National institute of public health and environment, RIVM, Bilthoven, the Netherlands.

Frette, V., et al. (1994), Fast, immiscible fluid-fluid displacement in three-dimensional porous media at finite viscosity contrast. Physical Review E 50(4): 2881-2890.

Frind, E.O., et al. (1990), Modeling of Multicomponent Transport with Microbial Transformation in Groundwater – the Fuhrberg Case. Water Resources Research 26(8): 1707-1719.

Fry, V.A., et al. (1995), Retardation of Dissolved-Oxygen Due to a Trapped Gas-Phase in Porous-Media. Ground Water 33(3): 391-398.

Fry, V.A., Selker, J.S. & Gorelick, S.M. (1997), Experimental investigations for trapping oxygen gas in saturated porous media for in situ bioremediation. Water Resources Research 33(12): 2687-2696.

Gardner, K.K. & Vogel, R.M. (2005), Predicting ground water nitrate concentration from land use. Ground Water 43(3): 343-352.

Geistlinger, H., Beckmann, A. & Lazik, D. (2005), Mass transfer between a multicomponent trapped gas phase and a mobile water phase: Experiment and theory. Water Resources Research 41(11): 1-15.

Geistlinger, H., et al. (2006), Direct gas injection into saturated glass beads: Transition from incoherent to coherent gas flow pattern. Water Resources Research 42(7): W07403.

Gerzabek, M.H., et al. (2007), The integrated project AquaTerra of the EU sixth framework lays foundations for better understanding of river-sediment-soil-groundwater systems. Journal of Environmental Management 84(2): 237-243.

Glass, R.J., Conrad, S.H. & Peplinski, W. (2000), Gravity-destabilized nonwetting phase invasion in macroheterogeneous porous media: Experimental observations of invasion dynamics and scale analysis. Water Resources Research 36(11): 3121-3137.

Glynn, P.D. & Plummer, L.N. (2005), Geochemistry and the understanding of ground-water systems. Hydrogeology Journal 13(1): 263-287.
Goodchild, R.G. (1998), EU policies for the reduction of nitrogen in water: the example of the Nitrates Directive. Environmental Pollution 102(1, Supplement 1): 737-740.
Goode, D.J. (1996), Direct simulation of groundwater age. Water Resources Research 32(2): 289-296.
Gourcy, L., et al. (2005), First investigations into the use of environmental tracers for age dating at the Brévilles experimental catchment (Chpt. 4). In Broers, H.P. and Visser, A., Report on concentration-depth, concentration-time and time-depth profiles in the Meuse basin and the Brévilles catchment (Deliverable T2.3). Utrecht, The Netherlands.
Grath, J., et al. (2001), The EU Water Framework Directive: Statistical aspects of the identification of groundwater pollution trends, and aggregation of monitoring results. Final Report, 41.046/01-IV1/00 and GZ 16 2500/2-I/6/00. Austrian Federal Ministry of Agriculture and Forestry, Environment and Water Management and European Commission, Vienna.
Grath, J., Ward, R. & Quevauviller, P. (2007), Common Implementation Strategy for the Water Framework Directive (2000/60/EC), Guidance Document No. 15, Guidance on Groundwater Monitoring. Technical Report – 002 – 2007. Office for Official Publications of the European Communities, Luxembourg.
Grath, J., et al. (2008), Guidance on Groundwater Status and Trend Assessment – Final Draft, Version 2.0, 15 October 2008. Working Group C – Groundwater, Activity WGC-2, "Status Compliance & Trends".
Griffioen, J. (2001), Potassium adsorption ratios as an indicator for the fate of agricultural potassium in groundwater. Journal of Hydrology 254(1-4): 244-254.
Griffioen, J., Passier, H.F. & Klein, J. (2008), Comparison of selection methods to deduce natural background levels for groundwater units. Environmental Science and Technology 42(13): 4863-4869.
Gupta, S.K., Lau, L.S. & Moravcik, P.S. (1994), Groundwater Tracing with Injected Helium. Ground Water 32(1): 96-102.
Happell, J.D., et al. (2003), Evidence for the removal of CFC-11, CFC-12, and CFC-113 at the groundwater-surface water interface in the Everglades. Journal of Hydrology 279(1-4): 94-105.
Harbaugh, A.W., et al. (2000), MODFLOW-2000, the U.S. Geological Survey modular ground-water model – User guide to modularization concepts and the Ground-Water Flow Process. USGS Open-File Report 00-92.
Harris, J., Loftis, J.C. & Montgomery, R.H. (1987), Statistical Methods for Characterizing Ground-Water Quality. Ground Water 25(2): 185-193.
Harter, T., et al. (2002), Shallow groundwater quality on dairy farms with irrigated forage crops. Journal of Contaminant Hydrology 55(3-4): 287-315.
Heaton, T.H.E. & Vogel, J.C. (1981), "Excess air" in groundwater. Journal of Hydrology 50: 201-216.
Helsel, D.R. & Hirsch, R.M. (1995), Statistical methods in water resources. Amsterdam, the Netherlands, Elsevier.
Hendrix, W.P.A.M. & Meinardi, C.R. (2004), Springs and streams in southern Limburg (in Dutch). National institute of public health and environment, RIVM, Bilthoven, the Netherlands.
Hinaman, K.C. & Tenbus, F.J. (2000), Hydrogeology and Simulation of Ground-Water Flow at Dover Air Force Base, Delaware. USGS Water-Resources Investigations Report 99-4224.
Hinsby, K., et al. (2007), Transport and degradation of chlorofluorocarbons (CFCs) in the pyritic Rabis Creek aquifer, Denmark. Water Resources Research 43: W10423.
Hirsch, R.M., Slack, J.R. & Smith, R.A. (1982), Techniques of trend analysis for monthly water quality data. Water Resources Research 18(1): 107-121.
Hirsch, R.M., Alexander, R.B. & Smith, R.A. (1991), Selection of methods for the detection and estimation of trends in water quality. Water Resources Research 27(5): 803-813.

Hiscock, K.M., Lloyd, J.W. & Lerner, D.N. (1991), Review of natural and artificial denitrification of groundwater. Water Research 25(9): 1099-1111.

Hoeks, P.A. (2002), Advice on fertilizing grassland and crops (in Dutch). Praktijkonderzoek Veehouderij, Lelystad, the Netherlands.

Holocher, J. (2002), Investigations of gas exchange in quasi-saturated porous media using noble gases as conservative tracers. PhD thesis. Swiss Federal Institute of Technology, Zurich.

Holocher, J., et al. (2002), Experimental investigations on the formation of excess air in quasi-saturated porous media. Geochimica et Cosmochimica Acta 66(23): 4103-4117.

Holocher, J., et al. (2003), Kinetic model of gas bubble dissolution in groundwater and its implications for the dissolved gas composition. Environmental Science and Technology 37(7): 1337-1343.

Holzner, C.P., et al. (2004), Assessment of methane emission from bubble plumes in the Black Sea by noble gases. Geochimica et Cosmochimica Acta 68(11): A323-A323.

Holzner, C.P., et al. (2008), Noble gas anomalies related to high-intensity methane gas seeps in the Black Sea. Earth and Planetary Science Letters 265(3-4): 396-409.

Horneman, A., et al. (2008), Degradation rates of CFC-11, CFC-12 and CFC-113 in anoxic shallow aquifers of Araihazar, Bangladesh. Journal of Contaminant Hydrology 97(1-2): 27-41.

Hudak, P.F. (2000), Regional trends in nitrate content of Texas groundwater. Journal of Hydrology 228(1-2): 37-47.

IAEA/WMO (2004), Global Network of Isotopes in Precipitation. The GNIP Database. Accessible at: http://isohis.iaea.org.

Istok, J.D., et al. (2007), An Experimental Investigation of Nitrogen Gas Produced during Denitrification. Ground Water 45(4): 461-467.

Jalali, M. & Kolahchi, Z. (2008), Groundwater quality in an irrigated, agricultural area of northern Malayer, western Iran. Nutrient Cycling in Agroecosystems 80(1): 95-105.

Janssen, G.M.C.M., Valstar, J.R. & Van Der Zee, S.E.A.T.M. (2006), Inverse modeling of multimodal conductivity distributions. Water Resources Research 42(3): W03410.

Janssen, G.M.C.M., Valstar, J.R. & Van Der Zee, S.E.A.T.M. (2008), Measurement network design including traveltime determinations to minimize model prediction uncertainty. Water Resources Research 44(2): W02405.

Jarvis, N.J. (1994), The MACRO model (version 3.1). Technical description and sample simulations. Reports and dissertations 19. Department of Soil Sciences. Swedish University of Agricultural Sciences, Uppsala, Sweden.

Jiang, Y., et al. (2006), Groundwater quality and land use change in a typical karst agricultural region: A case study of Xiaojiang watershed, Yunnan. Journal of Geographical Sciences 16(4): 405-414.

Joekar-Niasar, V., Hassanizadeh, S.M. & Leijnse, A. (2008), Insights into the relationships among capillary pressure, saturation, interfacial area and relative permeability using pore-network modeling. Transport in Porous Media 74(2): 201-219.

Johnston, C.T., et al. (1998), Ground Water Age and Nitrate Distribution Within a Glacial Aquifer Beneath a Thick Unsaturated Zone. Ground Water 36(1): 171-180.

Juhler, R.K. & Felding, G. (2003), Monitoring methyl tertiary butyl ether (MTBE) and other organic micropollutants in groundwater: Results from the Danish National Monitoring Program. Water, Air, and Soil Pollution 149(1-4): 145-161.

Katz, B.G., Chelette, A.R. & Pratt, T.R. (2004), Use of chemical and isotopic tracers to assess nitrate contamination and ground-water age, Woodville Karst Plain, USA. Journal of Hydrology 289(1-4): 36-61.

Kauffman, L.J., et al. (2001), Effects of Land Use and Travel Time on the Distribution of Nitrate in the Kirkwood-Cohansey Aquifer System in Southern New Jersey. USGS Water-Resources Investigations Report 01-4117.

Kaufman, S. & Libby, W.F. (1954), The Natural Distribution of Tritium. Physical Review 93(6): 1337-1344.

Kelly, B.P. (2004), Simulation of Ground-Water Flow, Contributing Recharge Areas, and Ground-Water Travel Time in the Missouri River Alluvial Aquifer near Ft. Leavenworth, Kansas. USGS Scientific Investigations Report 2004-5215.

Kelly, W.R. (1997), Heterogeneities in ground-water geochemistry in a sand aquifer beneath an irrigated field. Journal of Hydrology 198(1-4): 154-176.

Kendall, M.G. (1948), Rank Correlation Methods. London, Charles Griffin & Company.

Kim, N.J., Cho, M.J. & Woo, N.C. (1995), Developing A National Groundwater-Monitoring Network In Korea. Hydrogeology Journal 3(4): 89-94.

Kipfer, R., et al. (2002), Noble gases in lakes and ground waters. In Porcelli, D., Ballentine, C.J. and Wieler, R., Noble gases in geochemistry and cosmochemistry, volume 47 of Reviews in Mineralolgy and Geochemistry, Mineralogical Society of America. 47: 615-700.

Klump, S., et al. (2006), Groundwater Dynanics and Arsenic Mobilization in Bangladesh Assessed Using Noble Gases and Tritium. Environmental Science and Technology 40: 243-250.

Koeniger, P., et al. (2008), Tritium balance in macro-scale river basins analysed through distributed hydrological modelling. Hydrological Processes 22(5): 567-576.

Koh, D.-C., et al. (2006), Application of environmental tracers to mixing, evolution, and nitrate contamination of ground water in Jeju Island, Korea. Journal of Hydrology 327(1-2): 258-275.

Koh, D.C., et al. (2007), Evidence for terrigenic SF_6 in groundwater from basaltic aquifers, Jeju Island, Korea: Implications for groundwater dating. Journal of Hydrology 339(1-2): 93-104.

Kölle, W., Strebel, O. & Böttcher, J. (1985), Formation of sulfate by a microbial denitrification in a reducing aquifer. Water Supply 3(1): 35-40.

Korcz, M., et al. (2004), Spatial dataset for Elbe Basin (Chpt. 5). In Broers, H.P. and Visser, A., Documented spatial data set containing the subdivision of the basins into groundwater systems and subsystems, the selected locations per subsystem and a description of these sites, available data and projected additional measurements and equipment (Deliverable T2.1). Utrecht, The Netherlands.

Korcz, M., Dlugosz, J. & Bronder, J. (2007), Report which describes the approach used for inter well trend comparison with application to the Bille-Krückau watershed and comparison with classical multivariate analyses (Deliverable T2.9). Katowice, Poland.

Korom, S. (1992), Natural Denitrification in the Saturated Zone: A Review. Water Resources Research 28(6): 1657-1668.

Kumazawa, K. (2002), Nitrogen fertilization and nitrate pollution in groundwater in Japan: Present status and measures for sustainable agriculture. Nutrient Cycling in Agroecosystems 63(2): 129-137.

LaBolle, E.M., Fogg, G.E. & Eweis, J.B. (2006), Diffusive fractionation of ^3H and ^3He in groundwater and its impact on groundwater age estimates. Water Resources Research 42(7): W07202.

Laier, T. (2004), Nitrate monitoring and CFC-age dating of shallow groundwaters – an attempt to check the effect of restricted use of fertilizers. In Razowska-Jaworek, L. and Sadurski, A., Nitrate in Groundwaters, IAH Selected papers on hydrogeology. Leiden, the Netherlands, A.A. Balkema: 247-258.

Lapworth, D.J., et al. (2006), Pesticides in groundwater: some observations on temporal and spatial trends. Water and Environment Journal 20(2): 55-64.

Larsen, F. & Postma, D. (1997), Nickel Mobilization in a Groundwater Well Field: Release by Pyrite Oxidation and Desorption from Manganese Oxides. Environ. Sci. Technol. 31(9): 2589-2595.

Leahy, P.P., Ryan, B. & Johnson, I. (1993), An introduction to the U.S. geological surveys national water-quality assessment program. Water Resources Bulletin 29(4): 529-532.

Lee, J.Y., et al. (2007), A review of the National Groundwater Monitoring Network in Korea. Hydrological Processes 21(7): 907-919.

LEI (2006), Agricultural statistics (http://www3.lei.wur.nl/ltc/). Agricultural Economical Institute (LEI), Wageningen, the Netherlands, Wageningen.
Lenhard, R.J., Parker, J.C. & Mishra, S. (1989), On the Correspondence between Brooks-Corey and Van Genuchten Models. Journal of Irrigation and Drainage Engineering 115(4): 744-751.
Loftis, J.C., McBride, C.B. & Ellis, J.C. (1991a), Considerations of scale in water quality monitoring and data analysis. Water Resources Bulletin 27: 255-264.
Loftis, J.C., Taylor, C.H. & Chapman, P.L. (1991b), Multivariate tests for trend in water quality. Water Resources Research 27(7): 1419-1429.
Loftis, J.C. (1996), Trends in groundwater quality. Hydrological Processes 10: 335-355.
Lovley, D.R. & Woodward, J.C. (1992), Consumption of Freons CFC-11 and CFC-12 by Anaerobic Sediments and Soils. Environmental Science and Technology 26(5): 925-929.
Ma, L., Castro, M.C. & Hall, C.M. (2009), Atmospheric noble gas signatures in deep Michigan Basin brines as indicators of a past thermal event. Earth and Planetary Science Letters 277(1-2): 137.
MacDonald, A.M., et al. (2003), Identifying trends in groundwater quality using residence time indicators: an example from the Permian aquifer of Dumfries, Scotland. Hydrogeology Journal 11(4): 504-517.
MacDonnell, L.J. & Guy, D.J. (1991), Approaches to groundwater quality protection in the western United States. Water Resources Research 27(3): 259.
Maiss, M. & Brenninkmeijer, C.A.M. (1998), Atmospheric SF_6: Trends, sources, and prospects. Environmental Science and Technology 32(20): 3077-3086.
Maloszewski, P. & Zuber, A. (1993), Principles and practice of calibration and validation of mathematical models for the interpretation of environmental tracer data in aquifers. Advances in Water Resources 16(3): 173.
Maloszewski, P. & Zuber, A. (1998), A general lumped parameter model for the interpretation of tracer data and transit time calculation in hydrologic systems – Comments. Journal of Hydrology 204(1-4): 297-300.
Mann, H.B. (1945), Nonparametric tests against trend. Econimetrica 13: 245-259.
Manning, A.H., Solomon, D.K. & Sheldon, A.L. (2003), Applications of a total dissolved gas pressure probe in ground water studies. Ground Water 41(4): 440-448.
Manning, A.H., Solomon, D.K. & Thiros, S.A. (2005), H-3/He-3 age data in assessing the susceptibility of wells to contamination. Ground Water 43(3): 353-367.
Mayer, K.U., Frind, E.O. & Blowes, D.W. (2002), Multicomponent reactive transport modeling in variably saturated porous media using a generalized formulation for kinetically controlled reactions. Water Resources Research 38(9): 131.
McGuire, K.J. & McDonnell, J.J. (2006), A review and evaluation of catchment transit time modeling. Journal of Hydrology 330(3-4): 543-563.
McNab, W.W., et al. (2007), Assessing the impact of animal waste lagoon seepage on the geochemistry of an underling shallow aquifer. Environmental Science and Technology 41(3): 753-758.
Meinardi, C.R. (1994), Groundwater recharge and travel times in the sandy regions of The Netherlands. PhD thesis. VU University, Amsterdam, the Netherlands.
Menke, M.A. (1992), Pressures of fertilizers on soils in the Netherlands (in Dutch). Delft Hydraulics, Delft, the Netherlands.
Millington, R.J. & Quirk, J.P. (1959), Permeability of porous media. Nature 183(4658): 387.
Mol, G., Vriend, S.P. & van Gaans, P.F.M. (2001), Environmental Monitoring in The Netherlands: Past Developments and Future Challenges. Environmental Monitoring and Assessment 68(3): 313.
Molénat, J., et al. (2002), Mechanisms of Nitrate Transfer from Soil to Stream in an Agricultural Watershed of French Brittany. Water, Air, and Soil Pollution 133(1): 161-183.

Moncaster, S.J., et al. (1992), Sulphur isotope ratios as tracers of natural and anthropogenic sulphur in the Lincolnshire Limestone aquifer, eastern England. Water-rock Interaction: 813.

Mouvet, C., et al. (2004), PEGASE. Pesticides in European Groundwaters: detailed study of representative aquifers and simulation of possible evolution scenarios. In Dubus, I.G. and Mouvet, C., Final Report of the European Project #EVK1-CT1990-00028. BRGM/RP-52897-FR.

Mualem, Y. (1976), A new model for predicting the hydraulic conductivity of unsaturated porous media. Water Resources Research 12: 513-522.

Neumann, R.B., LaBolle, E.M. & Harvey, C.F. (2008), The Effects of Dual-Domain Mass Transfer on the Tritium/Helium-3 Dating Method. Environmental Science and Technology 42(13): 4837-4843.

Niessner, J. & Hassanizadeh, S.M. (2008), A model for two-phase flow in porous media including fluid-fluid interfacial area. Water Resources Research 44(8): W08439.

Nir, A. (1964), On the interpretation of tritium "age" measurements of groundwater. Journal of Geophysical Research 69(12): 2589.

Nolan, B.T., et al. (1997), Risk of nitrate in groundwaters of the United States – A national perspective. Environmental Science and Technology 31(8): 2229.

Oakes, D.B., Young, C.P. & Foster, S.S.D. (1981), The effects of farming practices on groundwater quality in the United Kingdom. Science of the Total Environment 21: 17-30.

Ojiambo, B.S., Poreda, R.J. & Lyons, W.B. (2001), Ground Water/Surface Water Interactions in Lake Naivasha, Kenya, Using $\delta^{18}O$, δD, and $^{3}H/^{3}He$ Age-Dating. Ground Water 39(4): 526-533.

Orban, P., Batlle-Aguilar, J. & Brouyère, S. (2005), Input data sets for groundwater and transport modelling in the Geer basin (Chpt. 3). In Broers, H.P. and Visser, A., Subsoil input data prepared for groundwater and reactive transport modelling in Dutch part of the Meuse basin (Deliverable T2.5). Utrecht, The Netherlands.

Orban, P. & Brouyère, S. (2007), Report with results of groundwater flow and reactive transport modelling in the Geer catchment (Chpt. 3). In Broers, H.P. and Visser, A., Report with results of groundwater flow and reactive transport modelling at selected test locations in Dutch part of the Meuse basin, the Brévilles' catchment and the Geer catchment (Deliverable T2.8). Utrecht, The Netherlands.

Orban, P., et al. (2008), Physically-deterministic determination and extrapolation of time trends in the Geer catchment (Chpt. 3). In Broers, H.P. and Visser, A., Report which describes the physically-deterministic determination and extrapolation of time trends at selected test locations in Dutch part of the Meuse basin, the Brévilles catchment and the Geer catchment (Deliverable T2.10). Utrecht, The Netherlands.

Osenbrück, K., et al. (2006), Timescales and development of groundwater pollution by nitrate in drinking water wells of the Jahna-Aue, Saxonia, Germany. Water Resources Research 42(12): W12416.

Oster, H., Sonntag, C. & Munnich, K.O. (1996), Groundwater age dating with chlorofluorocarbons. Water Resources Research 32(10): 2989-3001.

Ozima, M. & Podosek, F.A. (2002), Noble Gas Geochemistry. Cambridge, Cambridge University Press.

Parkhurst, D.L. & Appelo, C.A.J. (1999), User's guide to PHREEQC (version 2) – A computer program for speciation, batch-reaction, one-dimensional transport, and inverse geochemical calculations. USGS Water-Resources Investigations Report 99-4259.

Paschke, S.S. (2007), Hydrogeologic Settings and Ground-Water Flow Simulations for Regional Studies of the Transport of Anthropogenic and Natural Contaminants to Public-Supply Wells – Studies Begun in 2001. USGS Professional Paper 1737-A.

Pauwels, H., et al. (2001), Temporal variability of nitrate concentration in a schist aquifer and transfer to surface waters. Applied Geochemistry 16(6): 583.

Pebesma, E.J. & de Kwaadsteniet, J.W. (1997), Mapping groundwater quality in the Netherlands. Journal of Hydrology 200(1-4): 364.

Peeters, F., et al. (2003), Improving noble gas based paleoclimate reconstruction and groundwater dating using $^{20}Ne/^{22}Ne$ ratios. Geochimica et Cosmochimica Acta 67(4): 587-600.
Peterson, et al. (2001), Air-flow geometry in air sparging of fine-grained sands. Hydrogeology Journal 9(2): 168-176.
Pinault, J.-L., et al. (2005), Conventional and innovative approaches to trends analysis: a case study for the Brévilles catchment (Chpt. 4). In Broers, H.P. and Visser, A., Report on extrapolated time trends at test sites (Deliverable T2.4). Utrecht, The Netherlands.
Pinault, J.L. (2001), Manuel utilisateur de TEMPO: logiciel de traitement et de modélisation des séries temporelles en hydrogéologie et en hydrogéochemie. Projet Modhydro. Rap. BRGM/RP-51459. BRGM, Orleans.
Pinault, J.L. & Dubus, I.G. (2008), Stationary and non-stationary autoregressive processes with external inputs for predicting trends in water quality. Journal of Contaminant Hydrology 100(1-2): 22-29.
Plummer, L.N., et al. (2001), Groundwater residence times in Shenandoah National Park, Blue Ridge Mountains, Virginia, USA: a multi-tracer approach. Chemical Geology 179(1-4): 93-111.
Pollock, D.W. (1988), Semianalytical Computation of Path Lines for Finite-Difference Models. Ground Water 26(6): 743-750.
Pollock, D.W. (1994), User's Guide for MODPATH/MODPATH-PLOT, Version 3: A particle tracking post-processing package for MODFLOW, the U.S. Geological Survey finite-difference ground-water flow model. USGS Open-File Report 94-464.
Poreda, R.J., Cerling, T.E. & Salomon, D.K. (1988), Tritium and Helium-Isotopes as Hydrologic Tracers in a Shallow Unconfined Aquifer. Journal of Hydrology 103(1-2): 1-9.
Postma, D., et al. (1991), Nitrate Reduction in an Unconfined Sandy Aquifer – Water Chemistry, Reduction Processes, and Geochemical Modeling. Water Resources Research 27(8): 2027-2045.
Purtschert, R., et al. (2004), Estimation of groundwater flow velocities in a landfill leachate plume using ^{85}Kr measurements. Geochimica et Cosmochimica Acta 68(11): A494-A494.
Raats, P.A.C. (1977), Convective transport of solutes by steady flows II. Specific flow problems. Agricultural Water Management 1(3): 219-232.
Raats, P.A.C. (1981), Residence times of water and solutes within and below the root zone. Agricultural Water Management 4(1-3): 63-82.
Refsgaard, J.C., et al. (1999), Large scale modelling of groundwater contamination from nitrate leaching. Journal of Hydrology 221(3-4): 117-140.
Reid, R.C., Prausnitz, J.M. & Poling, B.E. (1987), The properties of gases and liquids. New York, McGraw-Hill.
Reijnders, H.F.R., et al. (1998), The quality of the groundwater in the Netherlands. Journal of Hydrology 207(3-4): 179-188.
Reijnders, H.F.R., et al. (2004), Quality of shallow and medium-deep groundwater in the Netherlands in 2000 including changes in the 1984-2000 period. (in Dutch) Report 714801030. National institute of public health and environment, RIVM, Bilthoven, the Netherlands.
Renken, R.A., et al. (2001), Approach for Delineation of Contributing Areas and Zones of Transport to Selected Public-Supply Wells Using a Regional Ground-Water Flow Model, Palm Beach County, Florida. USGS Water-Resources Investigations Report 01-4158.
Revesz, K., et al. (1995), Methane production and consumption monitored by stable H and C isotope ratios at a crude oil spill site, Bemidji, Minnesota. Applied Geochemistry 10(5): 505-516.
Reynolds-Vargas, J., Fraile-Merino, J. & Hirata, R. (2006), Trends in nitrate concentrations and determination of its origin using stable isotopes (^{18}O and ^{15}N) in groundwater of the western Central Valley, Costa Rica. Ambio 35(5): 229-236.

Ritter, A., et al. (2007), Agricultural land use and hydrology affect variability of shallow groundwater nitrate concentration in South Florida. Hydrological Processes 21(18): 2464-2473.

RIVM (1979-1981), Monitoring network assessing the chemical composition of precipitation in the Netherlands: annual report (1978-1980). National institute of public health and environment, RIVM, Bilthoven, the Netherlands.

RIVM (1986-1988), Chemical composition of precipitation over the Netherlands: annual report (1984-1987). National institute of public health and environment, RIVM, Bilthoven, the Netherlands.

RIVM (1989-1995), Netherlands precipitation chemistry network: monitoring results. National institute of public health and environment, RIVM, Bilthoven, the Netherlands.

RIVM. (2005), Chemical composition of precipitation over the Netherlands.

Robertson, W.D. & Cherry, J.A. (1989), Tritium as an indicator of recharge and dispersion in a groundwater system in Central Ontario. Water Resources Research 25: 1079-1109.

Robertson, W.D., Russell, B.M. & Cherry, J.A. (1996), Attenuation of nitrate in aquitard sediments of southern Ontario. Journal of Hydrology 180(1-4): 267-281.

Rose, S. (2007), Utilization of Decadal Tritium Variation for Assessing the Residence Time of Base Flow. Ground Water 45(3): 309-317.

Rosen, M.R. & Lapham, W.W. (2008), Introduction to the U.S. Geological Survey National Water-Quality Assessment (NAWQA) of ground-water quality trends and comparison to other national programs. Journal of Environmental Quality 37(S5): 190-198.

Rozemeijer, J.C. & Broers, H.P. (2007), The groundwater contribution to surface water contamination in a region with intensive agricultural land use (Noord-Brabant, The Netherlands). Environmental Pollution 148(3): 695.

Rueedi, J., et al. (2005), Estimating groundwater mixing ratios and their uncertainties using a statistical multi parameter approach. Journal of Hydrology 305(1-4): 1-14.

Rupert, M.G. (2008), Decadal-scale changes of nitrate in ground water of the United States, 1988-2004. Journal of Environmental Quality 37(S5): 240-248.

Saad, D.A. (2008), Agriculture-related trends in groundwater quality of the glacial deposits aquifer, central Wisconsin. Journal of Environmental Quality 37(S5): 209-225.

Salamon, P., Fernàndez-Garcia, D. & Gómez-Hernández, J.J. (2006), Modeling mass transfer processes using random walk particle tracking. Water Resources Research 42(11): W11417.

Santella, N., et al. (2003), Distribution of atmospheric SF_6 near a large urban area as recorded in the vadose zone. Environmental Science and Technology 37(6): 1069-1074.

Santella, N., et al. (2008), Widespread elevated atmospheric SF6 mixing ratios in the Northeastern United States: Implications for groundwater dating. Journal of Hydrology 349(1-2): 139-146.

Schlosser, P., et al. (1988), Tritium/^{3}He Dating of Shallow Groundwater. Earth and Planetary Science Letters 89(3-4): 353-362.

Schlosser, P., et al. (1989), Tritiogenic ^{3}He in Shallow Groundwater. Earth and Planetary Science Letters 94(3-4): 245-256.

Schwientek, M., et al. (2008), Evidence for denitrification regulated by pyrite oxidation in a heterogeneous porous groundwater system. Chemical Geology 255(1-2): 60-67.

Sebol, L.A., et al. (2007), Evidence of CFC degradation in groundwater under pyrite-oxidizing conditions. Journal of Hydrology 347(1-2): 1-12.

Shapiro, S.D., et al. (1999), Characterizing a sewage plume using the H-3-He-3 dating technique. Ground Water 37(6): 861-878.

Shapiro, S.S. & Wilk, M.B. (1965), An analysis of variance test for normality (complete samples). Biometrika 52: 591-611.

Shapiro, S.S. & Francia, R.S. (1972), An approximate analysis of variance test for normality. Journal of the American Statistical Association 67(337): 215-216.
Shoemaker, W.B., et al. (2004), Comparison of Estimated Areas Contributing Recharge to Selected Springs in North-Central Florida by Using Multiple Ground-Water Flow Models. USGS Open-File Report 03-448.
Singleton, M.J., et al. (2007), Saturated zone denitrification: Potential for natural attenuation of nitrate contamination in shallow groundwater under dairy operations. Environmental Science and Technology 41(3): 759-765.
Smethie, J.W.M., et al. (1992), Tracing groundwater flow in the Borden aquifer using krypton-85. Journal of Hydrology 130(1-4): 279-297.
Smith, R.L., Howes, B.L. & Duff, J.H. (1991), Denitrification in nitrate-contaminated groundwater: Occurrence in steep vertical geochemical gradients. Geochimica et Cosmochimica Acta 55(7): 1815-1825.
Solley, W.B., Pierce, R.R. & Perlman, H.A. (1993), Estimated Use of Water in the United States in 1990. U.S. Geological Survey, Circular 1081. Reston, VA.
Solomon, D.K. & Sudicky, E.A. (1991), Tritium and He-3 Isotope Ratios for Direct Estimation of Spatial Variations in Groundwater Recharge. Water Resources Research 27(9): 2309-2319.
Solomon, D.K., et al. (1992), Tritium and Helium 3 as Groundwater Age Tracers in the Borden Aquifer. Water Resources Research 28(3): 741-755.
Solomon, D.K., et al. (1993), A Validation of the $^{3}H/^{3}He$ Method for Determining Groundwater Recharge. Water Resources Research 29(9): 2951-2962.
Solomon, D.K., et al. (1995), Site Characterization Using H-3/He-3 Groundwater Ages, Cape-Cod, Ma. Ground Water 33(6): 988-996.
Spalding, R.F. & Exner, M.E. (1993), Occurrence of nitrate in groundwater – A review. Journal of Environmental Quality 22(3): 392-402.
Spitz, F.J., Nicholson, R.S. & Pope, D.A. (2001), A nested rediscretization method to improve pathline resolution by eliminating weak sinks representing wells. Ground Water 39(5): 778-785.
Strebel, O., Duynisveld, W.H.M. & Bo?ttcher, J. (1989), Nitrate pollution of groundwater in western Europe. Agriculture, Ecosystems and Environment 26(3-4): 189-214.
Stuart, M.E., et al. (2007), Screening for long-term trends in groundwater nitrate monitoring data. Quarterly Journal of Engineering Geology and Hydrogeology 40(4): 361-376.
Stute, M., et al. (1995), Cooling of Tropical Brazil (5°C) during the Last Glacial Maximum. Science 269(5222): 379.
Stuyfzand, P.J. (1991), The composition of rainwater along the coast of Holland (in Dutch). KIWA, Nieuwegein, the Netherlands.
Sültenfuß, J., Roether, W. & Rhein, M. (2004), The Bremen Mass Spectrometric Facility for the Measurement of Helium Isotopes, Neon, and Tritium in Water. IAEA International Symposium on Quality Assurance for Analytical Methods in Isotope Hydrology, Vienna, IAEA.
Takaoka, N. & Mizutani, Y. (1987), Tritiogenic ^{3}He in groundwater in Takaoka. Earth and Planetary Science Letters 85(1-3): 74-78.
Tesoriero, A.J., Liebscher, H. & Cox, S.E. (2000), Mechanism and rate of denitrification in an agricultural watershed: Electron and mass balance along groundwater flow paths. Water Resources Research 36(6): 1545-1559.
Tesoriero, A.J., et al. (2005), Nitrogen transport and transformations in a coastal plain watershed: Influence of geomorphology on flow paths and residence times. Water Resources Research 41(2): W02008.
Tesoriero, A.J., et al. (2007), Linking ground-water age and chemistry data along flow paths: Implications for trends and transformations of nitrate and pesticides. Journal of Contaminant Hydrology 94(1-2): 139-155.

Thiéry, D. (1990), Logiciel MARTHE- Modélisation d'Aquifére avec maillage Rectangulaire, Transport et HydrodynamiquE, version 4.3. BRGM report R 38210. BRGM, Orleans, France.

Thomas, J.M., et al. (2003), Noble gas loss may indicate groundwater flow across flow barriers in Southern Nevada. Environmental Geology 43(5): 568-579.

Thompson, G.M. & Hayes, J.M. (1979), Trichlorofluoromethane in groundwater – a possible tracer and indicator of groundwater age. Water Resources Research 15(3): 546-554.

TNO (2007), DINO Loket (http://dinoloket.nitg.tno.nl/). Netherlands Institute of Applied Geoscience TNO – National Geological Survey.

Tolstikhin, I.N. & Kamenski, I.L. (1969), Determination of groundwater age by the T-^{3}He method. Geochemistry International 6: 810-811.

USBR (2001), Lower Colorado River Accounting System – Demonstration of Technology (Calendar Year 2000). U.S. Department of the Interior – Bureau of Reclamation, Boulder City, Nevada.

Van Beek, C.G.E.M., Hettinga, F.A.M. & Straatman, R. (1989), The effects of manure spreading and acid deposition upon groundwater quality in Vierlingsbeek, the Netherlands. In Abriola, L.M., IAHS Publication 185. Wallingford, IAHS Press. 185: 155-162.

Van Breukelen, B.M., et al. (2003), Biogeochemistry and isotope geochemistry of a landfill leachate plume. Journal of Contaminant Hydrology 65(3-4): 245-268.

Van der Grift, B. & Van Beek, C.G.E.M. (1996), Hardness of abstracted groundwater: indicative predictions (in Dutch). Kiwa, Nieuwegein, the Netherlands.

Van der Grift, B. & Griffioen, J. (2008), Modelling assessment of regional groundwater contamination due to historic smelter emissions of heavy metals. Journal of Contaminant Hydrology 96(1-4): 48-68.

Van Drecht, G., et al. (1996), Groundwater quality in the Netherlands at a depth of 5 to 30 metres in the year 1992 and the change in the period 1984-1993. (in Dutch) Report 714801005. National institute of public health and environment, RIVM, Bilthoven, the Netherlands.

Van Duijvenbooden, W., Taat, J. & Gast, L.F.L. (1985), The National Groundwater Quality Monitoring Network: Final Report of the Installation Phase. (in Dutch) Report 840 382 001. National Institute of Public Health and the Environment, RIVM, Bilthoven, the Netherlands.

Van Duijvenbooden, W. (1993), Groundwater quality monitoring in the Netherlands. In Alley, W.M., Regional groundwater quality. New York, Van Nostrand Reinhold: 515-535.

Van Eerdt, M.M. (1999), Manure production and mineral secretion (in Dutch). Environmental Quarterly. 's-Gravenhage, Staatsuitgeverij/CBS-Publikaties. 16: 27-31.

Van Elburg, H., Engelen, G.B. & Hemker, C.J. (1992), FLOWNET User's manual (http://www.microfem.nl/). VU University, Amsterdam, the Netherlands.

Van Genuchten, M.T. (1980), A closed-form equation for predicting the hydraulic conductivity of unsaturated soils. Soil Science Society of America Journal 44: 892-898.

Van Maanen, J.M.S., et al. (2001), Pesticides and nitrate in groundwater and rainwater in The Province of Limburg in the Netherlands. Environmental Monitoring and Assessment 72(1): 95-114.

Van Ommen, H.C. (1986), Influence of diffuse sources of contamination on the quality of outflowing groundwater including non-equilibrium adsorption and decomposition. Journal of Hydrology 88(1-2): 79-95.

Varni, M. & Carrera, J. (1998), Simulation of groundwater age distributions. Water Resources Research 34(12): 3271-3281.

Visser, A., Broers, H.P. & Van der Grift, B. (2004), Spatial dataset for Meuse NL (Chpt. 2). In Broers, H.P. and Visser, A., Documented spatial data set containing the subdivision of the basins into groundwater systems and subsystems, the selected locations per subsystem and a description of these sites, available data and projected additional measurements and equipment (Deliverable T2.1). Utrecht, The Netherlands.

Visser, A., Broers, H.P. & Van der Grift, B. (2005a), Demonstrating trend reversal using tritium-helium age scaling: results for the Dutch Meuse subcatchment (Chpt. 2). In Broers, H.P. and Visser, A., Report on extrapolated time trends at test sites (Deliverable T2.4). Utrecht, The Netherlands.

Visser, A., Broers, H.P. & Van der Grift, B. (2005b), Concentration-depth, concentration-time and groundwater age-depth profiles in groundwater in dry agricultural areas of the lower Meuse basin NL (Chpt. 2). In Broers, H.P. and Visser, A., Report on concentration-depth, concentration-time and time-depth profiles in the Meuse basin and the Brévilles catchment (Deliverable T2.3). Utrecht, The Netherlands.

Visser, A., Van der Grift, B. & Broers, H.P. (2006), Subsoil input data prepared for groundwater and reactive transport modelling in Dutch part of the Meuse basin (Chpt. 2). In Broers, H.P. and Visser, A., Input data sets and short report describing the subsoil input data for groundwater and reactive transport modelling at test locations in Dutch part of the Meuse basin, the Brévilles' catchment and the Geer catchment (Deliverable T2.5). Utrecht, The Netherlands.

Visser, A., et al. (2008), Physically-deterministic determination and extrapolation of time trends at selected test locations in Dutch part of the Meuse basin (Chpt. 2). In Broers, H.P. and Visser, A., Report which describes the physically-deterministic determination and extrapolation of time trends at selected test locations in Dutch part of the Meuse basin, the Brévilles catchment and the Geer catchment (Deliverable T2.10). Utrecht, The Netherlands.

Vogel, J.C. (1967), Investigation of groundwater flow with radiocarbon. IAEA Symposium on Isotopes in Hydrology, 14-18 November 1966, Vienna, Austria, IAEA.

Walker, S.J., Weiss, R.F. & Salameh, P.K. (2000), Reconstructed histories of the annual mean atmospheric mole fractions for the halocarbons CFC-11, CFC-12, CFC-113, and carbon tetrachloride. Journal of Geophysical Research-Oceans 105(C6): 14285-14296.

Walter, D.A. & Masterson, J.P. (2003), Simulation of Advective Flow under Steady-State and Transient Recharge Conditions, Camp Edwards, Massachusetts Military Reservation, Cape Cod, Massachusetts. USGS Water-Resources Investigations Report 03-4053.

Walter, D.A. & Whealan, A.T. (2005), Simulated Water Sources and Effects of Pumping on Surface and Ground Water, Sagamore and Monomoy Flow Lenses, Cape Cod, Massachusetts. USGS Scientific Investigations Report 2004-5181.

Ward, R.S., et al. (2004), A framework for monitoring regional groundwater quality. Quarterly Journal of Engineering Geology and Hydrogeology 37(4): 271-281.

Wassenaar, L.I., Hendry, M.J. & Harrington, N. (2006), Decadal geochemical and isotopic trends for nitrate in a transboundary aquifer and implications for agricultural beneficial management practices. Environmental Science and Technology 40(15): 4626-4632.

Weissmann, G.S., et al. (2002), Dispersion of groundwater age in an alluvial aquifer system. Water Resources Research 38(10): -.

Wendland, F., et al. (1994), Potential nitrate pollution of groundwater in Germany: A supraregional differentiated model. Environmental Geology 24(1): 1-6.

White, M.D. & Oostrom, M. (2000), STOMP Subsurface Transport Over Multiple Phases: Theory Guide. Pacific Northwest National Laboratory, Richland, USA.

Williams, M.D. & Oostrom, M. (2000), Oxygenation of anoxic water in a fluctuating water table system: an experimental and numerical study. Journal of Hydrology 230(1-2): 70-85.

Williams, R.L., et al. (2007), Using dissolved gas analysis to investigate the performance of an organic carbon permeable reactive barrier for the treatment of mine drainage. Applied Geochemistry 22(1): 90-108.

Winckler, G., et al. (2002), Noble gases and radiocarbon in natural gas hydrates. Geophysical Research Letters 29(10): 1-4.

Wolman, M.G. (1971), The nation's rivers. Science 174(4012): 905-918.
Wösten, J.H.M. (1994), Water retention and permeabillity characteristics of top and subsoils in the Netherlands: the Staring series. New edition. (in Dutch). DLO-Staring Centrum, Wageningen, the Netherlands.
Xu, Y., Baker, L.A. & Johnson, P.C. (2007), Trends in Ground Water Nitrate Contamination in the Phoenix, Arizona Region. Ground Water Monitoring and Remediation 27(2): 49-56.
Yue, S., Pilon, P. & Cavadias, G. (2002), Power of the Mann-Kendall and Spearman's rho tests for detecting monotonic trends in hydrological series. Journal of Hydrology 259(1-4): 254-271.
Zhang, W.L., et al. (1996), Nitrate pollution of groundwater in northern China. Agriculture, Ecosystems and Environment 59(3): 223-231.
Zheng, C. (1994), Analysis of Particle Tracking Errors Associated with Spatial Discretization. Ground Water 32(5): 821-828.
Zheng, C. & Wang, P.P. (1999), MT3DMS: A modular three-dimensional multispecies transport model for simulation of advection, dispersion, and chemical reactions of contaminants in groundwater systems. Documentation and user's guide. Department of Geological Sciences, University of Alabama, Alabama.
Zinn, B.A. & Konikow, L.F. (2007a), Potential effects of regional pumpage on groundwater age distribution. Water Resources Research 43(6): W06418.
Zinn, B.A. & Konikow, L.F. (2007b), Effects of intraborehole flow on groundwater age distribution. Hydrogeology Journal 15(4): 633.
Zoellmann, K., Kinzelbach, W. & Fulda, C. (2001), Environmental tracer transport (^{3}H and SF_6) in the saturated and unsaturated zones and its use in nitrate pollution management. Journal of Hydrology 240(3-4): 187-205.
Zuber, A., et al. (2005), Groundwater dating with ^{3}H and SF_6 in relation to mixing patterns, transport modelling and hydrochemistry. Hydrological Processes 19(11): 2247-2275.

Summary

Groundwater is a valuable natural resource and as such should be protected from chemical pollution. Because of the long travel times of pollutants through groundwater bodies, early detection of deterioration is necessary to efficiently protect groundwater quality. Therefore, the European Union requires member states to demonstrate good groundwater chemical status, and also identify and reverse significant and sustained upward trends in the concentrations of pollutants that may threaten future groundwater quality.

The aim of this work was to develop and improve tools to detect trends in groundwater quality considering the reactive transport of pollutants from the ground surface to the monitoring screen. The working *hypothesis* was that including more information on pollutant transport, in particular travel time, in the analysis of groundwater quality monitoring data will lead to an improved efficiency to detect these trends and a better understanding of the detected trends. The general research question of this thesis was formulated as: *"What is the value of groundwater age in the detection of trends in groundwater quality?"*

The research presented in this thesis was conducted within the scope of work package TREND 2, named "Trends in groundwater and surface water quality", of the EU 6th Framework Program Integrated Project "AquaTerra" The study area of the research presented in this thesis was the province of Noord-Brabant, the Netherlands. Noord-Brabant is one of the areas in Europe which is most affected by agricultural pollution. The focus of this study was a selection of 14 monitoring wells located in agricultural recharge areas. These areas are especially vulnerable to diffuse groundwater pollution because groundwater and thus contaminants can easily reach deeper parts of the aquifer. The time-series from the selected wells of the groundwater quality monitoring network were used in this thesis, in conjunction with groundwater ages determined with $^{3}H/^{3}He$ in the 34 screens of the 14 wells in agricultural recharge areas.

The overall research question is elaborated through a series of sub-questions. Two lines of research are combined in this thesis: (1) investigating trends in groundwater quality in relation to groundwater ages and (2) determining groundwater age of sampled groundwater and in numerical models. The thesis consists of two parts. Each part deals with one line of research and consists of three chapters.

PART I: TRENDS IN GROUNDWATER QUALITY

Can we detect trends and demonstrate trend reversal in groundwater quality using groundwater age?
Chapter 2 discussed the potential of relating concentrations of pollutants in groundwater to the time of recharge, instead of the time of sampling, to demonstrate trend reversal. Concentrations of conservative pollutants showed an increase in groundwater that recharged before 1985, but also a decrease after 1990. Thereby, trend reversal of groundwater quality was demonstrated. This showed that $^{3}H/^{3}He$ dating is particularly useful to facilitate (re)interpretation of existing

groundwater quality data. Additionally, the measured concentrations related to time of recharge showed a strong correlation to a reconstruction of the contamination history that was based on historical records of the application of fertilizer and manure.

Can we understand the trends of concentrations of reactive solutes using groundwater age?
The purpose of Chapter 3 was to identify solute specific trends in concentrations that are influenced by reactions with sediment geochemistry. Three types of trends were distinguished. These are the result of: (1) the anthropogenic trends in historical concentrations in recharging groundwater unaltered during conservative transport through the groundwater body (e.g. chloride), (2) anthropogenic trends in recharge concentrations altered by reactions during transport (e.g. retardation of potassium), and (3) geochemical reactions in the subsurface that are triggered by anthropogenic changes in the recharge concentrations of other solutes (e.g. release of sulfate, iron, and arsenic by nitrate-induced pyrite oxidation). A combination of reactive transport modeling and the analysis of concentrations related to groundwater age provides an effective tool for revealing the appropriate hydrogeochemical processes that are responsible for trends in groundwater quality.

Which method is best suitable for the detection of trends in groundwater quality given a variety of available data, hydrogeological settings, and objectives?
Four methods for the detection and extrapolation of trends in groundwater quality were compared in Chapter 4: (1) statistical methods, (2) groundwater dating, (3) transfer functions, and (4) deterministic models. This chapter showed that there is no single optimal method to detect trends in groundwater quality across widely differing catchments. The selection of the method should firstly be made on the basis of the specific goals of the study (only trend detection or also extrapolation), and secondly on the system under study, and the available resources. For trend detection in groundwater quality, the most important difference between groundwater bodies is whether the character of the subsurface or the monitoring system causes mixing of groundwater with different travel times.

PART II: GROUNDWATER AGE

Can we date groundwater that is affected by geochemical reactions and subsequent degassing?
The production of gases in groundwater under contaminated locations by geochemical reactions is not uncommon. Degassing of these gases from groundwater and re-partitioning of noble gases between water and gas phase distorts groundwater dating by $^{3}H/^{3}He$.

To correct for the loss of tritiogenic ^{3}He due to degassing, a single-step equilibrium degassing model was presented in Chapter 5. The total dissolved gas pressure (TDG) at the monitoring screen was used to estimate the depth and timing of degassing, which is essential to estimate travel times from degassed samples. By propagating the uncertainties in the underlying measurements and assumptions through the travel time calculations, we found a travel time uncertainty of 3 years. This showed that $^{3}H/^{3}He$ dating provides valuable information on groundwater flow even at sites with strong degassing.

What is the fate of N_2 bubbles in the subsurface and how accurate are tracer ages of degassed groundwater?

Chapter 6 discussed the use of a two-phase flow and transport model (STOMP) to study the reliability of $^3H/^3He$, CFCs and SF_6 as groundwater age tracers under agricultural land where denitrification causes degassing. The TDG correction of the $^3H/^3He$ age presented in Chapter 5 overestimated the groundwater age by 2.1 years, due to the accumulation of $^3He^*$ in the gas phase. The total uncertainty of degassed $^3H/^3He$ ages of 6 years ($\pm$ 2 σ) is due to the correction of degassed $^3He^*$ using the TDG method, but also due to the travel time in the unsaturated zone and the diffusion of bomb peak $^3He^*$. CFCs appear to be subject to significant degradation in anoxic groundwater and SF_6 is highly susceptible to degassing. Based on the two-phase flow model results, $^3H/^3He$ appears to be the most reliable method to date degassed groundwater in the anoxic parts of an aquifer.

How can we derive accurate travel time distributions in regional scale models in order to predict trends in surface water quality?

The breakthrough of spatially diffuse contamination into the surface water is strongly related to the travel time distribution of discharging ground water. However, a travel time distribution based on a particle tracking analysis in a ground water model containing weak sinks is often uncertain, because weak sinks in the flow model pose a problem to the particle tracking theory. The probability-based method presented in Chapter 7 compares favorably with the solute transport solution and provides the most accurate travel time distribution that is based on a fine-resolution ground water model.

Main conclusions

Groundwater age is of utmost importance in the detection of trends in groundwater quality. In general, a conceptual understanding of the groundwater system is essential for the characterization of chemical status and the detection of trends. Groundwater age is in particular valuable for two reasons. First, the possibility to aggregate groundwater quality data from several independent monitoring locations across a groundwater body, with similar land use in their catchment area; and second, the possibility to link measurements of groundwater quality, and trends therein, related to time of recharge, directly to the contamination history. The value of groundwater age is demonstrated, apart from this thesis, by a growing number of studies using groundwater age in the detection of trends (Laier 2004; Daughney and Reeves 2006; Wassenaar *et al.* 2006; Tesoriero *et al.* 2007; Burow *et al.* 2008; Debrewer *et al.* 2008; Rupert 2008; Saad 2008). These studies agree that groundwater age is invaluable to the interpretation of existing time-series (Rosen and Lapham 2008).

Given the importance of travel times, they may be used to optimize the monitoring program or aid in the extension or improvement of the existing network. Although groundwater ages can only be determined after the installation of a monitoring location, groundwater age distributions estimated from simple analytical equations or complex models are practically essential for the design of a monitoring network (Van Duijvenbooden *et al.* 1985; Broers 2004a; Janssen *et al.* 2006)

Samenvatting

Trends in grondwaterkwaliteit in relatie tot grondwaterleeftijden

Introductie

"Grondwater is een waardevolle natuurlijke hulpbron die als zodanig voor achteruitgang en voor chemische verontreiniging moet worden behoed. Dit is in het bijzonder van belang voor grondwaterafhankelijke ecosystemen en voor het gebruik van grondwater ten behoeve van de voorziening van water bestemd voor menselijke consumptie." Met deze zinnen opent Richtlijn 2006/118/EG van het Europees Parlement en de Raad, in Nederland bekend als de Grondwater Richtlijn. Bij de bescherming van grondwater tegen verontreinigingen moet rekening worden gehouden met de lange reistijden van grondwater door de ondergrond. Veranderingen in de concentratie van verontreinigingen die vandaag in grondwater worden waargenomen, kunnen het gevolg zijn van verontreinigingen die jaren geleden hebben plaatsgevonden. Deze lange reistijden bemoeilijken ook het onderzoek naar trends in grondwaterkwaliteit. Naast de lange reistijden zijn er nog andere factoren van belang, zoals ruimtelijk variatie in uitspoeling van verontreinigingen en afbraak of vertraging van stoffen door reacties met de ondergrond. De uitspoeling van bijvoorbeeld nitraat is sterk afhankelijk van het langjarig gemiddelde neerslagoverschot en variaties daarin. Opeenvolgende natte jaren werken verdunnend en leiden tot lage nitraatgehalten. In een nat jaar dat op een aantal droge jaren volgt, kan juist extra veel nitraat uitspoelen dat zich in de droge jaren ervoor heeft opgehoopt. Bovendien is de uitspoeling van nitraat niet onder elk gewas hetzelfde. Nitraat kan in de ondergrond worden afgebroken door een reactie met sedimenten, bijvoorbeeld sedimenten waarin pyriet of veel organisch materiaal voorkomt. Andere stoffen, zoals kalium en zware metalen, adsorberen aan organisch materiaal en klei in de bodem, waardoor de uitspoeling van deze stoffen – en daarmee hun aankomst bij het filter van een meetlocatie – wordt vertraagd. Al deze factoren leiden tot de noodzaak om bij het onderzoeken en aantonen van trends in grondwaterkwaliteit rekening te houden met het transport van stoffen door grondwaterstroming en met chemische processen die tijdens dit transport plaats kunnen vinden.

Het doel van dit proefschrift is om trends in grondwaterkwaliteit aan te tonen, door specifiek rekening te houden met de reistijd van het bemonsterde grondwater. Daarbij is gebruik gemaakt van een groot aantal bestaande metingen van landbouwgerelateerde stoffen bemonsterd in putten van het meetnet grondwaterkwaliteit in landbouwgebieden in Brabant. Daarnaast behandelt dit proefschrift methodes om de reistijd of leeftijd van grondwater te bepalen aan de hand van verschillende "tracers" (het verval van de waterstofisotoop tritium en de verhouding met het vervalproduct helium, en de gehaltes chloorfluorkoolstofverbindingen (CFK's) en hexafluoride in

grondwater) en ook door numerieke modelsimulaties. Het onderzoek is uitgevoerd in het kader van het Europese onderzoeksprogramma AquaTerra.

Resultaten

De kwaliteit van grondwater in Brabantse landbouwgebieden is sinds 1990 verbeterd. De gehaltes van nitraat en andere landbouwgerelateerde stoffen zijn gedaald in grondwater dat na 1990 in de bodem is geïnfiltreerd. De verbetering van grondwaterkwaliteit is aangetoond door bestaande gegevens van het Landelijk en Provinciaal Meetnet Grondwaterkwaliteit in Brabant opnieuw te analyseren. Deze gegevens zijn gecombineerd met de leeftijd van het bemonsterde grondwater, bepaald aan de hand van tracers. Uit de leeftijd van het grondwater is het jaar van infiltratie afgeleid. Vervolgens zijn alle beschikbare metingen van nitraat en andere landbouwgerelateerde stoffen gerangschikt naar infiltratiejaar. Door alle metingen per stof samen in een figuur te tekenen, ontstaat de "geaggregeerde regionale trend". Voor nitraat leverde dat het beeld op dat voor 1980 de uitspoeling van nitraat toenam. Dankzij het mestbeleid is de uitspoeling van nitraat naar het grondwater sinds 1990 ook weer afgenomen. Daarmee is een trendbreuk aangetoond in de concentraties van nitraat ten opzichte van het jaar van infiltratie. Deze trend komt overeen met een reconstructie van nitraatuitspoeling in Brabant. Deze reconstructie is gebaseerd op cijfers over mestproductie en mestgebruik van het Centraal Bureau voor de Statistiek.

Naast nitraat zijn ook de trends van andere stoffen in het grondwater onderzocht om een compleet beeld van de grondwaterchemie te krijgen. Daaruit bleek dat de geaggregeerde regionale trends specifiek voor elke stof zijn, als gevolg van de chemische interacties tussen de verschillende stoffen en de ondergrond. Drie verschillende soorten stoffen zijn onderscheiden: "*conservatieve stoffen*", "*lokaal conservatieve stoffen*" en "*reactieve stoffen*". *Conservatieve stoffen* worden getransporteerd door grondwaterstroming zonder dat ze een interactie met de ondergrond aangaan. Transport zonder interacties met de ondergrond wordt conservatief genoemd. Een voorbeeld van een conservatieve stof is chloride, dat niet deelneemt aan reacties in de ondergrond. Stoffen die *lokaal conservatief* zijn, reageren slechts op een bepaalde plek in de ondergrond; daarvoor en daarna worden ze conservatief getransporteerd. Een voorbeeld van een *lokaal conservatieve stof* is nitraat. Nitraat, dat vanuit de bodem naar het grondwater is uitgespoeld, wordt pas afgebroken op het grensvlak tussen "oxisch" en "anoxisch" sediment. In anoxisch sediment bevindt zich reactief organisch materiaal en/of pyriet dat reageert met nitraat. De afbraak van nitraat gaat relatief snel, binnen enkele jaren, ten opzichte van de reistijden van grondwater. *Reactieve stoffen* zijn altijd onderhevig aan interacties met de ondergrond. De concentraties daarvan veranderen hierdoor continu tijdens hun weg door de ondergrond. Een voorbeeld van een *reactieve stof* is kalium. Kalium gaat kationuitwisselingen aan met klei en organisch materiaal in het sediment. Kalium wordt uitgewisseld voor een ander kation, veelal calcium, dat aan het sediment gebonden zat. Door deze uitwisseling verandert de waargenomen trend van kaliumconcentraties ten opzichte van de trends in de concentraties in infiltrerend grondwater.

De interacties van de meeste in grondwater aanwezige stoffen met de ondergrond zijn onderzocht met behulp van een numeriek chemisch-reactief-transportmodel. Daaruit blijkt

dat de trends in de concentraties van de kationen natrium, kalium, calcium, magnesium, ijzer, aluminium, nikkel en zink beïnvloed zijn door kationuitwisseling. De trends van nitraat, sulfaat, ijzer, zuurgraad (pH), arseen, nikkel en zink zijn beïnvloed door pyrietoxidatie: een reactie tussen pyriet in de ondergrond en nitraat uit het grondwater. Trends in pH en de concentraties van zuurstof en aluminium worden vooral bepaald door de chemische sedimenteigenschappen. Uit deze verschillen zijn drie soorten trends afgeleid: "conservatieve trends", "direct reactieve trends" en "indirect reactieve trends". Conservatieve trends worden gevonden voor conservatieve stoffen, zoals chloride. Direct reactieve trends worden gevonden voor landbouwgerelateerde stoffen die een reactie met de ondergrond aangaan. Voorbeelden daarvan zijn nitraat en kalium. Indirect reactieve trends worden gevonden voor stoffen die zelf niet aan landbouw gerelateerd zijn, maar wel door reacties tussen landbouwgerelateerde stoffen en de ondergrond beïnvloed worden. Voorbeelden hiervan zijn de stoffen gerelateerd aan pyrietoxidatie. Door de reactie tussen pyriet en nitraat worden sulfaat en ijzer geproduceerd, en komen ook zware metalen zoals nikkel en zink en arseen vrij. De trends die gevonden worden voor sulfaat, ijzer, nikkel en zink, zijn typisch voorbeelden van indirect reactieve trends. Om deze trends goed te verklaren is een begrip van reactief transport vereist. Voor het extrapoleren van deze trends is een chemisch-reactief-transportmodel noodzakelijk.

In het kader van het Europese onderzoeksprogramma AquaTerra zijn verschillende methoden voor het vinden en aantonen van trends met elkaar vergeleken. Deze methoden zijn door onderzoeksgroepen uit Nederland, België, Frankrijk en Polen toegepast op zeer verschillende geohydrologische systemen. Uit de vergelijking is gebleken dat er geen unieke methode bestaat om trends te onderzoeken, die geschikt is voor alle geohydrologische systemen die in Europa voorkomen. De methode om trends in grondwaterkwaliteit te onderzoeken moet afhangen van de volgende factoren: het doel van het onderzoek, enkel opsporen of ook extrapoleren, of zelfs een beter begrip van het systeem vergaren; de eigenschappen van de ondergrond en het meetnet; de reeds beschikbare gegevens en kennis over de ondergrond; en de middelen om nieuwe metingen te verrichten. Een belangrijk onderscheid moet gemaakt worden tussen grondwatermonsters die zijn genomen in specifieke monitoringsputten, en monsters die zijn genomen in bronnen, pompputten of drinkwaterwinningen. Monitoringsputten die zijn uitgerust met een kort filter op een bepaalde diepte leveren een monster met een specifieke grondwaterleeftijd. Bronnen, pompputten en drinkwatervoorzieningen daarentegen leveren veelal een mengsel van oud en jong grondwater. Door dit verschil in monstertype zijn ook verschillende methoden voor trendonderzoek vereist.

De leeftijd van grondwater is de tijd die verstreken is nadat het water als regen in de bodem is terechtgekomen. De leeftijden van grondwater in Brabant kunnen worden bepaald aan de hand van het verval van de waterstofisotoop tritium of aan de hand van de concentraties van CFK's en zwavelhexafluoride in grondwater. Bij het verval van tritium wordt een isotoop van helium geproduceerd. De halfwaardetijd van tritium is ongeveer twaalf jaar, waardoor tritium zeer geschikt is om grondwater dat jonger dan vijftig jaar is te dateren. De leeftijd van het grondwater wordt berekend uit de verhouding van de concentraties tritium en helium in grondwater. Naarmate er meer tritium vervalt, verschuift de verhouding meer naar de kant van helium, vergelijkbaar met een zandloper. Tritium in grondwater is onderdeel van de watermoleculen die het grondwater vormen. Helium is een edelgas dat chemisch inert is en daardoor opgelost

in grondwater conservatief wordt getransporteerd door grondwaterstroming. Sinds de jaren vijftig zijn CFK's gebruikt als drijfgas en koelmiddel, en sinds de jaren zeventig wordt zwavelhexafluoride gebruikt voor het isoleren van hoogspanningschakelaars. Daarbij zijn steeds grotere hoeveelheden ontsnapt waardoor hun concentratie in de atmosfeer over deze periode is toegenomen. Deze gassen zijn ook opgelost in regen te vinden, doordat ze in de atmosfeer oplossen in de druppeltjes van regenwolken. Daarmee zijn ook hun concentraties in grondwater, dat door infiltratie van regenwater over de afgelopen vijftig jaar is gevormd, toegenomen. Door de concentraties in grondwater nauwkeurig te meten is het mogelijk de leeftijd van het grondwater af te leiden. In de provincie Brabant zijn 34 monsters genomen uit 14 putten van het Landelijk en Provinciaal Meetnet Grondwaterkwaliteit. De meeste monsters zijn genomen van een diepte van 10 of 25 meter, enkele monsters zijn van een diepte van ongeveer 5 meter beneden het oppervlak. In deze monsters zijn de concentraties tritium, helium, CFK's en zwavelhexafluoride bepaald door laboratoria in Duitsland.

Uit de analyse van de monsters bleek dat helium deels uit het grondwater was verdwenen. De concentraties helium en neon, dat ter controle is gemeten, waren lager dan normaal in water worden aangetroffen. Het ontsnappen van helium kon verklaard worden door de productie van stikstofgas in de ondergrond. Zoals eerder vermeld reageert nitraat in de Brabantse ondergrond met pyriet. Naast ijzer en sulfaat wordt ook stikstofgas geproduceerd. Stikstofgas is chemisch inert. Onder normale omstandigheden zou het geproduceerde stikstofgas oplossen in het grondwater. De concentraties nitraat in Brabant zijn echter zo hoog dat het stikstofgas ontsnapt uit de oplossing en belletjes vormt in het sediment. Dit proces – ontgassing – is te vergelijken met het rijzen van deeg door de productie van koolzuur door gist. Tijdens het ontgassen worden edelgasatomen uitgewisseld tussen het grondwater, waarin ze opgelost zaten, en de nieuwgevormde belletjes. Als gevolg van deze uitwisseling nemen de opgeloste hoeveelheden helium en neon af, zoals uit de metingen bleek.

Doordat de concentraties helium en neon als gevolg van ontgassing waren veranderd, was het nodig een correctie toe te passen voordat een leeftijd kon worden berekend. Voor deze correctie is de totale gasdruk van de monsters bepaald, die een indicatie geeft van de diepte waarop ontgassing heeft plaatsgevonden. Met behulp van deze diepte zijn de heliumconcentraties gecorrigeerd voor ontgassing en de leeftijden van het grondwater bepaald. De nauwkeurigheid van de leeftijden is ongeveer drie jaar. Uit een vergelijking van de leeftijden met de diepte van de bemonstering bleek dat over het algemeen de leeftijd van het grondwater in de diepte toeneemt met ongeveer één jaar per meter. De leeftijden van het grondwater op een diepte van 25 meter zijn daardoor gemiddeld 25 jaar oud, maar de individuele leeftijden uit de afzonderlijke putten vertonen een spreiding van ongeveer twintig jaar. Hoewel de leeftijden dus gemiddeld met één jaar per meter toenemen, blijkt uit deze spreiding dat dateringen toch wel degelijk zinvol zijn.

Om te onderzoeken wat het lot is van de gevormde belletjes in het grondwater en ook om een beter beeld te krijgen van de nauwkeurigheid van grondwaterleeftijden die gebaseerd zijn op ontgaste monsters, is een numeriek model gebruikt dat het transport van water en gassen in sedimenten kan simuleren. De modelresultaten wijzen erop dat een groot deel van het gevormde stikstofgas wordt gevangen door het sediment. De belletjes zijn niet in staat om door de poriën van het sediment omhoog te bewegen. Daardoor kan zich een grote aaneengesloten gasfase

vormen waarin helium zich kan ophopen. De ophoping van helium beïnvloedt de verhouding tussen opgeloste concentraties tritium en helium. Als gevolg daarvan lijkt het water ongeveer twee jaar ouder dan het in werkelijkheid is. De onzekerheid van de leeftijden als gevolg van ontgassing en andere processen tijdens infiltratie en in de ondergrond is ook met het numerieke model onderzocht. Daaruit bleek dat de leeftijd van het grondwater op zes jaar nauwkeurig te bepalen is.

Uit een vergelijking tussen de gemeten hoeveelheden CFK's in grondwatermonsters en de modelresultaten bleek dat CFK's, net als nitraat, reageren met anoxische sedimenten. Daarnaast toonden een groot aantal monsters verontreiniging van CFK's door lokale bronnen aan. Mede daardoor zijn CFK's niet erg geschikt om grondwaterleeftijden mee te bepalen in Brabant. Zwavelhexafluoride is zeer gevoelig voor ontgassing, omdat de oplosbaarheid zeer laag is en er tijdens ontgassing relatief veel naar de belletjes ontsnapt. Bovendien is uit de gemeten hoeveelheid niet af te leiden of ontgassing heeft plaatsgevonden. Daardoor is ook zwavelhexafluoride minder geschikt voor het dateren van grondwatermonsters als ontgassing niet kan worden uitgesloten. De tritium-helium methode is daarom het meest geschikt om grondwatermonsters uit Brabant te dateren.

Met behulp van een numeriek model is de leeftijdsverdeling van het grondwater in het stroomgebied van de beek de Run in Brabant onderzocht. De leeftijdsverdeling van grondwater dat opkwelt naar de sloten en beken rondom de Run, bepaalt in zekere mate de kwaliteit van het water in de beek. Daarbij is de bijdrage van jong grondwater, dat minder dan 50 jaar oud is, van belang omdat dit deel beïnvloed kan zijn door de toegenomen intensieve landbouw in het gebied rondom de Run. Het aandeel ouder water verdunt juist de uitspoeling van nitraat naar beken en sloten. De leeftijdsverdeling is op verschillende manieren berekend met een grof en een fijn grondwatermodel. Beide modellen bestrijken een gebied van 35 bij 24 kilometer ten zuiden van Eindhoven. Het grove model heeft cellen van 100 bij 100 meter in de horizontaal; het fijne model heeft cellen van 25 bij 25 meter. Uit de vergelijking bleek dat de leeftijdsverdeling het beste kan worden berekend door het transport van een fictieve conservatieve stof te simuleren in een zeer fijn model. Dergelijke modellen zijn echter niet praktisch omdat ze veel rekentijd vergen. Een andere benadering, die fictieve deeltjes volgt door het grondwaterstromingsmodel, is wel toepasbaar op zeer fijne modellen. Deze *particle tracking* benadering kent echter een zwakte: het lot van deeltjes die in de buurt van kleine sloten of drainagebuizen terechtkomen is onzeker. Het is niet mogelijk te bepalen of het fictieve deeltje dan door de sloot wordt afgevoerd of doorstroomt naar de volgende sloot. Deze onzekerheid werkt door in de berekening van de leeftijdsverdeling van het uittredende grondwater. Door expliciet de kans dat een deeltje door de sloot wordt afgevoerd mee te nemen in de berekening van de reistijdenverdeling van grondwater kon deze onzekerheid worden weggenomen. Daardoor is het nu mogelijk op een zeer hoge resolutie betrouwbare leeftijdsverdelingen van grondwater te berekenen.

Conclusies

De verbetering van de grondwaterkwaliteit in Brabant kon worden aangetoond door de leeftijd van grondwatermonsters te bepalen. Voor onderzoek naar grondwaterkwaliteit is het essentieel

om de leeftijd van het bemonsterde grondwater te weten. Daarmee is het mogelijk een directe vergelijking te maken met reconstructies van nitraatuitspoeling op basis van statistische gegevens. Voor een gerichte monitoring van trends in grondwaterkwaliteit voor de Europese Kaderrichtlijn Water zou de leeftijd van het bemonsterde grondwater ter plaatse van alle bestaande locaties van het meetnet grondwaterkwaliteit bepaald moeten worden. Daarnaast zijn grondwaterleeftijden uitermate geschikt om het bestaande monitoringsprogramma te optimaliseren of het netwerk van monitoringsputten uit te breiden of te verbeteren. Hoewel grondwaterleeftijden in monitoringsputten pas na installatie van de put beschikbaar worden, zijn schattingen van grondwaterleeftijden of leeftijdsverdelingen essentieel voor het optimaal inrichten van een meetnet van grondwaterputten voor het monitoren van grondwaterkwaliteit.

Dankwoord

Dat was het dan. Het is af! Dit betekent het einde van een ontzettend leuke en leerzame periode, en het begin van mijn leven als doctor. Dr. Ate. Ik ben erg trots op het resultaat, maar ik ben vooral erg dankbaar dat ik kon vertrouwen op de wijze raad en steun en afleiding van heel veel mensen.

Allereerst mijn promotoren: Hans Peter Broers en Marc Bierkens. Hans Peter, bedankt voor de beste begeleiding die ik me had kunnen wensen. Jij hebt ontzettend scherpe ideeën over hoe je trends in grondwaterkwalitiet onderzoekt. Je wist precies wat je mij wilde laten doen, maar je vond het toch prima als ik het iets anders deed. Althans, je liet me de vrijheid. En met die vrijheid heb ik de krenten uit de pap kunnen vissen. En Marc, hartelijk dank voor het enthousiasme, de kritiek op al mijn werk, en de bereikbaarheid en openheid die weinig professoren eigen is. En voor de drive om te publiceren, publiceren, publiceren. Heren, het was een genoegen om jullie AIO te zijn!

Dank aan mijn collega's bij TNO, nu Deltares, op wiens schouders ik heb mogen staan om iets verder te kijken. Weinig promovendi hebben zoveel kennis en ervaring zo dicht om zich heen. Bas, Jasper, en vele anderen, voor jullie alomvattende kennis over grondwaterkwaliteit, geochemie en stoftransport. Bedankt Ruth, voor jouw onverbeterlijke enthousiasme en interesse voor mijn werk en R-gepiel. En voor het vertalen van mijn idiote ideeën en scriptjes naar een toepassing waar de rest van de wereld iets mee kan. Joachim en Ype, onder andere voor de leerzame en gezellige dagen naar Hupsel. Victor, Gijs, Annemieke, Janneke, en iedereen van Grondwaterkwaliteit en "BenO" die mijn tijd als AIO bij TNO zeer genoeglijk hebben gemaakt. En de collega-voetballers, voor de geweldige potjes voetbal en soms wat minder productieve donderdagmiddagen. En TNO en Deltares, als organisatie, voor de financiële, organisatorische en logistieke ondersteuning.

M'n collega's bij Fysische geografie voor lange doch inspirerende koffiepauzes, Juul voor de goede zorgen, en alle collega AIOs, Reinder, Sibren, Wiebe, Arien, Gilles, en anderen, voor de wijze raad en gedeelde sores. Bedankt Hanneke, een collega-TNO-AIO is wel de ideale kamergenoot in het laatste jaar bij TNO. Het was erg gezellig. En ook alle andere kamergenoten die ik in de afgelopen jaren bij TNO en de UU heb versleten, inmiddels te veel om op te noemen. Ik heb jullie aanwezigheid altijd erg gewaardeerd, al liet ik dat soms niet blijken.

Thanks to all citizens of the European Union for funding the 6th Framework Program Integrated Project AquaTerra and subsidizing my research and lifestyle. It has been a pleasure to be an AquaTerra PhD student. Thanks Johannes Barth for all your enthousiasm, reading all of our reports and making sensible comments, thanks Serge, Jordi, Philippe, Igor and Marek for the "T_2" collaboration, all inputs for our "deliverables" and interesting discussions about trends.

Thanks fellow AquaTerra PhD students for the good times abroad. Edda and Christian, it's always good to see you, at a conference or wherever, and discuss science, politics, life and everything else.

I owe many thanks to Peter Engesgaard and Klaus Hinsby for organizing the tremendously interesting and valuable FIVA PhD course in Copenhagen on environmental tracers in the hydrological cycle. This thesis would not have been nearly the same without the amazing lectures by Roland Purtschert and Kip Solomon. Thank you for all your knowledge, advice and answers.

Jürgen Sültenfuß, for the analysis of the $^{3}H/^{3}He$ samples. Thank you Jürgen, your comments on the noble gas measurements were very helpful to understand the "degassing" of groundwater, and to interpret these noble gas measurements to get a reliable age. Thanks Matthias Brennwald, for our discussion and your many valuable comments on an early version of Chapter 5. Thanks to Helmut Geistlinger, for providing a thorough review of Chapter 6. Mark White and Mart Oostrom are acknowledged supplying the STOMP code and their assistence while working with it.

En Joris! Bedankt voor het STOMP-werk. Je had de meest ondankbare taak om als stagiair uit te vogelen hoe het STOMP-model werkt en het aan de praat te krijgen, al ben je zelf geen modelleur. En toch is het je gelukt, terwijl ik op vakantie was nota bene. Knap. Het was erg goed en gezellig samenwerken. En dankzij jouw werk hebben we samen een paper in Journal of Contaminant Hydrology op onze naam staan! Bedankt!

Bedankt Ans, voor alle nachten in pension Kirchholtes tijdens veldwerk. Huiselijke gezelligheid tijdens veldwerk, met koud (!) bier in de koelkast. Perfect. En ook alle relaxte weekenden met Renske in Brabant waren voor mij kleine vakanties.

Uif en Ane, mijn paranimfen: dankzij of ondanks? Hoe dan ook: een geweldige tijd en bedankt voor alle afleiding. Heerlijk aan auto's klooien: lassen, kleppen stellen, stroomverdeler vastschroeven, bougies wisselen, olie verversen, Saab slopen, de 404 aan de praat krijgen, wat zijn we goed! Bootje varen, films, de Zotte en nog veel meer. Laat mij maar ouwehoeren over belletjes in bier. Bier? Reinder, Matthijs, Geert-Jan, en Maud, bedankt voor het klimmen, fietsen, concerten, feestjes, en heel veel gezelligheid.

Mieke, voor een veilig rommelig ordelijk thuis, voor de vrijheid van keuze, het sparren over hoe de wereld in elkaar zit, je rationele objectieve wereldbeeld waar plek genoeg is voor nuance, en het sorteren van m'n LEGO natuurlijk! ;-) Dirk, voor je liefde voor werk, niet van 9-5, maar door de enorme inzet in de uren dat we wel werken, en voor jouw aandacht voor taal en schrijven. Ik begin te begrijpen wat zo leuk is aan schrijven: gelezen worden. En Gerrit, voor het besef dat er meer is buiten mijn wetenschappelijke wereldje, en dat ik tijdens de verdediging enkel mijn werk belijd en niet mijn persoon.

En tot slot, natuurlijk, Renske! Dankjewel voor je geduld, het dulden van mijn gebrom en gemopper soms, en voor alle vakanties waartoe je me hebt verleid. Zonder jou had ik nooit door Thailand gefietst, of op Mt. Whitney gestaan. Promoveren is leuk, maar vakanties met jou

zijn zeker zo leuk. En soms vergeet ik dat. Help me herinneren! Dankjewel, voor alles met jou samen.

Curriculum Vitae

Ate Visser is geboren op 6 oktober 1979 te Amsterdam. Hij is de zoon van Mieke Krebber, universiteitsbibliothecaris, en Dirk Visser, journalist. Na de 6e Montessori-basisschool Anne Frank volgde hij het atheneum aan het Hervormd Lyceum Zuid in Amsterdam. Hij deed in de zomer van 1997 met goed gevolg eindexamen in negen vakken, waaronder geschiedenis en handelseconomie, maar geen aardrijkskunde.

Gefascineerd door de foto's en veldwerkmaterialen, koos hij na het atheneum voor de studie fysische geografie. Na het tweedejaarsveldwerk in Luxemburg, volgde hij enige vakken aan de universiteit van Michigan, waaronder politicologie en geschiedenis van de Verenigde Staten in de 20e eeuw. In zijn scriptie, geschreven onder begeleiding van Gerard Heuvelink en Willem Bouten, behandelde hij de mogelijkheden om de parameters van een bodemhydrologisch numeriek model te schatten met behulp van het Kalman-filter, een wiskundig algoritme om metingen en modelresultaten te combineren. Tijdens het afronden van zijn scriptie heeft hij enkele vakken van de minor Internationale Betrekkingen gevolgd. Vervolgens heeft hij stage gelopen bij het toenmalige Nederlands Instituut voor Toegepaste Geowetenschappen – TNO, tegenwoordig Deltares. Tijdens zijn stage, onder begeleiding van Roelof Stuurman en Marc Bierkens, heeft hij gewerkt aan een algoritme om de hydrologische toestand van een proefveld – bodemvochtgehalte en grondwaterstand – zo goed mogelijk te schatten. Daarvoor werden metingen van bodemvocht- en grondwaterstandsensoren en gecombineerd met een numeriek bodemvochtmodel en online gepresenteerd. De resultaten van deze studie zijn in 2006 gepubliceerd in Advances of Water Resources.

Op 16 september 2004 begon hij met zijn promotieonderzoek, op zoek naar trends in grondwaterkwaliteit, waarvan u het resultaat in handen heeft.

Publications

Published papers

Visser, A., et al. (2009), Trends in pollutant concentrations in relation to time of recharge and reactive transport at the groundwater body scale. Journal of Hydrology, in press, doi: 10.1016/j.jhydrol.2009.02.008.

Visser, A., et al. (2009), Travel time distributions derived from particle tracking in models with weak sinks. Ground Water 47(2): 237-245, doi: 10.1111/j.1745-6584.2008.00542.x.

Visser, A., et al. (2009), Degassing of $^{3}H/^{3}He$, CFCs and SF_6 by denitrification: measurements and two-phase transport simulations. Journal of Contaminant Hydrology 103(3-4): 206-218, doi:10.1016/j.jconhyd.2008.10.013.

Visser, A., Broers, H.P. & Bierkens, M.F.P. (2007), Dating degassed groundwater with $^{3}H/^{3}He$. Water Resources Research 43(10): WR10434, doi:10.1029/2006WR005847.

Visser, A., et al. (2007), Demonstrating Trend Reversal of Groundwater Quality in Relation to Time of Recharge determined by $^{3}H/^{3}He$. Environmental Pollution 148 (3): 797-807, doi:10.1016/j.envpol.2007.01.027.

Visser, A., Stuurman, R. & Bierkens, M.F.P. (2006), Real-time forecasting of water table depth and soil moisture profiles. Advances in Water Resources 29: 692-706, doi:10.1016/j.advwatres.2005.07.011.

Abstracts and conference proceedings

Visser, A., et al. (2008), Measurements and two-phase transport simulations of $^{3}H/^{3}He$, CFCs and SF_6 show degassing by denitrification and degradation of CFCs. In: B. Newman, proceedings of the International Workshop on Groundwater Dating using Environmental Tracers (G-DAT 2008), Leipzig, Germany, 5-7 March 2008, IAEA.

Visser, A., et al. (2007), Modelling two-phase transport of $^{3}H/^{3}He$. In: J.C. Refsgaard, K. Kovar, E. Haarder and E. Nygaard, proceedings of the ModelCARE 2007 Conference, Copenhagen, Denmark, 9-13 September 2007, IAHS publication 320: 226-232.

Broers, H.P., et al. (2007), Improving the prediction of future groundwater quality by analyzing concentration-depth profiles. In: T.D. Bullen and Y. Wang, proceedings of the 12th International Symposium on Water-Rock Interaction, Kunming, China, 31 July – 5 August 2007, Taylor & Francis, 1015-1019.

Visser, A., Broers, H.P. & Bierkens, M.F.P. (2006), Denitrification and degassing of groundwater: Implications for environmental tracer studies. Proceedings of the 16th Annual Goldschmidt Conference, Melbourne, Australia, 27 August – 1 September 2006, Geochimica et Cosmochimica Acta 70(18, Supplement 1): A674-A674.

Visser, A., Stuurman, R. & Bierkens, M.F.P. (2004), Real time forecasting of water table depth and soil moisture profiles. In: Teuling, A.J., Leijnse, H., Troch, P.A., Sheffield, J., and Wood, E.F., Proceedings of the 2nd international CAHMDA workshop on: The Terrestrial Water Cycle: Modelling and Data Assimilation Across Catchment Scales, Princeton, USA, 24-27 October 2004, pp. 117-121.

Press coverage

Brabants grondwater stuk schoner geworden, 3 May 2007, Brabants Dagblad

Grondwater schoner dankzij mestbeleid, 4 May 2007, BN – De Stem

Reports and chapters

Reports for the EU project AquaTerra are available online:
http://www.attempto-projects.de/aquaterra/57.0.html

NEDERLANDSE GEOGRAFISCHE STUDIES / NETHERLANDS GEOGRAPHICAL STUDIES

350 Z FÖLDI Neighbourhood dynamics in Inner-Budapest; A realist approach -- Utrecht 2006: Knag/Faculteit Geowetenschappen Universiteit Utrecht. 345 pp, 72 figs, 10 tabs, 34 pics. ISBN: 978-90-6809-391-9, Euro 35,00

351 S AGTERBOSCH Empowering wind power; On social and institutional conditions affecting the performance of entrepreneurs in the wind power supply market in the Netherlands -- Utrecht 2006: Knag/Copernicus Institute. 246 pp, 36 figs, 8 tabs. ISBN: 978-90-6809-392-6, Euro 27,50

352 C RINZIN On the middle path; The social basis for sustainable development in Bhutan -- Utrecht 2006: Knag/Copernicus Institute. 204 pp, 18 figs, 37 tabs, 5 box. ISBN: 90-6809-393-2, Euro 22,50

353 M VAN WIJK Airports as cityports in the city-region; Spatial-economic and institutional positions and institutional learning in Randstad-Schiphol (AMS), Frankfurt Rhein-Main (FRA), Tokyo Haneda (HND) and Narita (NRT) --Utrecht 2007: Knag/Faculteit Geowetenschappen Universiteit Utrecht. 323 pp, 59 figs, 18 tabs. ISBN: 978-90-6809-394-0, Euro 35,00

354 A C HELDERMAN Continuities in homeownership and residential relocations -- Utrecht/Amsterdam 2007: Knag/ Faculteit der Maatschappij- en Gedragswetenschappen Universiteit van Amsterdam. 125 pp, 15 figs, 14 tabs. ISBN: 978-90-6809-395-7, Euro 19,00

355 W BORREN Carbon exchange in Western Siberian watershed mires and implication for the greenhouse effect; A spatial temporal modeling approach -- Utrecht 2007: Knag/Faculteit Geowetenschappen Universiteit Utrecht. 125 pp, 36 figs, 17 tabs. ISBN: 978-90-6809-396-4, Euro 13,00

356 S O NEGRO Dynamics of technological innovation systems; The case of biomass energy -- Utrecht 2007: Knag/Copernicus Institute. 166 pp, 24 figs, 17 tabs. ISBN: 978-90-6809-397-1, Euro 18,00

357 R NAHUIS The politics of innovation in public transport; Issues, settings and displacements -- Utrecht 2007: Knag/Copernicus Institute. 184 pp, 9 figs, 40 tabs, 4 box. ISBN 978-90-6809-398-8, Euro 20,00

358 M STRAATSMA Hydrodynamic roughnesses of floodplain vegetation; Airborne parameterization and field validation -- Utrecht 2007: Knag/Faculteit Geowetenschappen Universiteit Utrecht. 180 pp, 55 figs, 28 tabs. ISBN: 978-90-6809-399-5, Euro 23,00

359 H KRUIZE On environmental equity; Exploring the distribution of environment quality among socio-economic categories in the Netherlands -- Utrecht 2007: Knag/Copernicus Institute. 219 pp, 76 figs, 25 tabs. ISBN: 978-90-6809-401-5, Euro 25,00

360 T VAN DER VALK Technology dynamics, network dynamics and partnering; The case of Dutch dedicated life sciences firms -- Utrecht 2007: Knag/Copernicus Institute. 143 pp, 23 figs, 25 tabs. ISBN: 978-90-6809-402-2, Euro 15,00

361 M A SCHOUTEN Patterns in biodiversity; Spatial organisation of biodiversity in the Netherlands -- Utrecht 2007: Knag/Copernicus Institute. 152 pp, 16 figs, 20 tabs. ISBN: 978-90-6809-403-9, Euro 20,00

362 M H J W VAN AMSTEL – VAN SAANE Twilight on self-regulation; A socio-legal evaluation of conservation and sustainable use of agrobiodiversity by industry self-regulation -- Utrecht 2007: Knag/Copernicus Institute. 167 pp, 15 figs, 13 tabs, 5 box. ISBN: 978-90-6809-404-6, Euro 20,00

363 S MUHAMMAD Future urbanization patterns in the Netherlands, under the influence of information and communication technologies -- Utrecht 2007: Knag/Faculteit Geowetenschappen Universiteit Utrecht. 187 pp, 82 figs, 20 tabs. ISBN: 978-90-6809-405-3, Euro 20,00

364 M GOUW Alluvial architecture of the Holocene Rhine-Meuse delta (The Netherlands) and the Lower Mississippi Valley (U.S.A.) -- Utrecht 2007: Knag/Faculteit Geowetenschappen Universiteit Utrecht. 192 pp, 55 figs, 14 tabs. ISBN: 978-90-6809-406-0**,** Euro 22,00

365 E HEERE & M STORMS Ormeling's cartography; Presented to Ferjan Ormeling on the occasion of his 65th birthday and his retirement as Professor of Cartography -- Utrecht 2007: Knag/Faculteit Geowetenschappen Universiteit Utrecht. ISBN: 978-90-6809-407-7, Euro 20,00

366 S QUARTEL Beachwatch; The effect of daily morphodynamics on seasonal beach evolution -- Utrecht 2007: Knag/Faculteit Geowetenschappen Universiteit Utrecht. 125 pp, 39 figs, 7 tabs. ISBN: 978-90-6809-408-4, Euro 12,50

367 R O VAN MERKERK Intervening in emerging nanotechnologies; A CTA of Lab-on-a-chip technology regulation -- Utrecht 2007: Knag/Copernicus Institute. 206 pp, 19 box, 35 figs, 12 tabs. ISBN: 978-90-6809-409-1, Euro 20,00

368 R M FRINGS From gravel to sand; Downstream fining of bed sediments in the lower river Rhine -- Utrecht 2007: Knag/Faculteit Geowetenschappen Universiteit Utrecht. ISBN: 978-90-6809-410-7**,** Euro 25,00

369 W IMMERZEEL Spatial modelling of the hydrological cycle, climate change and agriculture in mountainous basins -- Utrecht 2008: Knag/Faculteit Geowetenschappen Universiteit Utrecht. 147 pp, 54 figs, 12 tabs. ISBN: 978-90-6809-411-4, Euro 25,00

370 D S J MOURAD Patterns of nutrient transfer in lowland catchments; A case study from northeastern Europe -- Utrecht 2008: Knag/Faculteit Geowetenschappen Universiteit Utrecht. 176 pp, 44 figs, 19tabs. ISBN: 978-90-6809-412-1**,** Euro 20,00

371 M M H CHAPPIN Opening the black box of environmental innovation; Governmental policy and learning in the Dutch paper and board industry -- Utrecht 2008: Knag/Copernicus Institute. 202 pp, 41 figs, 30 tabs. ISBN: 978-90-6809-413-8, Euro 22,50

372 R P ODDENS & M VAN EGMOND Ormelings atlassen; Catalogus van atlassen geschonken aan de Universiteit Utrecht door de hoogleraren F.J. Ormeling sr. en jr. – Utrecht 2008: Knag/Faculteit Geowetenschappen Universiteit Utrechts. ISBN: 978-90-6809-415-2, Euro 15,00

373 R VAN MELIK Changing public space; The recent redevelopment of Dutch city squares – Utrecht 2008: Knag/Faculteit Geowetenschappen Universiteit Utrecht. 323 pp, 47 figs, 32 tabs. ISBN: 978-90-6809-416-9, Euro 20,00

374 E ANDRIESSE Institutions and regional development in Southeast Asia; A comparative analysis of Satun (Thailand) and Perlis (Malaysia) -- Utrecht 2008: Knag/Faculteit Geowetenschappen Universiteit Utrecht. 250 pp, 42 figs, 43 tabs, 18 box. ISBN: 978-90-6809-417-6, Euro 25,00

375 E HEERE GIS voor historisch landschapsonderzoek; Opzet en gebruik van een historisch GIS voor prekadastrale kaarten -- Utrecht 2008: Knag/Faculteit Geowetenschappen Universiteit Utrecht. 231 pp, 73 figs, 13 tabs. ISBN: 978-90-6809-418-3, Euro 30,00

376 V D MAMADOUH, S M DE JONG, J F C M THISSEN & J A VAN DER SCHEE Dutch windows on the Mediterranean; Dutch Geography 2004-2008 -- Utrecht 2008: Knag/International Geographical Union Section The Netherlands. 104 pp + cd-rom, 38 figs, 9 tabs. ISBN: 978-90-6809-419-0, Euro 10,00

377 E VAN MARISSING Buurten bij beleidsmakers; Stedelijke beleidsprocessen, bewonersparticipatie en sociale cohesie in vroeg-naoorlogse stadswijken in Nederland -- Utrecht 2008: Knag/Faculteit Geowetenschappen Universiteit Utrecht. 230 pp, 6 figs, 31 tabs. ISBN: 978-90-6809-420-6, Euro 25,00

378 M DE BEER, R C L BUITING, D J VAN DRUNEN & A J T GOORTS (Eds.) Water Wegen; Op zoek naar de balans in de ruimtelijke ordening -- Utrecht 2008: Knag/VUGS/Faculteit Geowetenschappen Universiteit Utrecht. 91 pp, 18 figs, 1 tab. ISBN: 978-90-6809-421-3, Euro 10,00

379 J M SCHUURMANS Hydrological now- and forecasting; Integration of operationally available remotely sensed and forecasted hydrometeorological variables into distributed hydrological models -- Utrecht 2008: Knag/Faculteit Geowetenschappen Universiteit Utrecht. 154 pp, 65 figs, 12 tabs. ISBN 978-90-6809-422-0, Euro 15,00

380 M VAN DEN BROECKE Ortelius' *Theatrum Orbis Terrarum* (1570-1641); Characteristics and development of a sample of *on verso* map texts -- Utrecht 2009: Knag/Faculteit Geowetenschappen Universiteit Utrecht. 304 pp + cd-rom, 9 figs, 65 tabs. ISBN 978-90-6809-423-7, Euro 30,00

381 J VAN DER KWAST Quantification of top soil moisture patterns; Evaluation of field methods, process-based modelling, remote sensing and an integrated approach -- Utrecht 2009: Knag/Faculteit Geowetenschappen Universiteit Utrecht. 313 pp, 108 figs, 47 tabs. ISBN 978-90-6809-424-4, Euro 30,00

382 T J ZANEN 'Actie, actie, actie…'; De vakbeweging in regio Noord-Nederland, 1960-1992 -- Utrecht/ Groningen 2009: Knag/Faculteit Ruimtelijke Wetenschappen Rijksuniversiteit Groningen. ISBN 978-90-6809-425-1, Euro 30,00

383 M PERMENTIER Reputation, neighbourhoods and behaviour -- Utrecht 2009: Knag/Faculteit Geowetenschappen Universiteit Utrecht. 146 pp, 10 figs, 19 tabs. ISBN 978-90-6809-426-8, Euro 15,00

384 A VISSER Trends in groundwater quality in relation to groundwater age -- Utrecht 2009: Knag/Faculteit Geowetenschappen Universiteit Utrecht. ISBN 978-90-6809-427-5, Euro, 20,00

For a complete list of NGS titles please visit www.knag.nl. Publications of this series can be ordered from KNAG / NETHERLANDS GEOGRAPHICAL STUDIES, P.O. Box 80123, 3508 TC Utrecht, The Netherlands (E-mail info@knag.nl; Fax +31 30 253 5523). Prices include packing and postage by surface mail. Orders should be prepaid, with cheques made payable to "Netherlands Geographical Studies". Please ensure that all banking charges are prepaid. Alternatively, American Express, Eurocard, Access, MasterCard, BankAmericard and Visa credit cards are accepted (please specify card number, name as on card, and expiration date with your signed order).